

**SCADA Software-based Techniques for the Management
and Improvement of Industrial Efficiency**

**Gwyn Robert Davies
(BEng.)**

A thesis submitted in candidature for the degree of Doctor of Philosophy
of the Cardiff University.

February 2010

**Intelligent Process Monitoring and Management Centre, Cardiff
School of Engineering, Cardiff University**

UMI Number: U585384

All rights reserved

INFORMATION TO ALL USERS

The quality of this reproduction is dependent upon the quality of the copy submitted.

In the unlikely event that the author did not send a complete manuscript and there are missing pages, these will be noted. Also, if material had to be removed, a note will indicate the deletion.



UMI U585384

Published by ProQuest LLC 2013. Copyright in the Dissertation held by the Author.
Microform Edition © ProQuest LLC.

All rights reserved. This work is protected against
unauthorized copying under Title 17, United States Code.



ProQuest LLC
789 East Eisenhower Parkway
P.O. Box 1346
Ann Arbor, MI 48106-1346

Declaration

This work has not previously been accepted in substance for any degree and is not currently submitted for candidature for any degree.

Signed..........(Candidate) Date...24/08/10.....


Statement 1

This thesis is being submitted in partial fulfilment of the requirements for the degree of PhD.

Signed..........(Candidate) Date...24/08/10.....

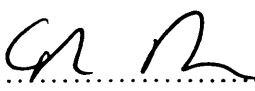
Statement 2

This thesis is the result of my own independent work/investigation, except where otherwise stated. Other sources are acknowledged by explicit references.

Signed..........(Candidate) Date...24/08/10.....

Statement 3

I hereby give consent for my thesis, if accepted, to be available for photocopying and for inter-library loan, and for the title to be made available to outside organisations.

Signed..........(Candidate) Date...24/08/10.....

Acknowledgments

In particular I would like to thank Dr. Roger Grosvenor, Mr Paul Prickett, Dr. Corby Lee and Mr Jon Wadley for their guidance and expertise during the course of this research.

I would also like to thank all the staff at Water Development Services Ltd and my research colleagues at the IPMM, for their comradeship over the last three years.

Finally, I wish to thank my family, Kay and Clio Davies, for their never ending love and support, which always helps me to achieve my goals.

Summary

SCADA, DCS and BMS systems are prevalent across a range of large industrial and commercial installations. The core research contribution of this thesis was to examine whether suitable, non-time critical, algorithms could be developed for deployment on these style of systems. The objective being to use the existing industry standard low frequency signals, for fault detection and diagnosis, condition based control and performance monitoring. This has indicated the potential for applying academic research in a new fashion across industry to improve operational efficiency. A representative SCADA system was used and the work focussed on the industrial water infrastructure in a deep bed filtration plant, a coal fired power station and a gas turbine research establishment.

In the water filtration plant innovative software was developed which diagnosed the location of pipe work blockages. A second programme was developed which passively monitored system variables, giving an indication of filter bed fouling and detecting abnormal system conditions. This functionality was used to provide a robust fault tolerant condition based backwash strategy for the filters. A third programme utilised a novel, threshold based, approach to diagnose the individual severity of combined blockages, allowing condition based back wash to continue, even under extreme abnormal blockage conditions.

The second area considered was based upon a cooling process located in a power station. An ideal condenser performance surface was successfully assimilated into SCADA software infrastructure, thus vastly improving on existing manual monitoring approaches and providing operators with real time efficiency information. Associated work at a gas turbine research facility demonstrated the further scope for gathering and displaying efficiency information using SCADA software.

The work undertaken proved that a research approach can be encapsulated in non-time critical, low frequency algorithms suitable for application to supervisory systems.

Contents

Declaration.....	I
Acknowledgements.....	II
Summary.....	III
Contents.....	IV
Acronyms.....	IX
Nomenclature.....	XII
List of Figures.....	XIV
List of Tables.....	XX
Chapter 1: Introduction and Research Motivation	1
1.1 Introduction.....	1
1.2 Research Motivation	2
1.3 Work Focus.....	4
1.4 Summary of Chapters.....	5
Chapter 2: Industrial SCADA Background	8
2.1 Introduction.....	8
2.2 Industrial SCADA.....	8
2.2.1 Background.....	8
2.2.2 Structure.....	10
2.2.3 Communications and Telemetry.....	11
2.2.4 Internet SCADA.....	13
2.2.5 Security.....	14
2.3 Conclusion.....	14
Chapter 3: Literature and Commercial Systems Review	17
3.1 Introduction.....	17
3.2 SCADA Review and Research Papers.....	17
3.3 IPMM Research.....	23
3.4 General Fault Detection and Diagnosis.....	24
3.4.1 FDD Review Papers.....	24

3.4.2	FDD Applications.....	26
3.5	Condition Based Control.....	29
3.6	Efficiency and Performance Monitoring.....	33
3.7	Commercial Monitoring and Control Systems Review.....	37
3.7.1	Section Introduction.....	37
3.7.2	Retrofitable Monitoring and Control Systems.....	37
3.7.3	Specialised Monitoring and Control Devices.....	41
3.8	Commercial SCADA and DCS System Review.....	43
3.9	Chapter Summary.....	45
3.10	Conclusion.....	46
 Chapter 4: Filtration Plant Single Blockage Location Diagnostic		47
4.1	Introduction.....	47
4.1.1	Context.....	47
4.1.2	Ideal System.....	47
4.1.3	Chapter Structure.....	48
4.1.4	Importance of Blockage Diagnosis.....	48
4.2	WRAP Rig Description.....	49
4.3	Electronic Hardware and Software – Experimental Set Up.....	52
4.3.1	Open Process Control (OPC).....	52
4.3.2	Citect.....	53
4.3.3	Description of Experimental Set Up.....	54
4.4	Blockage Location and Detection Literature Review.....	55
4.5	Blockage Response Testing.....	59
4.5.1	Section Introduction.....	59
4.5.2	PID Mode Blockage Tests.....	59
4.5.3	V5 Extended Transient Testing.....	62
4.6	SCADA Controlled Speed Request Test.....	64
4.7	Decision to Use the CUSUM Technique.....	67
4.8	Post Pump Blockage Discovery Work.....	71
4.8.1	Section Introduction.....	71
4.8.2	Retesting of Blockage Characteristics.....	72
4.8.3	42% Speed Request Test Cycle.....	73

4.8.4	The 55% Speed Request Test Cycle with Revised Procedure.....	75
4.9	Final Test Cycle.....	76
4.9.1	New V7 Model and Revised Test Cycle.....	76
4.9.2	Test Cycle Results.....	78
4.10	Diagnostic Programme Functionality.....	82
4.10.1	Threshold Based on Squared CUSUM Results.....	82
4.10.2	Effective Range of Diagnostic.....	83
4.10.3	Programme Description.....	85
4.11	Consideration of Internal Pump Blockage.....	86
4.12	Chapter Summary.....	87
4.13	Conclusion.....	88
 Chapter 5: Condition Based Backwash and Blockage Detection		90
5.1	Introduction.....	90
5.2	Chapter Structure.....	91
5.3	Filter Backwash Literature Review.....	92
5.4	Filter Bed Response Testing.....	96
5.4.1	Test Set Up.....	96
5.4.2	VF Testing.....	97
5.4.3	Blockage Pressure Response Theory.....	98
5.5	Filter Bed Fouling Monitoring Programme.....	102
5.6	V5 and V7 Testing.....	104
5.7	Combined Blockages.....	107
5.7.1	VF and V7 Combined Blockage Tests.....	107
5.7.2	Multivariate Blockage Signal Analysis.....	110
5.8	Condition Based Backwash and Blockage Detection Programme.....	112
5.8.1	Programme Concept.....	112
5.8.2	Variable Speed Request Region.....	112
5.8.3	Maximum Speed Request Region.....	114
5.8.4	Programme Functionality.....	117
5.8.5	Programme Testing.....	121
5.9	Chapter Summary.....	123
5.10	Conclusion.....	124

7.7.4	Back Pressure Performance Benchmarking.....	176
7.7.5	Real Time Contextualisation of Back Pressure Deviation Data...	178
7.7.6	Cross Unit Analysis Potential.....	180
7.7.7	Individual Unit Analysis.....	182
7.7.8	Potential Savings.....	184
7.7	Cooling Water Monitoring and Control.....	184
7.9	Chapter Summary.....	190
7.10	Conclusion.....	190
Chapter 8: Discussion		191
8.1	Relevance and Scope of Developed Methods.....	191
8.1.1	WRAP Rig.....	191
8.1.2	Coal Fired Power Station and GTRC.....	194
8.2	Systems Approach to Efficiency Using Supervisory Infrastructure.....	195
8.2.1	Systems Approach.....	195
8.2.2	Benefits of a Systems Approach.....	195
8.2.3	Structure of a Systems Approach.....	196
8.3	Benefits of Using a Supervisory System Based Approach	198
8.4	Practical Application.....	200
Chapter 9: Conclusions and Further Work		203
9.1	Main Contributions of the Research.....	203
9.2	Conclusion.....	205
9.3	Further Work.....	207
References.....		209
Appendix A: FMEA for the WRAP Rig		217
Appendix B: WRAP Rig Piping and Instrumentation Diagram.....		220
Appendix C: V5 Restriction Behaviour.....		221
Appendix D: Published Papers.....		227

Acronyms

AEM	Abnormal Event Management
BDTL	Blockage Dominance Transition Line
BP	Back Pressure
CAN	Controller Area Network
CPU	Central Processing Unit
CSA	Cross Sectional Area
CSV	Comma Separated Variable
CUSUM	Cumulative Summation
DCOM	Distributed Component Object Modelling
DCS	Distributed Control System
EEPROM	Electronically Erasable and Programmable Read Only Memory
FDD	Fault Detection and Diagnosis
FMEA	Failure Modes and Effects Analysis
FRD	Frequency Response Diagram
FT	Flow Transmitter
GPRS	General Packet Radio Service
GSM	Global System for Mobile communications
GTRC	Gas Turbine Research Centre
GUI	Graphical User Interface
HGL	Hydraulic Grade Line
HMI	Human Machine Interface
HTML	Hyper Text Markup Language
HTTP	Hypertext Transfer Protocol
HVAC	Heating, Ventilation and Air Conditioning

IDE	Integrated Development Environment
IP	Internet Protocol
IPMM	Intelligent Process Monitoring and Management
ISDN	Integrated Services Digital Network
ITA	Inverse Transient Analysis
LAN	Local Area Network
LSI	Langelier Saturation Index
MES	Manufacturing Execution System
MySQL	My Structured Query Language
OLE	Object Linking and Embedding
OPC	Open Process Control
OPCUA	Open Process Control Unified Architecture
ORP	Oxidation Reduction Potential
PC	Personal Computer
PCA	Principal Component Analysis
PCED	Process Control Event Diagram
PIC	Programmable Interface Controller
PID	Proportional Integral Derivative
PT	Pressure Transducer
PLC	Programmable Logic Controller
PSTN	Public Switched Telephone Network
RTU	Remote Terminal Unit
SCADA	Supervisory Control And Data Acquisition
SMS	Short Message Service
SQL	Structured Query Language
SR	Speed Request

TCP/IP	Transmission Control Protocol/Internet Protocol
TMP	Trans-Membrane Pressure
TTD	Terminal Temperature Difference
V5	Valve 5
V7	Valve 7
VBA	Visual Basic
VF	Filter Valve
VSPC	Virtual Supervision Parameter Control
WAP	Wireless Application Protocol
WAN	Wide Area Network
WRAP	Waste and Resources Action Programme
XML	Extensible Markup Language

Nomenclature

CW	Cooling water inlet temperature	$^{\circ}\text{C}$
C_0	Inlet concentration of filtered particles	Particles/ml
e	Effectiveness	
$F_{100\%}$	Flow rate at 100% Speed Request	m^3/h
$F_{55\%}$	Flow rate at 55% Speed Request	m^3/h
$F_{47\%}$	Flow rate at 47% Speed Request	m^3/h
ΔF_{ti}	Difference: actual flow and modelled V7 flow	m^3/h
F_{Actual}	Actual flow recorded	m^3/h
$F_{V7\text{Expected}}$	Flow expected based on equation 4.1.	m^3/h
FT2	Flow transmitter 2 reading	m^3/h
f_{R-A}	Slope of saturated air enthalpy curve at mid point	NA
g	Acceleration due to gravity	m/s^2
H	Total head loss	m
H_0	Initial clean filter head loss	m
H_p	Total dynamic head added by the pump	m
H_f	Friction and minor head losses	m
K	Deposition rate	Particles/s
L	Filter bed depth	m
P	Pressure	bar
PT3	Pressure transducer 3 reading	bar
Q_{Act}	Actual heat removal	kW
Q_{Max}	Maximum attainable heat removal	kW
T_{wb}	Wet bulb temperature	$^{\circ}\text{C}$
T_{w1}	Tower inlet temperature	$^{\circ}\text{C}$
T_{w2}	Tower outlet temperature	$^{\circ}\text{C}$
T_{db}	Dry bulb temperature	$^{\circ}\text{C}$
W_p	Pump energy added	J
W_t	Turbine energy added	J
W_f	Frictional and other losses	J
z	Height of point from datum	m
σ	Quantity of deposit per unit filter volume	particles/ m^3

v	Approach velocity	m/s
ρ	Fluid density	kg/m ³
ϵ_{Tower}	Tower thermal effectiveness	
Φ	Humidity	%

List of Figures

Figure	Title	Page
Figure 1.1	Simplified representation of the cooling water infrastructure in a generalised large scale industrial process.	4
Figure 2.1	Generalised representation of a SCADA infrastructure.	10
Figure 4.1	Simplified representation of the cooling water infrastructure in a generalised large scale industrial process with water filtration plant highlighted.	47
Figure 4.2	The WRAP water filtration rig.	50
Figure 4.3	Experimental electronic connection on the filter 2 sub-system in the WRAP Rig.	55
Figure 4.4	Flow and speed request response to V7 restrictions of approximately 25%, 50%, 75% and 100%.	60
Figure 4.5	Flow and speed request response for V5 closures of approximately 25%, 50%, 75% and 100% flow restriction.	61
Figure 4.6	Example of flow characteristics seen for a V5 blockage exhibiting the extended transient.	62
Figure 4.7	Example of ramped up speed request test cycle with a V5 restriction of approximately 77%.	64
Figure 4.8	Generalised representation of the characteristic responses of V7 and V5 restrictions with identical Base Flow rates.	66

Figure 4.9	Base Flow and 100% speed request flow for a range of V7 restrictions.	67
Figure 4.10	Representation of V5 and V7 flow rates at 100% speed request for identical base flow rates and expected V7 flow rate.	68
Figure 4.11	Example of a full test, run during a V5 medium closure.	70
Figure 4.12	CUSUM results for a number of V5 and V7 blockages.	71
Figure 4.13	Series of example test cycles run with V5 closures with no tape blockage.	72
Figure 4.14	Example of 42% speed request base test cycle and a cycle modification attempting to prevent flow crash.	74
Figure 4.15	Example of revised test cycle with no second period at 100% speed request shown with a V5 restriction.	76
Figure 4.16	V7 closure flow responses to decrease from 100% speed request to 55% speed request and associated line of best fit.	77
Figure 4.17	100% to 55% speed request test cycle with CUSUM of deviation from expected V7 closure flow response.	78
Figure 4.18	Test results for 100% to 55% speed request test cycle.	79
Figure 4.19	Further test results focussed on areas of ambiguity.	80
Figure 4.20	Test cycle repeated on ambiguous V5 result	81
Figure 4.21	CUSUM results with ambiguous results subjected to double test cycle.	82

Figure 4.22	Spread of CUSUM squared data following repeated test strategy showing decision threshold.	83
Figure 4.23	Flow diagram representing the final functionality of the Blockage Location Programme.	85
Figure 5.1	Generic profile of a membrane system operating with a periodic backwash cycle.	94
Figure 5.2	Profile of a closed loop control system applied to a membrane system.	95
Figure 5.3	Simplified Schematic of the filter 2 subsystem showing filter fouling simulation valve VF.	96
Figure 5.4	Total head loss varying with time.	97
Figure 5.5	System response to VF blockages in PID mode.	98
Figure 5.6	HGL for system with no blockages.	100
Figure 5.7	HGL for an isolated VF restriction.	101
Figure 5.8	Filter bed 2 sub-system process mimic.	103
Figure 5.9	System response to closures of V5 and V7 in PID mode.	104
Figure 5.10	Hydraulic model results for V5 and V7 restrictions.	106
Figure 5.11	Gradual V7 closure performed at four different VF blockage levels.	108
Figure 5.12	60%VF only variable values cross referenced with variable response of combined 20% VF and increasing V7 restriction.	110

Figure 5.13	Speed request and PT3 relationship for a range of VF blockage levels in the ‘Variable Speed Request Region’.	112
Figure 5.14	PT3 and FT2 relationship for a range of VF blockage levels in the Maximum ‘Speed Request Region’.	114
Figure 5.15	PT3 and FT2 relationship for a range of VF blockage levels and the results for VF blockages combined with 10% and 20% V7 blockages.	115
Figure 5.16	Diagnostic thresholds for combined blockage cases.	116
Figure 5.17	Modified process mimic.	118
Figure 5.18	Flow diagram of the Condition Based Backwash and Blockage Detection programme functionality.	120
Figure 6.1	Combined VF and V7 blockage results.	128
Figure 6.2	Combined VF and V7 blockage results showing synergistic behaviour.	129
Figure 6.3	Hydroflow model flow for a VF 0.2” diameter pipe restriction with various diameter V7 pipe restrictions.	130
Figure 6.4	V5 combined blockage test results.	131
Figure 6.5	Combined VF and pipe valve blockage tests results with diagnostic thresholds.	132
Figure 6.6	Threshold template.	134
Figure 6.7	Diagnostic requiring single threshold calculation.	135

Figure 6.8	Diagnostic requiring double threshold calculation.	136
Figure 6.9	Diagnostic requiring no threshold calculation.	137
Figure 6.10	Flow diagram for case where the 42% speed request flow rate fell into zone 3.	139
Figure 6.11	Explanation of combined blockage diagnostic test results.	141
Figure 7.1	Simplified representation of the cooling water infrastructure in a generalised large scale industrial process with heat exchanger highlighted.	145
Figure 7.2	Simplified representation of a coal fired power station.	146
Figure 7.3	Effect of tower inlet water temperature and flow on tower outlet temperature and effectiveness.	147
Figure 7.4	Enthalpy verses temperature diagram for a cooling process.	149
Figure 7.5	Relative costs of running a medium size station and Sankey diagram of heat flow for a 500MW generating unit.	153
Figure 7.6	Optimum economic operating point	154
Figure 7.7	Design condenser back pressure related to condenser cooling water inlet temperature and generated load.	161
Figure 7.8	Variation of coefficients and constant of equation 7.6 with varying generated load.	162
Figure 7.9	Design back pressure equation error profile.	163

Figure 7.10	Manipulated design back pressure equation error profile.	164
Figure 7.11	Simulation system functionality.	166
Figure 7.12	Process mimic for one of the three generating units.	167
Figure 7.13	Station-wide condenser efficiency overview screen.	169
Figure 7.14	Two successive generating periods of Unit 1.	171
Figure 7.15	Condenser cooling water temperature rise and TTD for a typical condenser.	174
Figure 7.16	Back pressure deviation data with lines of best fit for each unit.	176
Figure 7.17	Efficiency level contextualisation using performance benchmark envelope.	179
Figure 7.18	Steam rate characteristics for the three units across the generating range.	181
Figure 7.19	Effects of condenser cooling water inlet temperature on back pressure deviation for a limited range of generated load.	183
Figure 7.20	Gas Turbine Research Centre	185
Figure 7.21	L8 and chemical use manual input page.	186
Figure 7.22	Process mimic with LSI indicator.	187
Figure 7.23	Cooling tower cost savings page.	188

Figure 7.24	Test day temperature data.	189
Figure 8.1	Simplified representation of a SCADA based efficiency management system for a coal fired power plant.	197

List of Tables

Table	Title	Page
Table 5.1	PID response to VF restriction.	102
Table 5.2	VF only and combined VF/V7 variable cross referencing results.	111
Table 5.3	VF/V5 and VF/V7 combined blockage results.	122
Table 6.1	VF Dominant combined blockage test set	126
Table 6.2	V7 Dominant combined blockage test set	126
Table 6.3	Combined blockage diagnostic testing results.	140
Table 7.1	Predicted tower performance	151
Table 7.2	Design back pressure expressed in inches of mercury.	160
Table 7.3	Example of cost penalty error.	171
Table 7.4	Method for deducing back pressure deviation causes	175

Chapter 1

Introduction and Research Motivation

1.1 Introduction

Within power generation and distribution, the water sector, manufacturing, asset management, logistics, buildings and virtually any large scale system which requires regulation and control, the electronic collection and interpretation of data has become vital to safety and competitiveness. The engineering community and human kind in general is facing potentially its biggest ever challenge from the threat of dwindling resources. As a result, the use computer technology to improve efficiency within industrial applications has never been of more importance or emphasis.

In recent years, financial driving forces have been the prime motivation towards a general acceptance of the need for greater efficiency within industry. With ever increasing levels of legislation, efficiency has become more critical and visible. Large industry often involves the teamwork of hundreds of individuals from within a company, and ever increasingly, sub-contracted personnel. As a result of the technical and organisational complexity of the systems involved, the collective desire for change does not necessarily translate into appropriate action, leading to potential efficiency savings being overlooked.

At the core of this research is the concept that this problem can be addressed by the development of a systems style approach to plant efficiency improvement, deployed using the existing software and hardware infrastructure already installed on site. In deference to the constraints of current and future supervisory systems, non-time critical methods for using standard low frequency data streams are researched. The concept of the non-time critical low frequency approach is the core theme underlying all the applications presented in this thesis. These innovative methodologies are implemented on representative SCADA software, to demonstrate to other researchers the applicability of the underlying approach.

1.2 Research Motivation

The specific background of this research involved a deep level of collaboration with a UK based medium-sized enterprise offering bespoke solutions and consultancy to the waste water treatment and industrial water treatment sectors. The partner company design and install small to mid-scale water treatment and water conditioning plant, often integrating this plant into large pre-existing industrial infrastructures. Examples include the installation of demineralisation, deep bed filtration, chemical removal, chlorination and chemical dosing equipment. As a result of the collaboration with the company partner, the author gained experience of system installation and integration at more than thirty heavy industrial, manufacturing and local authority sites during the course of the research. Sectors included steel production, pharmaceuticals, power generation, food and beverage, academic campuses and hospitals.

The company perceived an opportunity to capitalise on its experience by offering consultancy and management services in the industrial water sector, via means of innovative and cost effective application of electronic technology and software. In many ways, the key commercial aspect of this was the potential for capital gain through consultancy work addressing the efficiency improvements mentioned in the introduction. The use of water within industrial processes is an example of how inefficiency can occur due to the fact that the water related process is often seen as a subordinate system to the core process. The plant management will often have a high level of process specific knowledge, but a far lower level of knowledge about the supporting water systems. This is despite the fact that these systems are expensive to run and have a direct impact on the efficiency of the core process.

The methodologies developed in this research were required to have the immediate potential for efficiency improvement in industry; this helped to focus the style of research. It quickly became apparent to the author that, at the majority of sites visited; the data needed for more effective process management was already available from the installed instrumentation. Much of this however, remained unutilised for the purposes of performance monitoring and improvement. It was also the case that this data was being

collected by a Supervisory Control and Data Acquisition (SCADA) system or Distributed Control System (DCS), which displayed the process variables and triggered alarms when thresholds were crossed. These systems however, did nothing to actively improve the process or contextualise the data. A further striking technical feature, which is discussed in detail in Chapter 2, was the complexity of the communication architectures which linked the instrumentation to the SCADA or DCS and the database. This complexity represented a large barrier to the retrofit of efficiency hardware or software.

An elegant approach was to investigate whether non-time critical, low data frequency, methodologies could be researched which would be suitable for application using the processing power of the existing, deployed SCADA or DCS systems. Producing non-time critical, low data frequency methodologies was vital in order satisfy the constraints of an already deployed system, in terms of continued robust operation and the existing low frequency data streams available, which were often in the order of 0.2 to 0.1Hz. The benefit of utilising a deployed SCADA or DCS system is that the communications integration has already been achieved. Thus, the time, expense and disruption of deploying efficiency related algorithms would be vastly reduced. Also by placing the new algorithms at the supervisory level the robust operation of the PLC at the regulatory level would not be undermined.

The work would be of merit to the academic community as it would indicate to researchers the potential for modifying their own research concepts for rapid application using existing site software. It was decided to focus on using representative SCADA software for the research. Demonstration versions and other salient information were more readily available for SCADA software packages than for highly proprietary DCS software.

The pivotal aim of the thesis was to research non-time critical standard low data frequency applications, suitable for deployment using existing on site software, such as the SCADA system. It would be shown that Fault Detection and Diagnosis (FDD), condition based control and performance monitoring were possible using this approach to demonstrate its validity and flexibility.

1.3 Work Focus

The work is focussed specifically on the monitoring and operation of industrial cooling water infrastructure. This was considered an ideal candidate for the extended application of SCADA technology, as the general system structure, shown in Figure 1.1, is common both in heavy industry and power generation. This guaranteed that the research would be of wide relevance.

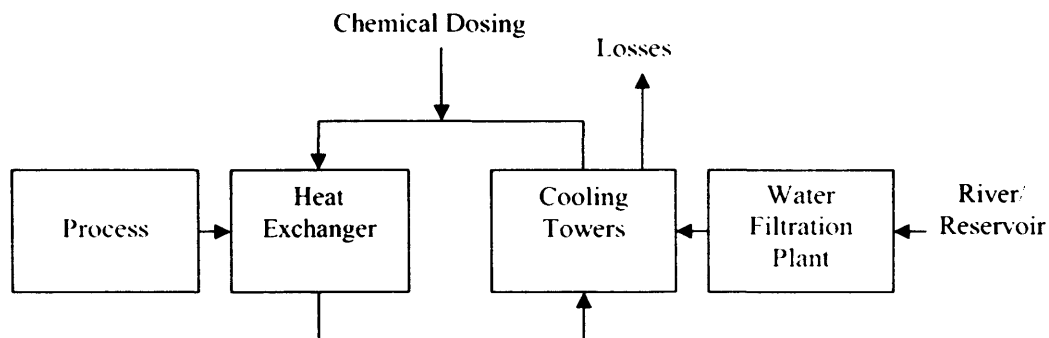


Figure 1.1: Simplified representation of the cooling water infrastructure in a generalised large scale industrial process.

In the generalised process shown in Figure 1.1, water is abstracted from a river or reservoir to feed the cooling system. For large scale water users, receiving water from the mains supply would be uneconomical and in many cases unfeasible due to the volumes required. This water is treated before it enters the cooling tower system, often using a deep bed filtration plant. Here water is pumped through sand filtration media to remove particles, which would otherwise clog the cooling system. After a timed period of operation, the filter bed is backwashed by pumping processed water back through the bed. This backwash water is discharged to drain, so removing the particles which had been filtered from the unprocessed water during service.

The cooling system comprises a number of, so called, wet cooling towers which are connected to the process heat exchange unit via a pumped water circuit. All cooling towers work in a thermodynamically similar fashion, by a process of evaporative cooling. In practice this involves the heated cooling water, from the process heat exchanger, being sprayed from nozzles located high in the tower. As it descends, the water transfers heat energy, by a process of evaporation, to the air which is being forced through the tower. The iconic and hyperbolic shaped natural draft cooling tower uses the Venturi effect to

draw air from the base of the tower, creating a counter flow with the descending water. Alternatively mechanical draft towers use fans to force air through the tower, either drawing air from the base creating a counter flow with the descending cooling water, or from the side, creating a cross flow with the descending water. All cooling towers contain packing of some form which increases the air-water contact time. They also have a pond at the base, where the descending water is captured for re-circulation.

All cooling towers suffer from water loss through evaporation, drift (the lost of small airborne droplets), and intentional blow down. Blow down is the procedure of dumping a percentage of the cooling water to a drain. This is performed when the concentration of contaminants in the cooling water, caused by the evaporation cycle, reaches a critical level. All such losses are replaced from the 'make up' supply provided by the filtration plant. In the process heat exchanger, pipes containing the cooling water come into contact with the hot process fluids, such as steam or exhaust gasses, removing waste heat from the process, before then transferring it to atmosphere via the cooling towers.

At a point, usually upstream of the process heat exchanger, a variety of chemicals are added or "dosed" to the cooling system. These can vary immensely as a function of the water quality and construction materials used at the specific site. A biocide and pH regulating chemical will always be present, often accompanied by a mix of corrosion and scale inhibitors.

In order to examine the potential applications of SCADA software across the water infrastructure, and connected processes, work was undertaken at three plants. Water filtration plant applications were developed using the Waste and Resources Action Programme (WRAP) filtration rig provided by the company partner. Research on the efficient management of the heat exchange process was conducted at a coal fired power station. Research into the management of chemical dosing and cooling water was undertaken at the Gas Turbine Research Centre.

1.4 Summary of Chapters

Initial research was conducted to establish the potential benefits and justification of utilising the innate functionality of deployed supervisory system software. With this established, algorithms were researched and applied using a SCADA package

experimentally to assess the validity of the approach for efficiency related tasks. A summary of the chapters presenting this work is as follows;

Chapter 2 contains an overview of the range of SCADA structures commonly found in industry and details the involved nature of the communications and database infrastructure. This provides a basis to consider the potential methods which could be used to retrofit efficiency management functionality into an existing SCADA system. The conclusion drawn is that using the innate functionality of the SCADA software offers significant potential advantages over other methods.

Chapter 3 contains a review of research literature and commercially available retrofitable monitoring systems. A review of research conducted using SCADA is presented first. It is concluded that although the potential of utilising data gathered by the SCADA system has been recognised, little research has been conducted to explore how the functionality of the SCADA software itself, can be better utilised. A review of the efficiency related tasks considered in this thesis, namely FDD, condition based control and performance monitoring reveals that some of the approaches taken would be suitable for the development of SCADA based efficiency systems.

Chapter 4 presents the first element of experimental research which was undertaken on the WRAP water treatment rig. A short review of research into blockage detection and diagnosis is presented. The SCADA system and electrical set up used in this research is described, along with the functionality of the WRAP water filtration rig. The work undertaken to develop a blockage diagnosis algorithm suitable for the SCADA software is then presented. The system response to blockages upstream and downstream of the pump is initially explored. The characteristic behaviour captured is then used to develop an automated test cycle, using code in the SCADA software. This is shown to distinguish between potentially damaging upstream pipe restrictions, and less serious downstream blockages. It is thus demonstrated that non-time critical low frequency algorithms applied using the SCADA package can successfully achieve fault diagnostics.

The next stage of work on the WRAP Rig is presented in Chapter 5. This involves research into passive monitoring and condition based control. A short review of previous research into filter backwashing strategies is included. A methodology is developed for

passively assessing the fouling level in the filter bed and using this to automatically trigger backwashing of the bed, based on condition. This is in contrast to the existing, time based strategy, which does not account for filter condition. A level of fault detection is also included to prevent erroneous backwashing based on the data obtained under fault conditions.

Chapter 6 explores the possibility of running more complicated fault diagnostics in the WRAP Rig using threshold based techniques within the SCADA software. A programme is realised which can diagnose the individual blockage levels of combined filter bed and pipe blockages. It is shown that this could be applied, under very severe blockage conditions, in order to allow condition based control to continue.

Chapter 7 presents work undertaken at a Coal Fired Power Station, in the area of efficiency monitoring. A review of research in the field of cooling tower and condenser efficiency is presented. The assimilation of a condenser performance surface into the SCADA software is described. A simulation is conducted within the SCADA software using historical process data from the station and hence the limitations of the existing efficiency monitoring strategy are revealed. Methods for the application of the SCADA package for improved condenser efficiency monitoring at the station are discussed. Work undertaken at the Gas Turbine Research Centre is also presented. This covers the potential for using SCADA to manage chemical dosing and cooling tower operation.

Chapter 8 provides a discussion of the work undertaken. The wider relevance of the research and recommendations for the practical application of extended supervisory software functionality are covered.

Chapter 9 gives the conclusions drawn from the work and a concise list of the research contributions of the thesis. Finally a list of further recommended research activity is presented.

Chapter 2

Industrial SCADA Background

2.1 Introduction

The implementation of SCADA systems varies widely across industry [1]. The often complicated interrelations between the SCADA system components are explored in this chapter, to identify the potential advantages of using innate SCADA software functionality for efficiency improvement.

2.2 Industrial SCADA

2.2.1 Background

Industrial SCADA systems have effectively been in operation since the very first control systems were implemented. The original embodiment of SCADA involved panels of dials and switches, each individually hardwired to a particular instrument or contact set, using current or voltage signals. Data logging was achieved through the use of strip recorders. The operator effectively exercised centralised supervisory control by manipulating the control panel. This style of system was limited because the amount of wiring would become unmanageable, as more sensors were added. As this complexity grew, historical data became difficult to archive, and the panels required 24 hour supervision.

The key developments which heralded the beginning of the modern SCADA system were, the inclusion of network communications in the system architecture and the invention of the Central Processing Unit (CPU) [1]. In early automated plants, relay logic was used for control. The invention of the CPU allowed this logic to be hosted within field a processor, such as a Remote Terminal Unit (RTU) or a Programmable Logic Controller (PLC) at a regulatory level. From this point forward, the term “field processor” will be used in place of RTU and PLC where a statement is relevant to both. As the value of data and tighter process control became apparent, more sensors and actuators were added to processes. The constantly evolving power of the CPU meant that it became most effective

to deal with the control of sub-processes locally, creating a highly distributed system. The use of telemetry was vital to this as it allowed connection of these distributed controllers to a central PC, facilitating the modern SCADA architecture.

As a further dissemination of control, the use of intelligent sensor units has also become common [1]. These units possess some of the functionality of a field processor, allowing them to execute simple code. Typically they may be able to execute PID control, provide digital switching and also support more than one sensor. They are usually configurable within the limits of the intended task, such as cooling water chemical dosing control.

In the modern industrial setting the distinction between DCSs and networked PLCs has become highly blurred. Indeed, in the experience of the author, definitions change from site to site. In practice the majority of systems are unique. The fact that they combine a mixture of legacy equipment further complicates the issue. Originally, it could be argued that DCSs were proprietary entities, with all RTUs being of the same brand and communicating using a proprietary protocol. Today however, systems which may contain a number of different brands of PLC networked together will often be referred to by site engineers as the DCS.

SCADA software can be categorised into two types: proprietary or open. Proprietary systems only support the communication protocol of hardware from the same company. These systems will often be marketed as turn key solutions, citing simplicity and rapid deployment as advantages. However, there is a major disadvantage to the customer, who becomes totally dependent on one supplier, with no flexibility. If more advanced or cheaper hardware becomes available from another supplier, this cannot be used. This can severely limit plant upgrade and competitiveness, if the supplier does not stay at the cutting edge of new developments. Open software, on the other hand, provides hardware and software interoperability. The system can utilise the field processor best suited to each application. This may be more complicated to integrate at the beginning, but can offer major benefits in performance and upgradeability in the long term.

2.2.2 Structure

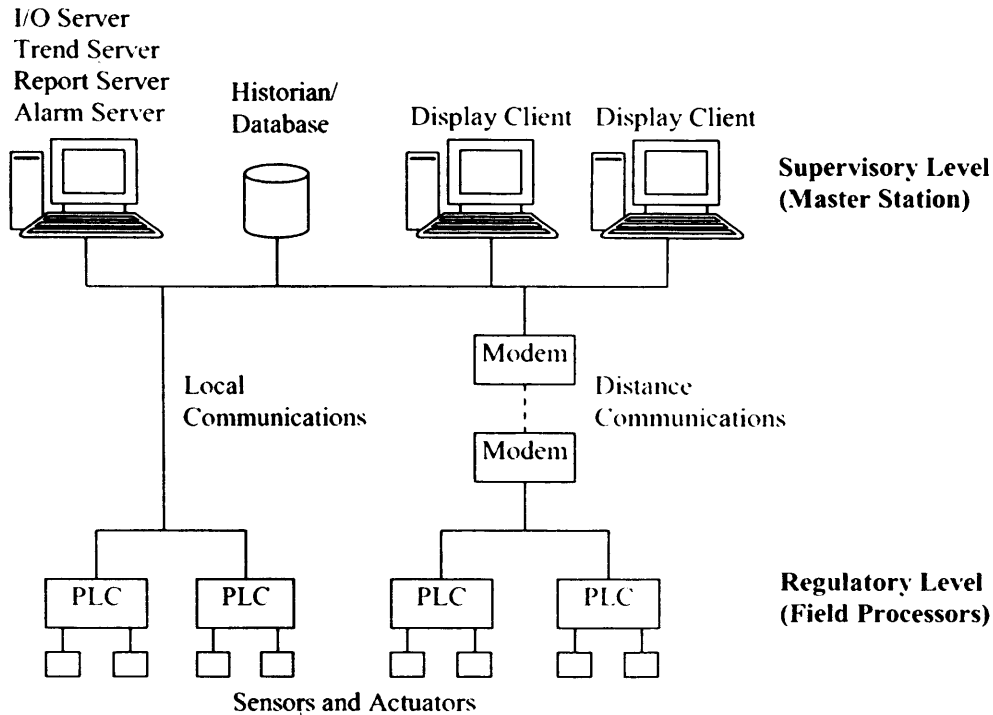


Figure 2.1: Generalised representation of a SCADA infrastructure.

A generalised representation of a SCADA infrastructure is shown in Figure 2.1. At the regulatory level field processors use sensor data and actuators to control a particular process within the confines of defined set points. At the supervisory level, a typical SCADA Master Station configuration is shown. Here the I/O, Trending, Report and Alarm Servers are hosted on a single Personal Computer (PC). This PC is linked via the Local Area Network (LAN) to the PC containing the database and a number of PCs which act as display clients. There are a number of methods for achieving the communication connections between devices, which are shown as lines in the diagram. The geographical layout, legacy equipment in place and isolated system upgrades combine to produce a unique and often hybrid communication structure, when a plant is operated for a number of years. As such, Figure 2.1 is considered as a generalised representation, with some of the possible configurations explained below

The I/O Server is the part of the software which deals with communications with all the field processors. In an open SCADA package, the correct drivers must be included for each device. The Trend Server deals with the real time update of the Graphical User

Interface (GUI) and access to historical trend data. The Report Server contains formatted reports and facilitates the population of these reports with relevant data from the historian. The Alarm Server handles the prioritising and display of configured alarms, which may be coming from a number of the field processors simultaneously. If required in larger systems, to improve performance, it is possible to host each of these servers on a different PC on the LAN. The Display Clients, hosted on networked PCs, are software portals which allow operators to view all the SCADA screens allowing, for example, the handling of alarms and changing of set points. The Display Clients allow simultaneous access to the SCADA package for a number of operators allowing one SCADA package to cover all the separately managed areas of an industrial site. The Database or Historian can be hosted on a separate PC, as shown in the figure. The SCADA system may use a proprietary historian package or a relational database, normally configured and managed using Structured Query Language (SQL) code.

2.2.3 Communications and Telemetry

In large applications Master Station computers will usually be networked together on an Ethernet based LAN. The term Ethernet refers to a group of frame based protocols standardised under the remit of IEEE802.3. A large modern industrial Ethernet is composed of twisted pair cables which connect end systems to a network hub that reframes the data for transmission via the higher speed Fibre Optic backbone of the LAN. The usual protocol used in industry is TCP/IP with other protocols such as NetBeui and Netbios becoming obsolete. Smaller Ethernets may not include a fibre optic backbone. On larger scale Ethernets segmenting may be used to prevent congestion. In this case a bridge or a switch is used to divide the Ethernet. The divided Ethernet segments allow free communication between nodes in the segment, but prevent unnecessary communication between segments. The segments remain linked however, as those Ethernet broadcasts which are required to reach all nodes on the LAN, are allowed to pass. Switches have become increasingly important in large industrial Ethernets. They contain a level of intelligence which allows them to identify the intended recipient of a package. The switch can be connected to a number of nodes in a radial pattern. Rather than a packet being seen by all the nodes on a series network, the switch is the first to receive all packets, and as such can select the correct recipient and send the packet directly, so reducing network traffic. A further form of Ethernet traffic control, called sub net masking, is also often

used. A device on the network has an IP address and also a sub net mask. The subnet mask can be configured to limit the devices that this IP address can communicate with, effectively applying a limited privilege level.

Many modern field processors can now be fitted with Ethernet modules, or come with these as standard. In applied SCADA systems which use Ethernet for local communications, a control cabinet DIN rail mounted switch will connect devices, such as the PLC and Human Machine Interface (HMI) screen in the cabinet to the backbone. This facilitates the link between SCADA software and field devices. Unlike the PCs on the network, the field devices may be utilising industry standard Ethernet protocols, such as Modbus-TCP/IP or Profinet. There is a move within in industry towards having Ethernet as the standard industrial communication media [2]. This is reflected by the number of new devices such as PLCs which offer Ethernet capability as standard.

In many cases, the field processor will not be Ethernet capable but will use serial protocols for local communication, such as Modbus RTU, Profibus, CAN or Devicenet. A group of field processors will be networked together using a twisted pair cable and communicating using one of these serial protocols. In many cases the RS485 standard will be used for the physical connection due to its interference tolerance and distance capabilities. In order to connect to the Ethernet a gateway protocol convertor can be used which formats packets configured in the serial protocol for Ethernet transport and vice versa. As an example, a Modbus packet would actually be contained in the payload of a normal Ethernet frame, which ensures it reaches the correct node. The device on this node then reveals the payload and uses the Modbus protocol to decode the information. This form of communication is relatively inefficient but the benefits of a common Ethernet communication medium and robust operation are significant. More commonly the field processor network will be connected to a field PC containing the correct serial communications card. In master-slave based protocols, such as Profibus, the PC will be the master and provide the link between Ethernet and serial networks.

In cases where geographical separation is an issue, the distance communication between field devices and master station may be facilitated by use of a Wide Area Network (WAN) utilising radio frequency, GSM or landline connection. In the case of radio and GSM WANs, the field processor will be connected to the relevant modem, which

communicates to another modem at the master station. This modem is connected directly to one of the PCs, or is actually a node on the LAN. For land line based systems, the actual line may be privately owned across a large site, or may be leased from a public telephone company. Once again an appropriate modem provides the gateway at either end.

It is worth mentioning that due to the myriad of industrial applications, the complexity of integration, the presence of legacy systems and the personal preferences of engineers, there is no standard SCADA implementation within industry. For example, even at some large sites there may be no Ethernet LAN at the Master Station level. All Field devices may simply be linked to a single SCADA hosting PC, via a field bus, running a serial protocol. In reality, fully understanding a deployed SCADA system often involves obtaining information from several departments and piecing together the evidence to create a clear picture.

2.2.4 Internet SCADA

Many modern SCADA packages such as iFix and Citect offer “bolt on” web clients. These have a similar functionality to a standard display client except they are designed to allow the SCADA interface to be accessed via the Internet. This functionality may be useful, for example, to allow a line manager or process engineer to monitor the running of the factory from an external location.

A more radical concept for connection to remote equipment is the web hosted SCADA system. As the majority of field processors do not currently possess the ability to connect to the Internet, they may instead be networked to a PC which provides an interface with the Internet. A lower cost solution is the use of a so called Internet gateway device. This ruggedized unit communicates with the field processor via a serial link, and then converts the data obtained into HTML or XML format. The device has an IP address and supports either the full TCP/IP stack or a streamlined version. The SCADA connects to the remote devices via the Internet. The main SCADA package may reside with the end user but in a true application of web based SCADA a service provider hosts the SCADA software. The process operators, in the control room, access the SCADA interface via means of a standard web browser.

2.2.5 Security

As previously discussed, there is a strong trend towards more open architectures, with the adoption of mainstream technologies such as Ethernet, TCP/IP and web browsers within the SCADA industry. These are effectively replacing the specialised proprietary systems originally deployed. This offers significant business benefits in terms of capital cost, time savings and improved process efficiency. However, the increased connectivity has suddenly exposed systems to cyber threats such as worms, viruses and hackers, which they are ill prepared to deal with [3]. The desire for increased connection with the wider supply chain must be offset against considerations of how the system can become open to threat. For example, tank level data from the plant may be used to automatically reorder products. This exposes the SCADA system to the potentially poorly protected system of the supplier. The implications of Cyber attacks on SCADA systems range from loss of service right through to major contamination and loss of life.

All Internet connections should have firewall protection. Often, if the industrial LAN is connected to a corporate LAN running business software, there will also be a firewall between the two networks, providing protection to the SCADA system from internal attack. However Cai et al [4] state that these traditional measures are designed for an IT infrastructure and are seldom fully suited to the protection of SCADA systems. They give the example of Distributed Component Object Modelling (DCOM), which forms the underlying protocol of both OPC and Profibus, to support their argument. It uses the Microsoft remote procedure call service which has known vulnerabilities to Cyber attack. Also, DCOM opens a wide range of ports, which can be extremely difficult to filter using the fire wall. It is clear that SCADA security will become an ever more pressing problem in the future and it should be considered every time a new SCADA implementation or modification is proposed.

2.3 Conclusion

The overview indicates the level of variation and complexity which can exist in industrial applications of a SCADA system. Retrofitting and integrating efficiency management and optimisation functionality into the existing infrastructure would be an involved task. One

possibility would be to attempt to retrofit external stand alone hardware systems. If this was achieved by accessing signals between the regulatory and supervisory layer, the integration could clearly be a problem due to the range of protocols and knowledge required to successfully deploy the system, without compromising the existing communications infrastructure. Alternatively, the hardware may be designed to acquire instrument signals before they reached the PLC, or deploy new sensors. This may necessitate expensive opto-isolation devices, which would also require time consuming and disruptive installation. Finally, the question of integration of the system at the supervisory level could be a problem. A stand alone system would potentially require a separate monitor in the control room. It would be difficult to integrate the information produced by the new system into the existing database. Adding another system could lead to a far more complicated overall structure, which may then cause more harm than good. The merits of some commercial systems are considered in the next chapter to reinforce this argument.

Alternatively, the PLC could be used to increase functionality. This is also not an ideal solution for a number of reasons. As mentioned, at the regulatory level the PLC controls variables around predefined set points. The PLC is also responsible for emergency shutdown activity and other safety related tasks. The sequential programming languages used in the PLC are designed to be highly robust. They have less functionality than procedural languages but are also less susceptible to errors, and easier to troubleshoot. Using the sequential PLC code, to enact higher and less critical functionality, could interfere with the core functionality and safety objectives of the PLC. Due to the simplistic nature of the sequential languages the code would be ungainly and could lower execution times of the PLC. Also the ease of troubleshooting could be reduced leading to extra downtime. As PLCs are programmed in proprietary code, the portability of the applications developed across the plant could also be limited. Although modern PLCs can be programmed over the network this practice is not always used. Therefore, any changes that needed to be made to the PLC programming would require a visit to the PLC location. Hosting all the efficiency related software in a central location rather than distributed across many PLCs offers a better chance for fast maintenance and a more integrated and manageable approach. It also ensures that the critical regulatory control provided by the PLC remains intact with the new algorithms located a step removed from the process, at the supervisory level. As a result even if an erroneous request comes from

the supervisory level, the existing alarming or emergency shutdown thresholds within the PLC will ensure safety is not compromised.

A third possibility would be to add additional optimisation software linked to the SCADA system at the supervisory level. The retrofit of this could also have significant disadvantages and not provide the required functionality. The new software would most likely be linked to the SCADA system by use of the database. This statement is supported by evidence presented in the literature review in the next chapter. The first problem is that connecting to an existing database can be extremely difficult, and cause major problems to the existing infrastructure, possibly undermining the current functionality of the SCADA system. Blaha [5] conducted a reverse engineering process on thirty five industrial databases to assess the uniformity and suitability of the approaches taken to configure the databases. It was found that a low level of uniformity existed across the analysed databases. Therefore, the author of this thesis asserts that the integration of new software with the existing database is likely to be a time consuming and disruptive task. The use of this method would also lead to an increase in database traffic and an almost inevitable decrease in the reaction time of the efficiency system.

Use of the SCADA system alone offers a number of advantages over the other methods outlined. No communications or database integration is required, as this has already been achieved. No hardware installation is required, as this already exists. All the code of the new efficiency system is held in one place and in one programming language. The efficiency system is effectively hosted as close to the process as possible without compromising emergency performance, as could be the case using the PLC. This leads to seamless integration with the existing operator screens and fast reaction times. Also the code developed for one part of the plant can be easily modified and deployed to act on other similar parts of the plant, from a centralised location. Based on these arguments it is proposed that using the innate programmability of the already deployed SCADA system offers an elegant solution. This thesis considers deploying efficiency monitoring and optimisation to an existing industrial infrastructure, using examples drawn from water infrastructure plant. In the next chapter a review of literature and commercial systems is presented to support this and to explore the potential applications of SCADA technology.

Chapter 3

Literature and Commercial Systems Review

3.1 Introduction

This chapter contains a review of previous research into the application of technology at the supervisory level and the development of methods for FDD, condition based control and performance monitoring. An overview of research containing relevant concepts is presented in this chapter. This is supported in later chapters by further short review sections dedicated to research pertaining to the specific plant and problems considered in those chapters. Much of the research presented emanates from the water industry but where appropriate, papers of interest from other industrial sectors are included.

The review of SCADA research reveals that the potential value of SCADA systems is recognised by academia and industry. However, it is shown that little research has been conducted on exploring the full functionality of the actual SCADA packages deployed. A consideration of strategies reported by researchers in the fields of FDD, condition based control and performance monitoring demonstrates that techniques are available which could potentially be deployed using SCADA software. Finally, an evaluation of existing commercial technology is provided, comparing their functionality to the requirements of this research. The conclusion reached suggested that using the existing SCADA software offered a more readily integrateable solution.

3.2 SCADA Review and Research Papers

A number of researchers have utilised SCADA technology as part of experimental apparatus, while others have attempted to implement SCADA systems linked to process optimisation or expert system software. Starting with review papers and moving on to relevant research, this section demonstrates that, although the potential of SCADA application is recognised, little research has been conducted on exploring the possible benefits of deploying pure SCADA software functionality to achieve the intended goals.

Garrett et al [6] published a paper chronicling and reviewing the developments in technology and thinking in the field of instrumentation, control and automation in the U.S. water industry from 1975 to 1997. The paper describes the rise of PLC technology and distributed control systems and notes the rapid increase in the use of water quality optimisation models during the 80's. These were facilitated by the reducing cost and increasing processing power of the PC, although the models were not implemented in real time. An example is given of how despite the implementation of multi-million dollar SCADA systems, much of the capacity of these systems was not used. Reports were still being compiled by hand and valuable data was being collected but essentially then ignored. The paper closes by saying that "The need for optimally controlled plants will increase due to tightening permit requirements and the ever present need to reduce costs."

Dieu [7] published a paper describing in detail the implementation and refinement of a SCADA package, on the City of Houston's waste water system. The structure and interface design of the system was relatively standard. The paper is of note to this research as examples are given of how better information allowed rapid improvement in the control, and efficiency of the chlorination process. Previously undetectable control strategy flaws were unmasked by the new systems' ability to show simple trend data, making the water system more comprehensible to operators and field technicians.

Patel et al [8] effectively developed a SCADA system based on the Labview software using the additional functionality of the Data Logging and Control module. The system was designed to be highly flexible as it was to be employed to run laboratory testing on an ever changing range of renewable energy generation equipment. An Open Process Control (OPC) server was used for all communications with industry standard devices such as PLCs. OPC was used to maximise the flexibility of the system and was also considered the easiest option for industrial device communications. The system is notable in the context of this research as it shows a SCADA system developed with a different intended use from standard applications. For example, the software comes with functions for calculating and logging figures such as the maximum, minimum and standard deviation values of a set of experimental data. This is indicative of the diverse range of applications the modern SCADA package could be used for.

Ozdemir et al [9] considered the integration of a WAP enabled mobile phone as a display client for a modern SCADA package. The Siemens WinCC SCADA software was networked to an S7-300 PLC which controlled a model crane. The mobile phone had mimic, alarm, data table and remote control pages. The SCADA could transmit data to the Java enabled phone via WAP or GPRS. The ability to connect a mobile phone to a leading industrial SCADA illustrates the ever widening scope of SCADA technology.

Duong [10] provided an overview of SCADA architecture and functionality applied to the management of oil pipelines. The increase in processing power, online memory and off line storage capacity is reported to result in computationally intensive operations being achieved within a real time framework. It also results in large amounts of process data being retained for analysis. The use of specific leak detection software utilising data collected by the SCADA system is outlined.

The author of this thesis considers that the use of such software has become commonplace in the oil and gas transport industry due to the massive safety, environmental and ultimately financial implications of leakages. Therefore, a large economic and political justification exists for the time and expense required to retrofit software to the SCADA system, which is not present in many other industries. The leak detection software packages will usually be deployed by the manufacturer and integrated with the existing SCADA system in partnership with the pipeline operator, as explained by Theakston [11].

Chan et al [12] describe the implementation and evolution of the Public Utilities Board of Singapore's 22kV power distribution network SCADA system, which was connected to 1330 substations. The system, which was still under development at the time this paper was published, was intended to eventually connect to 3000 substations. The vast size of the system meant that the decision was taken to split the master station into two sites dealing with separate parts of the country. They are connected via the public telephone network. A brief description of the development of an expert system linked to the SCADA system is given. The system was intended to provide artificial intelligence for the analysis of disturbances and the proposal of new switching sequences. The expert system was based in a PC connected to the master station LAN and an object oriented programming approach was taken using the Lisp programming language. The expert system could access the SCADA database directly and deployed programming functions

evaluated the data to assess the network topology. These results were then stored as objects in the knowledge base and called upon for disturbance analysis. The system is said to adopt both model and rule based fault diagnostics and it was intended that eventually, all alarms and circuit breaker changes would be utilised for diagnostics by the expert system, using an internal event manager function. This is an example of the work being undertaken to push the boundaries of SCADA beyond basic control functions, although external add-on software was used rather than the innate functionality of the SCADA software. The use of external software connected to the SCADA system was practical, in this case, as it was included at the design phase, and therefore, a successful integration was more likely.

Valsalam et al [13] set out that, according to the International Energy Agency, world energy needs will increase by 50% by 2030. It is stated that, given this backdrop, the application of SCADA systems to extract maximum efficiency from power production by efficient use of resources will become increasingly important. The system described in the paper is based on a top level SCADA package connecting the individual SCADA systems of three hydroelectric power plants by means of Radio WAN. The newly deployed SCADA package had all the usual elements but also included specific analysis modules for fault detection. It was not made clear where the programming for these modules lay but the functions did utilise SCADA tag data directly. This meant that data streams being collected by the SCADA system could be sampled and the values utilised by the programme code. The example provided concerns a pressurised system leak detection module. After pressurisation the gradient of the pressure loss was calculated from the last sixty samples. A least squares algorithm was used to produce the line of best fit. Once the slope was calculated it was tested and if found to be significantly different from the expected decay slope, an alarm was triggered. Other modules mentioned include further leak detection applications and optimisation of water flow through generating units.

Bernard et al [14] explained the problem of alarm showers faced by the control room operators of Hydro-Quebec. The nine regional control rooms were responsible for the supervision and remote control of more than 350 generating stations and substations, with each operator handling on average 15 facilities. Alarms were displayed on a traditional SCADA alarm page, where alarm strings were listed down the page. It was reported that some incidents could generate hundreds of alarms within seconds, as a ripple effect

emanated from the original event caused by the automatic shutdown. It was stated in these cases that most of the alarms were not relevant to the diagnosis of the fault. Diagnosis of the fault was often critical as the effect of certain shutdowns may overload neighbouring equipment and lead to system instability. The expert system developed and partially implemented to address the problem was model based. There was a rule based component which held information on the alarm grouping related to a specific control action and a descriptive component which contained information on the equipment contained in each facility. The system worked by recognising patterns in generated alarms to suggest possible faults. The system was also capable of requesting tag data from the SCADA system to help confirm results. The expert system was hosted on a computer on the control room LAN and was able to read alarm information from the SCADA system database. The results from the expert system were then transmitted to a HMI module installed on each operator computer on the LAN. The system was partially implemented and tested. It was estimated that the full application would take many more laborious man-months of work, at each control room, to populate and test the expert model. In the specific case of this paper, it can be said that in recent times there has been increased emphasis on designing out the possibility of alarm showers at the development stage of a SCADA installation. There are now guidelines restricting the number of alarms which should be faced by an operator in the time period following a system event.

In a recent paper, Reynard et al [15] developed an educational SCADA system for use in the training of SCADA configuration, PLC programming and industrial communications. Reflective of the burgeoning acceptance of Internet SCADA, the Schneider Vijeo Look SCADA software was networked to the PLCs via the Internet, communicating by means of an OPC server. The fact that this style of system was chosen for use in classes, by a teaching university, is indicative of the trend towards the acceptance of control systems with Internet components, despite the security issues outlined in the previous chapter.

Yang et al [16] outlined a considered approach to the design of internet-based process control systems. The major benefits of a move to web enabled control systems are cited as the enabling of remote monitoring and control, collaboration between skilled plant managers in different locations and the ability to relocate the geographical position of plant management staff in response to business needs. In the paper, five key design issues are considered: requirements specification, architecture, interface design, supervision

control and system safety checking. In each case the effects of the new web related phenomena of traffic delay, concurrent user access, security and varying working load are considered. The mentality adopted in the approach is that internet-based process control systems should be used to enhance, rather than replace, computer based systems. As a result the point of Internet interface is discussed with reference to a traditional DCS or SCADA style architecture. The possibility of connection at the regulatory, supervisory or management level is considered. The effect of Internet time delay is considered in detail with the conclusion that a control architecture which is insensitive to time delay is needed for Internet control. Virtual Supervision Parameter Control (VSPC) where only set points and PID parameters are altered via the Internet with the regulatory tasks remaining with the PLC is discussed as the ideal solution. Security issues are addressed and procedures such as the development of user privilege levels are discussed. A Process Control Event Diagram (PCED) is demonstrated as a tool for assessing the robustness of the system in terms of dealing with delays and security issues. The approach outlined was applied by the researchers to a simple water tank control problem. The VSPC approach was taken to overcome time delay and the user interface was designed to run using standard Internet web browsers. The regulatory control of the process was actually handled by the same computer which was acting as the Internet server. The embodiment of the system was achieved through the use of Labview software and Java applet technology. Although this provided a suitable test bed for the procedures outlined, this arrangement of technology and software selection is not reflective of current industrial control systems. It is concluded by the authors that the use of VSPC over the Internet provides similar results to its use in traditional LAN, WAN and serial field bus networked structures but security issues remain the single largest obstacle to successful deployment of Internet enabled systems.

Kim et al [17] developed an Internet monitoring system for an agricultural storage facility. A purpose specific food process controller, which had a number of sensor inputs and digital outputs for actuator control, was linked to an on site PC. The onsite PC running a LINUX server was TCP/IP and HTTP enabled allowing computers with different operating systems to access the server via Internet. The mySQL database was also located in the onsite PC and a number of task specific programmes were written in visual C++ to allow data basing, data transfer and remote control. Communications between the on site controller and PC was accomplished via an RS232 link set up in windows. The system

was successfully demonstrated, and represents a successful connection to a pre-existing proprietary controller in an industrial setting. The issue of security is not however fully addressed in the paper.

It was clear from the many and varied activities described in this section, that industry and academia has accepted the potential which the application of SCADA offers. However, in all the papers reviewed little evidence was found that the full functionality of the SCADA software used had been explored. In some cases external software packages were linked to the SCADA software but as discussed previously in Chapter 2, the retrofit of new software to an existing SCADA implementation can be time consuming and problematic. In the examples, only very specific problems, in very large systems, were addressed using add-on software. Having concluded that the application of pure SCADA technology offered potential benefits and was worthy of research effort, an examination of the techniques and methodologies, which could potentially be included in a pure SCADA system configuration, was now explored. A review of previous research in these is presented over the following sections.

3.3 IPMM Research

The Intelligent Process Monitoring and Management (IPMM) group, of which the author is a member, have previously researched the cost effective deployment of condition monitoring technology for FDD, performance and safety purposes. Prickett and Grosvenor [18] for example, utilised analysis of existing sensor data for the monitoring of a machine tool. This approach eliminated the need to deploy new sensors minimising cost and downtime for system deployment. This is also a core aim of the research presented in this thesis. A Petri-net model was applied to the milling machine and this was updated by the detection of state changes, through consideration of controller signals and embedded sensor data. For fault detection, the axis feed drive signals of the milling machine were captured and analysed, with controller driven fluctuations being used to infer the health of the cutting tool.

The IPMM has also undertaken work involved with remote process monitoring. Frankowiak et al [19] reported the deployment of a number of PIC microcontrollers as monitoring modules, networked using the industry standard CAN bus protocol. These

modules were then connected to the Internet via a connectivity module. A management PC handled the database of collected data and provided a visual representation of the Petri-net model which had essentially been encoded onto the PICs. Ahsan et al [20] also utilised a similar PIC based Internet enabled system for fault detection on a batch process simulation rig. Blockages and leaks were detected by consideration of the flow rate, tank level and pump power signal from the PLC. Both time and frequency domain techniques were applied for the fault detection and identification. This work was of particular interest as the style of fault detection methods applied was heavily influenced by the limitations of the 8 bit controllers used. Modifying and simplifying the FDD approaches used in order to maintain proper SCADA functionality would present similar challenges in this research.

Alyami et al [21], utilising the more advanced dsPIC microcontroller, used a time domain analysis of the pressure response of a pneumatically actuated gripper for fault detection. The high frequency component of the data was removed via use of a moving average process to smooth the data. The squared rate of change of the pressure was used to identify key points in the gripping process and thus calculate closure time. This information was then compared to the expected closure time to grasp a component, to detect incorrect or misaligned parts. A similar method was also utilised by Alyami et al [22] to assess the extension of a linear pneumatic actuator. In both cases numerous test cycles produced response surfaces linking time, pressure and closure/distance. These were programmed into the software and then used to estimate expected closure time or distance travelled, for the gripper and linear actuator respectively. This approach of assimilating performance curves into software was expected to be a major feature of the approach favoured for use with the SCADA package, in this present research.

3.4 General Fault Detection and Diagnosis

3.4.1 FDD Review Papers

The field of FDD is a wide and heavily researched area. In this review section a representative cross section of methods is presented along with applications which are related to the water industry or of relevance to this research.

Classical methods of fault detection involve the limit checking of a process variable as stated by Isermann [23], who goes on to explain that as this does not give a deeper understanding of the process, it does not facilitate fault diagnosis. As a result, model based methods have been adopted and in this paper Isermann summarises the widely used model based methods for fault detection, and then identification in general terms.

In an earlier paper Isermann et al [24] reviewed research trends in the application of model based fault detection and diagnosis to industrial processes between 1991 and 1995. It was found that approximately 50% of the process fault detection applications considered used a parameter estimation method to detect faults. Trends for fault identification were less clear but the growing application of neural networks and fuzzy logic was acknowledged.

Venkatasubramanian et al conducted a very thorough review and comparison of FDD methods used across industry in a series of three papers. The importance of the correct and increased application of FDD technology is explained, with reference to the industrial costs incurred, such as the 20 Billion dollars lost annually by the US petrochemical industry as a result of poor Abnormal Event Management (AEM).

In the first paper [25] of the series, the ten most desirable characteristics for a FDD system were listed and explained. Features considered included reliability, robustness, fast response and adaptability. It was noted that a single approach will not be able to fulfil all these criteria but that a good system will be a compromise between these factors. After this general series introduction the first paper goes on to review quantitative model based approaches. The approach of residuals was fully covered, where deviations, or residuals, of the measured process variables from the developed model can be used for FDD. The need for robust models in these residual techniques was discussed. The limitation of quantitative model techniques to applications involving non-linear systems was discussed.

In the second paper [26], a review of qualitative models and search strategies was undertaken. The technique for visual representation of fault analysis using so called Signed Digraphs was explained. Here a diagram was produced which had positively or negatively signed arcs connecting 'cause' and 'effect' nodes. Further adaptations of Signed Digraphs were then explored, as well as the concept of fault tree analysis. The

area of qualitative physics or common sense reasoning was discussed in detail. Strategies such as dividing processes into sub-systems to reduce complexity, by either structural or functional decomposition were explained. Finally, so called search techniques for fault diagnosis were explained and categorised into two approaches; Topographic methods that perform malfunction analysis using a template of normal operation and symptomatic searches which look for symptomatic signatures to direct the search towards a fault diagnosis.

The final paper [27] considers the use of historical process data. The extraction of important features from the data is discussed with reference to many of the techniques already outlined in the previous papers. In conclusion to the series, the lack of literature on real world industrial applications of diagnostic systems is highlighted, with commercial secrecy being cited as the potential cause of this. It was also pointed out that most researchers, particularly in academia, treat diagnosis and control as separate issues, despite their inherent link. It is asserted that the integration of the two is vital if real progress is to be made in the field. This proposition is embraced by work presented in Chapter 5 of this research. An increase in the ease of deployment and adaptability of systems is also put forward as a requirement for their increased uptake in industry. Improving the ease of deployment was a core driver for this research.

3.4.2 FDD Applications

A wide array of practical research has been undertaken applying FDD to industrial systems. Some pertinent examples from the wider literature are provided here, with further, more specific, examples relevant to the WRAP water treatment rig application reviewed in Chapter 4.

Zumoffen et al [28] developed and tested, through simulation, a highly involved fault detection, isolation and estimation system for a waste water treatment plant. Sensor and actuator faults were concentrated upon in particular but it was also stated that the methodologies outlined could be applied to diagnosing process faults. Process variables over a period of days were considered by the system to detect faults. Both fuzzy logic and neural network sub-systems were employed for model development and data analysis.

The eventual goal of the research was to provide a fault tolerant system by adjusting the PID loop parameters in real time to compensate for the diagnosed fault.

Xin et al [29] developed an expert system for a water treatment plant based on the capture of operator knowledge. It is stated that in the case of a water treatment plant, operators often rely on knowledge built up over many years of experience. Also, the decisions made may result from the co-operation of a number of experts including for example, operators, technicians and chemists. As a result of no single person having responsibility, the documenting and capture of this information was said to be quite poor. The researchers used an expert system shell to develop a prototype system. The prototype was populated using information gained in a number of interviews with plant staff. This approach is used in research presented in this thesis in the Coal Fired Power Station work in Chapter 7. The system was tested with operator comments being used to make modifications. During the testing it was found that even experienced operators benefited from using the system, as it provided a useful memory aid to the recall of correct procedures in the event of unusual occurrences. The system was not fully deployed to the extent of stand alone operation.

Grieu at al [30] developed a method of fault diagnosis for four faults in a water treatment plant, based on fuzzy logic. The system was embodied through the use of the Fuzzy Toolbox in Matlab and first developed on a simulated plant. The model was later verified on a waste water treatment plant for the City of Perpignan. The time scales involved were extended as some of the data used was only collected daily. For a full application of the method it was stated that additional online sensors would be required. In the author's opinion, this would increase installation cost and disruption; the use of extra sensors is avoided in the research approaches presented later in this thesis.

Chen et al [31] applied the Principal Component Analysis (PCA) approach to detecting faults in an air source heat pump, used for water heating and cooling in an office building. The PCA method involves the mathematical manipulation of process variables into fewer integrated variables termed the principal components. This is achieved by the eigenvalue decomposition of a matrix containing samples of original variables, taken during normal operation. Data obtained during a fault condition is then compared to these original principal components, via further mathematical means, to produce a measure of the error between the normal and abnormal data. The need for great care in choosing the amount of

training data for the PCA model is discussed, as data from too long a time period may contain natural fluctuations which will desensitise the model. In the particular case of the heat pump, only inlet and outlet temperatures for the water, refrigerant and air used by the system were considered. Faults were applied to the system by the partial blockage of the air inlet. The applied method was found to have a good degree of success in detecting fouling of the intake.

Cho et al [32] studied transient analysis for FDD in a Heating Ventilation and Air Conditioning (HVAC) system. Faults were created and responses tested in a climate controllable environmental test chamber. Residuals were used to detect and define single faults but for combined fault analysis, the residual development over time was considered. In the study, single faults were introduced in a temperature sensor, fan and damper actuator. Each of these faults was then tested in combination with a VAV damper controller fault. The VAV controller controls the dampers which regulate the air supply to rooms based on requirement. The VAV damper control faults were tested at normal, high and low gain settings, to mimic a poorly tuned controller. It was found that only by consideration of the transient development could the combined nature of the fault be deduced. Also, as the HVAC system took of the order of 60 minutes to reach a steady state following the development of a fault, it was stated that on-line fault diagnosis without consideration of recovery time would lead to erroneous results. This consideration was noted by the author of this thesis, as it was likely that extended transient behaviour would be present within the industrial water systems to be considered.

Thornhill [33] considered the root cause isolation of plant wide oscillations, in a complex industrial chemical process. Data on process variables, set points and controller outputs, pertaining to 15 control loops within the process, was available. The oscillation was detected by analysis of routine plant data stored in the database. Visual inspection showed the presence of an oscillation with a period of approximately two hours and this affected so many of the readings, that the phenomenon could be considered plant wide. Mathematical manipulation of data from similar amplitude points of the oscillation, using the nearest neighbour technique, was used to create a non linearity index. The loop with the highest non linearity index was considered the most likely root cause. This diagnosis was then confirmed by the application of existing process knowledge and a faulty valve was isolated as the root cause. This work illustrates the high level of variable and control

interrelation within industrial systems and the complexity of approach often required to solve problems that may not be immediately apparent to operators.

A range of FDD approaches is documented in this section of the review, ranging from implementations of neural networks, to the collection and application of operator knowledge. Of particular interest to this research, were the methods which were programmed to detect and identify faults from the signature which the variables produced under fault conditions. One of the aims of this thesis was to use readily available signals. As such, the signature analysis style of approach, if tailored to accommodate the limitations of the SCADA package, offered great potential. In many cases the research presented has used heuristic methods to first evaluate normal and abnormal plant states, before capturing this information in code, and utilising it in real time, to detect and characterise faults. The application of SCADA for fault diagnosis is suited to this style of approach as real time analysis of a complicated system, can be reduced to the simpler task of testing for deviations from the expected characteristics. The use of the results of offline neural network or PCA analysis approaches is also of interest. Using these approaches, the key variables and behaviours can potentially be outlined and simplified. For example the SCADA system database can provide historical plant data for use in the training phase of a neural network and then the key fault behaviours can potentially be simplified and encapsulated in the SCADA programming to give alerts. The use of Fuzzy Logic approaches may also be viable using SCADA. For example Grieu [30] utilise a list of condition based rules for the inference phase of the fuzzy decision process. This list style approach could be implemented using conditional executors within the SCADA software, such as the Case Select function of the Citect SCADA software (see Section 4.3.2) used in this thesis work.

3.5 Condition Based Control

Research papers in the field of condition based and adaptive control are numerous. A brief review is presented here, of research which compliments the style of approach used in this thesis, with further more specific examples presented in Chapter 5. In the context of this thesis condition based control is implemented as condition based monitoring, over a number of hours, which then triggers a system response if a pre-defined threshold is reached. The papers presented below tackle more complex or high frequency problems

and thus take a more involved approach. The papers are however of relevance to this research, as many of the techniques or approaches used may be of relevance to low frequency applications.

Bloch et al [34] considered the use of neural networks in industry and focused in part on the application of neural network techniques to a water treatment process. Particular attention was paid to the significance of selecting appropriate process variables to facilitate the training of the network. The possibility of training a network to behave like the inverse of a process, in order to then control the process, is also discussed. It is stated that the development of neural networks for control is often an 'excessively heavy task'. In the case study presented, a neural network is used to model the coagulation process in a water treatment plant, with the aim of optimising the amount of coagulant dosed to the system. The model is developed into a control algorithm and is designed to self teach, potentially allowing the wide spread low cost deployment of the system to other coagulation processes. One year's worth of data was used to train the model. A method was outlined for the detection and compensation of defective process sensor signals. Savings on coagulant chemical use were reported along with the intention to deploy the system on further sites. A key benefit of neural networks was put forward as their ability to capture unwritten empirical operator knowledge and utilise it electronically. The technology described does appear to have the potential to optimise non-linear systems and research in this field is potentially of great value. However, the complicated nature and heavy processing workload involved in the application of an on line, self teaching neural network, as put forward here by Bloch, may not lend itself to the more limited capabilities of a SCADA system.

Soyguder et al [35] presented an adaptive control approach, implemented on the dampers of a HVAC system, using fuzzy logic. It is stated that most HVAC systems exercise control based solely on the required room temperature, with humidity being left to find its own level. Fuzzy logic is used in this study to adaptively define the Proportional Integral Derivative (PID) loop parameters used to control two dampers, allowing the regulation of both temperature and humidity in the room. It is unclear from the paper whether the fuzzy calculation of PID parameters is actually achieved in real time, using the PLC, or if parameters pre-calculated using fuzzy logic were programmed into the PLC. The eventual

aim of the research was clearly, to develop an adaptive tuning of the HVAC PID loops to improve the performance of the system.

Tzoneva [36] implemented two methods of PID loop tuning for the control of dissolved oxygen in the aeration tank of an activated sludge water treatment process. It is stated that in most activated sludge plants SCADA systems are used. However, they are only ever utilised to monitor variables and never to realise advanced control of the process, based on environmental conditions and process dynamics. The fact that water treatment plants operate for very long periods, often with parameters only tuned once, is also discussed. The general ethos of the work was that adaptive tuning of PID parameters based on current dissolved oxygen levels, signs of impending disturbances and process dynamics would result in increased processed effluent quality and a reduction in costs. The functionality of the system was realised using a layered structure of hardware and software. The process signals were input to a PLC which also contained the PID control algorithm. Sitting above the PLC was the Adroit SCADA software. This had a communications link with a MySQL database which in turn had a communications link with Matlab software which was all hosted on a PC. Process data was displayed on the SCADA screen and also passed to the database. The user could select the tuning method to be used via the SCADA screen. The actual optimisation software was enacted within the Matlab environment and the resulting set point recommendations were sent to the SCADA via the database. At this point, the operator could compare the recommendations with the existing set points and choose to accept or decline the modifications. In the authors opinion, the use of Matlab for the execution of the optimisation algorithms and the resulting need for an intermediary database to facilitate communications, significantly increased system complexity requiring knowledge of both data basing and Matlab programming and potentially diminished robustness. However, the Matlab programming environment is very well suited to the development of optimisation strategies and did provided advantages to the developer.

Radhakrishnan [37] also considers optimisation using Matlab software. It is put forward that, in the particular case of a ball grinding mill, PLCs are capable of maintaining the process around desired set points. However, a supervisory level control system, based on a system model, is required to optimise the process as a whole. A model of the ball mill was constructed within Matlab, this was then used to identify the three key optimisation

parameters. This model was then used to develop an ideal response surface for these parameters, represented by a second order polynomial. This was then combined with an economic objective function to produce the optimisation building blocks. It is stated that the optimisation was tested using a simulation. It is presumed that the entire development and simulation took place within the Matlab environment. This work recognises the potential for turning SCADA collected data into real time information and action. The author of this thesis puts forward that the type of equations developed here, could be embedded in the coding of a modern SCADA package.

Cambrano et al [38] reported an approach for the optimal control of the City of Barcelona's urban drainage system. The system was comprised of a network of sewers which carried waste water and rain water to terminal locations, where it was treated and/or discharged into the environment. In high intensity rain events, the system could become inundated, leading to flooding or combined sewer overflows. The paper describes the first stage implementation of an advanced urban drainage approach. This involved the installation of large capacity detention tanks and the development of a predictive, adaptive control strategy, for the diversion of excess flow into these tanks. As part of the new strategy, some new telemetry was added to the existing SCADA system. This facilitated the addition of new rain sensors, as well as flow, level and water quality sensors in the sewer system. The new control strategy followed a global approach, where real time data from the whole water system was used to make system level decisions. This is said to differ from the local approach used in most urban drainage systems, where flow is regulated to set points based only on local data. The new control approach involved first mathematically modelling the drainage system using Matlab. Next a cost function was developed to act as the measure of optimality of the system. This equation was a mathematical expression of the main aims of the system; which were to prevent flooding, and minimise combined sewer overflows. The cost function penalised unwanted behaviour, such as positive deviations from design sewer flows. The combination of system modelling and the application of the cost function were used to develop a 30 minute prediction horizon of the expected system loading. This prediction was used to derive an optimal control strategy for the use of detention tanks, using real time data provided by the SCADA system. A simulation was conducted using historical data and the new approach was found to offer advantages. The application of the new control

approach was underway at the time the paper was published but no indication is given that the new software had been successfully integrated with the existing database.

Gao et al [39] presented a method for adaptive control learning. The aim of the approach was to identify the key parameters which should be altered by an adaptive control algorithm under different conditions, to optimise a given system. In the example used, the positional control of a large space antenna was considered. A cost function was utilised as the performance index based on the weighted sum of the root square error, the maximum error and the settling time. A simulation model of the antenna was built using C and a knowledge based system was applied to this using CxPERT, an expert system shell. To perform the analysis and learning, the Hooke and Jeeves search method was employed, to optimise the performance index, by altering all the available parameters. During this iterative process, a sensitivity analysis was conducted for each of the terms of the cost function at each stage. When the optimum performance solution was reached, the sensitivities were averaged over the steps and put into a database table. The testing of the system conducted proved that the system had the potential to define the most relevant control parameters and, then assign the optimum values to them.

In much of the condition based control and adaptive control work outlined, the inclusion of a performance index was at the core of the research. This was then often used to optimise the adaptive control by the minimisation of deviation from the ideal performance. This style of approach is suited to SCADA software functionality. However, the more computationally expensive and complicated approaches, such as the real time prediction horizon calculations used by Cambrano et al [38], may not be suited to implementation within SCADA software. Although this may not always be the case as SCADA processing power increases. The potential for automated condition based control to increase efficiency through optimisation was clear from the background research. This is explored explicitly in this thesis in Chapter 5 through work performed on back wash initiation in the WRAP filtration rig.

3.6 Efficiency and Performance Monitoring

This section considers efficiency and performance monitoring research. Examples illustrating general techniques that have been applied are presented. These examples come

from a range of industrial applications but are included as the concepts could be applied to industrial water infrastructure. Further examples, specifically pertaining to the work done at the coal fired power station, are reviewed at the start of Chapter 7.

Prasad et al [40] proposed a performance monitoring strategy for thermal power plant operations. The plant considered was a 200MW oil/gas fired station. Matlab Simulink was used to develop a plant model based on 14 first order nonlinear differential equations and 120 algebraic equations. Artificial noise signals, to mimic real plant conditions, were included in this thorough model. One important aspect of the performance monitoring approach discussed was the perceived importance of using actual best condition plant operating data, rather than original design data, to assess the deviation in the performance of the plant. It was stated that the plant personnel felt that the design performance was an unattainable goal. As a result, poor performance which was referenced against the design value did not create a real sense of urgency. A neural network approach was adopted, to discover the best condition plant operating benchmark, for the steam circuit. The work presented remained theoretical but the intention was stated to apply the findings to the plant, although no strategy was outlined. The use of modelling techniques, to evaluate the ideal performance, is a useful tool and if the results can be mathematically simplified the performance measures could potentially be implemented on SCADA software.

Studzinski [41] broadly described the use of monitoring techniques in environmental engineering, presenting three short case studies, where monitoring was used to develop models and maintain processes. Firstly, the application of computer based models to a waste water treatment plant was discussed. These models were used to support operator decision making, and were only made possible due to the availability of database technology. The second example considered a system used to support operational decision making in a communal water network. The system had modules dealing with modelling and optimisation, which communicated via a shared database, and provided information on expected water demand. Finally, the use of a neural network to predict ambient temperature, or to fill in gaps in the data caused by equipment failure, was briefly covered and reported to be successful.

Sardeshpande et al [42] considered an approach for the energy benchmarking of a complex industrial process, in the form of a glass furnace. The differences based on

process, scale of operations and age of plant are cited as examples of why formulating a uniform energy benchmarking approach can be difficult for industrial systems. Data from an analysis of 123 glass furnace operations around the world was presented, with the conclusion being drawn that even the best performing furnaces could be improved by modifications of design and operation. The researchers conducted a thorough analysis of all aspects of the glass furnace, and hence formulated mass and energy balance equations describing the behaviour of relevant sections of the furnace. A systematic review of all design and operational variables which could affect the model was presented. The model was developed in Matlab but a further version was developed in Excel, utilising Visual Basic Application coding to run the required iterations and produce a user interface. The second model was produced as a result of feedback from a workshop held with Indian glass industry officials. This demonstrates the extent to which software selection influences the uptake of research in industry, with well known industry standard packages always favoured. The final model produced a prediction of minimum possible energy consumption for a furnace based on design and operating parameters. A case study was presented where the model was also used for a parameter sensitivity analysis, which further aided process optimisation. The model was designed to be applicable to a wide variety of furnaces. It is stated that the approach could also be adopted for other industrial processes to provide a rational basis for target setting and energy performance improvement. It is suggested by the author of this thesis that the simplified outcomes of studies such as this, which indicate important process variable relationships and credible efficiency targets, can be embodied in the existing supervisory control infrastructure, to facilitate rapid operational improvement.

Kim et al [43] describe the application of a commercially available on-line, real time, performance monitoring system, to two combined cycle gas turbine power stations. The EfficiencyMap software, from General Electric, was chosen because it had been previously used in combined cycle gas turbine plants. The plants featured the Infi-90 DCS system, with each turbine in the plants having a separate DCS block. Plant data was fed from the regulatory level to PC buffer nodes, which acted as gateways onto the LAN, allowing data to be fed to the system server PC which hosted a real time database. The performance monitoring and optimisation software applied was connected to the real time database, which was vital for its operation. The author of this thesis asserts that many

plants will not have a sophisticated real time database, which would make the integration of this system highly complicated and expensive.

Before performance calculations were commenced, the software package first validated the data by checking that the variables agreed with the laws of conservation of mass and energy. This procedure was performed as it is stated that measured data can be subject to random and systematic error. Once the data was validated, the software predicted the expected performance of important plant parameters and then compared them with the real readings obtained. The prediction was facilitated by a plant model developed using proprietary code within the software. Another performance indicator, calculated by the software, was the corrected value of process variables which was found by correcting the current value back to a standard reference condition. This provided an indication of how the plant would be performing under the standard reference condition, which removes the current influence of load and ambient conditions. As a result, this value should not change over time unless the physical performance of the equipment changes. Therefore, a trend of corrected performance should form a horizontal line unless plant performance changes.

A number of examples are given of how the new performance monitoring was used. Corrected values of gas turbine power output were plotted before and after a plant overhaul and the expected increase in performance could be clearly seen as a rise in the horizontal data line. It was observed that plant operators and maintenance staff were now empowered. They could detect performance degradation quickly themselves, without recourse to consult plant technical staff, or review traditional plant test data. The new system also allowed the effect of operational changes to be assessed. In the example given the opening of the inlet guide vane to a turbine was modulated and trends of turbine power and unit efficiency were correlated with the degree of guide vane closure, indicating the optimum position. It was stated that the "Quicker identification of equipment performance change with respect to any changes of operation parameters resulted in improving overall plant capacity and efficiency". An optimum load allocation algorithm was also enacted. This indicated to operators what generation levels each of the turbines should be run at to achieve the required plant output. This decision was made based on the individual gas turbine heat rate for a given load. Over time the turbines were said to degrade differently, so choosing to run only the best turbines, when full capacity was not required, boosted efficiency. Overall, it was reported that the new system

produced an average improvement of 0.45% in the total efficiency of the two plants. This was significant as the combined output of the plants was 3800MW.

The importance of correctly selecting performance measures came through strongly in a number of the papers reported in this section. The concepts of referring current performance back to expected performance, or to baseline performance, were both discussed in the papers. The rationale used to present efficiency data to operators is a matter explicitly covered in Chapter 7 of this thesis, with reference to the coal fired power station work presented.

3.7 Commercial Monitoring and Control Systems Review

3.7.1 Section Introduction

Before the decision was made to concentrate solely on the application of the SCADA package, a background review of monitoring and control devices which could work alongside the SCADA system was conducted, to assess if they offered any distinct advantage. A consideration of how well they could be integrated into a modern industrial infrastructure and an assessment of their processing capabilities and potential for higher level application was undertaken.

3.7.2 Retrofittable Monitoring and Control Systems

The Red Lion Data Station Plus [44] is designed specifically to address the difficulties of integrating a data acquisition system into a legacy industrial control framework. The system claims to have a wide range of servers for data mapping to PLCs, PCs and SCADA systems. The Ethernet port can communicate in four Ethernet protocols simultaneously and the system also features two RS232 ports and an RS422/485 port for communication with legacy equipment. Upgrade cards are available to allow communications using CANopen, Devicenet and Profibus. Historical data is held in a Comma Separated Variable (CSV) format, for manipulation by programmes such as Excel. The unit has an embedded web server, which can support a configurable HMI screen, displaying dynamic content. This can be accessed using a standard web browser, without the need for proprietary software. The system is also capable of supporting an

independent threshold based alarm strategy. It appeared that the programming facilities offered could not accommodate the level of sophistication required for this research, as configuration was achieved using a simple scripted language. This would mean the code would be bulky and inefficient for more complicated tasks. The lack of procedural call functionality in the scripted language would also reduce execution time.

The ACT'L eWON system [45] is based around an embedded web server, which can be configured using the BASIC language, to provide historical data trending and process mimic screens with dynamic content. These can be viewed using a standard web browser and no proprietary software is required on the end users computer. The unit is Ethernet enabled and can export data directly to a remote user via an optional PSTN, GSM/GPRS or ISDN modem. The Unit can have its own alarming capability, independent of the alarm strategy incorporated by the control device. This includes thresholds, dead-bands and optional activation delays. A remote user can receive alarm notification via SMS or email which can be programmed to automatically include attached data logs for a time running up to the fault.

Local data acquisition, from the control device, can be accomplished via the Ethernet or Serial port on the eWON. The company supports a number of servers which are compatible with many of the top PLCs. Once data is retrieved from the PLC memory map by the server, a user defined tag database links data streams in the server to the required elements on the GUI or process mimic software, held on the embedded web server. This tag system is analogous to that used for linking data from an OPC server to an OPC client. However, the servers used to connect a PLC to the eWON do not comply with OPC standards. They are designed singly to interface with the eWON as a client, rather than being compatible with the full range of OPC clients available. This appeared to be a capable device which had the potential to apply higher level functionality, using the BASIC language format. However, this device and the previous Data Station Plus device both sit between the PLC and SCADA package, which diminishes the robustness of the system by adding an extra data conduit which could potentially malfunction.

The MSL Dataweb [46] is designed to acquire signals directly from the sensor, or alternatively, obtain signals that are retransmitted from a control device. The user can connect to the device via Ethernet or RS232 interface. A remote user can access real time

point data, or historical CSV files, via a server hosted by the company. Data is transmitted from the unit to the company server via GPRS or PSTN connection. The basic package offers no inbuilt data trending or process mimic capability. However, it is possible to purchase SCADA software named Orchestrator. This can display trend graphs, mimic screens and has a degree of programmable data manipulation functionality. The software can also act as an OPC client, so that information from legacy equipment with an OPC server can be added to data coming from the Dataweb unit. This solution is offered as a service for the management of distributed assets. A monthly fee is required and the system is essentially stand alone, and not designed to be integrated with an industrial SCADA package.

The Nortech NX-30 [47] System can acquire both analogue and digital input signals for monitoring, and has 8 digital outputs for control. A sub-board is available providing the ability to monitor opto-isolated inputs. The system has been designed to allow the user to integrate it as a separate monitoring layer, above any existing control hardware. Input signals used by the control device can be acquired and monitored without alterations to the existing control framework. A further indication of the retrofit ability of the system is the fact that it will accept digital inputs from volt free (dry) contact sets, providing its own wetting current from within the unit. The wetting current is the minimum current needed to flow through a newly closed mechanical switch or relay, in order to overcome any oxidation which may have occurred on the contacts while open. Nortech offer the "i-Host Platform" software for use with the NX-30. This server can be accessed using a standard web browser. Data is transmitted to the server via GSM network, Ethernet or serial connection. The server provides a human interface which gives information on alarms and provides historical trending. The system does not support procedural programming code and is designed as a passive monitoring and alarming system.

The Powelectrics IN4MA GSM RTU [48] communicates data from the field in GPRS format, over the 900 and 1800 GSM network, to the "Gateway" server hosted by Powelectrics. The unit can take up to sixteen analogue inputs and has an analogue and digital output capability. Alarm thresholds can be programmed, which trigger email alerts, via the "Gateway" server or direct SMS text alerts to customer mobiles. The "Gateway" server can be accessed via the web by customers. The data can be viewed in interactive charts or downloaded in CSV format. The system can be remotely configured via the

website using a product specific scripted language. The unit does feature an RS-232 port for communication with serial enabled devices but does not have an Ethernet port. The system is not well equipped for integration into a modern large scale industrial site. The unit appears to be aimed more towards smaller stand alone sites.

The Sentry GSM3D Multi [49] is a GSM enabled device which allows the monitoring and control of eleven I/O ports. Data is transmitted from the device via SMS or GPRS. Alarms, data and status information can be sent to up to 120 individual mobiles via SMS. The four digital outputs can be used for relay control autonomously, as a result of a change of input state, or via SMS message from the user. The device has an RS232 port for communication with a PLC or HMI. Historical data held in the PLC memory map can be accessed and reported. The unit can be remotely configured using Windows based software. The Sentry GSM3D Logger [50] Utilises the same communications framework as the Multi but fulfils a metering role. It has one MB of internal non-volatile memory allowing data from the ten digital input and two analogue input ports to be logged and periodically downloaded to a server. This can generate an email to the customer or be accessed directly via the web. Neither device supports Ethernet or any industrial sensing and control protocols such as Profibus or Modbus. They are intended for remote monitoring purposes rather than large industrial applications.

The IPC systems i-LOG EDM [51] will support a wireless, PSTN or GSM/GPRS modem using Hayes commands, which are more commonly referred to as AT commands. The system can log four analogue and four digital inputs and has two digital relay outputs. These can be controlled remotely by the user or triggered automatically in the event of an alarm. The unit can support Internet communications and has two active web pages held on an internal server. There is a non-volatile memory which is capable of holding 40000 channel logs. Data and recorded events can be downloaded via email. The digital relay outputs provide scope to allow the unit to trigger visual or audio alarms in the event that a programmed threshold is breached. The i-LOG EDM is ideally intended for stand alone metering applications.

The range of products available, illustrates that there is a high demand for stand alone monitoring and control systems that are capable of integrating with a variety of legacy

equipment. Some systems are designed purely to use Ethernet and serial protocols to obtain data, while others have the added capability of their own analogue and digital inputs and outputs, for limited control. Their use to apply more advanced efficiency strategies and monitoring to industrial cooling water infrastructure could offer benefits. A generic system developed using one of these technologies could be implemented at many sites, with the code of the core algorithms created, remaining unchanged. Also, many of the systems offer the potential for remote operation. This could allow a third party expert water consultancy company to liberate efficiency activity from, the less specialised plant operators. Integrating these add-on systems at an existing plant would however, present significant data communication challenges at every installation. As discussed, there was also the potential for these systems to undermine the robustness of the existing communications structure. On reflection, it was decided that the pre-existing, on site SCADA package, would provide the most integrated and wide spread opportunity to improve plant efficiency. Also, as SCADA software is an industrially recognised product group, its advanced application offered broader opportunities for the findings of this research to be practically applied, than if a lesser known product were utilised.

3.7.3 Specialised Monitoring and Control Devices

There are a number of industry specific monitoring and control devices available with limited programmability but which already contain powerful and configurable task specific functions. Two such devices, which are directed at the industrial water market, are included here as a representation of the state of the art of this technology.

Pulsar offers a range of water utility system monitoring and control equipment. Of particular note is the Zenith 140 Pump Station Controller [52], which is designed specifically to reduce costs, and improve the monitoring and management of pumping stations on the mains water network. The unit can be connected to various modems using AT commands via the RS232 port and can also support Modbus and Profibus.

The system has a variety of task specific, pre-programmed functions; for example the "Tariff Guard" function can be set to fill the station well, using the pumps, at off peak electricity periods. The well can be set to fill to a different height each cycle to prevent a ring, of surface solids, building up around the edge. Data logging is available via the

addition of an EEPROM upgrade card. Data is delivered in CSV format. Software is available which provides trend graphs and will also automatically arrange data into the reporting format required by the UK Environment Agency. The addition of a more capable control and monitoring system to all pumping stations on the network has a variety of benefits. Logging of flow rates can allow the development of a detailed loading profile for the network. This can aid in planning for storm events and, pinpointing overloading, which may be caused by the needs of a new building development, for example. As utility companies reduce the number of operatives on the ground, this level of monitoring is becoming vital to the functionality of the mains water system.

The Walchem Web Master One [53] is a controller used extensively for the chemical dosing and control of cooling towers, boilers and other industrial water systems. The various incarnations come equipped with a set of sensors suited to the intended application, such as conductivity, pH and Oxidation Reduction Potential (ORP). An upgrade card can also provide an extra eight digital and nine analogue inputs. The unit also has eight digital outputs for control and can be upgraded to provide four analogue outputs, which could be used to allow variable speed control of a pump via an inverter, or to retransmit a signal should the requirement arise.

The unit is Ethernet enabled and can support Modbus TCP/IP, facilitating connection to many available SCADA systems. The unit can be connected to a land line or GSM modem and, multiple units can utilise the same modem, which is connected to the master controller, if they are configured as slaves on an Ethernet LAN. The Internet communications system is based around the patented "Shoulder Tap" technology. This was designed to allow access to the embedded web server, without the need for a permanent Internet connection. The user logs into the Walchem website and enters the phone number of the required controller. The server sends a request to the webmaster, which then dials up the local Internet Service Provider (ISP), and logs on to the Internet. The user is then connected to the Web Master where a controller specific ID and pass is requested. The server provides real time dynamic data in tabular format.

These two task specific devices are capable solutions to the problem of controlling specific water infrastructure tasks. However, particularly in the case of the Walchem device, they can lead to a higher degree of monitoring and control strategy segmentation,

if not fully integrated with the existing site SCADA system. This is in contrast to the concept of increased integration at the core of this research.

3.8 Commercial SCADA and DCS System Review

There are a range of SCADA and DCS software packages on the market. A selection of the most well recognised and accepted products, which it was felt had the functionality to enact higher level integrated efficiency activity, is presented.

Wonderware offer a highly modular range of software products with an open architecture [54]. An overall SCADA package is built by system integrators, for a particular installation, by the combination of relevant modules. The highly open architecture is put forward as a major selling point of the software. As well as providing drivers for the leading PLCs, the company also has a partnership with Kepware. Kepware is a leading force in the development of industrial hardware communications software, in particular OPC servers. Although a proprietary historian data basing package is offered, the software is also capable of communicating with an SQL database.

GE Fanuc offer an open architecture SCADA package called iFix [55]. The software contains drivers for most major PLC brands and is also an OPC client, allowing connection to field devices via a third party OPC server. The package comes complete with built-in historian and alarm handling. The software can utilise the Visual Basic programming language for configuration. Specific add-ons are also available aimed at the water and power industry. A web client is available which is designed to integrate seamlessly with the developed SCADA, providing a secure web portal for external access.

ABB has a SCADA style offering called Extended Automation System 800xA [56]. The system claims to have an open architecture and supports OPC, Profibus, Foundation Fieldbus and the Hart device management system. One unusual aspect of the software is the in-house, patented, Aspect Object Technology. This allows the linking of documentation such as point listings, engineering drawings and safety information to a specific physical item such as a pump or controller, represented on screen. This is potentially of high value in a large plant, where generations of modification, and a lack of continuity in archiving, can lead to highly inefficient maintenance and upgrade activity.

ABB concentrate mainly on the power industry. They offer a wide range of hardware devices such as PLCs. Although the software has an open architecture, it is likely to be optimised for use with own brand hardware.

The Siemens SCADA offering is called WinCC [57] and is widely used process visualisation software in industry. It offers all the standard functionality such as alarming and trending. All software for connection to the range of Siemens controllers comes as standard and once again, in the move towards open architecture, protocols such as Allen Bradley Ethernet IP, Modbus TCP/IP and Profinet are supported. No drivers for non Siemens controllers are provided but the software is fully OPC compliant, meaning that if the correct OPC server is available, all field devices from other manufacturers can be communicated with. This reliance on OPC, as the main conduit for cross manufacturer hardware communications, differs from the approach of other open architecture SCADA providers, such as Citect and Wonderware. These companies include drivers for all major PLC brands as part of the software suite. Data archiving is achieved through the use of a Microsoft SQL server. Detailed configuration is achieved via a proprietary scripting language.

Siemens also offers an integrated DCS called SINAUT, for geographically distributed assets, such as found in the waste water industry. The software and hardware including controllers and various modems are proprietary Siemens products. For less demanding systems the SINAUT Micro architecture is used which is based on the WinCC or WinCC Flexible interface, using the S7-200 PLC for field control and GPRS WAN communications. For larger more complex systems SINAUT ST7 is based on WinCC or PCS7 using the SIMATIC S7-300 and S7-400 for field control. All forms of WAN communications are supported, with Siemens modems available for all except radio communications. Both the solutions come complete with OPC server software, which allows the hardware to communicate with third party OPC clients, such as SCADA software from other vendors. This highlights the ever increasing industry desire for flexibility, in that, even a largely proprietary product from a market giant, presented mainly as a turn key solution, still has the capacity to interface with third party software. This move prevents the alienation of potential customer sites that already have a commitment to a certain SCADA package from a different supplier.

Rockwell Automation offers a manufacturing targeted SCADA package called Factory Talk [58]. Emphasis is placed on increased integration of the SCADA level with the enterprise software level. Communications is provided with Rockwell's own Logix controllers and interoperability with other brands of controllers is also stated to be possible. The range of products is highly modular with specific packages for areas such as display, communications and specific manufacturing tasks, like batch production control and scheduling.

Trend is a major player in the European HVAC control market. The company offers a PC based client/server software for control and interrogation of remote devices [59]. This can communicate, via Ethernet, directly with Trend control devices, non proprietary variable speed drives that are Ethernet/ TCP/IP enabled, or Ethernet routers which provide access to sub-networks of Trend controllers. Trend sub-networks communicate via a proprietary RS232 protocol. All devices on the network have equal status. A controller receives all network data but only acts upon that which pertains to it. The data address frame has dual levels. An instruction can be addressed to an individual controller or addressed to all the controllers in a particular group. The Trend system offers much of the same functionality as a SCADA package.

3.9 Chapter Summary

In the literature review of SCADA research in Section 3.2, the potential for utilising the plant encompassing, data gathering, capability of the SCADA implementations was clearly recognised by researchers. However, it was shown that little research had been conducted on utilising the full functionality of the SCADA package. This is believed to be the case as in the papers presented the researchers had used the software best suited to their applications. For example, Sardeshpande et al [42] had chosen to use Matlab to conduct their research. However, after industry feedback the model was then implemented on Excel, despite this not being the ideal software, as this is the industry standard. This example encapsulates one of the key drivers behind this thesis, which is the value of making research methodologies readily applicable to the industries they are designed for.

Most research relied on the integration of add-on software packages. The FDD review in Section 3.4 revealed that work had been undertaken utilising available process signals and that a number of the less computationally expensive strategies could have potential for

application using a SCADA package. In the condition based control and efficiency monitoring research reviewed in Section 3.5, it was found that the use of performance indicators, such as cost functions, were applicable for control optimisation. The presentation of performance data, contextualised with referenced to ideal and benchmark performance was of importance in efficiency monitoring. In both cases, heuristic system models could be used to define system targets and it is suggested by the author that these targets would form the ideal data for assimilation into a SCADA package configuration. The use of complicated online plant models, for real time calculation of control targets, was felt to be beyond the sensible scope of SCADA functionality.

A review of commercially available retrofitable monitoring systems revealed that there was a large demand for retrofit equipment within industry. However, due to the limitations of these systems and the difficulty of integration, it was concluded that the use of the existing SCADA system offered potential for meaningful research. A review of a number of leading SCADA software packages confirmed that such systems had the potential to be programmed for efficiency monitoring and optimisation tasks.

3.10 Conclusion

Based on the background research into industrial SCADA implementations, presented in Chapter 2, and the review of academic work and commercially available products in this chapter, it was decided that research into the extended application of SCADA would produce a high value contribution to the research knowledge base. The use of SCADA, for the implementation of efficiency tasks at existing plants, was believed to have significant advantages over other options, in terms of ease of integration, cost, system maintenance and safety. The encapsulation of research based techniques within a trusted industrial product, already in place at the industrial site, vastly broadened the practical relevance of the work, thus offering the potential to positively change research thinking and practice. In order to discover if non-time critical, low frequency, algorithms suitable for SCADA software could be effectively used for efficiency activity, so answering the main question of the thesis, attention was first turned to the water filtration side of industrial water infrastructure. The first implementation of the SCADA software is presented in the next chapter.

Chapter 4

Filtration Plant Single Blockage Location Diagnostic

4.1 Introduction

4.1.1 Context

The first experimental application of non-time critical low frequency algorithms embedded in SCADA software is presented in this chapter. The work in this and the next two chapters is focussed on the WRAP water filtration plant. This plant could form an integral part of the industrial water infrastructure considered in this thesis, as highlighted in Figure 4.1.

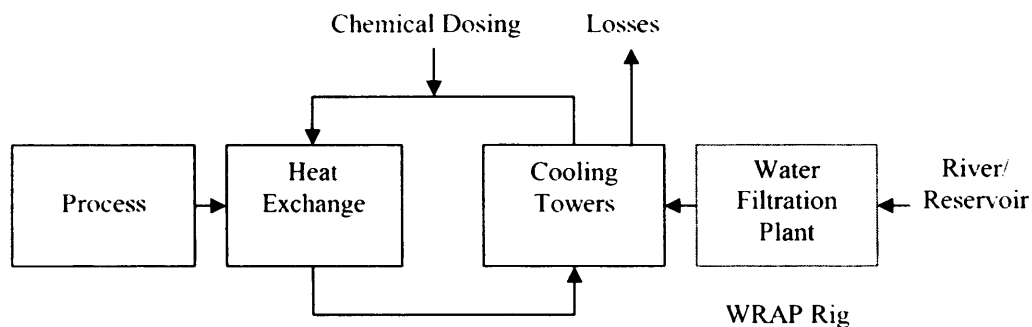


Figure 4.1: Simplified representation of the cooling water infrastructure in a generalised large scale industrial process with water filtration plant highlighted.

4.1.2 Ideal System

A Failure Modes and Effects Analysis (FMEA), conducted by the author on the WRAP Rig, resulted in highest scores for pipe blockage and fouled filter bed occurrences. This FMEA was based on the methodology set out by the Ford Motor Company FMEA manual [60], and is provided as Appendix A. Both these occurrences could lead to damage and reduce operational efficiency. Thus it was considered that an ideal water filtration efficiency system would possess the following capabilities;

- The ability to diagnose pipe restriction, preventing permanent damage and directing remedial maintenance activity.
- The ability to trigger backwash of the filter beds based on condition, thus reducing power consumption and water use.

These requirements and their justification are discussed in more detail in the relevant chapters. This chapter presents work focussed on the diagnosis of pipe restrictions, fulfilling the first criteria of an ideal system. The following two chapters present work focussed on robust condition based control of filter backwash process, thus fulfilling the second criteria.

4.1.3 Chapter Structure

This chapter considers the problem of pipe blockage diagnosis. It gives a detailed description of the WRAP water treatment rig and the experimental electronic hardware and software configuration used. A brief literature review of the previous research done by others on blockage detection and location is also included. The extensive testing of the WRAP system response to varying levels of pre and post-pump valve closure is summarised and the development of the first Blockage Location Diagnostic programme, implemented using the SCADA-based code, is explained.

The later part of the chapter describes the necessary remedial modifications that were made to the developed programme, as a result of the discovery that the pump was suffering from an internal blockage, during the first stage of experimentation. This blockage took the form of a piece of transparent sticking tape wrapped around the pump impellor. This fault had altered the system characteristics. The performance of the modified programme is described and an explanation of the full execution strategy of the diagnostic is presented.

4.1.4 Importance of Blockage Diagnosis

Blockage diagnosis was considered a problem worthy of investigation as restrictions of the inlet or outlet pipe work are two of the four main pump fault conditions [61]. The

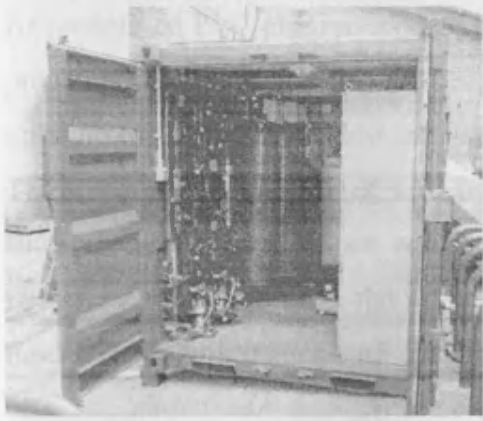
detection and management of abnormal events such as these has become increasingly relevant in the drive to improve industrial plant efficiency [25]. Pipe blockage also accrued one of the highest scores in the FMEA conducted by the author on the WRAP filtration rig, supplied by the company partner, as presented in Appendix A.

It is desirable to know the location and severity of a pipe blockage relative to the pump. In the WRAP Rig, for example, a pre-pump blockage could starve the pump of fluid potentially leading to permanent cavitation damage. A post-pump blockage, while effecting plant efficiency, will normally cause no damage to the pump. An understanding of the location of the blockage allows an abnormal blockage, or valve closure event, to be more effectively managed. This information may also be an aid to maintenance efficiency: if the attending technicians know the location of the blockage they can quickly remedy the problem. If the location is not known, a time consuming systematic dismantling of the pipe work is often the only option.

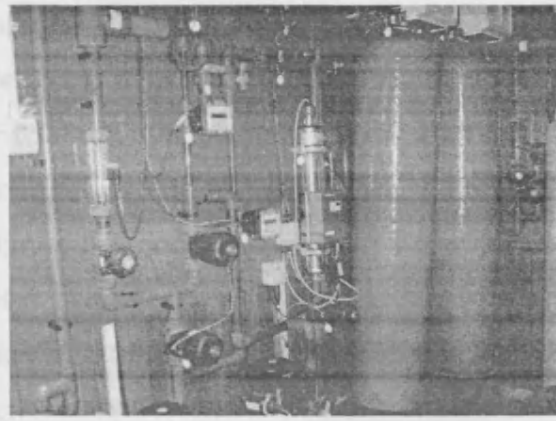
4.2 WRAP Rig Description

The WRAP Rig is a mobile filtration demonstration platform, one of three designed and manufactured by the company partner, Water Development Services. The system was designed to allow a direct performance comparison between two differing types of filtration media, as they process effluent from a single source and also to showcase the company's engineering prowess. Specifically the rig was used to show the performance of Recycled Glass Media (RGM) compared to a conventional filtration media such as sand.

The system, which was housed in a small sized shipping container, can be seen in Figure 4.2, and could be transported to demonstration sites where effluent was pumped directly into the unit. The rig utilised in this research was recently used to process wash down water from a dairy production line, similar rigs were used for varying applications such as the removal of bio fouling and bird excrement from nature reserve reservoirs.



(a) Outside view



(b) Inside view of filters and piping

Figure 4.2: The WRAP water filtration rig.

The piping and instrumentation diagram of the rig is included as Appendix B and the full functionality of the rig is described here for completeness, although only one of the filter subsystems was used. For the purposes of the experiments the external pump, P1, was disconnected as no external open reservoir existed. Pumps P2 and P3 (Grundfos CRI3) delivered unprocessed liquor from the external tank T1 to filters F1 and F2 respectively. The valves V8, V9 and V10 could be used to alter this relationship for operational flexibility. The PLC controlled, pneumatically actuated, diaphragm valves VA5A and VA5B were used to select flow from either of the unprocessed effluent streams entering F1 or F2 for analysis by the suspended solids analyser SS1. (Note; the ion specific analyser IS1 is no longer fitted to the rig). The flow rate into each filter was maintained at a pre-programmed set point by a PID loop. The analogue signals from the flow transmitters FT1 and FT2 (Burkert 8045 MID) were manipulated via the PID loop algorithm by the PLC to provide a 0-10V output to the invertors (Toshiba VF-S11), which controlled pumps P2 and P3. Thus, the speed of the pumps was controlled to maintain the desired flow rate into the filters.

Following filtration the liquor from F1 and F2 was passed through the UV sterilisers UV1 and UV2 respectively. The PLC controlled valves VA6A to VA6D were used during automated control to select which processed liquor stream was fed to the second suspended solids analyser SS2. (Note; the ion specific analyser IS2 is no longer fitted to the rig). Processed liquor is finally deposited into tank T2.

At predefined PLC programmed service intervals, the filter beds were backwashed using processed liquor from tank T2. This was delivered by pump P4, controlled by a PID loop utilising the signal from flow transmitter FT3, to maintain a desired backwash flow rate. The software was configured so that only one filter could be backwashed at a time. If the filter service interval of one bed ended during the backwash cycle of the other bed, it remained in service until the other bed had been backwashed and returned to service mode. The required backwash cycle was then initiated by the PLC.

The rig was installed with an air blower AB1, which could be used during the backwash cycle to agitate the compacted bed. The access of unprocessed liquor, backwash water or air into filters F1 and F2 was controlled by backwash controllers BWC1 and BWC2 respectively. The backwash controllers featured an electromechanically operated three way valve. This was operated by a timer cycle triggered by the PLC at the start of a backwash cycle. This valve opened for a mechanically programmed set time interval allowing backwash flow from P4 and then air flow from AB1, before returning to the service position. The PLC control strategy utilised these time windows to run the backwash pump and air blower.

For convenience in this research, as no effluent was to be used, the overflow from the processed liquor tank T2 was connected to the unprocessed liquor tank T1. This created a self contained system that operated by re-circulating clean water. The beds were thoroughly backwashed to drain before experimentation began, to ensure the filter media was clean. The backwash discharge was then connected to T1 to maintain the water volume in the system during the actual testing.

The system was controlled by two Cylon UC32.24 PLCs [62], networked using a proprietary serial protocol. These in turn were networked to a communications module which contained a GSM modem and two RS232 ports for providing the connection to external devices. Chemwatch [62], Cylon's proprietary SCADA system, was used for the original operation of the rig. The system was configured to display two process mimic screens that showed real time values of the various sensor readings. A number of alarm and control screens were also present, allowing an appropriately privileged operator to alter alarm thresholds, control parameters and to manually override system components such as pumps.

4.3 Electronic Hardware and Software - Experimental Set Up

4.3.1 Open Process Control (OPC)

It was decided to use OPC software to facilitate communications between the chosen SCADA software and the PLC. OPC has been at the forefront of the move towards a fully open SCADA system architecture. Object Linking and Embedding (OLE) was the precursor of OPC and was developed to overcome the need for hardware drivers, such as printer drivers, to be written for each new software item created. By defining a standard interface, Microsoft enabled the hardware manufacturers to develop only a single OLE server for their equipment. The software, which required access to the hardware, simply conformed to the framework, producing a compatible OLE client for the server. The potential of this technology for improving the interoperability of hardware and software within industry soon became apparent, leading to the development of OPC and the creation of the OPC Foundation [63] to regulate and define OPC standards.

The first defined standard was OPC Data Access (OPCDA) which provided a format for real time data exchange. Since then further standards have followed, such as OPC Alarms and Events (OPC A&E) and OPC Historical Data Access (OPC HAD). These are to be usurped by the OPC Unified Architecture (OPCUA). The OPCUA standard is designed to allow the technology to function with software other than Windows based applications and to bring the existing specifications under one umbrella. The original OPC was based on the Component Object Model (COM) standard. This is becoming less used by Microsoft in favour of cross platform standards such as Web Services and Service Orientated Architecture (SOA). This development is also addressed by the OPCUA standard.

Operationally, if an OPC server is available for a hardware item, it will be installed on a PC in the Master Station. Any OPC compatible client software, such as the SCADA package, can then exchange data with the device via the server. In configuration terms the tags, which are identifiers placed on each process signal in the SCADA client, are linked to corresponding tags in the OPC server. These are interfaced to specific addresses in the PLC memory providing a simple to use interoperability solution.

4.3.2 Citect

The Citect SCADA software [64] was chosen as the generic software for experimental use in this work. Citect is an Australian company founded in 1973, which was taken over by the Schneider Electric Group in 2006. It is a major software developer in the global SCADA market and Citect software can be found in all major industrial and manufacturing fields. As well as offering technical site installation and integration services, the company also offers an overall package called Professional Services. This involves consideration of the business goals of the client and cultural change management to achieve all possible benefits during the operational phase of project life cycle. This reflects the fact that optimisation systems, no matter how good, will not bring about improvements if business and operational processes are not adjusted accordingly.

At the same level as the SCADA software, Citect also offers the Facilities software designed for the management of property. A top level package called Ampla, which utilises data from the SCADA and/or Facilities software, is also available. This Manufacturing Execution System (MES) software supports the implementation of continuous improvement methodologies such as Lean and Six Sigma. This allows the efficient management and presentation of the large volumes of information which these approaches generate.

Citect SCADA is currently on version 7.1 and offers an extensive range of proprietary drivers for communications with field devices from numerous manufacturers. Citect is also an OPC Foundation partner. As such there is an option to use separately acquired OPC drivers as a means of communication with external devices, as was the case in this research.

Citect SCADA allows the integration engineer to design dynamic process mimic pages. Multiple digital or threshold triggered analogue alarms can be configured and are displayed, prioritised and handled by the operator via an alarm page. A GUI is also available which can trend up to eight selected process variables simultaneously. A higher level GUI also exists which combines selected events and alarms with trend data to provide an annotated plot.

Much of the basic design of these functions is achieved by configuration windows containing check boxes. However, more advanced configuration is achieved via the use of the proprietary procedural Cicode programming language. Cicode code can be used in the configuration windows for minor operations. However, for more complex programmes, a Cicode Integrated Development Environment (IDE) is provided within the Citect configuration Environment. Citect variable tags can be used directly by Cicode functions. The Cicode language was included in Citect to allow complex configurations and flexibility. A form of the Visual Basic language called CitectVBA is also supported.

Citect was an ideal choice for this research due to its commitment to an open architecture approach. Part of the remit of the research and company partner aims, was to assess how optimisation systems could be applied to sites which demanded a certain brand of PLC, or contained a variety of legacy systems. The range of drivers offered and the OPC compliance of the software lent itself to this task. Other benefits were the potential for twenty four hour phone support and UK based training courses. The application of Citect SCADA in a variety of industries globally and the affiliation with the giant Schneider Group guaranteed mainstream acceptance.

4.3.3 Description of Experimental Set Up

The Cylon PLCs, used to control the rig, were more usually implemented as part of a building management system and are not widely known or accepted within the process industry. The company partner expressed a desire to focus on a more widely accepted PLC. The Siemens S7-200 was chosen as the PLC for use in this research due to its general acceptance and low cost. It was judged to be impractical to remove the Cylon PLC and replace with an S7-200, as this would have required the extensive plant automation programming to be recreated on the Siemens PLC. Instead the system was configured so that relevant process signals were 'piggy backed' from the Cylon by the S7-200 as represented in Figure 4.3. The figure confirms the use of only one of the two available filter beds and provides a simplified schematic diagram, compared to the piping and instrumentation diagram of Appendix B.

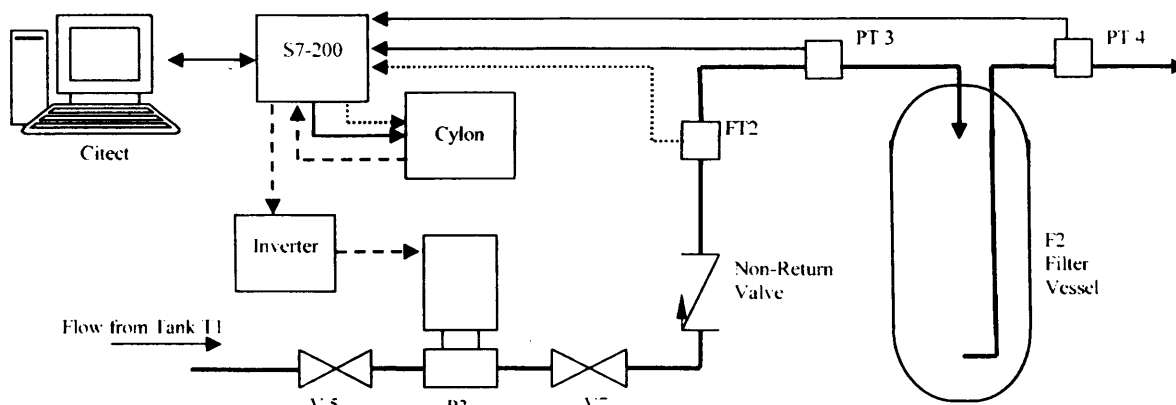


Figure 4.3: Experimental electronic connection on the filter 2 sub system in the WRAP rig

The pressure transducer PT3 and flow transmitter FT2 sensor signals (4-20mA) were 'piggy backed' by running the signal cables into the S7-200 analogue inputs. These same terminals were then wired to the analogue inputs of the Cylon. This allowed the S7-200 to measure the process variable signal on its way to the controlling Cylon PLC. It was confirmed that this had no effect on the value transmitted to the Cylon PLC. The 0-10V speed request signal, from the Cylon to the inverter, was taken into an analogue input and retransmitted to an analogue output terminal on the S7-200 which was wired to the inverter. To allow the manual control of the speed request, an override button was configured on the Citect mimic screen which toggled a digital tag. In the manual speed request mode, this tag was switched off which altered the S7-200 programme, substituting the retransmitted Cylon speed request value for an on screen value, set by the operator using the Citect interface. The Citect software and S7-200 PC Access OPC server software were both hosted on the same PC. The Citect software communicated with the OPC server, which in turn communicated with the PLC over a Siemens RS232 PC/PPI Multimaster cable.

4.4 Blockage Detection and Location Literature Review

Blockage detection and location diagnosis could be of importance in a number of sectors. Various methods have been developed by researchers in order to achieve such procedures. A relevant cross-section of current research is presented in this section. This review helped to formulate the approach taken in this thesis and is presented in addition to the review in Chapter 3 in order to give a perspective to the work undertaken in this chapter.

Higham et al [61] assert that probably half of all measurements made in the process industry are of pressure and flow. These were two signals readily available in the WRAP Rig. They present a method for distinguishing between what they call the four important operational fault conditions in a pump, using information gained from analysis of pressure and flow in the system. They identify the four key pump fault conditions as obstruction of the inlet, obstruction of the outlet, damage to the impeller and 'tank run dry'. Their method centres around the analysis of the noise component of the mA signal received from the pressure and flow transmitters. In operational applications this noise, which is defined as any part of the signal with a frequency above 5Hz, is filtered out to give a steady reading for the controller to utilise. The paper states that by examining this noise component, rather than discarding it, it is feasible to identify the type of fault on a pump, as well the severity of the fault, using the frequency spectra analysis. The importance of studying the operational characteristics of the plant, in order to distinguish them from a fault condition, is also discussed.

Parrondo et al [65] looked specifically at the diagnosis of cavitation and pump inlet blockages of a centrifugal pump using pressure and vibration responses. The addition of the fluid transient behaviour to the natural behaviour of the pump was put forward as one of the biggest problems in pump fault diagnostics. They concluded that as a result of the complexity, no generic fault diagnostic could be developed for pumps. In their approach the pressure response was captured at the pump inlet and outlet and the vibration was recorded by accelerometers attached to the pump casing. The variables were measured with a sample frequency of 400Hz. Using a frequency component analysis, at four frequencies for each fault tested, a fault library was created. It was found that this approach was effective when using the pressure response but that the vibration response was not clear enough due to noise generated by other structures mechanically coupled to the pump. In the context of this research it should be noted that this style of fault diagnosis requires the addition of sensors to the system.

Wang et al [66] described a method for the detection and location of partial pipe blockages. They consider that the development of blockages in the energy, chemical and water industry is a common problem. They cite the possible causes as localised chemical or physical deposition or erroneous valve closures. Their method was first developed

mathematically by consideration of the governing equations for pipe flow and orifice plates. A simplified governing equation was produced and its solutions expressed as a Fourier series. It was found that for each individual harmonic, the damping coefficient changed with respect to the magnitude and location of a blockage. As a result, the magnitude of the blockage could be determined by the magnitude of the damping coefficient and its location deduced from the ratio of damping rates in the respective harmonics. The derived method was successfully tested using laboratory based experimentation.

Lee et al [67] proposed the use of Frequency Response Diagram (FRD) shapes to locate and size multiple blockages in a straight pipeline. A fluid transient was applied to the pipe by means of a discharge valve and the resulting pressure response analysed and turned into a FRD. The peaks of the FRD were analysed by Fourier transform which resulted in unique signatures for the size, location and number of blockages in all but exceptional cases. The method was tested theoretically using a model but not through experimentation. A number of short falls were explained, such as the reliance on orifice equations to simulate blockages, which in real world applications would not be uniform. The developed method would be highly complex to automate and there is no explanation of how pumped and bent pipe transportation systems would react.

Scott et al [68] evaluated the use of a technique based upon back pressure monitoring for partial blockage detection and characterisation in gas flow pipelines. The detection of blockages in oil and gas pipelines has significant financial advantages. This work was particularly concerned with blockages in full well stream production pipelines, which pump unprocessed reservoir fluids long distances before reaching the production facility. In these cases the formation of blockages is often very slow and thus indistinguishable from normal reservoir depletion. Using only routine data the developed method quantifies partial blockages by comparing production data to a baseline performance curve. A standard gas back pressure equation was applied and combined with modifications to describe a blockage. This produced a coefficient termed as the "blockage factor". It was found that blockages in horizontal pipelines produced deviations from the backpressure curve in predictable ways, which could be quantified by the blockage factor. It was also discovered that the time to steady state restoration following a rate change was dependent on the severity and location of the blockage. It was set out that further work was needed

assessing the effects of extra valves and equipment located on the pipe line in real applications. It appears that, as with all these methods, the physical layout of the mechanical components can have a significant effect on the effectiveness of the approach.

Stephens et al [69] attempted to use Inverse Transient Analysis (ITA) to detect partial blockages in a small part of a water distribution network. ITA involves the variation of the parameters of a transient model to develop a set of predicted responses to known events. These responses are then compared to actual responses for the events by means of an objective function. In this paper a least squares method was developed by summing the squared differences between the actual and predicted data. These researchers used a pre-existing software-based search algorithm to conduct the ITA process. Transients were added to the system by the actuation of a valve. Real world distribution networks contain many mechanical complexities such as residential connections and rubber joints. It was determined that when the real data resulting from the introduced transients was compared to the model, there was a high degree of error. It was concluded that the simulation error prevented the use of ITA for blockage detection and analysis. This work demonstrates the difficulties of transplanting controlled laboratory generated techniques to real world applications. It was decided in this research to try and investigate methods which would function despite the presence of a number of system complications such as pipe elbows and narrow cross sections.

It may be concluded from the brief literature review that the frequency analysis based methods described offer great potential. However, the high data rates of 5Hz and above, and processing overhead required, would not be practical for implementation using an industry standard networked SCADA system, where frequencies higher than 2Hz are rarely used due to bandwidth considerations. The use of time based analysis of available lower frequency process variable data, presented by Scott et al [68], fitted most closely with the expected capabilities of the SCADA package which was at the core of this research.

4.5 Blockage Response Testing

4.5.1 Section Introduction

An investigation into the time domain response of the flow and PID pump speed request variables during pipe restriction events, up and downstream of the pump, was now undertaken. The focus of the investigation was to uncover any differences in the response of upstream and downstream blockages. This could potentially be used to distinguish between the two with a non-time critical low frequency fault diagnosis programme, implemented using the SCADA software. As explained in the chapter introduction, the first part of the research was undertaken with an unknown fault present in the form of an internal pump blockage. The development work conducted under this fault condition is presented as it formed the basis of the diagnostic programme produced. The remedial work conducted after the discovery of the internal blockage is then presented which resulted in the final embodiment of the diagnostic programme.

4.5.2 PID Mode Blockage Tests

For the purposes of this investigation it was decided to use only the Filter 2 subsystem. In order to characterise the system response to pipe restrictions, a series of closure tests was planned using Valve 5 (V5), which was situated upstream of the pump, and Valve 7 (V7) which is situated downstream of the pump, as shown in Figure 4.3. To calibrate the valves, and thus provide a context for the testing, the speed request to the pump was manually overridden. In manual mode the speed request generated by the PID loop in the Cylon PLC was substituted with a speed request defined in percentage terms by the user via the SCADA interface. This process was necessary as the PID control would attempt to maintain flow, as indeed it should, and hence negate the effect of the valve being partially closed. A flow rate of $1\text{m}^3/\text{h}$ was attained by a speed request of 47%. To calibrate a valve the speed request was set to a constant 47% and the valve handle was turned causing a reduction in the flow rate. The valve was adjusted to attain flow rates of 0.25, 0.5 and $0.75\text{m}^3/\text{h}$, which it was assumed corresponded to flow restriction levels of 75%, 50% and 25% respectively. Once the valves had been calibrated, tests were undertaken with the system returned to the normal PID mode.

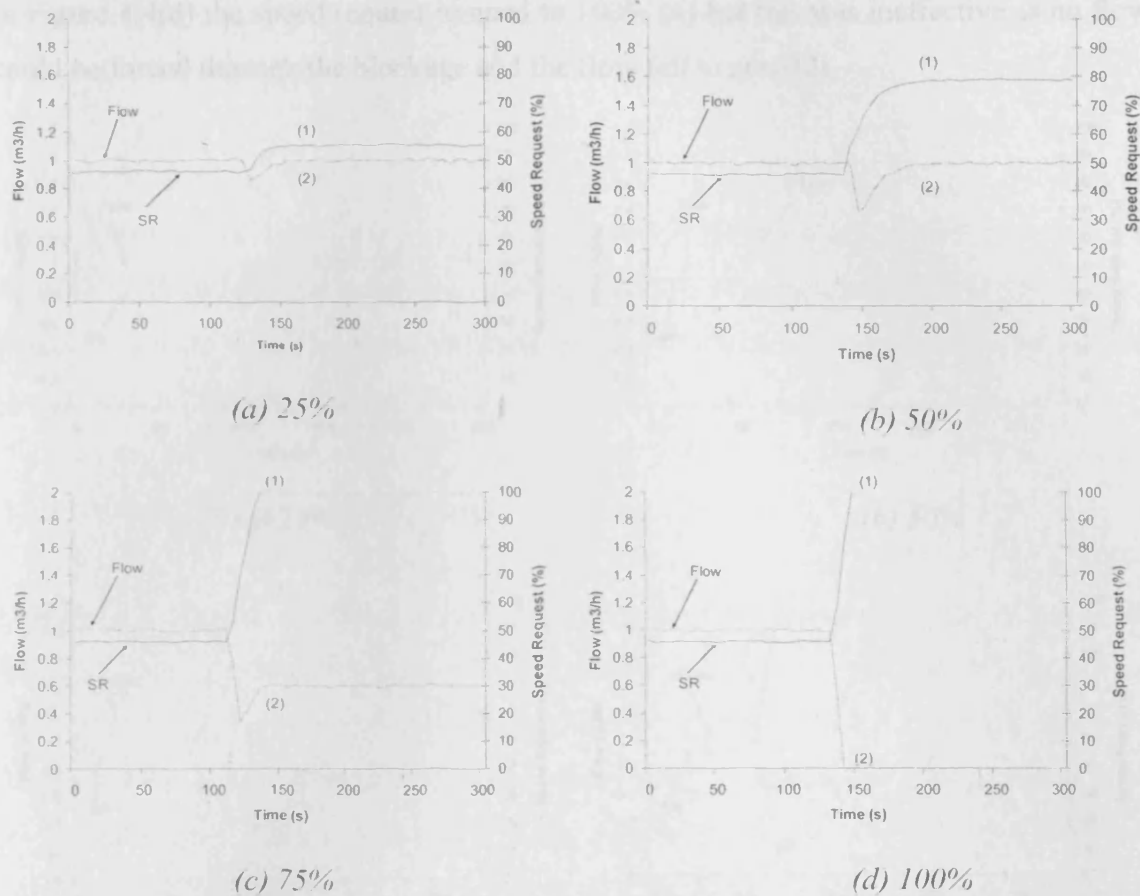


Figure 4.4: Flow and speed request response to V7 restrictions of approximately 25%, 50%, 75% and 100%.

Figure 4.4 shows examples of the tests conducted at V7 flow restrictions of 25%, 50%, 75% and 100%. The system was in automatic mode and as such the PID loop controlling the flow, in an attempt to maintain a $1\text{m}^3/\text{h}$, was uninhibited. For each test the valve was manually set to the positions which were defined during the calibration process. In the following explanation the numbered points refer to the area of the plot under consideration. As can be seen in all cases, the flow signal from FT2 initially falls sharply when the valve is closed. The PID response quickly increases the speed request to compensate. In the 25% and 50% closure cases of Figure 4.4(a) and 4.4(b) the speed request reached a point which was sufficient to produce the required flow rate (1) and the flow entered a steady state (2). For the 75% restriction case in Figure 4.4(c) a maximum pump speed request of 100% was insufficient to achieve the desired flow due to the severity of the blockage. As such, the PID loop increased the speed request to 100% (1) but the flow rate only reached a steady state below $1\text{m}^3/\text{h}$ (2). At 100% restriction as seen

in Figure 4.4(d) the speed request jumped to 100% (1) but this was ineffective as no flow could be forced through the blockage and the flow fell to zero (2).

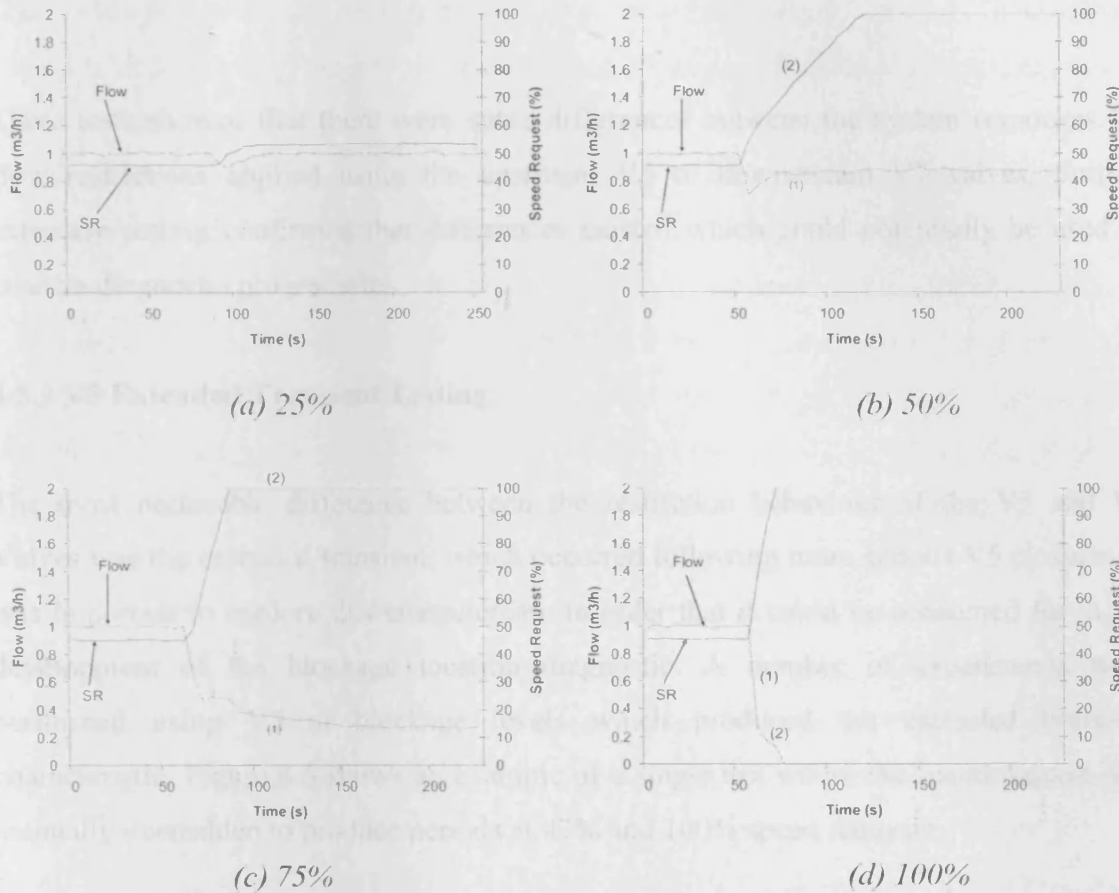


Figure 4.5: Flow and speed request response for V5 closures of approximately 25%, 50%, 75% and 100% flow restriction.

The procedure followed for the V5 valve closure tests was identical to that for V7. As can be seen in Figure 4.5(a) the 25% restrictions showed a similar characteristic to the V7 25% restrictions. However, the 50% V5 restriction shown in Figure 4.5(c) caused the flow to fall below $1\text{m}^3/\text{h}$ (1) despite the actions of the PID loop and the speed request response of the PID loop also exhibited an extended transient (2) when compared with the V7 speed request in Figure 4.4(b), which was quick to reach steady the state at 100%.

The 75% V5 blockage level of Figure 4.5(c) also showed a different characteristic to that of 75% V7 (Figure 4.4(c)). The flow rate was seen to be in a state of transient for an extended period (1). There was decay in the flow rate following the valve closure event despite the speed request maintaining a steady 100% (2). For the V5 100% restriction case shown in Figure 4.5(d) there was also a difference in the flow rate characteristic. Rather

than the exceedingly sharp drop to zero flow witnessed in the V7 tests the flow, as shown in Figure 4.5(d) first dropped rapidly (1) but then the slope of the decent lessened slightly (2).

These tests showed that there were some differences between the system responses for flow restrictions applied using the upstream V5 or downstream V7 valves. Further extensive testing confirmed that differences existed which could potentially be used to create a diagnostic programme.

4.5.3 V5 Extended Transient Testing

The most noticeable difference between the restriction behaviour of the V5 and V7 Valves was the extended transient, which occurred following more serious V5 closures. It was important to explore this characteristic in order that it could be accounted for in the development of the blockage location diagnostic. A number of experiments were performed using V5 at blockage levels which produced the extended transient characteristic. Figure 4.6 shows an example of a single test where the speed request was manually overridden to produce periods at 47% and 100% speed requests.

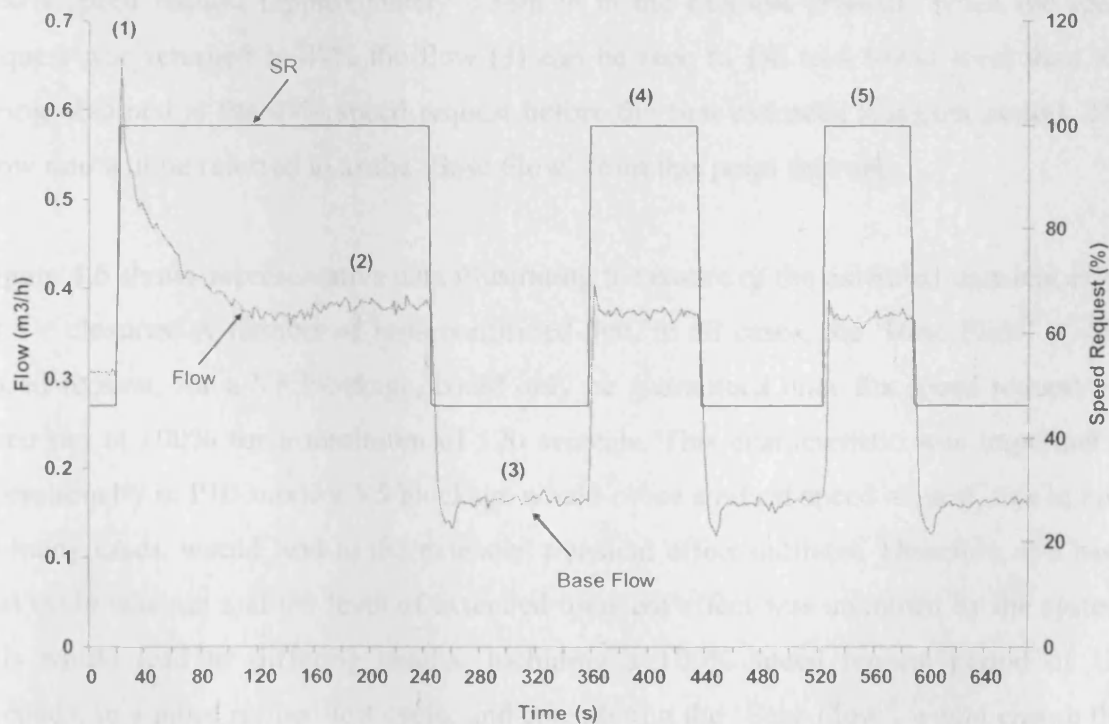


Figure 4.6: Example of flow characteristics seen for a V5 blockage exhibiting the extended transient.

Figure 4.6 shows the extended transient characteristic of the V5 valve. The pre-set V5 blockage, that was applied at a speed request of 47%, caused the flow to reduce to a steady state of $0.3\text{m}^3/\text{h}$, as seen in the first 20 seconds of the figure. The data in Figure 4.6 begins after this steady flow state was reached. The speed request was manually set to 100% and the flow rose to a peak (1) and then gradually fell to a relatively steady state (2). The system was then returned to 47% speed request and the flow was found to settle at just over $0.15\text{m}^3/\text{h}$ (3). When the speed request profile was cycled a further two times, (4) and (5), it was observed that the same 'Base Flow' rates occurred. The first period at 100% speed request appeared to have altered the flow rate which could be generated by the pump at this level of V5 restriction. As a result the subsequent 'Base Flow' rate of approximately $0.15\text{m}^3/\text{h}$ is lower than the original flow rate of approximately $0.3\text{m}^3/\text{h}$. The nature of the V5 transient behaviour is discussed further later in the chapter.

Figure 4.6 demonstrates the general characteristic for cases where an extended flow transient existed for a V5 closure. The flow rate would reach what could be considered a steady state after approximately 120 seconds (at the maximum speed request). This can be seen in Figure 4.6 in the first period at 100% speed request (2). The steady state flow after the 120 seconds represented the maximum steady state flow that the valve would allow at 100% speed request (approximately $0.38\text{m}^3/\text{h}$ in the example shown). When the speed request was returned to 47% the flow (3) can be seen to fall to a lower level than was being obtained at the 47% speed request before the first extended transient period. This flow rate will be referred to as the 'Base Flow' from this point forwards.

Figure 4.6 shows representative data illustrating the nature of the extended transient effect of 5V closures. A number of tests confirmed that, in all cases, the 'Base Flow' at 47% speed request, for a V5 blockage, could only be guaranteed once the speed request had been run at 100% for a minimum of 120 seconds. This characteristic was important as operationally in PID mode a V5 blockage would cause a raised speed request, this in turn, in many cases, would lead to the extended transient effect outlined. Therefore, if a basic test cycle was run and the level of extended transient effect was unknown by the system, this would lead to differing results. Including a 100% speed request period of 120 seconds, in a more refined test cycle, and considering the 'Base Flow', would ensure that results would be standardised and consistent, irrespective of the state of the system before a test cycle began.

4.6 SCADA Controlled Speed Request Tests

In order to find a robust method to distinguish between the V5 and V7 valve restrictions it was necessary to fully characterise the flow response of the system. It was decided to experiment with a subtle ramp up of the speed request from 47% to 100%. It was thought that the manner in which the 'Base Flow' rate altered with the increasing speed request may provide a discernible difference between V5 and V7 valve restrictions. A procedural code test function was therefore written in Cicode, which smoothly ramped up the speed request using conditional executors.

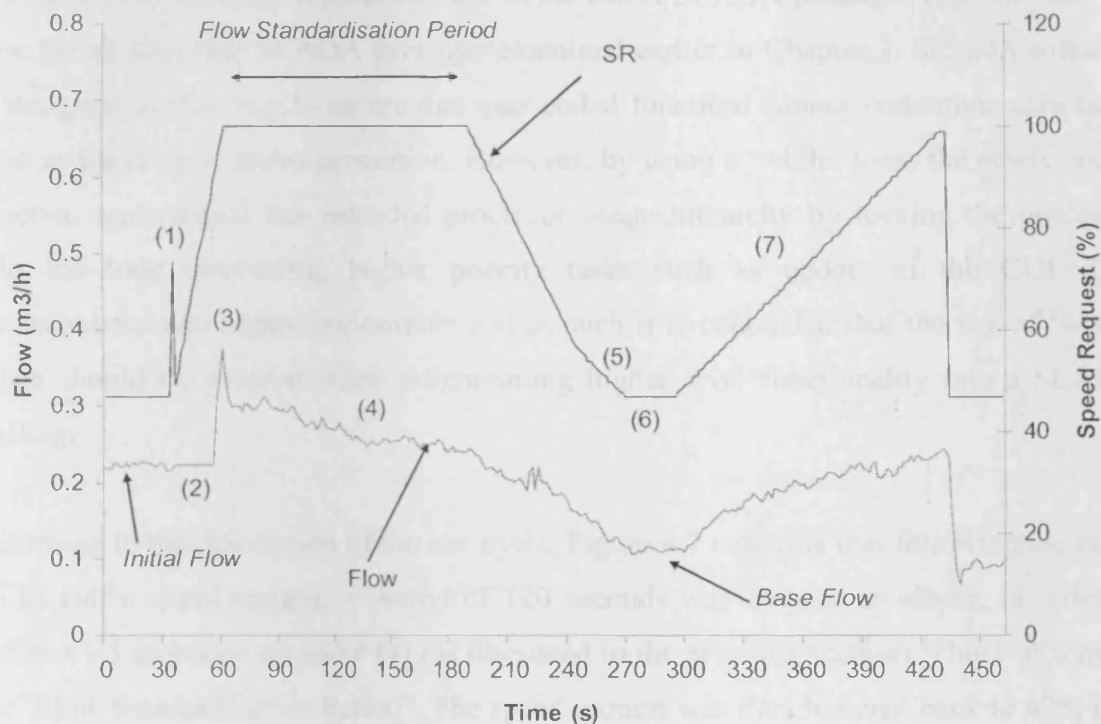


Figure 4.7: Example of ramped up speed request test cycle with a V5 restriction of approximately 77%.

Figure 4.7 shows the programmed speed request test cycle. To test blockages the speed request was first manually set to 47% and the blockage applied once a steady state had been reached. The automatic test cycle was then triggered using a button configured on the SCADA process mimic screen. The test cycle first ramped up the speed request to 100%. A 'while' conditional execution loop was used to perform this operation on the speed request value. This is noted since the selection of this style of loop had certain implications for the function of the SCADA package. As evident in the figure, at the start of the speed request ramp up, a spike is produced (1). This feature occurred on

approximately half of all cycles run and could not be fully explained. If the flow signature is analysed during the ramp up it can be seen that at the start, the flow signal appears to lose its natural variability (2) and then suddenly takes a large step up near the end of the cycle (3). This of course was not a true reflection of the flow response. On further investigation it was determined that the while loop had effectively frozen the update of the SCADA GUI, which was being used to record the results. It was thus the indicated flow response that had been affected, not the actual flow response.

Further investigation determined that user written procedural code functions have the lowest priority in terms of processor use in the Citect SCADA package. This was also the case for all the other SCADA packages examined earlier in Chapter 3. SCADA software is designed in this way to ensure that user coded functions cannot undermine core tasks such as trending or alarm generation. However, by using a 'while' loop, the newly coded function undermined this intended processor usage hierarchy by locking the processor into the loop, preventing higher priority tasks such as update of the GUI. This characteristic was highly undesirable and as such it is concluded that the use of 'while' loops should be avoided when programming higher level functionality into a SCADA package.

Returning to the description of the test cycle, Figure 4.7 confirms that following the ramp up to 100% speed request, a period of 120 seconds was allowed to elapse, in order to exhaust V5 extended transient (4) (as discussed in the previous section). This was termed the 'Flow Standardisation Period'. The speed request was then lowered back to 47% in a controlled fashion. The rate of change of the speed request reduction was decreased as the 47% was approached (5), in order to prevent an impulse response. This had been seen to cause the flow to drop to zero when severe blockages were tested. For this phase of the test cycle a 'For' loop was utilised. Following each iteration of the 'For' loop, the programme exits the loop before the next iteration. This allows the priority of critical functions such as trending to be recognised by the processor. As a result no undesirable freezing of the GUI or other side effects were witnessed.

Once the speed request had been brought back to 47%, this level was maintained for 20 seconds (6) to allow the flow to stabilise. Following this, the actual speed request ramp up test cycle (7) was initiated, this time using a 'For' loop. A range of V5 and V7 valve

restrictions were now subjected to the new test cycle and a complete set of results were obtained.

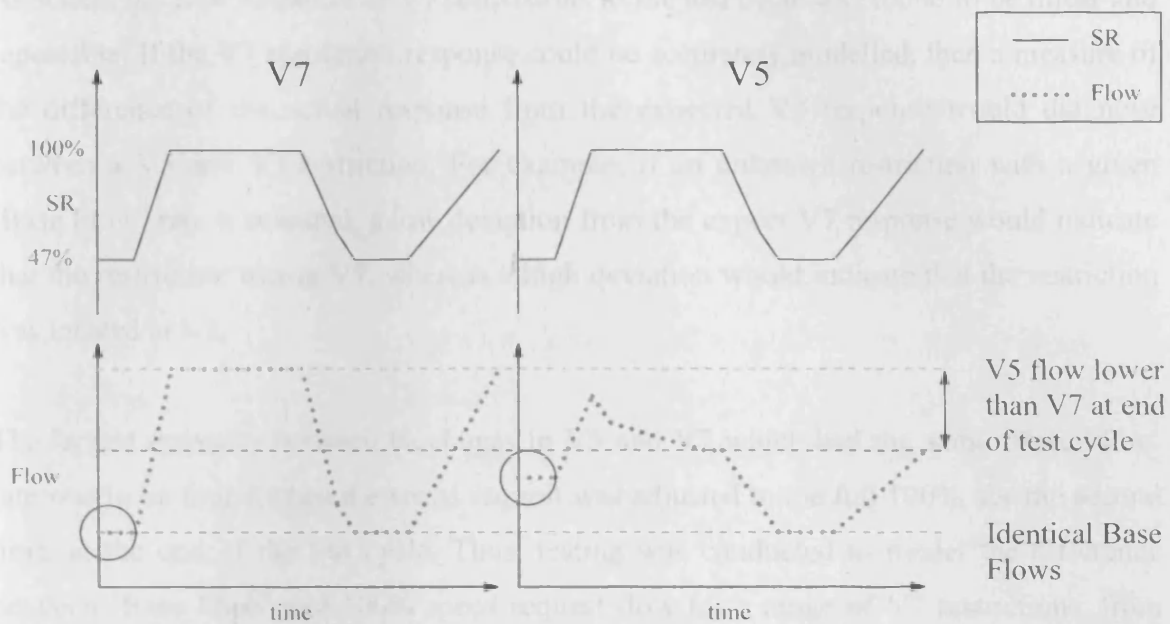


Figure 4.8: Generalised representation of the characteristic responses of V7 and V5 restrictions with identical 'Base Flow' rates.

A general pattern which could be used to distinguish between V5 and V7 restrictions became apparent from the range of closures applied, as illustrated in the generalised trends in Figure 4.8. The key distinguishing feature was that for individual V5 and V7 restrictions which gave identical 'Base Flow' rates, V5 always exhibited a lower flow rate at the end of the test cycle with the speed request at 100%.

Moreover, the V7 response was found to be highly linear and repeatable, whereas the V5 response was far more erratic. V7 restrictions would always exhibit a 'Base flow' after the 'Flow Standardisation Period' which was identical to the initial flow, as no extended transient and associated flow degradation behaviour existed for V7 restrictions. V5 and V7 restrictions which exhibited the same 'Base Flow' did not have the same initial flow rate as demonstrated by the circles in Figure 4.8 and were therefore not considered to be the same blockage level. This indicated that the characteristic (at this stage) did not account for blockage level but simply provided a method for distinguishing between V5 and V7 restrictions.

4.7 Decision to Use the CUSUM Technique

As stated, the flow response of V7 restrictions to the test cycle was found to be linear and repeatable. If the V7 restriction response could be accurately modelled, then a measure of the difference of the actual response from the expected V7 response would diagnose between a V5 and V7 restriction. For example, if an unknown restriction with a given 'Base Flow' rate was tested, a low deviation from the expected V7 response would indicate that the restriction was at V7, whereas a high deviation would indicate that the restriction was located at V5.

The largest disparity between blockages in V5 and V7 which had the same 'Base Flow' rate was to be found when the speed request was adjusted to the full 100%, for the second time, at the end of the test cycle. Thus, testing was conducted to model the difference between 'Base Flow' and 100% speed request flow for a range of V7 restrictions, from 40% upwards. Blockages below 40% were not tested at this stage since it was not clear whether the resulting higher flow rates would compact the filter bed adversely affecting the rig.

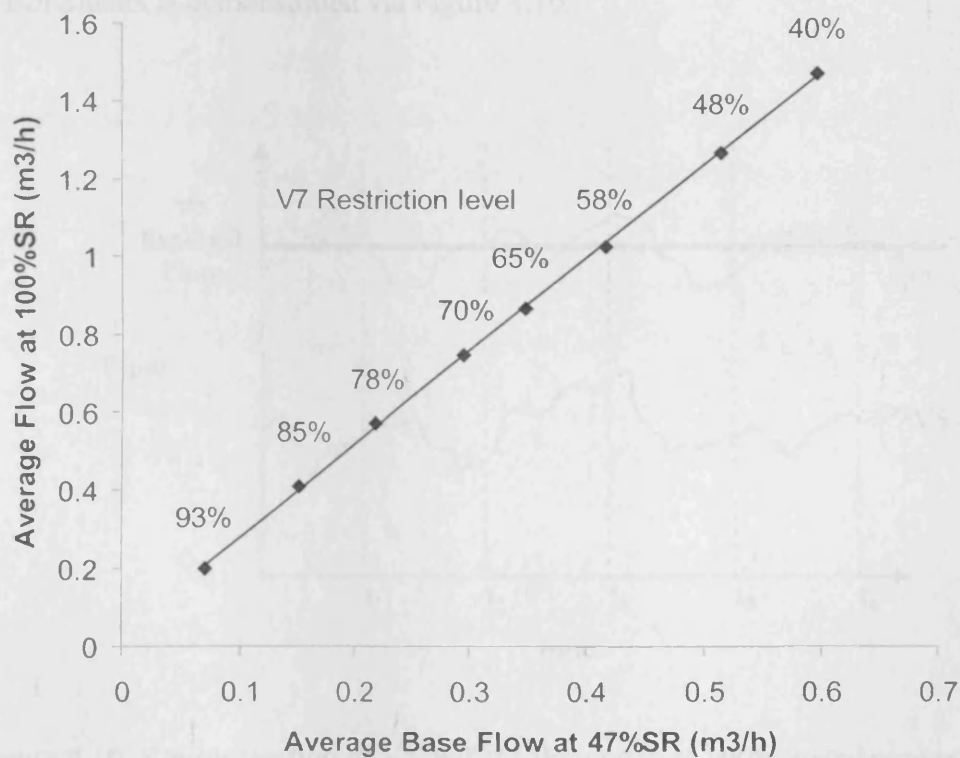


Figure 4.9: 'Base Flow' and 100% speed request flow for a range of V7 restrictions.

A line of best fit was produced for the data in Figure 4.9 which had the equation;

$$F_{100\%} = 2.38F_{47\%} + 0.041 \quad (4.1)$$

Where $F_{100\%}$ was the flow rate at 100% speed request and $F_{47\%}$ was the flow rate at 47% speed request for a V7 blockage.

It would now be possible to calculate the expected 100% speed request flow response of a V7 blockage, from the average measured 'Base Flow'. The difference of the actual response at 100% from that of the calculated V7 response could then, as proposed, be used to distinguish between a V5 and V7 restrictions.

It was decided that utilising a CUSUM technique [70], offered a potential method for accentuating any difference between the modelled V7 response and the actual measured flow response. This would allow a diagnostic programme to clearly distinguish between a V7 and V5 restriction. The technique used for a cumulative summation of repeated measurements is demonstrated via Figure 4.10.

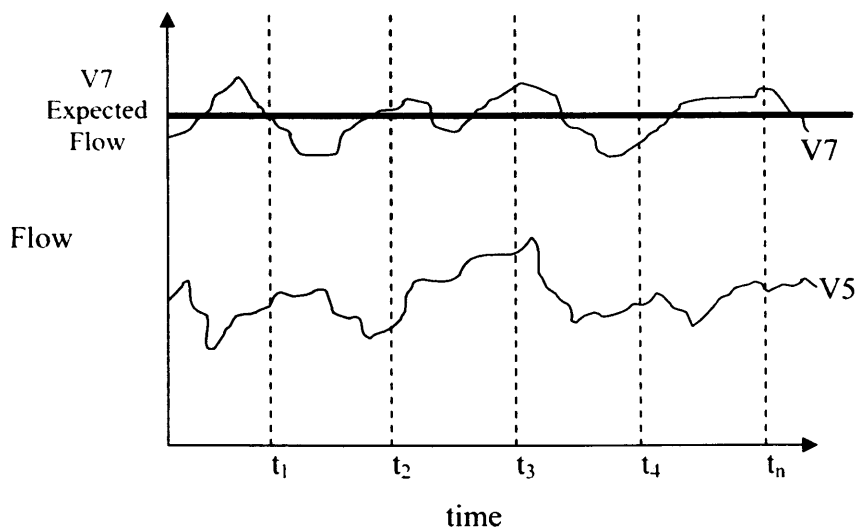


Figure 4.10: Representation of V5 and V7 flow rates at 100% speed request for identical 'Base Flow' rates and expected V7 flow rate.

Figure 4.10 is a representation of how closures in V5 and V7, which result in an identical average ‘Base Flow’ rate at 47% speed request, would differ when the speed request was increased to 100%. The expected average V7 restriction flow rate that would be calculated from equation 4.1 is also shown. If at the times t_1 to t_n the expected flow rate is subtracted from the actual flow rate, this would represent the difference of the actual flow rate from that of a V7 modelled blockage at each specific time. This can be represented as equation 4.2;

$$\Delta F_{ii} = F_{Actual} - F_{V7Expected} \quad (4.2)$$

Where ΔF_{ii} is the difference between the actual flow and the modelled V7 flow at time t_i , F_{Actual} is the actual flow recorded and $F_{V7Expected}$ is the flow expected based on equation 4.1. If the difference between the actual flow and the modelled V7 flow for each sample are added together, then a cumulative sum is produced:

$$CUSUM = \sum_{i=1}^n (\Delta F_{ii}) \quad (4.3)$$

Consideration of how V5 and V7 restrictions would react (with reference to Figure 4.10) confirms that V5 would generate a large negative CUSUM. V7 however would generate a small positive or negative CUSUM, as the difference between the actual flow and the model V7 flow would always be small. Also, as the V7 deviation fluctuated from positive to negative, a degree of ‘cancelling’ would take place causing the V7 restriction CUSUM to tend to zero. This method of analysis was then written into the test cycle as shown in Figure 4.7.

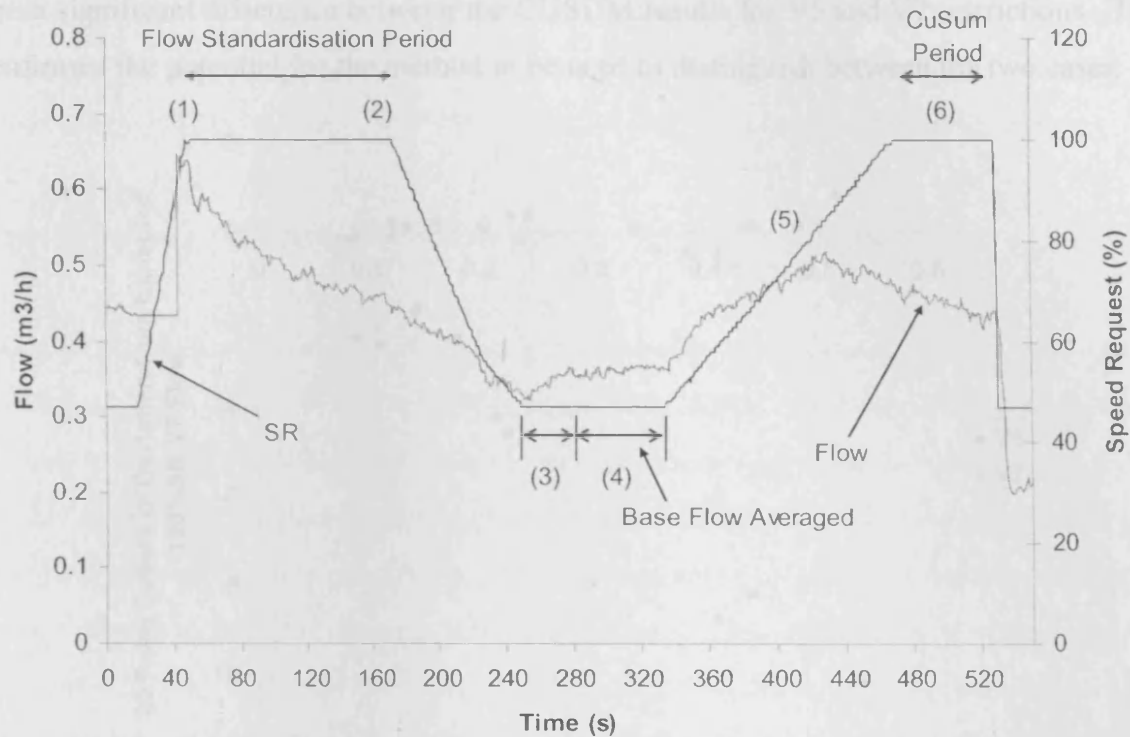


Figure 4.11: Example of a full test run during a V5 medium closure.

As demonstrated in Figure 4.11 the programme first ramped up the speed request to 100% (1). The programme ran the 'Flow Standardisation Period', at 100% speed request for 120 seconds (1)-(2) to exhaust the extended transient, seen as the flow falling away during this period. Although this period is not required for a V7 restriction, the location of a real restriction would be unknown operationally and the full test sequence would always need to be run. The speed request was then reduced back to 47% as previously described. The speed request ran at 47% for a short period (3), to allow the flow signal to settle, before taking a 20 point average (4) that was stored as 'Base Flow'. The 'Base Flow' was substituted into equation 4.1 by the function to generate a value for the expected flow that would be attained at the subsequent 100% speed request, if the closure was located at V7. Next the function gradually ramped up the speed request to 100% (to avoid an unwanted impulse response). During the new section of the test (6) the difference of 20 actual flow values from the expected V7 flow were then calculated and summed using equation 4.3.

The results from a series of V5 and V7 restriction tests can be seen in Figure 4.12. Each test cycle lasted over eight minutes and it was only possible to perform approximately five test cycles an hour at this development stage. It can be seen from the initial tests that there

was a significant difference between the CUSUM results for V5 and V7 restrictions. This confirmed the potential for the method to be used to distinguish between the two cases.

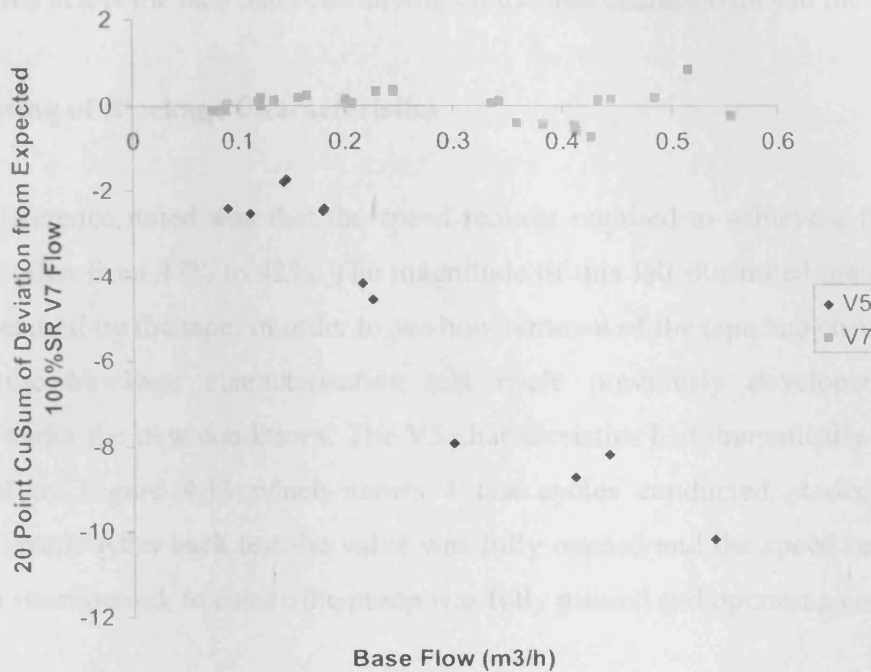


Figure 4.12: CUSUM results for a number of V5 and V7 blockages.

In summary, a test cycle had been developed based on the studied system characteristics which could potentially be used to distinguish between V5 and V7 blockages. The full development and testing of this new method was however cut short, as the previously unforeseen internal fault with the pump was discovered. This would have altered the system characteristics compared to a pristine state. This meant that a re-characterisation of the response to V5 and V7 restrictions was needed. The general approach described ultimately did still prove to be valid and as previously discussed was deemed to merit the inclusion of the results in this section.

4.8 Post Pump Blockage Discovery Work

4.8.1 Section Introduction

The pump was opened for routine maintenance and a 15 cm piece of transparent sticking tape was found wrapped around the base impellor. The tape was creating a blockage restricting flow into the first stage impellor and consequently all following impellors. It was reasonable to assume that this tape had been present since before the rig's delivery to

the University. The rig was believed to be in its normal operating condition and the discovery of the tape was entirely unforeseen. An investigation was conducted to ascertain what affect the tape had been having on the true characteristics of the pump.

4.8.2 Retesting of Blockage Characteristics

The first difference noted was that the speed request required to achieve a flow rate of $1\text{m}^3/\text{h}$ had fallen from 47% to 42%. The magnitude of this fall illustrated the scale of the restriction caused by the tape. In order to see how removal of the tape had changed the V5 response, the blockage characterisation test cycle previously developed was run repeatedly under the new conditions. The V5 characteristics had dramatically changed as exemplified by Figure 4.13 which shows 4 test cycles conducted at decreasing V5 restriction levels. After each test the valve was fully opened and the speed request set to 100% for a short period, to ensure the pump was fully primed and operating correctly.

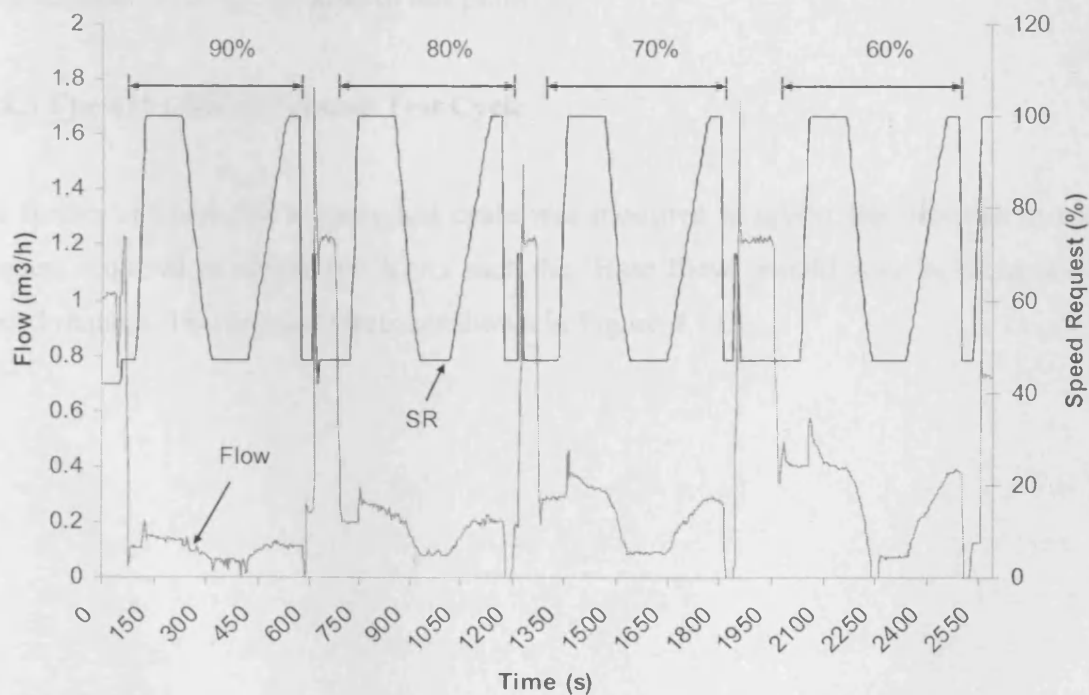


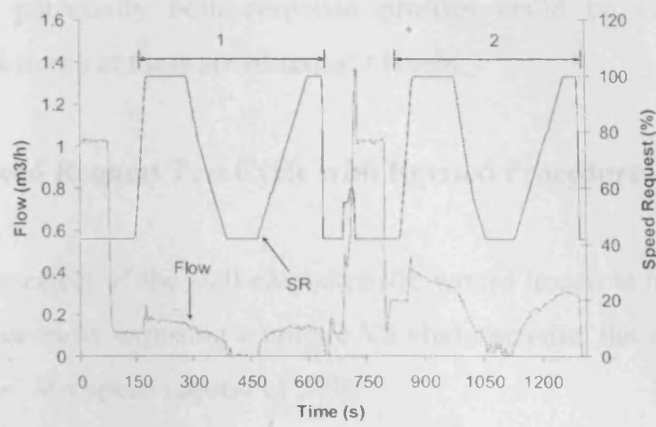
Figure 4.13: Series of example test cycles run with V5 closures with no tape blockage.

As in previous tests V5 closure was set with the speed request at a constant 47% to obtain the desired flow restriction. The test cycle was then triggered which initiated the 'Flow Standardisation Period' at 100% speed request. However, without the tape in place the

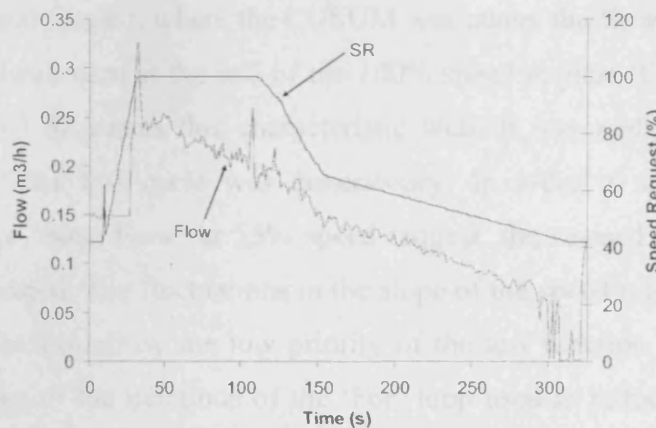
flow, rather than falling to a unique 'Base Flow' level after the 'Flow Standardisation Period' now seemed to always fall to a similar level of between 0.7 and 0.9m³/h. Also a more severe V5 restriction did not necessarily lead to a lower 'Base Flow' following the 'Flow Standardisation Period'. This is illustrated by 80% and 60% restriction tests in Figure 4.13. The 60% test had a far less severe V5 closure than the 80% test, which is shown by the fact that the 47% speed request flow obtained before the 'Flow Standardisation Period' is far higher. However, following the 'Flow Standardisation Period' the 'Base Flow' in the 60% test actually falls to a lower level than the 80% test. This was an entirely different characteristic to that witnessed with the tape in place. With the tape present, following the 'Flow Standardisation Period', V5 blockages had always led to a test result where the increase in flow from the 47% speed request to the 100% speed request was less than that seen for a V7 blockage. Now it appeared that in some cases V5 restrictions might actually show a larger flow increase than V7 restrictions. Further testing confirmed that in some cases V5 would now give the same increase as V7 when subjected to the test cycle. This undermined the analytical strategy used by the characterisation programme up to this point.

4.8.3 The 42% Speed Request Test Cycle

As further research the existing test cycle was modified to reflect the decrease in speed request required to obtain 1m³/h. As such the 'Base Flow' would now be taken at 42% speed request. Two example tests are shown in Figure 4.14.



(a) 42% base test cycle



(b) 42% base modified test cycle

Figure 4.14: Example of 42% speed request base test cycle and a cycle modification attempting to prevent flow crash.

Figure 4.14(a) is illustrative of the testing that took place with the revised 42% speed request 'Base Flow' test cycle. With the new lower speed request, severe to medium V5 closures now showed a tendency to drop to zero following the 'Flow Standardisation Period'. Hence, the ramp down (following the 'Flow Standardisation Period') was altered, as can be seen in Figure 4.14(b), to try and prevent the flow dropping to zero. The failure of the extended ramp down test indicated that the pump without tape had a much stronger stalling characteristic. With the base speed request at 42% the pump would always stall with severe to medium V5 blockage levels. With the 'Base Flow' taken at 47% speed request severe to medium blockages would always fall to between 0.7 and 0.9m³/h. It was

hypothesised that potentially both response profiles could be caused by the stall characteristic of the pump at these speed request levels.

4.8.4 The 55% Speed Request Test Cycle with Revised Procedure

To determine if the effect of the stall characteristic would lessen at higher speed request levels, possibly once more exposing a unique V5 characteristic, the test was modified to take the 'Base Flow' at a speed request of 55%.

It had also been noted that in all cases, both with and without tape, that in the second period at 100% speed request, where the CUSUM was taken, the flow always attained the same level as had been seen at the end of the 100% speed request 'Flow Standardisation Period'. Figure 4.13 illustrates this characteristic well. It was realised that the second ramp up phase of the test cycle was unnecessary. In order to explore the no tape characteristics for a 'Base Flow' at 55% speed request, the revised test cycle shown in Figure 4.15 was created. The fluctuations in the slope of the speed request ramp down (1) are considered to be caused by the low priority of the test function within the SCADA package. The timing of the iterations of the 'For' loop used to reduce the speed request are not uniform, as other higher priority SCADA tasks are undertaken between each iteration.

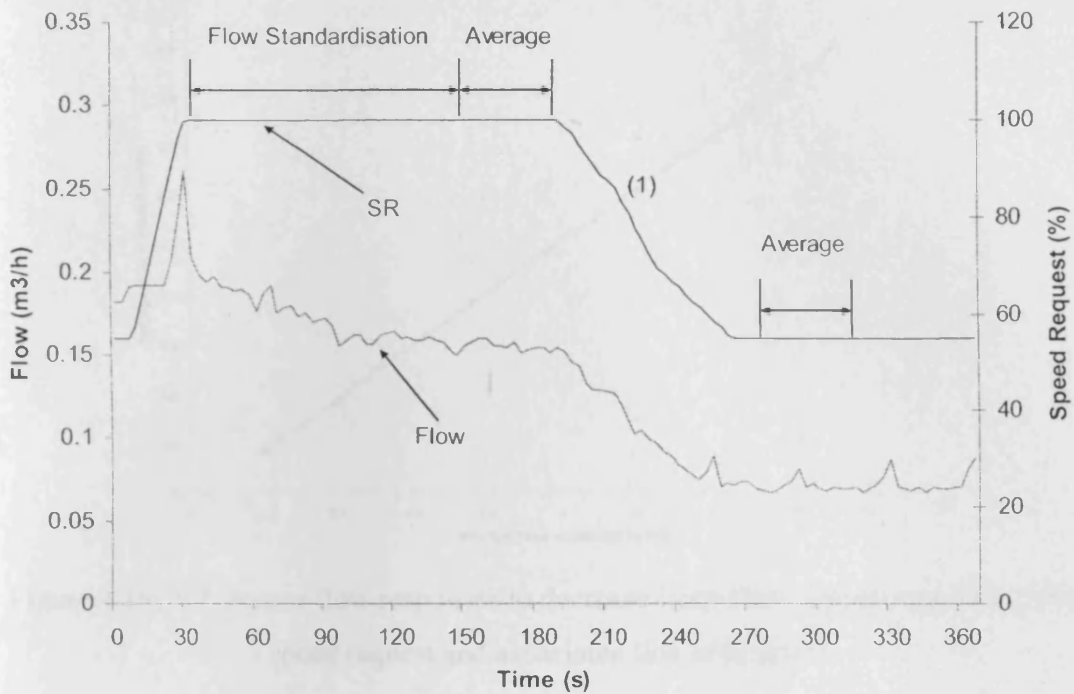


Figure 4.15: Example of revised test cycle with no second period at 100% speed request shown with a V5 restriction.

The new test cycle shown in Figure 4.15 was applied to V5. Once again, despite the increase in speed request which attempted to mitigate the new stall characteristics, severe to medium blockages still resulted in similar flow rates after the 'Flow Standardisation Period'.

4.9 Final Test Cycle

4.9.1 New V7 Model and Revised Test Cycle

With the tape in the pump, a severe to medium V5 blockage had always resulted in a lower flow rate than V7, when the speed request was ramped up from the base speed request to 100%. This simple and useful characteristic was clearly no longer apparent now that the tape was removed and the pump was allowed to exhibit its true behaviour. However, the linearity of V7 closures behaviour seemed to have been unaffected by the removal of the tape. To confirm this, the test cycle shown in Figure 4.15 was run at a variety of V7 closures to create the plot shown in Figure 4.16.

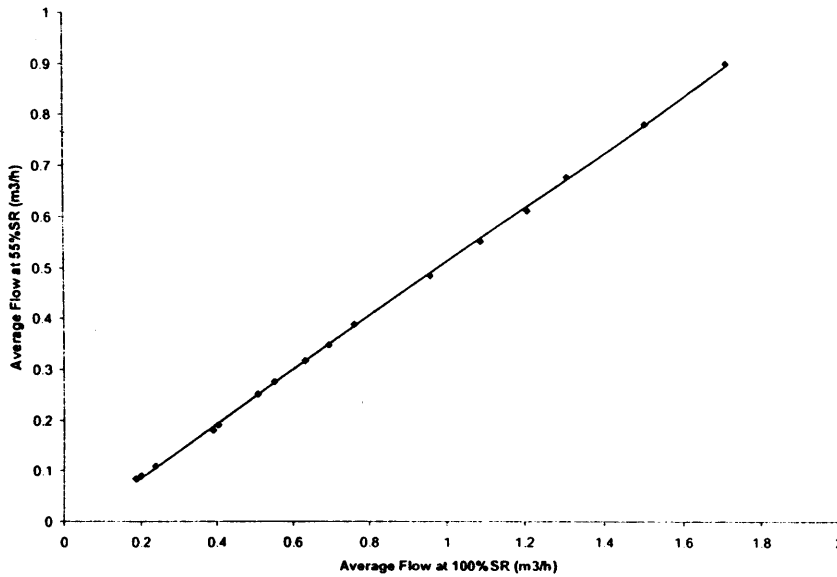


Figure 4.16: V7 closure flow responses to decrease from 100% speed request to 55% speed request and associated line of best fit.

The data shown in Figure 4.16 confirmed that the V7 flow response was still highly linear with the pump in its normal state. The V5 response had drastically changed but it was still conceivable that the V5 restriction response would differ from the V7 response. This difference would occur in a less predictable manner than had been witnessed with the tape in place. It would be necessary to fully explore the new behaviour and this was achieved using the previously developed mechanisms. A line of best fit for the data shown in Figure 4.16 was thus used to generate equation 4.4. This characterised the expected V7 response for a given 100% speed request flow rate, when the speed request was reduced to 55%.

$$F_{55\%} = 0.533F_{100\%} - 0.02 \quad (4.4)$$

Where $F_{55\%}$ is the flow at 55% speed request and $F_{100\%}$ was the flow at 100%. Equation 4.4 was then used to develop the test cycle seen in Figure 4.17.

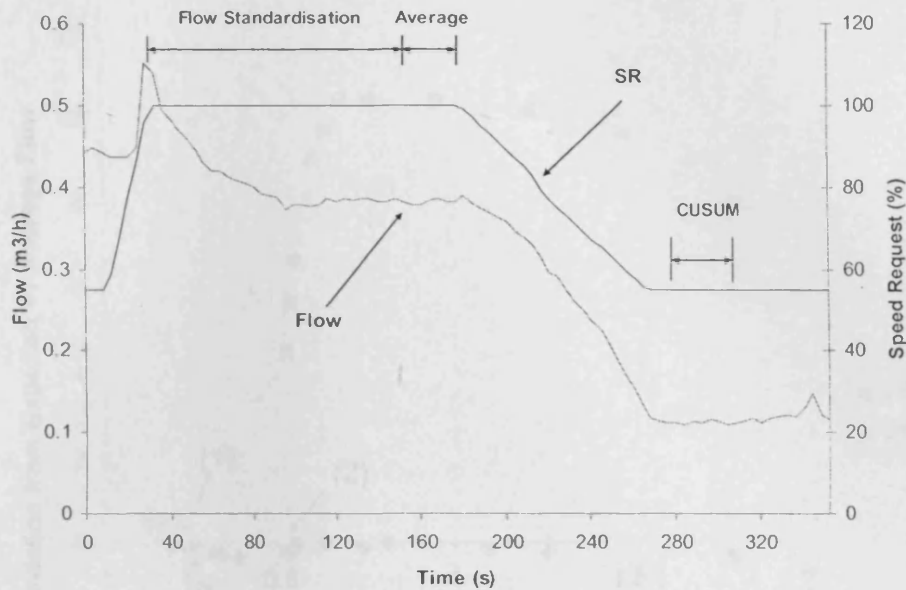


Figure 4.17: 100% to 55% speed request test cycle with CUSUM of deviation from expected V7 closure flow response.

When the test cycle shown in Figure 4.17 was triggered, the speed request quickly ramped up to 100%. This level was maintained for 120 seconds (as in previous cycles) to standardise the flow. At the end of the 'Flow Standardisation Period' a 20 point average of the flow was taken with the speed request still at 100%. The programme then substituted this value into equation 4.4 to generate the expected V7 model average flow at 55%. Once the 100% speed request average flow had been taken, the programme ramped down the speed request to 55%. After a short 10 second pause, the 20 point CUSUM of the difference between the actual flow and the modelled V7 flow was triggered by the programme.

4.9.2 Test Cycle Results

The overriding concept of the test was to examine the difference between the flow rate obtained at 100%, following the 'Flow Standardisation Period' and the 'Base Flow' then obtained at 55% speed request. With test cycles taking over five minutes, plus set up time, it was only possible to obtain approximately six tests per hour. The results of the testing are shown in Figure 4.18.

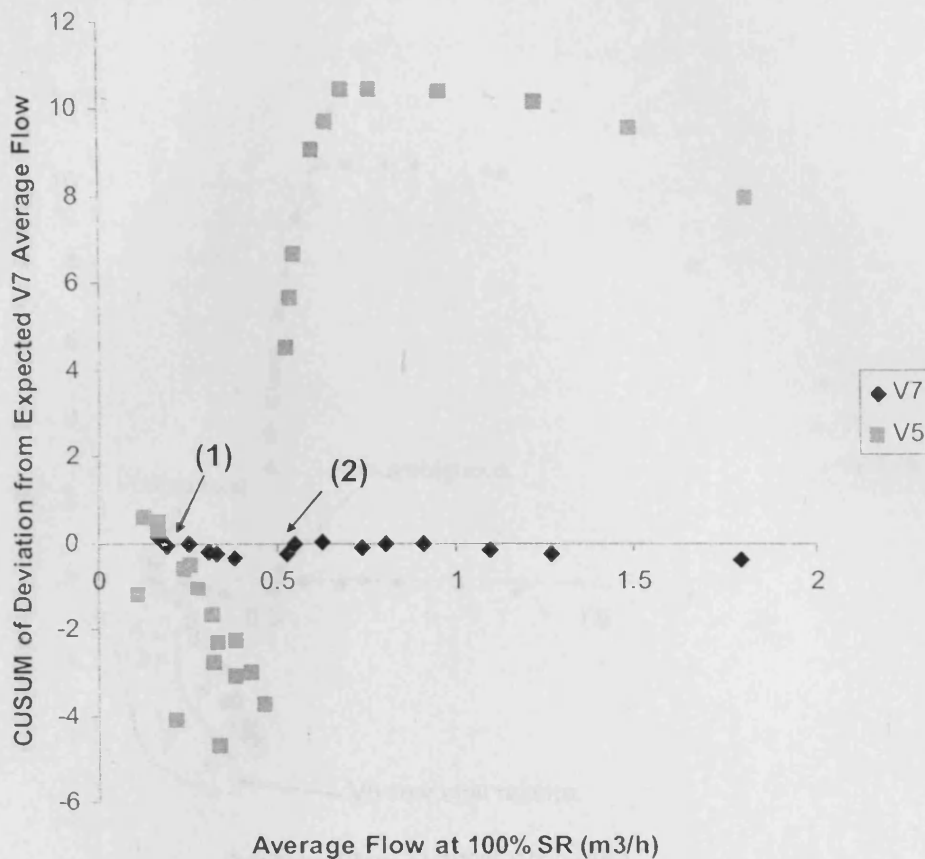


Figure 4.18: Test results for 100% to 55% speed request test cycle.

The spread of the V5 CUSUM values in Figure 4.18 goes from positive to negative and back. This was in stark contrast to the all negative V5 results seen with the tape still in place, which was shown in Figure 4.12. The results illustrated that there was still, in most cases, a strong difference between the response of V5 and V7 closures subjected to the test cycle. There were, however, two main areas of ambiguity. The first was where the downward trend of V5 results intersected with the V7 results marked as (1). The second occurred where the V5 results transitioned very rapidly from negative to positive CUSUM results shown as (2). Based on the initial results, this second area of ambiguity appeared to present less of a problem than the first, as the transition was extremely rapid. There was therefore, a much reduced chance of the V5 restriction producing the same result as a V7 restriction. To understand if the new characteristics could still be used to diagnose a V5 or V7 restriction, a further 50 test cycles were conducted on V5, focussing on the two areas of ambiguity. The new results can be seen in Figure 4.19.

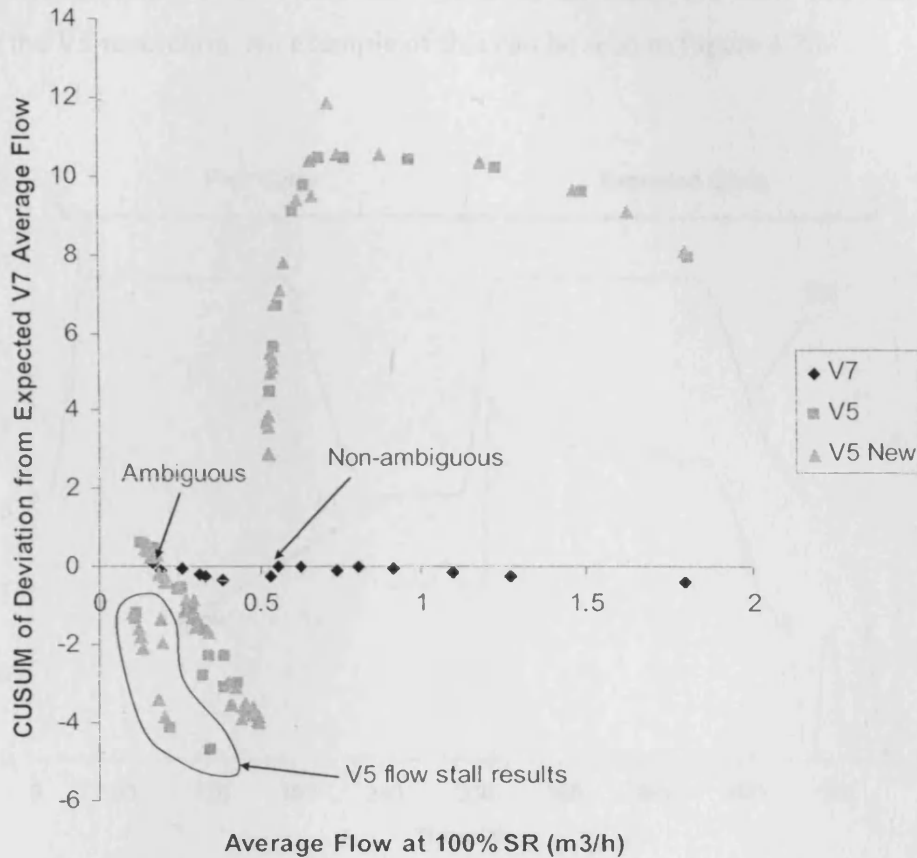


Figure 4.19: Further test results focussed on areas of ambiguity.

The new test findings confirmed that the first suspected area of ambiguity was a significant problem. The second area did not however present ambiguous results, as the sign transition was considered to be a step change in the behaviour of the pump. To support and explain these observations a thorough analysis of the V5 restriction results was undertaken. The flow characteristics resulting from V5 restrictions were considered to be the result of cavitation behaviour, caused by the upstream V5 starving the pump of water. A full explanation of the analysis undertaken is presented as Appendix C.

The possibility of ambiguity for restrictions which gave values lower than 0.25 m³/h at 100% speed request still remained. However, as discussed in Appendix C, some V5 restrictions in this range would actually cause the flow to stall preventing ambiguity, shown as 'V5 flow stall results' in Figure 4.19. To exploit this fact, it was decided to do further testing on V5 closures in this limited region, to see if the flow stall could be artificially brought about. Tests were conducted on V5 restrictions which showed flows below 0.25m³/h. Those tests which showed CUSUM values close to V7 were then

immediately subjected to a second test cycle. In all cases the flow did stall to zero exposing the V5 restriction. An example of this can be seen in Figure 4.20.

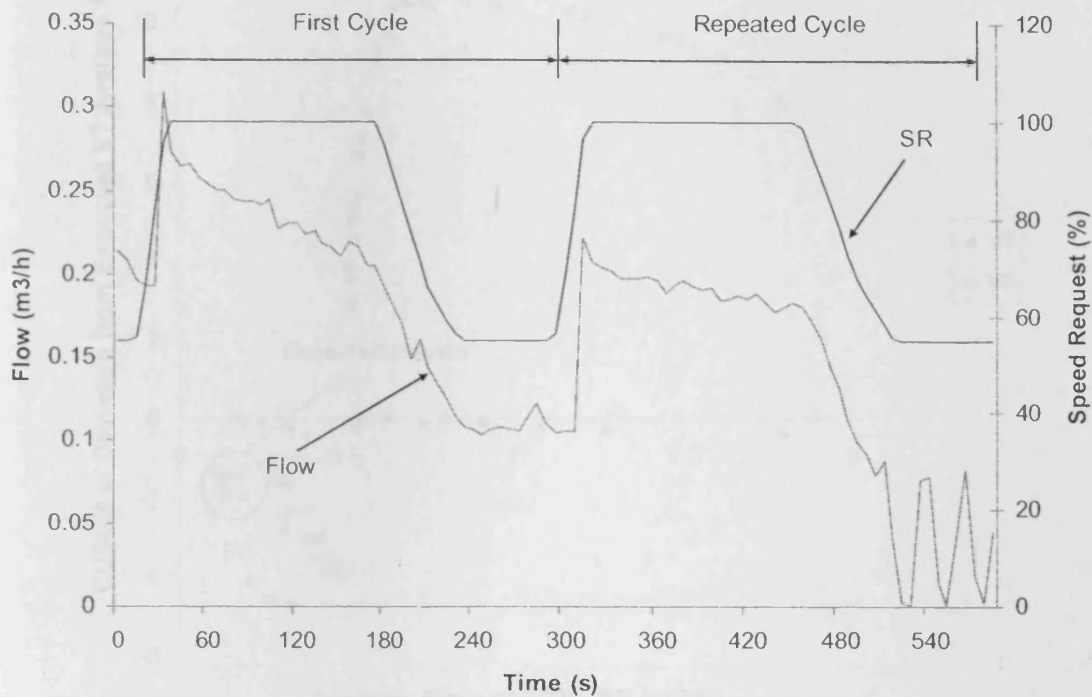


Figure 4.20: Test cycle repeated on ambiguous V5 result.

The example shown in Figure 4.20 illustrates the characteristic seen on initiating the second test cycle. It can be seen that in the second CUSUM period at 55%, the flow falls to zero. The pump does however struggle to re-establish flow, and large fluctuations can be seen. The CUSUM produced as a result of these fluctuations, while being more than negative enough to distinguish it from a V7 fault, is not as negative as was seen for the cases where the flow naturally stalled, as seen in Figure 4.19. The new spread of CUSUM data is presented in Figure 4.21. This data represents the test outcome if all ambiguous V5 results are discarded and the immediate retest results plotted. The results show that using the double test technique for ambiguous results leads to a clear differentiation between V5 and V7 closures.

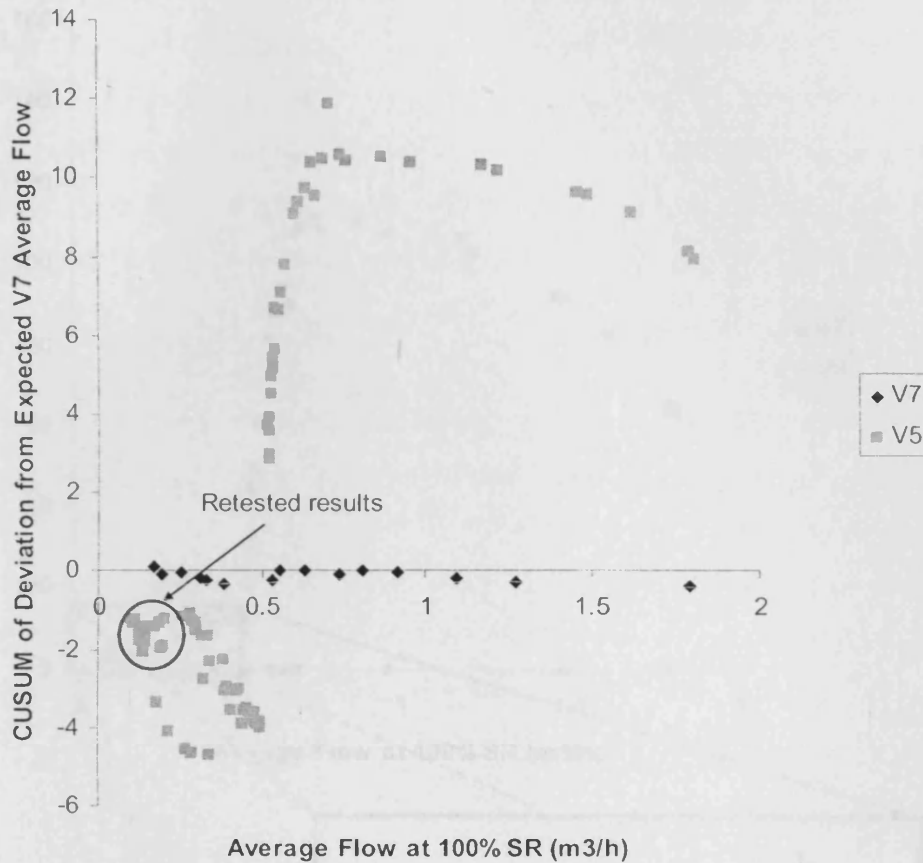


Figure 4.21: CUSUM results with ambiguous results subjected to double test cycle.

4.10 Diagnostic Programme Functionality

4.10.1 Threshold Based on Squared CUSUM Results

Using the new method a V5/V7 restriction diagnostic programme could now be completed. In order to magnify the difference between V5 and V7 restriction CUSUM results and standardise the sign so that a single threshold could be used, it was decided to square the CUSUM results as demonstrated by Figure 4.22. The highest V7 result was 0.18, whereas the closest V5 result was 1.2. As such a reliable decision threshold between V5 and V7 CUSUM² results of 0.7 was decided upon.

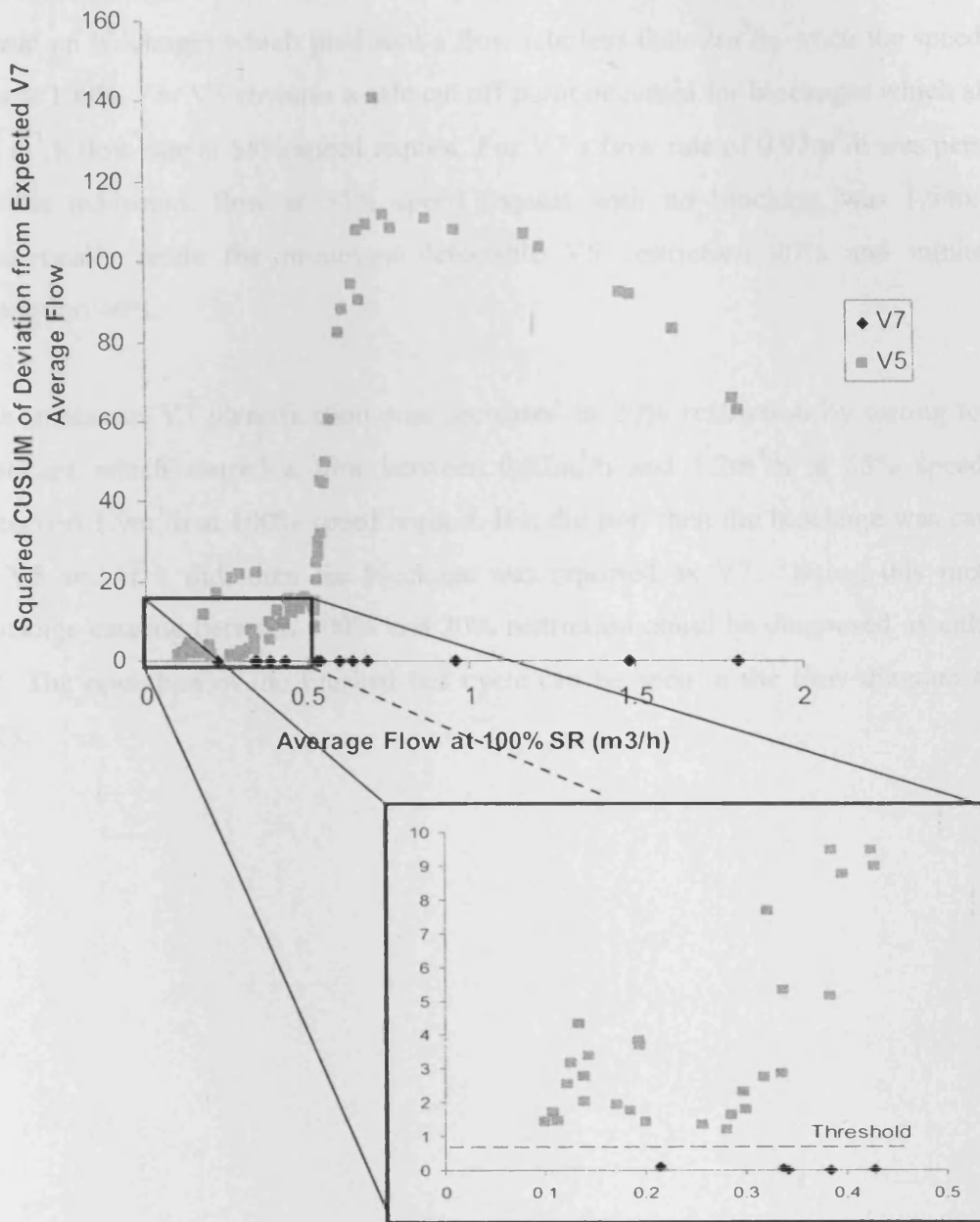


Figure 4.22: Spread of CUSUM squared data following repeated test strategy showing decision threshold.

4.10.2 Effective Range of Diagnostic

The effective range of the V5/V7 restriction diagnostic programme was good. At the severe end of the spectrum, any blockage that allowed a flow at 55% speed request could be tested. If the flow possible at 55% was used as an indication of blockage severity, this meant that blockage levels up 99.9% could be tested. At the minor blockage end of the spectrum the use of the programme was more limited. In order to preserve the filter bed it

was undesirable to run the flow rate higher than $2\text{m}^3/\text{h}$. As such the test cycle could only be run on blockages which produced a flow rate less than $2\text{m}^3/\text{h}$, when the speed request was at 100%. For V5 closures a safe cut off point occurred for blockages which allowed a $1.2\text{m}^3/\text{h}$ flow rate at 55% speed request. For V7 a flow rate of $0.92\text{m}^3/\text{h}$ was permissible. As the maximum flow at 55% speed request with no blockage was $1.54\text{m}^3/\text{h}$, this theoretically made the minimum detectable V5 restriction 20% and minimum V7 restriction 40%.

The minimum V7 identification was decreased to 20% restriction by testing to see if a blockage which caused a flow between $0.92\text{m}^3/\text{h}$ and $1.2\text{m}^3/\text{h}$ at 55% speed request exceeded $1.9\text{m}^3/\text{h}$ at 100% speed request. If it did not, then the blockage was categorised as V5 and if it did, then the blockage was reported as V7. Using this method any blockage causing between 100% and 20% restriction could be diagnosed as either V5 or V7. The operation of the finished test cycle can be seen in the flow diagram of Figure 4.23.

4.10.3 Programme Description

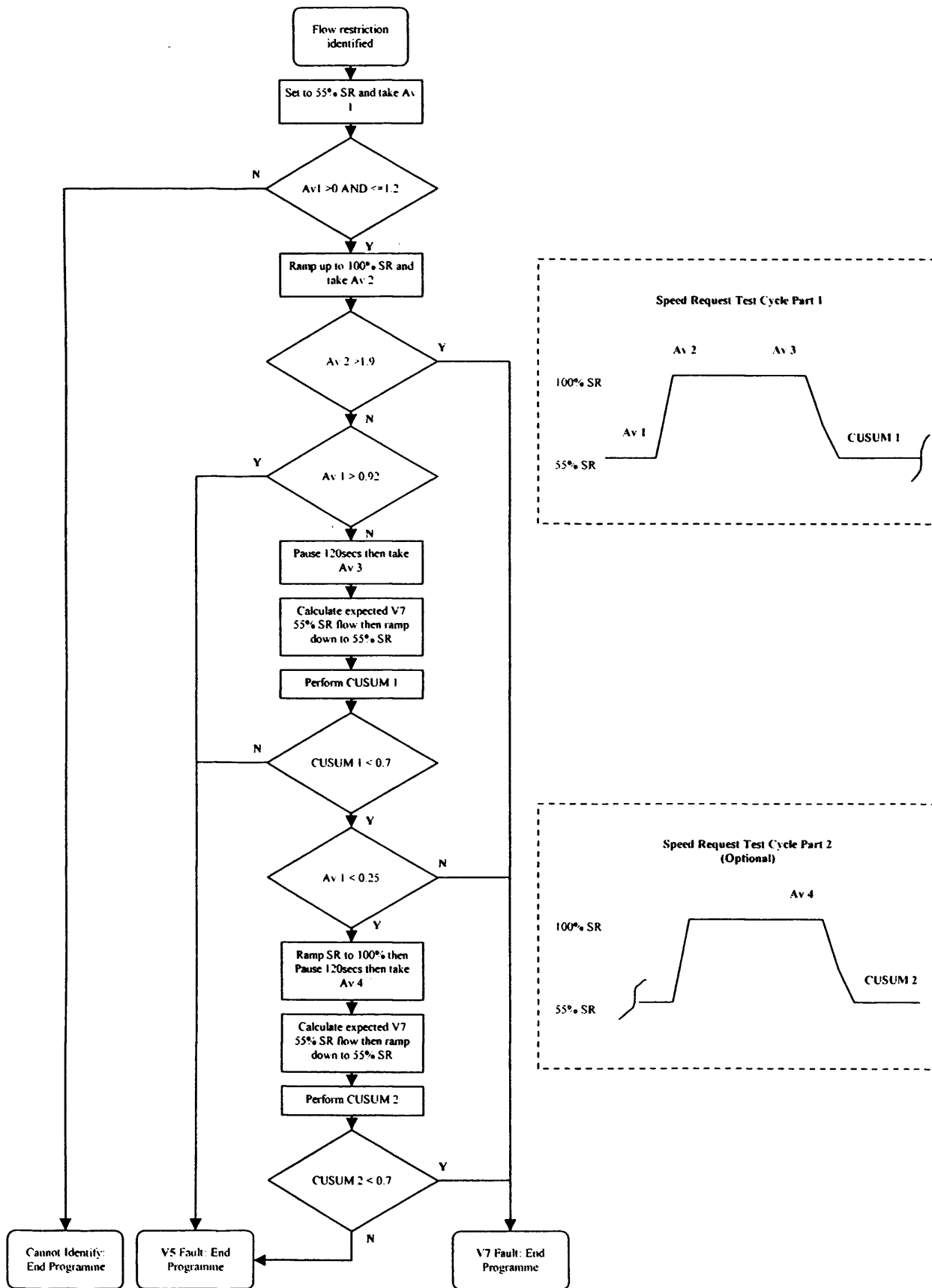


Figure 4.23: Flow diagram representing the final functionality of the Blockage Location Programme.

When the programme was triggered the speed request was set to 55% and a 20 point average taken. If the average was found to be greater than zero but also less than $1.2\text{m}^3/\text{h}$, it was within the acceptable region for the diagnostic to continue. If not, the SCADA process mimic screen was updated to inform the operator that the restriction could not be diagnosed and the programme terminated. If the blockage could not be diagnosed at this stage, the speed request was increased to 100% and a 5 point average was taken. If this was above $1.9\text{m}^3/\text{h}$ then the restriction must be V7. If this was not the case but the average was still greater than $0.92\text{m}^3/\text{h}$, then the blockage was diagnosed as V5. In either situation the operator was informed of the result on screen and the programme was terminated.

If the restriction remained undiagnosed at this point, the full 120 second 'Flow Standardisation Period' at 100% speed request was conducted and then a third average was taken. This was used to calculate the model V7 response expected when the speed request was dropped to 55%. Following this the speed request was dropped to 55% and the 20 point CUSUM procedure conducted. If the squared CUSUM value was found to be above the 0.7 threshold, then the restriction was diagnosed as V5. If this was not the case, then the restriction was most likely at V7. However, there was still a possibility that the restriction could be a severe V5 blockage. Therefore, the stored average 1, shown in Figure 4.23, was now retested to see if it was below $0.25\text{m}^3/\text{h}$, indicating a severe blockage. If this was not the case, then a V7 restriction was diagnosed. If the restriction still remained undiagnosed at this point then an immediate retest was the only option and this was undertaken to finally diagnose the location of the restriction and inform the operator.

4.11 Consideration of Internal Pump Blockage

It was not possible to recreate the tape blockage discovered in the pump but it was important to consider how the diagnostic would have reacted to this type of blockage. It was difficult to compare the results from before and after discovery of the tape as the diagnostic test cycle was changed with the speed request used to obtain the 'Base Flow' being altered.

When the tape was removed the flow rate produced by a given speed request increased. It can therefore be concluded that the tape was acting as a flow restriction and could be detected by monitoring of the speed request.

The blockage was not severe enough to fall in the range of the test cycle as at 100% speed request, with no valve blockage, the 2m³/h maximum flow was reached. Therefore, the blockage could not have been diagnosed by the current programme. In the case of larger internal blockages, which fall into the range of the programme, a distinction is likely to occur. As the diagnostic uses the presence of cavitation behaviour to distinguish between blockages, it is most probable that an internal pump blockage at the base of the impellor stack would cause cavitation and thus be diagnosed as a V5 blockage. An internal blockage which had formed near the outlet of the pump would not cause cavitation and would thus be diagnosed as a V7 restriction. In a real world application a restriction diagnosed as V5 could therefore produce a text string stating “Pipe blockage upstream of pump or internal pump inlet blockage present”, for example.

4.12 Chapter Summary

In this chapter the relevance of the WRAP Rig in an industrial water infrastructure was presented. The ideal capabilities of a deep bed water filtration plant efficiency system were defined as the ability to diagnose faults and control backwash based on filter bed condition. The WRAP Rig and experimental set up was described and a short literature review focussed on blockage diagnosis presented. This pointed towards time domain analysis of existing PLC signals as the best option for development of a SCADA-based diagnostic programme.

Initial testing revealed that there was a difference in the flow response caused by restrictions in the V5 Valve upstream of the pump and the downstream V7 Valve. This difference was linked to the extended transient behaviour present for V5 restrictions. A SCADA based function was written which ran an automatic pump speed request test cycle to expose the differing characteristics of V5 and V7 restrictions. This was achieved by performing a CUSUM of the difference between the actual flow response and the expected V7 response.

The discovery and removal of an internal pump blockage altered the flow characteristics produced by valve restrictions and a modification to the test cycle was required. However, the existing diagnostic concept was found to remain valid. A full diagnostic programme was developed which had the ability to distinguish between a V5 or V7 restriction of between 20% and 99.9%.

4.13 Conclusion

The work done had successfully demonstrated that non-time critical, low frequency algorithms could be used for blockage diagnostics. This was achieved using heuristically developed fault models which were then used by the programme to distinguish between two blockage locations. The methodology was shown to be suitable for application using SCADA software. Blockage diagnosis was defined as an important requirement of a filtration plant efficiency improvement system. It had also become clear that to achieve this, any functions written within the package must be mindful of the limitations of the software; firstly care must be taken to ensure the primary functions of the SCADA package are not compromised, as was the case when a 'While' loop was used for speed request control. Secondly, as user written functions have the lowest priority in terms of processor usage, programmes designed with highly time critical elements should not be used. In the developed diagnostic programme a pause in the execution of the code of up to a few seconds would have no impact on the final outcome of the test, as the steady state rather than the transient characteristics of the system were used in the diagnostic process. The developed approach and programme could also be applied to other similar plant with a minimum of effort. To do this the downstream blockage behaviour would be modelled as in Figure 4.16 and an equation of the line of best fit produced and substituted into the existing code. A small number of other tests would also be performed to define the range of the programme and some of the other decision values but once again, these could be substituted into the existing code.

It is noted that this was a first application and as such would require further development. Work to increase the range of the programme, to include smaller blockages, would be of value. The test results had shown that a strong CUSUM deviation still existed for the smallest blockages which were in the range of the programme. The range was limited by the need to keep the flow rate below $2\text{m}^3/\text{h}$. Therefore, one possibility would be to

experiment with using lower speed request values to obtain 'Base Flow' and produce CUSUM values for smaller blockages. It was decided not to investigate this further as the main objective of demonstrating that an applied SCADA system could be used for fault diagnostics had been achieved. In particular the level of analysis possible and the ability to initiate, control and manage a test cycle as part of the diagnostic process had been achieved. Considering the time consuming nature of the research work, it was decided to now move on to the task of developing a condition based filter backwash initiation programme.

Chapter 5

Condition Based Backwash and Blockage Detection

5.1 Introduction

The operational control strategy of a filter bed drastically affects the quality of the processed effluent produced and the efficiency of the water treatment system. The desired filter throughput is calculated at the design phase, being determined by the size of the filter, the type of filtration media, the unprocessed influent quality and the required water output quality. The system should be engineered to ensure that the throughput provides the best compromise between power efficiency, processed effluent quality and output of processed water.

When in operation, the filter bed will naturally begin to foul up as contaminants are filtered from the unprocessed liquor. This operational decay of filter bed permeability leads to increased power consumption as the pump has to work harder to maintain the set flow rate. The filter can be cleared of this contamination by means of backwashing. In this process clean water, often taken from the processed liquor tank if the process permits, is pumped backwards through the filter and discharged to drain. The backwash fluidises the filter media allowing the contamination to be released and flushed from the granules. The backwash flow rate is always higher than the filtration flow rate, to ensure that the maximum level of contamination is removed.

In the WRAP Rig the control of backwashing was achieved through a time based strategy. The time period between backwashing operations could be manually re-configured within the process control framework. The time period was initially configured through judgement, by the commissioning engineer and could be modified over time through trial and error by the operators. In most deep bed filtration plant pressure transducers are provided, upstream and downstream of the bed, in order that the level of fouling in the filter can be deduced. A raised pressure differential indicates a raised level of blockage. Examination and consideration of this differential at the backwash trigger points from historical data could help to refine the backwash timing. For example, if the differential

was low when backwash commenced, it can be deduced that the filter was not particularly fouled and the time between backwashes can be increased without any detrimental affects. Conversely, if the pressure differential was high the filter was over fouled and time between backwashes should be reduced.

It is important to optimise the time between backwashes as there are a number of financial and operational implications. In the case of excessive backwashing, production is halted too often so reducing output. Excessive backwashing also uses up processed liquor or fresh mains water, which has an associated cost. In many cases the backwash discharge to drain is monitored and charged for by the utility company. Backwash cycles also use significantly more power than normal service operation due to the high flow rates involved. In the case of infrequent backwashing, overall pump power consumption is increased due to the added effort needed to overcome a more completely fouled filter. This, in principal, increases the likelihood of pump failures. Processed effluent quality can also be affected by a fouled filter and the longevity of the filtration media can be reduced.

In light of the detrimental affects of over or under backwashing, it was asserted that the timing of backwashes could potentially be more efficiently controlled by a condition based strategy. Using appropriate non-time critical, low frequency algorithms this could be implemented in the SCADA software, using the filter bed pressure reading to trigger backwash, based on the level of fouling in the filter media. Work was thus undertaken to explore if a programme could be developed that would implement a condition based back wash initiation strategy. This would need to be robust enough to prevent unrelated faults, such as pipe blockages, triggering unneeded backwashes or masking fouled filter characteristics thus delaying required backwashes.

5.2 Chapter Structure

Accordingly, in this chapter, a review of previous work on filtration optimisation is given, and then the new research is presented. Tests results are used to demonstrate that filter blockage level does have a dramatic effect on pre-filter pressure and this allowed the development of the proposed SCADA-based filter blockage diagnostic for back wash initiation. In order to determine the robustness of this approach, the implications of pipe

blockages and combined filter and pipe blockages were explored via experimental test results.

5.3 Filter Backwash Literature Review

The concept of adaptive control of backwash duration (not triggering) was explored by Infalco Degremont Inc who produced a patent for an automatic backwash control system, for filter beds in a series arrangement[71]. The system pumped backwash liquor through each filter sequentially. When the measured particle count of the effluent from a particular filter fell below a pre-determined level, confirming successful backwash had been achieved, the backwash flow was redirected to the next filter in the series and so on, until all filters were cleansed. This approach required the addition of turbidity measurement instrumentation.

Amburgey [72] described the problem of filter “Ripening”. This refers to the increased passage of particles and micro organisms through granular filtration media, such as sand, in the period of time immediately following backwash. A technique, termed extended terminal subfluidisation wash, is outlined as a strategy to overcome this problem. Following the main backwash, a period of reduced flow backwash is initiated. The duration of this is sufficient to completely replace the volume of water held in the filter. In principle this subfluidisation wash will remove the main backwash remnant particles suspended in the filter, without dislodging more particles from the filtration media.

Other solutions to the problem of “Ripening” have been proposed and reported. Chipps et al [73] describe a procedure termed “Delayed Start” which involved refilling the filter with unprocessed liquor and then leaving it out of service for a set period, before resuming filtration. Chipps et al [73] also outline a “Slow Start” concept and a similar strategy was proposed by Colton et al [74]. “Slow Start” involves reducing the flow rate for a period directly following backwash, thus allowing the filter more time to deal with the increased turbidity of the “Ripened” water. These methods are not adaptive and could easily be implemented using PLC logic. Suthaker et al [75] however, put forward evidence that the particle passage through the filter during “Slow Start” could be managed by control of the influent solids flux rate (filtration rate multiplied by influent particle concentration), which represents an approach towards adaptive optimisation.

Bhargava et al [76] developed a mathematical method for determining the variation of backwash water turbidity with respect to duration of backwash, for a rapid sand filter. It was proposed that with knowledge of the grain size and volume of each layer of filter media, the required backwash duration could be calculated. It was asserted that this information could be used to optimise backwash duration. Continuing this modelling theme, Delgrange-Vincent et al [77] developed a neural network to predict the productivity of an ultra filtration pilot plant. The pilot plant utilised a cellulose acetate hollow fibre module as the filter. This generally behaved in a similar fashion to a deep bed sand filter, in that over the course of an operational cycle the filter became fouled so increasing resistance. The pilot plant operated on a sequential backwash regime. Experimental data was obtained from the rig with varying flow rates over numerous cycles. The transmembrane pressure which was calculated using data from pressure transducers, before and after the filter, was one of the variables considered along with the turbidity of the influent. The neural network model was refined to make use of the most pertinent variables. Thought was also given to removing those variables which would be most operationally expensive to obtain. The developed neural network showed a good degree of accuracy in predicting the expected resistance caused by fouling over long term time scales (in excess of 100 filtration cycles). The intention stated was to apply the neural network to the control strategy of the pilot plant. In the author's opinion, the double neural network model proposed, combined with the need for training, puts the system into a high complexity bracket. It is also not clear how transferrable the method may be to other ultra filtration plant, which present differing membrane Cross Sectional Area (CSA) for example.

Yigit et al [78] explored the impact of seven general backwash strategies on the fouling characteristics of a submerged membrane bioreactor. The pilot plant used was fed with domestic waste generated by a university campus. It was found that fouling rates and membrane resistances, generally decreased with more frequent backwashing (i.e. shorter filtration periods). It was also observed that the detrimental effects of too long a filtration duration on membrane resistance, out-weighed the positive effects of optimised backwash duration. This indicated that the key parameter for an efficient backwash regime was a correctly timed initiation of the backwash cycle. This supports the decision to consider backwash initiation timing in this research.

A highly relevant paper by Smith et al [79] proposed a pressure based approach to backwash initiation of a membrane based filtration system. Fouling is considered a major problem in the application of this technology. In a similar fashion to sand filtration, increased fouling leads to permeability decline and therefore higher energy demands to maintain a constant permeate flux. It is reported that previous studies on membrane cleaning using complex models, statistical approaches and trial and error have produced promising results, in terms of evaluating the ideal time between backwashes. However, all these results rely on a constant permeate flux and level of influent contamination, which is stated not to be the operational reality. Membranes differ from sand in that, in the relatively short term, a certain level of irreversible fouling occurs, which cannot be removed by backwash and this is reflected in the Trans-membrane Pressure (TMP) time profile as shown in Figure 5.1.

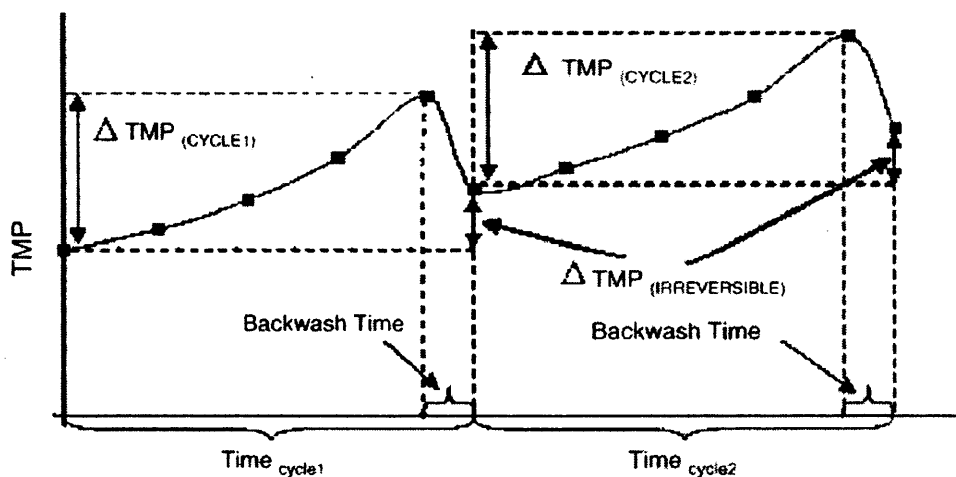


Figure 5.1: Generic profile of a membrane system operating with a periodic backwash cycle. (Smith et al [79])

It can be seen in the figure that after the backwashes the TMP has been reduced by fouling removal but the irreversible fouling prevents a return to the base TMP. Eventually, the membrane must be removed for physical or chemical cleaning. Analysis of the problem, using a mathematical model, confirmed that fluctuation in flux and contamination levels indeed undermined the effective operation of a fixed time between backwash approach. Too short a period, led to unnecessary backwashes wasting time and reducing the possible throughput. Too much time between backwashes led to increased energy consumption and also increased the level of irreversible fouling. To optimise the backwashing the researchers proposed a closed feed back loop based on the TMP. The

build up of irreversible TMP however, caused a problem if a TMP threshold based backwash approach was used, as can be seen in Figure 5.2.

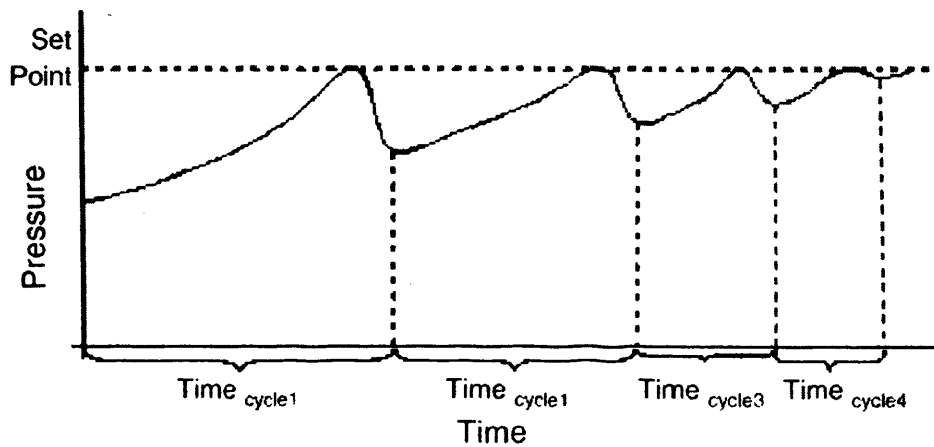


Figure 5.2: Profile of a closed loop control system applied to a membrane system.

(Smith et al [79])

The researchers argued that with this method of control the amount of TMP increase allowed in each cycle diminishes, leading to decreased production as the cycle times decreased. Therefore, a revised strategy which used the relative increase in TMP was developed. To test the new system an experimental rig simulating industrial conditions was constructed. Then a set of fixed filtration time between backwash, and backwash duration combinations, were tested to find the optimum configuration for the system. Having found the optimum setting, this data was used for comparison with the new adaptive control method. As mentioned, the level of irreversible TMP increases with each cycle until production must be stopped for cleaning. This level of TMP was set to 50kPa in their tests. As a result of the initial testing, it was found that a rise in TMP of approximately 3% of the total allowable rise gave the best performance. Therefore, a single set TMP value was not used, as was the case in Figure 5.2. Backwash was instead triggered each cycle by a rise of 3% of the last TMP (following the previous backwash). When the results for the new control system were compared with the optimum fixed time results, it was found that although the increase of TMP with operational time remained similar, the number of backwashes required was reduced by 40%. This work demonstrated the possible benefits of adaptive backwash control based on the pressure response and provided valuable insight into how this may possibly be achieved for the deep bed sand filter in the WRAP Rig.



5.4 Filter Bed Response Testing

5.4.1 Test Set Up

In order to simulate the pressure response caused by a reduction of flow across the filter bed, a 1" ball valve identical in dimensions to those already installed was added to the rig and designated VF. The valve was added between the outflow from filter F2 and the inflow to the pressure transducer PT4 as illustrated in Figure 5.3.

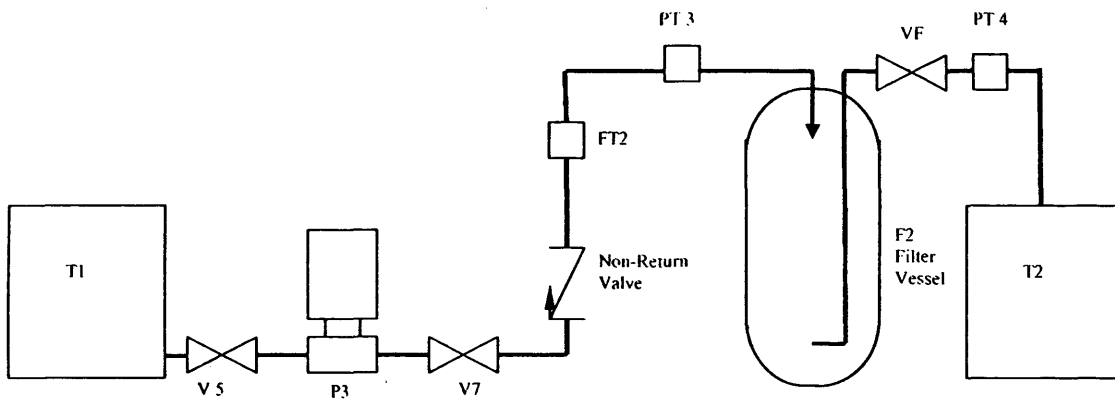


Figure 5.3: Simplified Schematic of the filter 2 subsystem showing filter fouling simulation valve VF.

This modification was utilised as fouling the bed using actual particulate matter was deemed to be impractical, due to the excessive testing time required to backwash and re-contaminate the bed. Also obtaining a good level of repeatability for testing would have been difficult, considering the inexact nature of fouling the bed manually.

The addition of a valve to simulate filter head loss due to fouling was considered a good approximation, as shown by the explanation of loss of head due to fouling adapted from Svarovsky [80] and summarised in the following:

The accumulation of deposits in a layer of the bed decreases the layer's permeability. For a filter operated at constant rate there is a consequent increase in the hydraulic pressure across the layer which is proportional to the quantity of deposit present.

$$\frac{\partial H}{\partial L} = \left(\frac{dH}{dL} \right)_0 + K\sigma \quad (5.1)$$

Where $(dH/dL)_0$ is the initial hydraulic gradient across the clean filter material and σ is the quantity of deposit per unit filter volume (which is dimensionless). K is the deposition rate in m^3/s . The total head loss H , across the combined layers of the filter, is obtained from integration of this equation with respect to the depth L at any time t .

$$H = H_0 + KvC_0t \quad (5.2)$$

Where H_0 is the initial clean filter head loss across the layers, v is the approach velocity in m/s equal to the volumetric flow rate per unit face area of the filter and C_0 is the inlet concentration. This equation is illustrated in Figure 5.4.

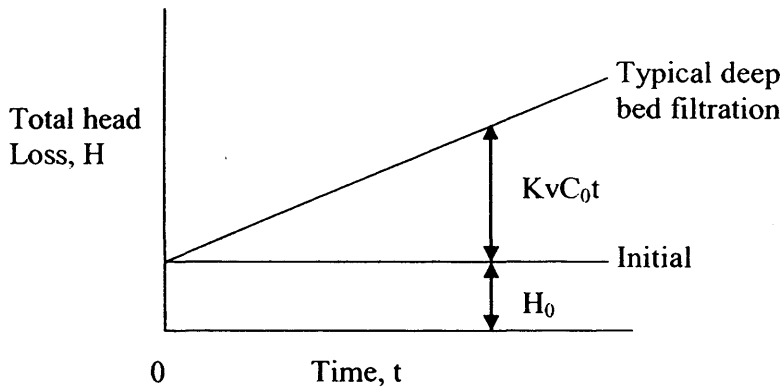


Figure 5.4: Total head loss varying with time.

The reduction of permeability across the filter can thus adequately be reproduced by a valve, which can be set to provide a reduction in head. After calibration the valve can be used to represent the level of expected natural decay at varying points in time.

5.4.2 VF Testing

In order to determine the system response to filter fouling, under operational conditions, the characteristics produced by restrictions of VF were examined, with the rig under PID control.

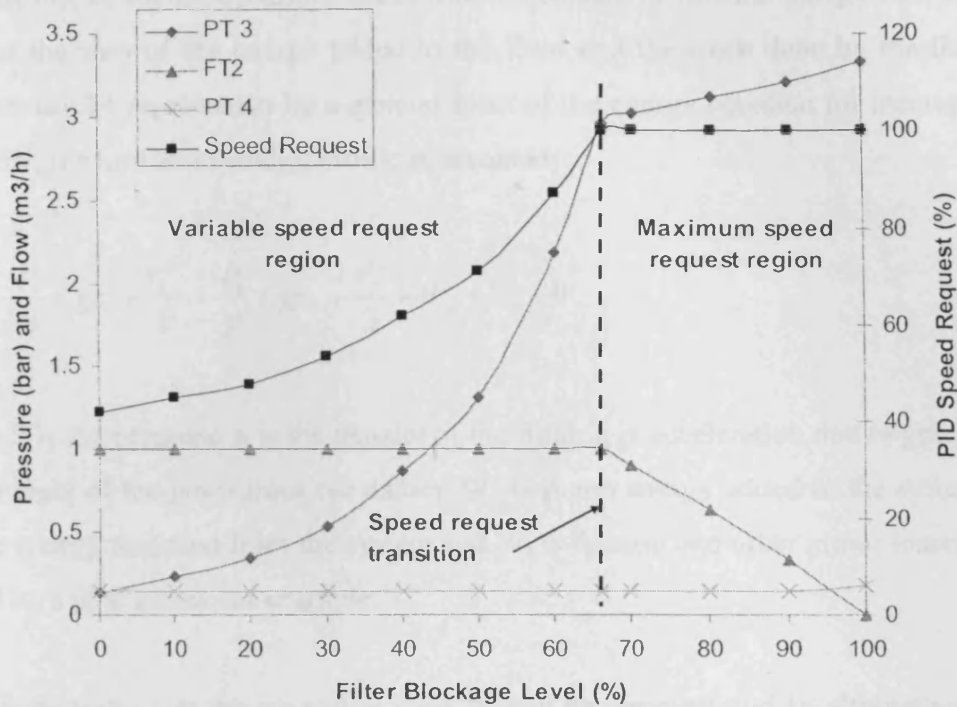


Figure 5.5: System response to VF blockages in PID mode.

Figure 5.5 demonstrates the response of the system to VF restriction levels from 0 to 100%. In the 'Variable Speed Request Region' the increase of blockage level caused the PID speed request to increase in an attempt to maintain the target flow of 1m³/h. As a result, the pressure built up behind the VF restriction which resulted in the pronounced PT3 response. Once the blockage became severe enough to cause maximum speed request the steep rise of PT3 pressure changed to a more gradual rise versus blockage level. In the 'Maximum Speed Request Region', the flow was now seen to fall, as the increasing VF restriction was no longer counteracted by the flow maintaining action of the PID. From these tests, PT3 showed the most pronounced response, whereas PT4 remained virtually unaffected. Thus it was decided to concentrate on PT3 as a potential indicator of filter blockage level.

5.4.3 Blockage Pressure Response Theory

If the pressure response was to be used for diagnostic purposes, it was important to understand the theory behind the observed behaviour. This would confirm that the behaviour was the result of repeatable system characteristics and that the approach would have the potential to be deployed to other systems.

The first law of thermodynamics states that the change of internal energy of a system is equal to the sum of the energy added to the fluid and the work done by the fluid [81]. This law can be represented by a general form of the energy equation for incompressible pipe flow, if a uniform velocity profile is assumed;

$$\frac{P_1}{\rho} + gz_1 + \frac{V_1^2}{2} = \frac{P_2}{\rho} + gz_2 + \frac{V_2^2}{2} - W_p + W_t + W_f \quad (5.3)$$

Where P is the pressure, ρ is the density of the fluid, g is acceleration due to gravity and z is the height of the point from the datum. W_p is pump energy added to the system, W_t is turbine energy removed from the system and W_f is friction and other minor losses such as caused by a pipe elbow for example.

There is no turbine in the rig and as such W_t can be removed and an alternative form of the energy equation can be produced if equation 5.3 is divided by g;

$$\frac{P_1}{\rho g} + z_1 + \frac{V_1^2}{2g} = \frac{P_2}{\rho g} + z_2 + \frac{V_2^2}{2g} - H_p + H_f \quad (5.4)$$

Where $P/\rho g$ is the pressure head, z the elevation head and $V^2/2g$ the velocity head. H_p is the total dynamic head added by the pump and H_f represents friction and minor head losses. The units are energy per unit weight of liquid in Nm/N, which can be simplified to leave units of meters (m). A calculated value represents the elevation that the fluid would reach under atmospheric pressure. This is a direct measure of the pressure at that point, since 1 metre of head is approximately equal to 0.1bar of pressure. If the results given for all points along a pipeline are plotted, this is known as the Hydraulic Grade Line (HGL).

In order to plot the HGL for the rig, the Hydroflo piped system design engineering software was utilised [82]. A model of the WRAP rig filter 2 sub-system was created within the software. The intention of the model was to provide an approximation of the PT3 pressure response, caused by different blockage conditions, for theoretical confirmation of experimental results. It was not judged practical or necessary to create a highly accurate model as the physical embodiment of the rig was complicated. The purpose of the model was for comparative analysis of general trends, rather than

quantitative analysis of exact pressure response. The appropriate heights were programmed in for the system elements. PVC friction calculation details for pipe work were selected from the software and appropriate pipe lengths set. Elbows were omitted as their effects were minimal and would not undermine the theoretical verification required from the model. The pump performance curve for the Grundfos CRI 3-6 was incorporated into the software. The HGL obtained for the system model with no blockages can be seen in Figure 5.6.

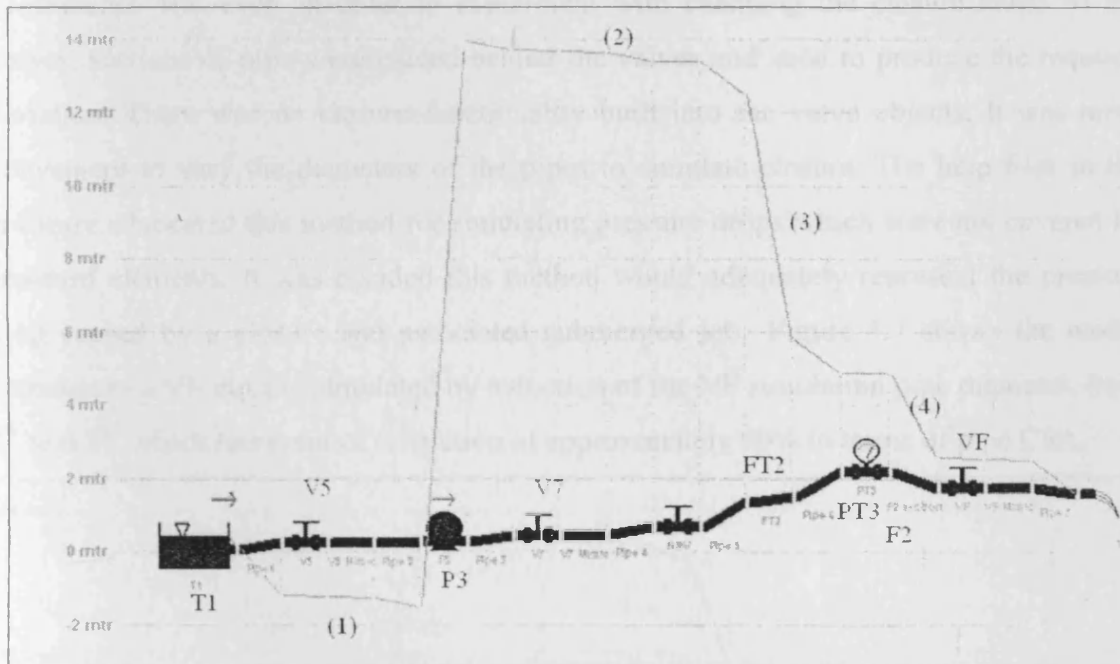


Figure 5.6: HGL for system with no blockages.

The model representation in Figure 5.6 gives the system elements a standard width to simplify interpretation. The water level in T1 and the P3, PT3 and outlet height were all entered into the software. The height arrangement of the elements between these is an arbitrary result of the model diagram and has no effect on the results. It can be seen that between T1 and P3 the HGL is negative (1). This is due to the fact that P3 is higher than the T1 outlet. After P3 the HGL rises which is a result of the energy fed into the system by the pump. Between P3 and FT2 the losses caused by the various pipe runs and valves can be seen (2). There is a large loss of pressure across FT2 (3) as the diameter of the pipe is reduced from 1" to 0.5", due to the design of the flow transmitter. There is also a significant drop (4) across the pipe marked F2. For this element the distance was set to 5m, to approximate the transit of the water through the unblocked F2 filter bed. The exact

level of head loss caused by the clean filter, due to the added friction of the granular media, was not researched. A restriction caused by filter fouling would be created by adjusting the VF simulation valve, as was the case in the actual rig experiments. In the simulation the pump is running at maximum speed request.

The pressure drop seen across a partially closed valve is a result of the generation and dissipation of turbulent eddies, in the high shear layer around the submerged jet [83]. In the model, the valves V5, V7 and VF were set as ball valves with appropriate flow coefficients. However, in order to experiment with changing the closure levels of the valves, sections of pipe were placed behind the valves and used to produce the required variation. There was no closure functionality built into the valve objects. It was more convenient to vary the diameters of the pipes to simulate closure. The help files in the software advocated this method for simulating pressure drops which were not covered by standard elements. It was decided this method would adequately represent the pressure drop caused by a closure and associated submerged jet. Figure 5.7 shows the model response to a VF closure simulated by reduction of the VF simulation pipe diameter, from 1" to 0.3", which represents a restriction of approximately 90% in terms of pipe CSA.

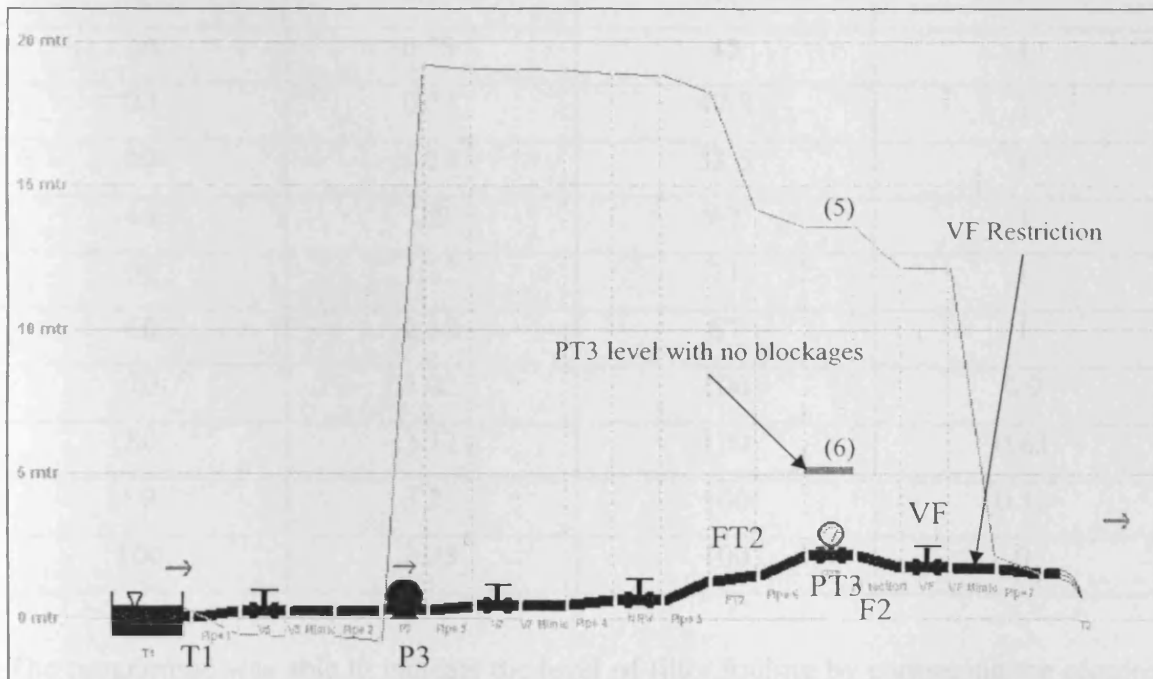


Figure 5.7: HGL for an isolated VF restriction.

It can be seen in Figure 5.7 that the pressure registered at PT3 (5), with a VF restriction in place, had dramatically increased compared with the blockage free case (6), transferred from Figure 5.6. With the blockage now downstream of PT3, the effect of back pressure

would be registered by the pressure transducer. This profile concurred with the pressure data seen for VF closures, in the 'Maximum Speed Request Region' of Figure 5.5, where an increase of restriction at VF, resulted in an increase in the pressure registered by PT3. This analysis further confirmed that the pressure response witnessed was a true reflection of the system characteristics, and could reliably be used as the basis for further investigation.

5.5 Filter Bed Fouling Monitoring Programme

The response of PT3 to varying filter blockage levels was used to create a simple real time filter bed fouling indication programme. The results from Figure 5.5 are now shown in tabulated form in Table 5.1. It was the PT3 pressure response and corresponding filter blockage level data that were utilised by the programme as highlighted in yellow.

Table 5.1: PID response to VF restriction.

VF blockage level (%)	PT3 response in PID mode (bar)	SR response in PID mode (%)	FT2 response in PID mode (m ³ /h)
0	0.13	42	1
10	0.23	45	1
20	0.34	47.8	1
30	0.54	53.5	1
40	0.9	62	1
50	1.32	71	1
60	2.18	87	1
70	3.02	100	0.9
80	3.12	100	0.63
90	3.21	100	0.33
100	3.33	100	0

The programme was able to indicate the level of filter fouling by comparing the acquired PT3 pre-filter pressure reading with the pressure data contained in Table 5.1. The categories shown in the table were used to express the general blockage level. For example, if the PT3 pressure was found to be 1.5bar, this lay between the values seen for blockages of 50% to 60% in the programme look up table. A process mimic of the filter 2

sub-system was created using the HMI functionality of the SCADA package and is shown in Figure 5.8.

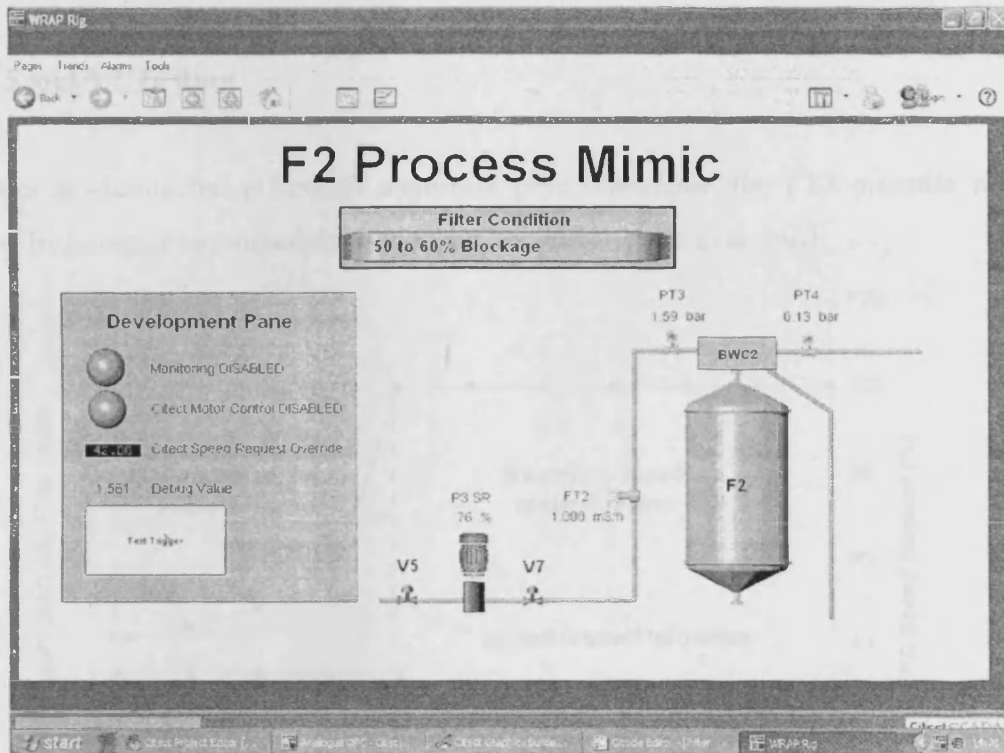


Figure 5.8: Filter bed 2 sub system process mimic.

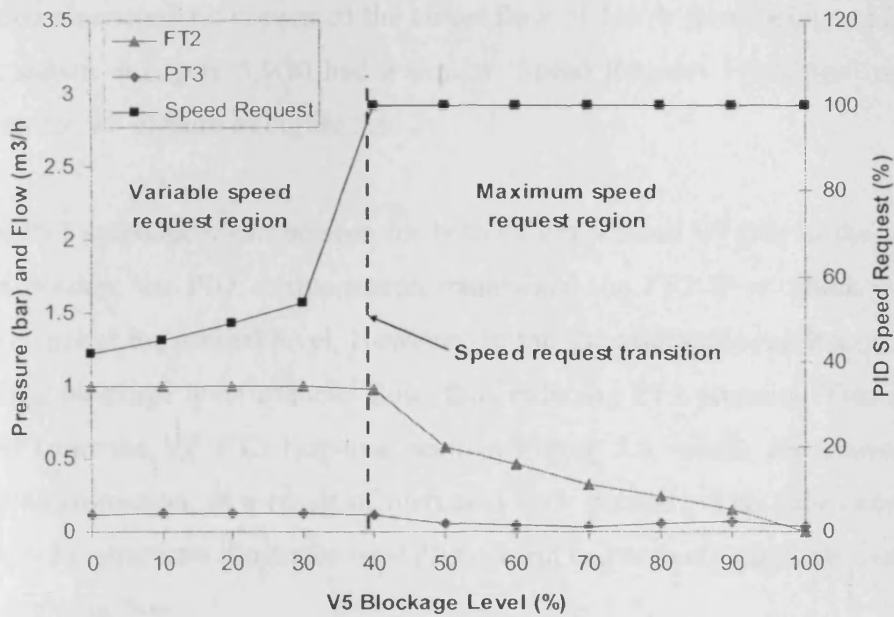
The values of the process variable tags such as the PT3 and PT4 pressures were represented in real time, next to the relevant system elements, on the process mimic of Figure 5.8. A repeating 'Event' was set up using the configuration boxes within Citect (see section 4.3.2). This event could be configured to trigger at any time interval. The triggering of the 'Event' was configured to call up the Filter Bed Fouling Monitoring Programme, which was written in Cicode using the Integrated Development Environment provided within the software. This function read the current value of the PT3 variables from the Citect I/O Server and compared this with the coded version of Table 5.1 to assess the level of filter fouling. The programme then selected an appropriate message from another coded look up table and by means of a text string variable, linked to the process mimic, displayed this in the Filter Condition box seen at the top of Figure 5.8.

As a result the programme was able to continually update the Filter Condition. This simple programme functioned correctly and could potentially be used to trigger backwash based on the level of blockage in the filter. However, it was deemed important to discover

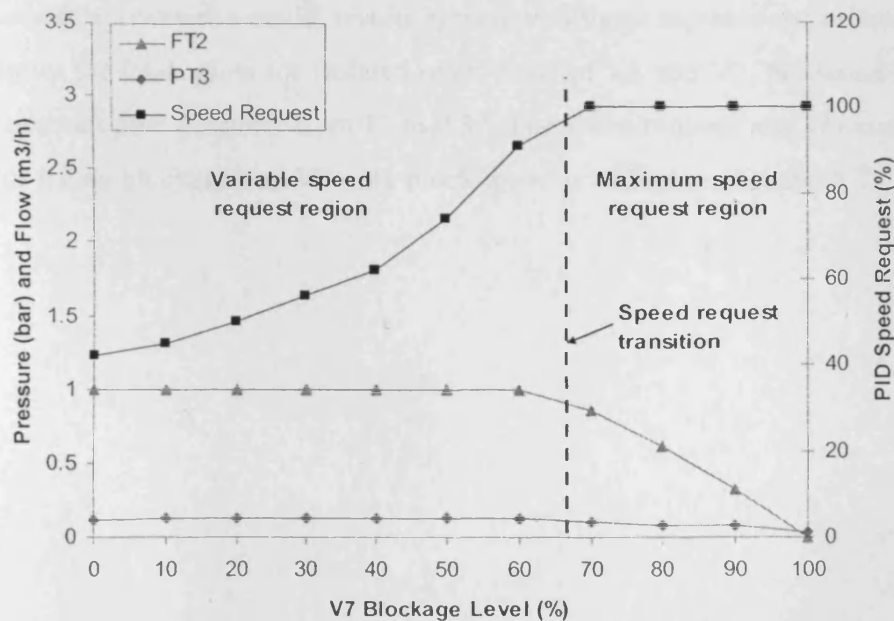
if other blockages in the system would alter the PT3 pressure response, thereby undermining this simple approach.

5.6 V5 and V7 Testing

In order to define the effects of abnormal pipe blockages, the PT3 pressure response caused by isolated individual restrictions at V5 and V7 was examined.



(a) V5 Response



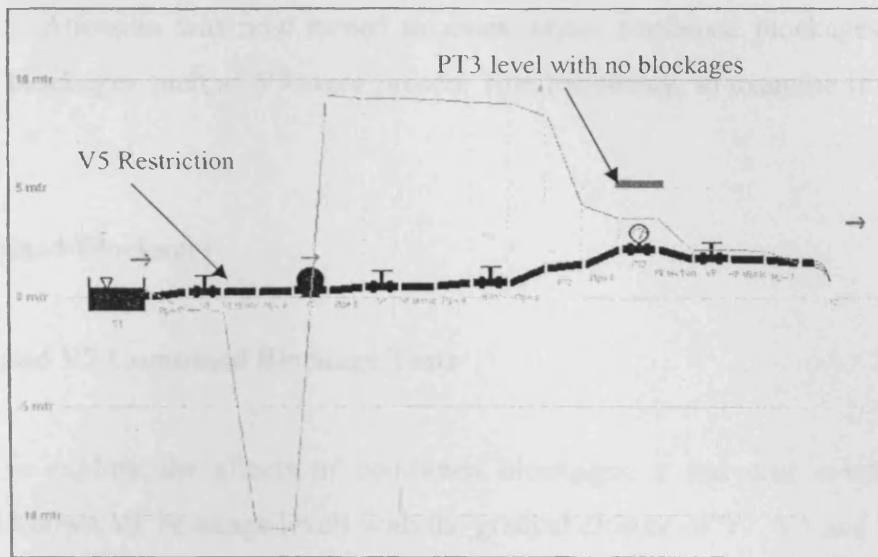
(b) V7 Response

Figure 5.9: System response to closures of V5 and V7 in PID mode.

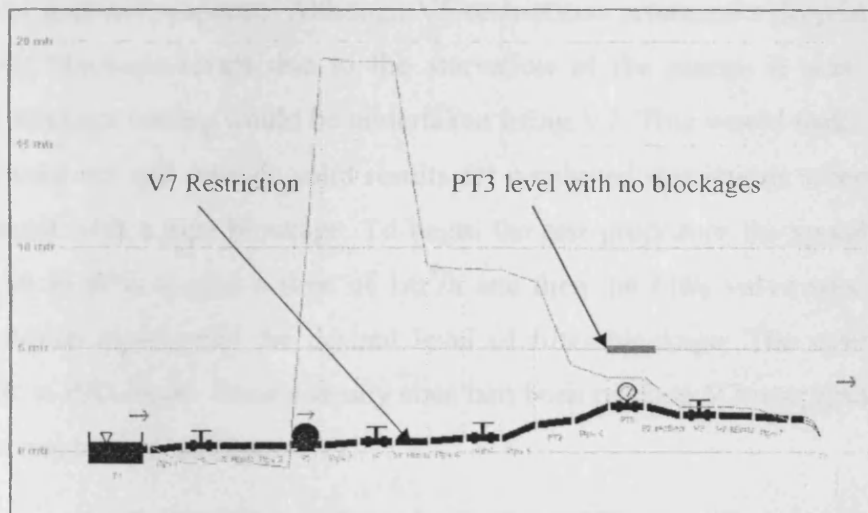
The V5 and V7 restrictions showed a similar general pattern to VF restrictions for FT2 and speed request responses. The V5 results shown in Figure 5.9(a) experienced the 'Speed Request Transition' at a much lower blockage level (40%) than the VF results shown in Figure 5.5. This was symptomatic of the position of the valve relative to the pump. V5 was upstream of the pump and as such caused pump starvation when closed. The V5 response reached a critical point around the 30% closure level, where the starvation characteristic prevented the target flow of $1\text{m}^3/\text{h}$ from being achieved. The V7 results shown in Figure 5.9(b) had a similar 'Speed Request Transition' point (66%) to that seen for VF closure in Figure 5.5.

For the PT3 response it can be seen for both valves V5 and V7 that in the variable speed request portion, the PID compensation maintained the FT2 flow which maintained the PT3 pressure at the normal level. However, in the 'Maximum Speed Request Region' the increasing blockage level reduced flow, thus reducing PT3 pressure. This PT3 response differed from the VF PT3 response seen in Figure 5.5, where the pressure rose with increasing restriction, as a result of increased back pressure. The behaviour seen for the V5 and V7 restrictions illustrates how PID control can actively mask abnormal blockages by maintaining flow.

The theoretical hydraulic model results agreed with those captured experimentally. Figure 5.10 shows the HGL plots for isolated restrictions of V5 and V7, produced by narrowing of the relevant pipe diameter from 1" to 0.3". The speed request was at maximum, as was done for the no blockage and VF only blockage tests of Figures 5.6 and 5.7.



(a) *V5 Restriction.*



(b) *V7 Restriction*

Figure 5.10: Hydraulic model results for V5 and V7 restrictions.

In both V5 and V7 restrictions the pressure at PT3 was lower than the level obtained with no blockages in place. Figure 5.10(a) shows that a highly negative pressure is created before the pump by a V5 restriction. This is termed a suction head and creates the ideal conditions for the cavitation behaviour discussed in Appendix C.

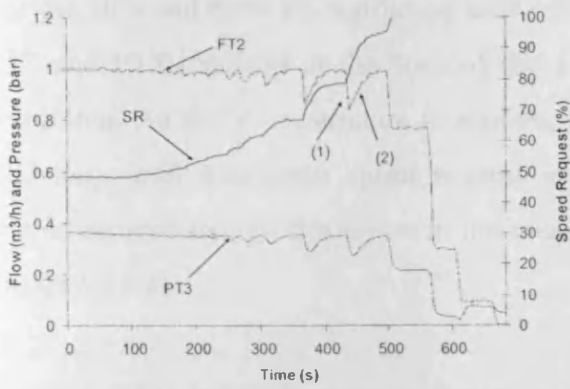
These tests demonstrated that abnormal blockages could lower the PT3 pressure response. It was hypothesised that in a scenario where an isolated filter blockage heightened the PT3 pressure, this would then be reduced if an abnormal pipe blockage was added to the system. If this were the case, the abnormal blockage would lower the level of filter blockage perceived by the Filter Bed Fouling Monitoring Programme, described in

section 5.5. Attention was now turned to cases where combined blockages of VF and abnormal blockages such as V7 were present simultaneously, to examine if this was the case.

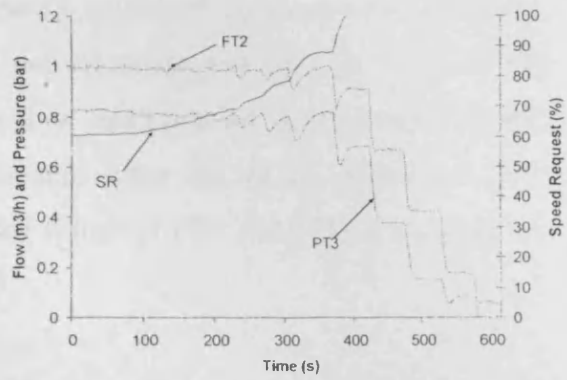
5.7 Combined Blockages

5.7.1 VF and V7 Combined Blockage Tests

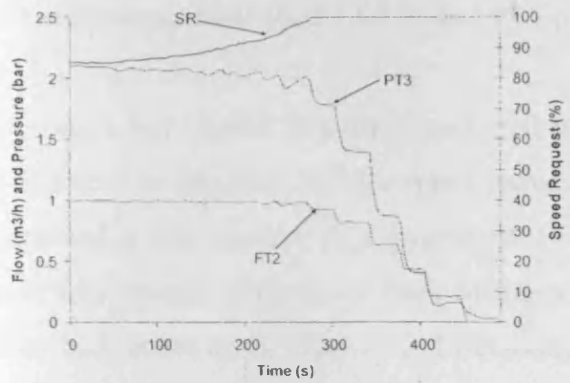
In order to explore the affects of combined blockages, a test was conducted which combined known VF blockage levels with the gradual closure of V7. V5 and V7 had been shown to produce similar overall characteristics in terms of the effect of a restriction on the pre-filter pressure response. Although V5 restrictions produced a drop in the pressure at far lower blockage levels due to the starvation of the pump. It was decided that combined blockage testing would be undertaken using V7. This would make testing more straightforward but still provide valid results for combined restrictions where VF fouling was combined with a pipe blockage. To begin the test procedure the speed request was manually set to 42% to give a flow of $1\text{m}^3/\text{h}$ and then the filter valve was set to give a flow rate which represented the desired level of filter blockage. The system was then turned back to PID mode. Once a steady state had been reached V7 was gradually closed. The results can be seen in Figure 5.11.



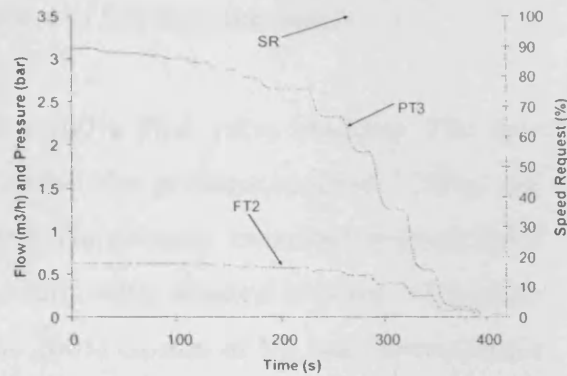
(a) VF 20% Closure



(b) VF 40% Closure



(c) VF 60% Closure



(d) VF 80% Closure

Figure 5.11: Gradual V7 closure performed at four different VF blockage levels.

Figure 5.11(a) is a combination of a gradually increasing V7 restriction, applied with a constant VF restriction of 20% already in place. The steps seen in the data were considered to be a result of the stiffness of V7 preventing smooth closure. For example, the sudden fall in flow marked (1) in Figure 5.11(a) was a result of V7 being closed by a small but finite amount. The flow recovery caused by the PID loop speed request response is marked as (2). It can be seen in Figure 5.11(a) that at the start of the test the speed request is slightly raised due to the VF blockage. The PT3 pressure is also higher than the normal 0.13bar. As the V7 restriction is increased, the speed request gradually rises to compensate, which maintains the flow measured by FT2. The fact that the flow rate is maintained results in the pressure measured by PT3 being maintained at the starting level. This continues until the V7 restriction becomes so severe that the speed request reaches saturation. After this the further increases in V7 restriction led to a drastic reduction in the FT2 and PT3 measured values.

For the 40% and 60% VF restriction tests of Figure 5.11(b) and (c), it can be seen that the FT2 and PT3 readings at the start of the test are raised, in line with the level of VF restriction. As the V7 restriction is applied, the flow and pressure are maintained by the PID loop until maximum speed request is reached. After this point, increases in V7 restriction lead to significant loss in the measured values of FT2 and PT3, as was seen in Figure 5.11(a).

Figure 5.11(d) differs as at the beginning of the test, the VF restriction of 80% is already severe enough to require maximum speed request. As a result, the gradual addition of a V7 restriction causes the FT2 flow and PT3 pressure to fall from the outset.

The same test regime was also conducted with a 100% filter valve blockage. The flow was found to be zero and the speed request 100%. The pressure reached 3.33bar and remained at this level as V7 was gradually closed. The pressure remained, even after V7 was fully closed. This was a result of the non-return valve situated between V7 and the filter bed, as shown in Figure 5.3. Effectively the 100% closure of VF and the non-return valve turned this section of the pipe into a pressure vessel. P3 pumped water into the pipe, which became pressurised due to the blockage at VF. Even when the pump was stopped, the non-return valve prevented the pressure escaping. A separate test conducted confirmed this. The speed request was set to 100% and VF was fully closed. The pre-filter pressure was seen to rise to 3.33bar. The speed request was then set to 0%. The section of pipe remained pressurised. Over the next twenty minutes there was only a slight decay of 0.03bar pressure, which can be attributed to minor leakage from the non-return valve.

The test results had demonstrated that in the 'Variable Speed Request Region' the action of the PID loop maintained the FT2 flow. Thus, the PT3 pressure caused by the VF restriction was also maintained, despite the addition of a V7 restriction. This indicated that in the 'Variable Speed Request Region' the programme developed in Section 5.5 would still correctly assess the level of filter restriction, despite the addition of an abnormal blockage. The speed request however, did alter with the addition of the V7 restriction, offering a potential indication of the presence of an abnormal blockage. In the 'Maximum Speed Request Region' the addition of an abnormal restriction drastically altered the PT3 pressure response thus undermining the programme described in section 5.5.

A more in depth evaluation of the system variable responses to combined blockages was undertaken. The objective was to extend the functionality of a condition based backwash programme into the 'Maximum Speed Request Region' and to determine if the speed request could be used for abnormal blockage detection in the 'Variable Speed Request Region'.

5.7.2 Multivariate Blockage Signature Analysis

It was decided to examine if the combined response of all three variables differed, depending on whether a filter bed only blockage or a combined filter bed and a pipe blockage was present.

In order to do this the speed request, FT2 and PT3 results from the VF only blockage tests shown in Figure 5.5 and summarised in Table 5.1, were cross referenced with the Figure 5.11 combined blockage test results. Figure 5.12 shows an example of one of the forty comparisons undertaken, to explain the procedure.

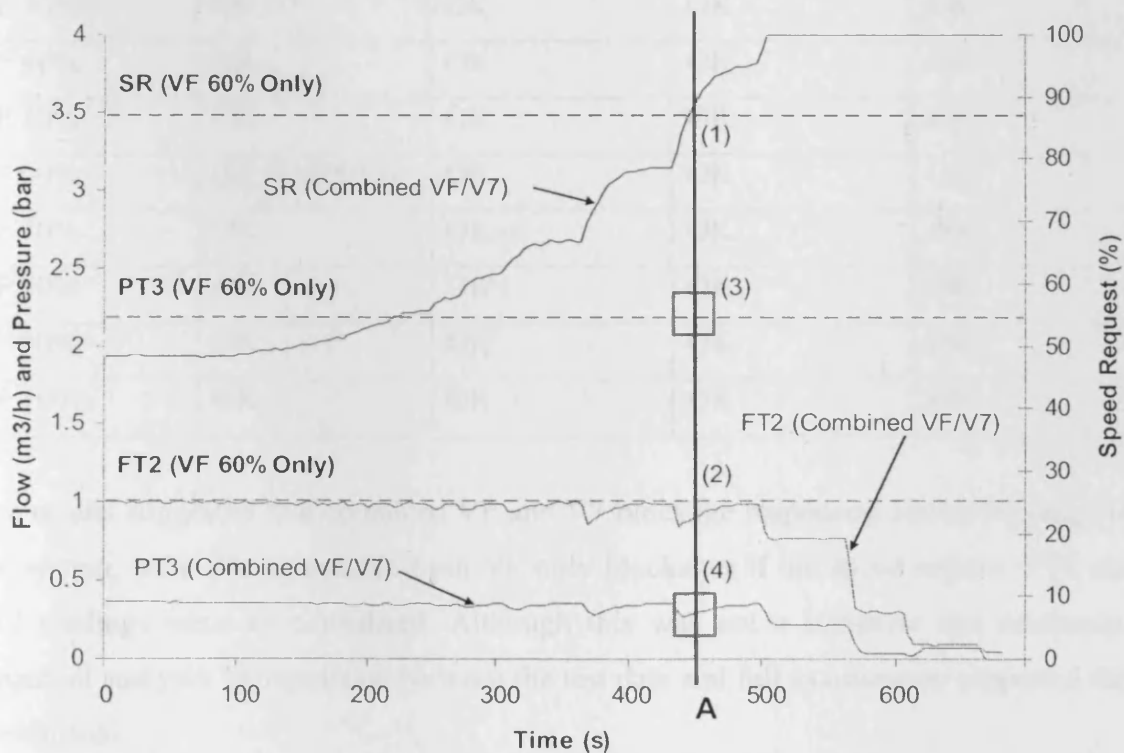


Figure 5.12: 60%VF only variable values cross referenced with variable response of combined 20% VF and increasing V7 restriction test.

In Figure 5.12 straight dashed lines representing the speed request, FT2 and PT3 readings for a 60% VF only blockage (as taken from Table 5.1) are applied to the combined blockage test results form Figure 5.11(a). It can be seen that after time A, the speed request (1) and the FT2 (2) readings for the VF only blockage are similar to the combined blockage readings. However, at this time the PT3 readings obtained for the VF only (3) and combined blockage (4) are very different, as highlighted by the squares. Therefore, in this test, it is concluded that at no point does a VF only blockage have an identical signature to a combined blockage if all three variables are considered. The results of the entire cross referencing process are shown in Table 5.2 with “OK” denoting that the VF only and combined blockages always had unique signatures. The test featured in Figure 5.12 is highlighted in the table.

Table 5.2: VF only and combined VF/V7 variable cross referencing results.

	VF 20%/V7	VF 40%/V7	VF 60%/V7	VF 80%/V7
VF 10%	OK	OK	OK	OK
VF 20%	OK	OK	OK	OK
VF 30%	OK	OK	OK	OK
VF 40%	OK	OK	OK	OK
VF 50%	OK	OK	OK	OK
VF 60%	OK (Fig. 5.12)	OK	OK	OK
VF 70%	OK	OK	OK	OK
VF 80%	OK	OK	OK	OK
VF 90%	OK	OK	OK	OK
VF 100%	OK	OK	OK	OK

The results suggested that combined VF and V7 blockage responses, across the range of the system, were distinguishable from VF only blockages if the speed request, PT3 and FT2 readings were all considered. Although this was not a complete and continuous empirical analysis, extrapolation between the test data and full examination supported this conclusion.

5.8 Condition Based Backwash and Blockage Detection Programme

5.8.1 Programme Concept

The approach used to facilitate robust operation of the programme was to model the response of the system variables to VF only restrictions, and then tests for deviations from this model to detect abnormal pipe blockages.

The VF only restriction system response fell into two distinct regions, as indicated in Figure 5.5. In the 'Variable Speed Request Region', the FT2 reading is maintained at $1\text{m}^3/\text{h}$ by the action of the PID loop. The speed request and PT3 response are seen to be the VF blockage level dependant variables. In the 'Maximum Speed Request Region' the FT2 and PT3 readings are the blockage dependant variables, as the speed request has reached saturation. Due to this change in blockage dependant variables, it was decided to create separate models for the two regions.

5.8.2 Variable Speed Request Region

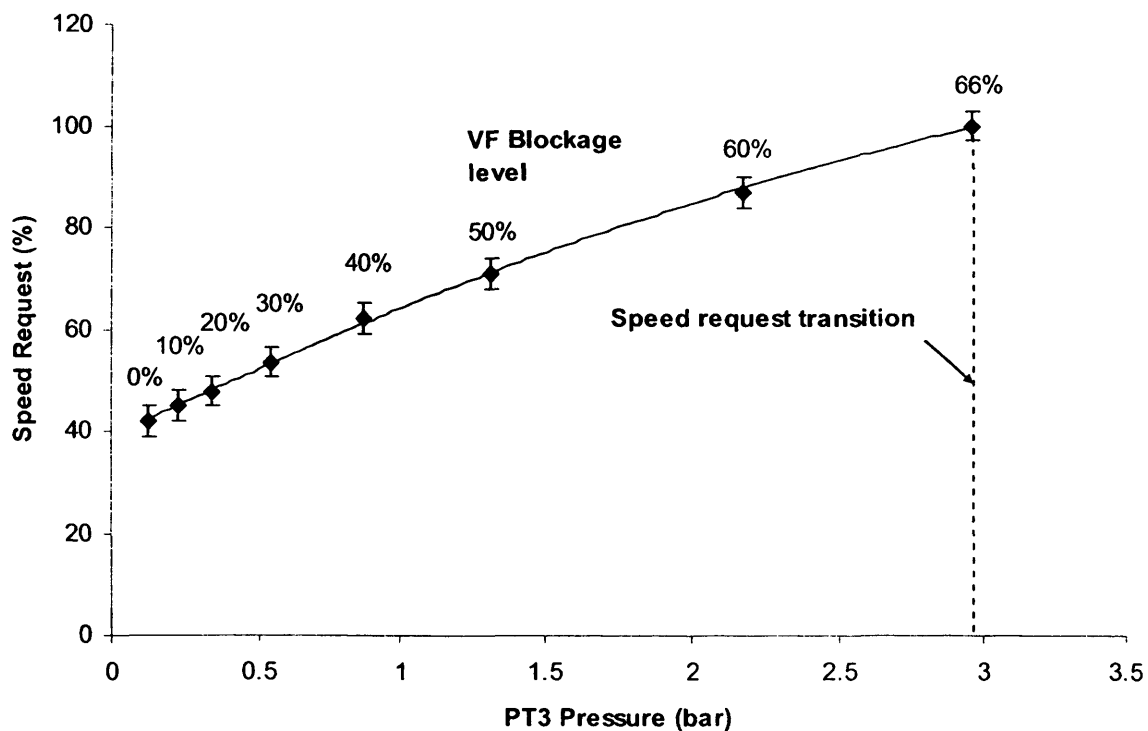


Figure 5.13: Speed request and PT3 relationship for a range of VF blockage levels in the 'Variable Speed Request Region'.

The relationship between the speed request and PT3 data from the 'Variable Speed Request Region' of Figure 5.5 was plotted to give Figure 5.13. A convincing line of best fit was possible and had the equation;

$$SR = -2.43PT3^2 + 27.74PT3 + 38.83 \quad (5.5)$$

This equation could potentially be used within a programme to decide if an unknown blockage was the result of pure filter bed fouling, or if the behaviour moves away from this, other blockages were present. An error band would have to be applied to the curve to account for signal fluctuation. The size of the allowable error was critical, as too large an error allowance would desensitise the system, leading to combined faults being diagnosed as filter bed only blockages. Too small an error band would lead to normal signal fluctuation, seen in a filter only blockage, causing an incorrect combined blockage diagnosis. It was found, from testing, that for lower VF blockage levels the addition of a 10% V7 blockage would cause the speed request to rise by approximately 3%. For higher VF blockage levels, the addition of a 10% V7 blockage, only produced a 2% increase in speed request. The V7 blockage level had to be increased to 15% to attain a 3% increase in speed request. It was also seen that the pressure was unaffected by the addition of the V7 blockages, as the corrective action of the PID loop maintained flow and thus pressure. As a compromise between over and under sensitivity, an error of $\pm 3\%$ was chosen and is represented on Figure 5.13. This meant that in the most extreme case, a VF blockage combined with a V7 blockage of 15% would be misdiagnosed as filter only fouling. This was a comparatively minor pipe blockage level for the system to miss but ensured that the more serious situation of normal filter fouling being diagnosed as a combined blockage, was highly unlikely.

It should be noted that pipe blockages may require maintenance action by personnel. This approach means that unnecessary actions arising due to the misdiagnosis of a filter bed blockage, as a pipe blockage, will be avoided. The worst case scenario will be the delay of appropriate maintenance action which, given the low level of blockage present, is not a concern due to the limited damage and cost.

A benefit of this style of approach is that the method and code may be applied to any similar set up. The line of best fit in equation 5.5 would need to be re-established, if

changes to the set up were introduced, but this process would be straightforward and would continue to support effective blockage detection.

5.8.3 Maximum Speed Request Region

In the ‘Maximum Speed Request Region’ it was necessary to consider the relationship between FT2 and PT3, as these were now the blockage dependent variables. The results can be seen in Figure 5.14.

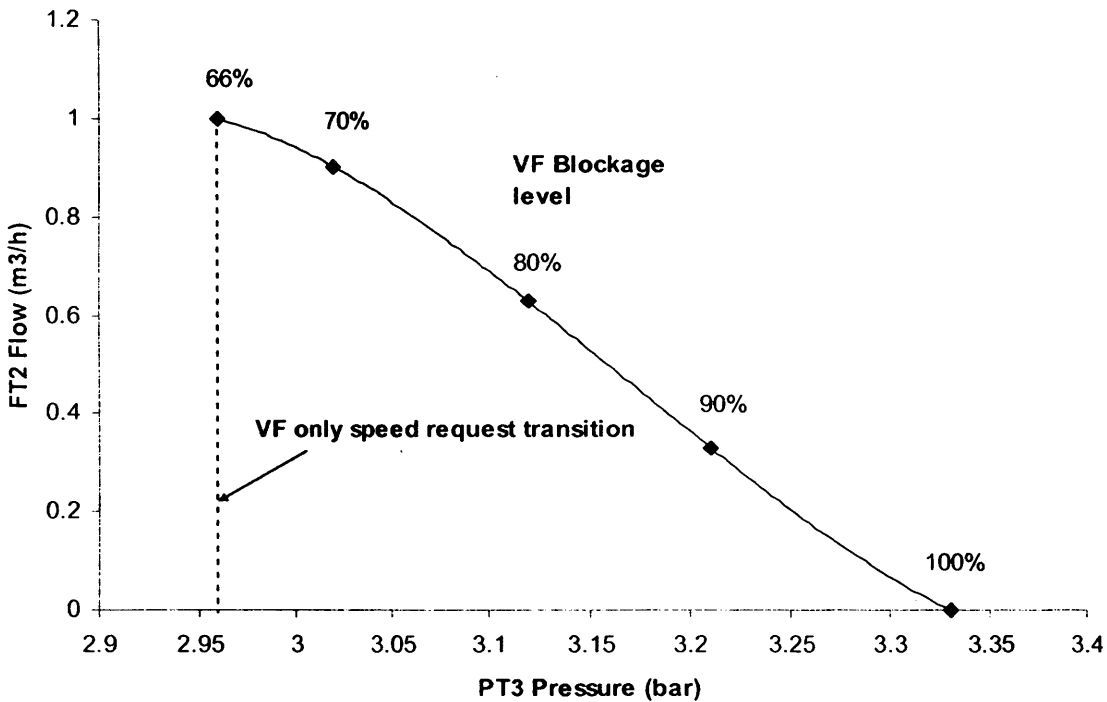


Figure 5.14: PT3 and FT2 relationship for a range of VF blockage levels in the ‘Maximum Speed Request Region’.

Figure 5.14 also shows the line of best fit for the data which had the equation;

$$FT2 = 17.11PT3^3 - 162.79PT3^2 + 512.98PT3 - 534.86 \quad (5.6)$$

Once again there was potential to use this line of best fit to decide if a blockage was producing a typical filter bed fouling response. In order to test the suitability of the line of best fit, blockages of VF, from the ‘Maximum Speed Request Region’, were combined with 10% and 20% V7 blockages. The resulting combined blockage data can be seen in Figure 5.15.

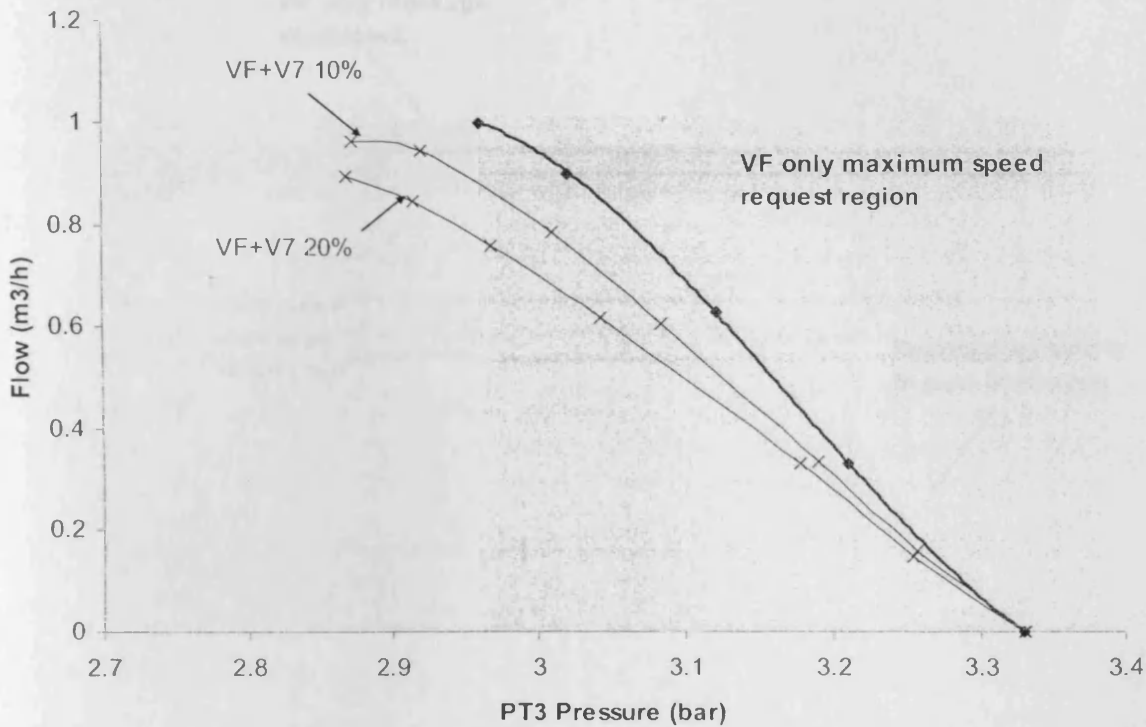


Figure 5.15: PT3 and FT2 relationship for a range of VF blockage levels and the results for VF blockages combined with 10% and 20% V7 blockages.

As discussed previously, in the VF only 'Maximum Speed Request Region', any addition of V7 closure resulted in a decrease in FT2 flow and PT3 pressure, as the PID loop could no longer raise the speed request to compensate. As a result when V7 components were added to pure VF blockages, which fell close to the edge of the VF only 'Maximum Speed Request Region', the reduction in PT3 pressure moved the resulting data points outside the limits of the line of best fit.

In order to account for combined results which fell outside the realm of the line of best fit, thresholds were imposed as can be seen in Figure 5.16. If a result with a speed request of 100% had a PT3 pressure less than 2.9bar it would be diagnosed as not being a pure VF blockage regardless of FT2 flow. If the pressure fell between 2.9bar and 2.96bar then results with a flow rate above the maximum flow threshold of $0.95\text{m}^3/\text{h}$ would be diagnosed as pure VF blockages. Those below were diagnosed as being not pure VF blockages. As a result test points which fell into the green box would be treated as pure VF blockages. In the worst case scenario, for this part of the method, a V7 blockage just over 10% would be overlooked.

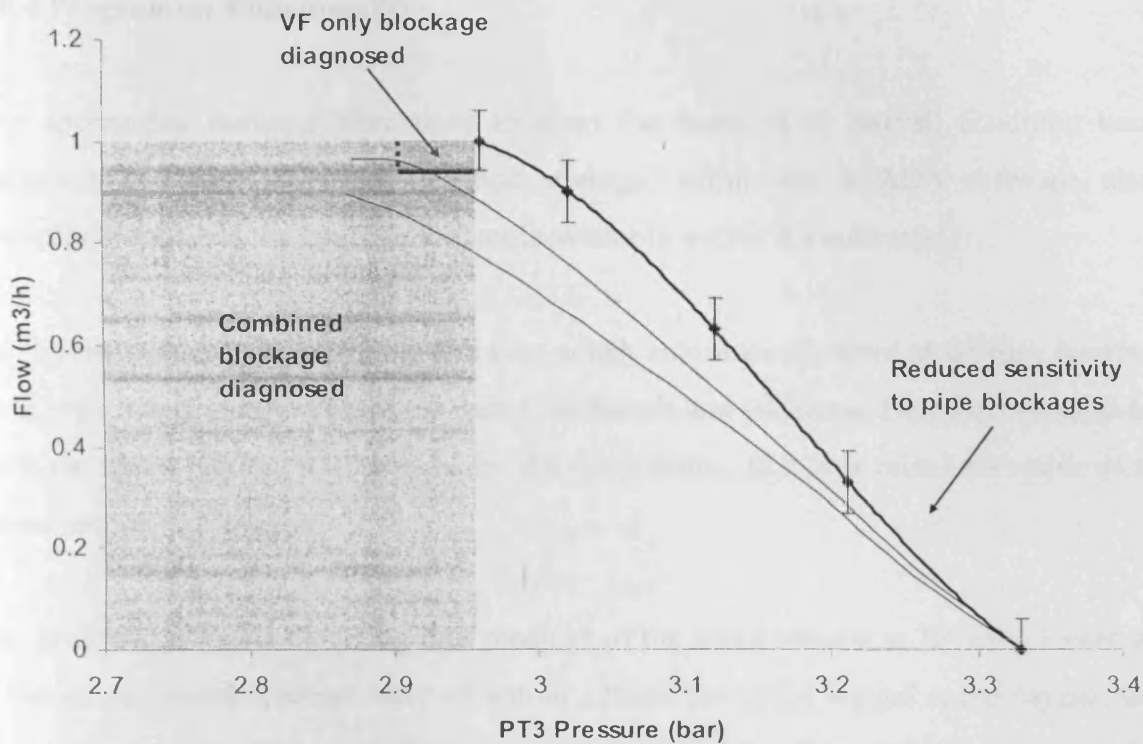


Figure 5.16: Diagnostic thresholds for combined blockage cases.

As a compromise, once again between over and under sensitivity, a margin for error for the line of best fit for the FT2 flow signal was selected. $\pm 0.06 \text{ m}^3/\text{h}$ was chosen and is represented by the error bars in Figure 5.16. The flow signal usually only fluctuated around the average by $0.01 \text{ m}^3/\text{h}$ in normal operation and under blockage conditions, where larger fluctuations were seen, variations were still only $0.02 \text{ m}^3/\text{h}$ different from the average.

The error bars in Figure 5.16 demonstrate that for less severe VF blockages, in the 100% speed request region, the system would overlook additional V7 blockages up to around 5%. For very severe VF blockages the system would become far less sensitive to the addition of pipe blockages, as indicated in Figure 5.16. This was of minor importance as operationally the filter bed should never be allowed to foul up to these levels. If it were to happen, then a backwash would be the only sensible course of action and following this, the reduced level of filter blockage would expose the pipe blockage to the programme. The parameters used in the best fit equation (5.6), could be updated as required by a change in set up and the established method is robust and could be deployed as required.

5.8.4 Programme Functionality

The approaches outlined were used to form the basis of an overall condition based backwash and pipe blockage detection strategy, within the SCADA software, using procedural code and the configurable tools available within the software.

An 'Event' was configured in the software which automatically fired at set time intervals. This event triggered the Condition Based Backwash and Blockage Detection programme. First the speed request was checked by the programme. If it was raised the value of the speed request was logged.

The programme began by taking four readings of the speed request at 30 second intervals. If the speed request readings were all within $\pm 2\%$ of the initial logged speed request, then the system was designated as being in steady state and the diagnostic was continued. If this was not the case then the programme terminated.

If a steady state was reached and the speed request was less than 100%, then the programme utilised the line of best fit and the equation for the 'Variable Speed Request Region' seen in Figure 5.13. The pressure was substituted into equation 5.5. The speed request was compared with the expected speed request value just calculated. If the speed request was within $\pm 3\%$ of the expected, then a VF only blockage was diagnosed. If the speed request fell outside this an abnormal blockage condition was diagnosed.

If the speed request was 100%, then the decision lines for the 'Maximum Speed Request Region' seen in Figure 5.16 were used. If the pressure was found to be above 2.96bar then the line of best fit described by equation 5.6 was used. The pressure value was substituted into the equation and the expected pure VF blockage flow calculated. If the flow was within $\pm 0.06\text{m}^3/\text{h}$ of the calculated line of best fit flow, then a pure VF blockage was diagnosed.

If the pressure was found to be between 2.9bar and 2.96bar then a flow above $0.95\text{m}^3/\text{h}$ was diagnosed as a pure VF blockage. Flow below this was diagnosed as an abnormal blockage fault. If a pressure below 2.9bar was found then an abnormal pipe blockage was also diagnosed.

In all cases where a VF only blockage was diagnosed, the pressure was then compared with the data in Table 5.1 using the functionality of the original programme presented in Section 5.5. The level of filter bed fouling was thus diagnosed and the on screen Filter Condition indicator was updated accordingly. Also the new System Condition indicator shown to the top right of Figure 5.17 was updated to read “Normal”. The programme was configured such that backwash was triggered if the filter blockage level reached a user defined blockage level or above. Therefore, after diagnosing the filter blockage level, it was compared against a user defined backwash threshold. If the backwash threshold was reached, a pop up box recommending backwash was triggered, as can be seen in Figure 5.17. In this work this pop up box was used in place of an actual backwash for practicality. The software could be quickly modified to control the actual backwash triggering tag in the PLC for operational use.



Figure 5.17: Modified process mimic

In cases where the speed request was 100% and an abnormal pipe blockage was detected, the Filter Condition indicator was updated to read “Unknown”. The new System Condition indicator was set to read “Abnormal Blockage Present”. A pop up box was triggered which informed the user that the automatic pressure based backwash had been suspended and the Condition Based Backwash and Blockage Detection programme was terminated. Operationally in this situation the system could revert to the time based backwash initiation strategy, until the abnormal blockage was remedied.

In cases where the speed request was less than 100% i.e. in the 'Variable Speed Request Region', and an abnormal blockage was diagnosed, a different approach was taken. Testing had shown that in the 'Variable Speed Request Region' the PID maintained a pressure indicative of the filter blockage. As such in these cases the filter bed blockage level could still be diagnosed despite the presence of a pipe blockage. So the programme diagnosed the filter blockage level based on pressure and updated the Filter Indicator. The System Condition Indicator was set to read "Abnormal Blockage Present". The filter blockage level was then tested against the backwash threshold as usual and a decision made in the same way as a VF only blockage would be handled. The full operation of the programme can be seen in the flow diagram of Figure 5.18.

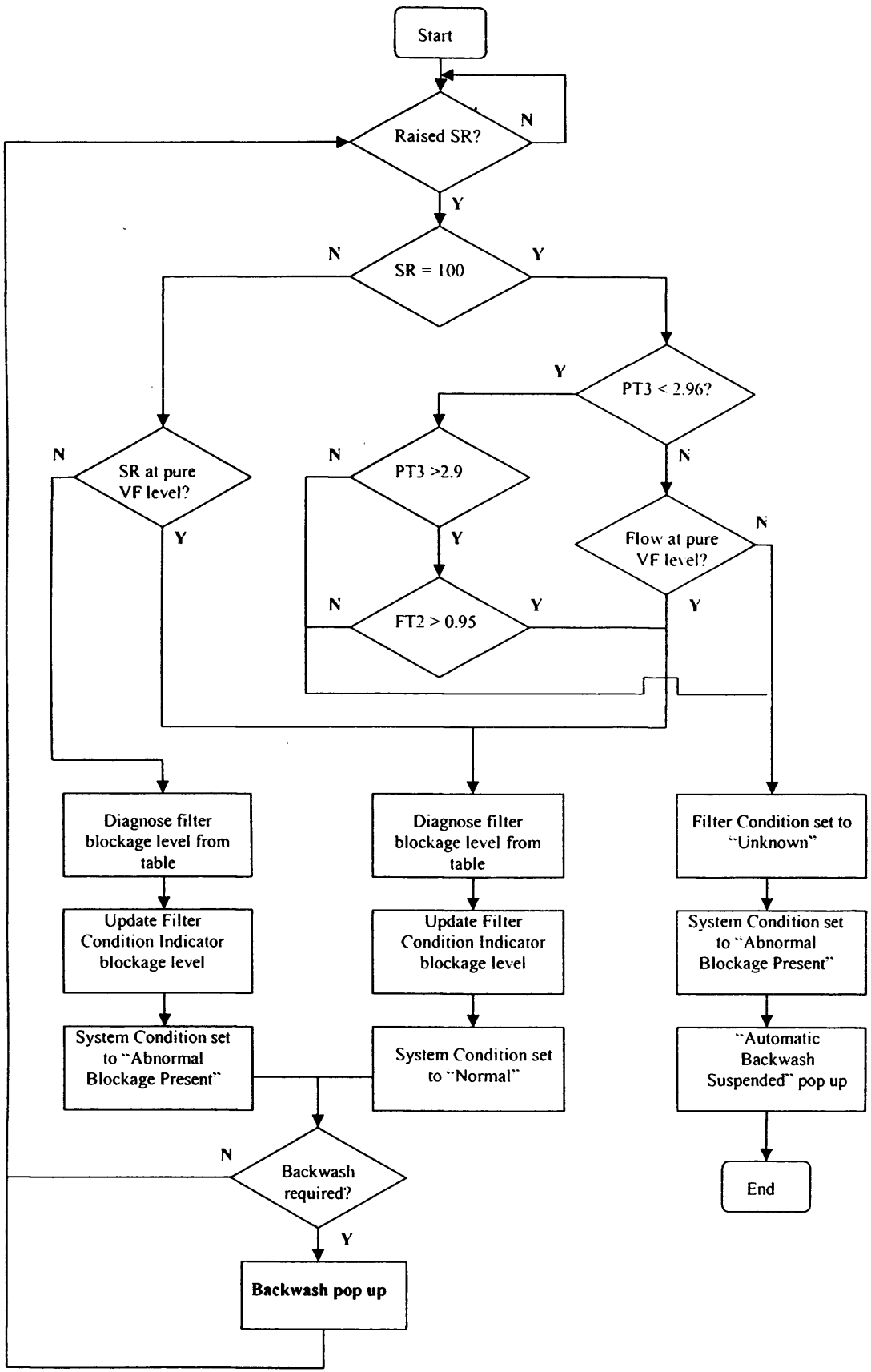


Figure 5.18: Flow diagram of the Condition Based Backwash and Blockage Detection programme functionality.

5.8.5 Programme Testing

The programme was tested across a range of combined blockages and the results can be seen in Table 5.3. The pipe valve blockages were calibrated and set first, based on reduction of flow at constant speed request. The VF level was then set with reference to marks on the valve. This was checked once the programme had executed, by opening the pipe valve and reading the flow reduction caused by the VF restriction at fixed speed request. The blockage values stated in the table are accurate to $\pm 3\%$. The VF blockage levels were chosen to fall in the centre of the blockage level categories of the programme to give clear results. An “Unknown” message was produced when the blockage condition forced the system into the ‘Maximum Speed Request Region’. This onscreen message in the Filter Condition box denotes that the conditions had fallen outside the diagnostic capability of the system. Therefore an “Unknown” message shows that the system has successfully identified its own limitations. It does not mean that the system has lost functionality or failed in its intended task on robust monitoring.


Table 5.3: VF/V5 and VF/V7 combined blockage results.


V5	10%		20%		30%		40%		50%		60%		70%		80%		90%		100%	
VF	SC	FC	SC	FC	SC	FC	SC	FC	SC	FC	SC	FC	SC	FC	SC	FC	SC	FC	SC	FC
5%	AB	OK	AB	OK	AB	OK	AB	U	AB	U	AB	U	AB	U	AB	U	AB	U	AB	U
15%	AB	OK	AB	OK	AB	OK	AB	U	AB	U	AB	U	AB	U	AB	U	AB	U	AB	U
25%	AB	OK	AB	OK	AB	OK	AB	U	AB	U	AB	U	AB	U	AB	U	AB	U	AB	U
35%	AB	OK	AB	OK	AB	OK	AB	U	AB	U	AB	U	AB	U	AB	U	AB	U	AB	U
45%	N	OK	AB	OK	AB	OK	AB	U	AB	U	AB	U	AB	U	AB	U	AB	U	AB	U
55%	N	OK	AB	OK	AB	OK	AB	U	AB	U	AB	U	AB	U	AB	U	AB	U	AB	U
65%	AB	U	AB	U	AB	U	AB	U	AB	U	AB	U	AB	U	AB	U	AB	U	AB	U
75%	AB	U	AB	U	AB	U	AB	U	AB	U	AB	U	AB	U	AB	U	AB	U	AB	U
85%	AB	U	AB	U	AB	U	AB	U	AB	U	AB	U	AB	U	AB	U	AB	U	AB	U
95%	N	OK	N	OK	AB	U	AB	U	AB	U	AB	U	AB	U	AB	U	AB	U	AB	U
V7	10%		20%		30%		40%		50%		60%		70%		80%		90%		100%	
VF	SC	FC	SC	FC	SC	FC	SC	FC	SC	FC	SC	FC	SC	FC	SC	FC	SC	FC	SC	FC
5%	AB	OK	AB	OK	AB	OK	AB	OK	AB	OK	AB	OK	AB	U	AB	U	AB	U	AB	U
15%	AB	OK	AB	OK	AB	OK	AB	OK	AB	OK	AB	OK	AB	U	AB	U	AB	U	AB	U
25%	AB	OK	AB	OK	AB	OK	AB	OK	AB	OK	AB	OK	AB	U	AB	U	AB	U	AB	U
35%	N	OK	AB	OK	AB	OK	AB	OK	AB	OK	AB	U	AB	U	AB	U	AB	U	AB	U
45%	N	OK	AB	OK	AB	OK	AB	OK	AB	OK	AB	U	AB	U	AB	U	AB	U	AB	U
55%	N	OK	AB	OK	AB	OK	AB	OK	AB	OK	AB	U	AB	U	AB	U	AB	U	AB	U
65%	AB	U	AB	OK	AB	U	AB	U	AB	U	AB	U	AB	U	AB	U	AB	U	AB	U
75%	AB	U	AB	U	AB	U	AB	U	AB	U	AB	U	AB	U	AB	U	AB	U	AB	U
85%	AB	U	AB	U	AB	U	AB	U	AB	U	AB	U	AB	U	AB	U	AB	U	AB	U
95%	N	OK	N	OK	N	OK	AB	U	AB	U	AB	U	AB	U	AB	U	AB	U	AB	U

Key:

SC = System Condition

FC = Filter Condition

 = Correct

 = Incorrect

N = "Normal" message

AB = "Abnormal Blockage" message

OK = Correct VF blockage diagnosed

U = "Unknown" message

The programme performed as expected and produced correct outputs in the majority of tests. For VF/V5 combined blockages, a 10% blockage of V5 was not diagnosed when combined with 45% and 55% VF restrictions. This was a result of the slightly lower sensitivity of the variable speed request line of best fit at higher VF blockage levels. Both 10% and 20% V5 blockages were missed by the programme when combined with VF restrictions of 95%. This was due to the loss of sensitivity for severe VF blockages in the 'Maximum Speed Request Region', labelled in Figure 5.16. As a result of the V5 flow degradation behaviour, believed to be caused by pump cavitation, the majority of V5 combined tests fell into the 'Maximum Speed Request Region'. The detected presence of the pipe restriction thus led to the programme delivering the desired 'Unknown' result for the filter bed condition.

V7 combined blockages showed similar results to V5, except that far more of the results fell into the 'Variable Speed Request Region' and as such, the programme was able to diagnose the VF blockage level. The correct filter condition result was obtained in all cases tested, demonstrating the developed method was a robust approach, for use in condition based backwash initiation.

Due to the multivariate style of analysis used by the programme, the presence of other faults such as the internal tape blockage in the pump, witnessed in chapter 4, should also be detected. The tape had caused a raised speed request and as such this would take the speed request out of the tolerance of the line of best fit used for filter fouling level detection in the 'Variable Speed Request Region'. With the existing programme this would result in an "Abnormal Blockage" diagnosis.

5.9 Chapter Summary

A short literature review focused on filter backwash control was presented. This suggested that efficiency improvements could be made by initiating backwash based on filter blockage level. The addition of VF, a valve used to simulate filter blockages, was described and test results obtained using VF in PID mode presented. The results demonstrated that filter blockages had a marked effect on the pre-filter pressure obtained from PT3. A theoretical software model of the WRAP Rig system concurred with these findings.

A filter blockage level diagnosis programme was described which was capable of ascertaining the level of filter blockage to within 10% using the PT3 response. The effect of isolated pipe blockages and combined VF/V7 blockages on the PT3 response was demonstrated. It was shown that both types of blockage had an effect on the PT3 response. The evidence also strongly suggested that if speed request, PT3 pressure and FT2 flow were all considered, VF only, and combined VF blockages had unique signatures. A method for modelling the VF response using these three variables was described and this model was coded into the software. A programme was thus developed which could deliver robust condition based backwash and pipe blockage detection, by comparing measured system variables with the model VF response. The testing results for the programme were included, demonstrating the success of the method.

5.10 Conclusion

An effective, passive, Condition Based Backwash and Blockage Detection programme was realised using non-time critical, standard frequency algorithms. These were applied using the in-built functionality of the SCADA package. Heuristic methods were used to develop a model of normal operation. With this model assimilated into the programme by means of equations, system condition and abnormal events could be monitored. Once again, the diagnostics were based on the steady state response of the system, to prevent programme execution pauses caused by the low priority of the procedural code, from distorting the results. The execution of the programme had no adverse effects on the functionality of the SCADA software. The style of approach ensured that recalibration to reflect system changes, or a new calibration process for application of the software to a similar plant, would be straightforward. It had been shown that by fully exploiting the capabilities of the SCADA software, potential improvements in operational efficiency and early detection of energy wasting system faults could be achieved.

Chapter 6

Combined Blockage Level Diagnostic

6.1 Introduction

The Condition Based Backwash and Blockage Detection programme allowed filter only blockage level to be diagnosed, facilitating condition based backwash triggering for a range of conditions. This included the case of combined blockages for which the PID response fell within the 'Variable Speed Request Region'. The programme however, was not capable of diagnosing the level of pipe restriction with combined blockages present. The level of filter bed fouling also remained unknown for combined blockage cases, which fell into the 'Maximum Speed Request Region'. Automatic backwash was disabled, by the programme, in these cases.

The significant potential benefits, if a method could be devised which overcame these limitations, were sufficient to merit further investigation. Diagnosis of pipe blockage severity for example, would be useful for maintenance prioritisation. The ability to diagnose filter blockage levels even in the 'Maximum Speed Request Region' would also be valuable, as this would allow condition based backwash to continue in all cases.

Improved abnormal blockage tolerability was desirable, as in many cases a maintenance technician may not be able to attend the site for days or weeks. In some wider applications the filtration system maybe supplying a critical batch process which would make immediate repair unviable. From a research viewpoint it was deemed important to fully explore the capability boundaries of the SCADA software. If even more complicated diagnostic functionality was possible, this would demonstrate an extended scope for advanced SCADA configuration applications in industrial plant.

6.2 Blockage Dominance Based Approach

6.2.1 Concept

It was hypothesised that in combined blockage cases the larger, or dominant, restriction would dictate the flow rate. Testing not presented here supported this theory. It had also been shown, through the testing presented in Chapter 5, that the presence of pipe and filter restrictions had an effect on the pre-filter pressure measured at PT3. A test strategy was developed to examine the blockage dominance and pressure behaviour, with a view to extending the diagnostic capabilities of the system.

6.2.2 V7 and VF Combined Testing

A test method was devised for pure and combined VF and V7 blockages. It was decided that for each test the FT2 flow rate at 42% would be taken. The speed request would then be increased to 100% and the PT3 pressure recorded. It was premised that the FT2 flow at the 42% speed request would give an indication of the dominant blockage severity and the PT3 pressure would give an indication of the subordinate blockage severity.

The tests were conducted by setting the severity of the dominant blockage first, by flow calibration at 42% speed request, and then setting the subordinate blockage, albeit more approximately, with reference to the physical marks on the valve handle. For example, the tests in the first two columns (shown in red) of table 6.1, were obtained as follows; in each of the nine tests the dominant VF blockage was calibrated (between 100% and 20%) and V7 was left at 0% blockage, before the test result was noted. For the next two columns (shown in green), the VF blockage level was set first (between 90% and 25%) and the subordinate V7 blockage was then set to 25% in all cases. The same approach was used to conduct the remaining tests shown in the table. The testing process was then reversed, with the now dominant V7 set first and VF set second, as shown in Table 6.2.

Table 6.1: VF Dominant combined blockage test set

V7 Blockage (%)	VF Blockage (%)	V7 Blockage (%)	VF Blockage (%)	V7 Blockage (%)	VF Blockage (%)	V7 Blockage (%)	VF Blockage (%)
0	100	25	90	50	90	75	90
0	90	25	80	50	80	75	80
0	80	25	70	50	70	75	75
0	70	25	60	50	60	X	X
0	60	25	50	50	50	X	X
0	50	25	40	X	X	X	X
0	40	25	30	X	X	X	X
0	30	25	25	X	X	X	X
0	20	X	X	X	X	X	X

Table 6.2: V7 Dominant combined blockage test set

VF Blockage (%)	V7 Blockage (%)	VF Blockage (%)	V7 Blockage (%)	VF Blockage (%)	V7 Blockage (%)	VF Blockage (%)	V7 Blockage (%)
0	100	25	90	50	90	75	90
0	90	25	80	50	80	75	80
0	80	25	70	50	70	75	75
0	70	25	60	50	60	X	X
0	60	25	50	50	50	X	X
0	50	25	40	X	X	X	X
0	40	25	30	X	X	X	X
0	30	25	25	X	X	X	X
0	20	X	X	X	X	X	X

The results from these fifty tests were plotted and results for each subordinate blockage level joined, to expose trends in the data, as shown in Figure 6.1. The colour coding of the tests in Table 6.1 corresponds to the colours of the resulting lines in the top half of Figure 6.1 to demonstrate how the plot was constructed.

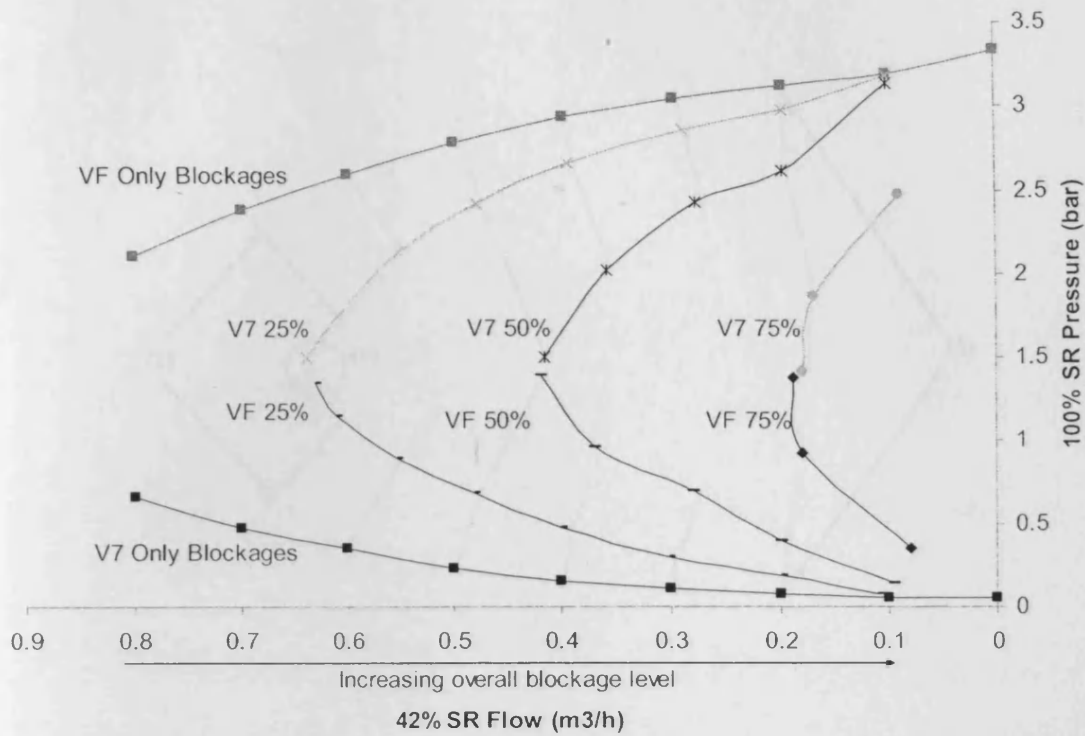


Figure 6.1: Combined VF and V7 blockage results.

The VF dominant combined blockages are positioned in the top half of the Figure 6.1 plot and the V7 dominant combined blockages in the lower half. The subordinate 25%, 50% and 75% blockages, in each half of the plot, had produced thresholds which could potentially be used to identify the approximate severity of the subordinate blockage.

6.2.3 Blockage Synergy

In most cases the flow rates for the combined blockages were seen to be less than was expected. For example, if the 25%/25% tests, shown as (1) in Figure 6.2, are considered, the flow rates were seen to be approximately $6.4 \text{ m}^3/\text{h}$. A single 25% blockage would only reduce flow to $0.75 \text{ m}^3/\text{h}$. This suggested that rather than the dominant blockage being entirely responsible for the flow rate, there was a degree of synergy in the flow restriction caused.

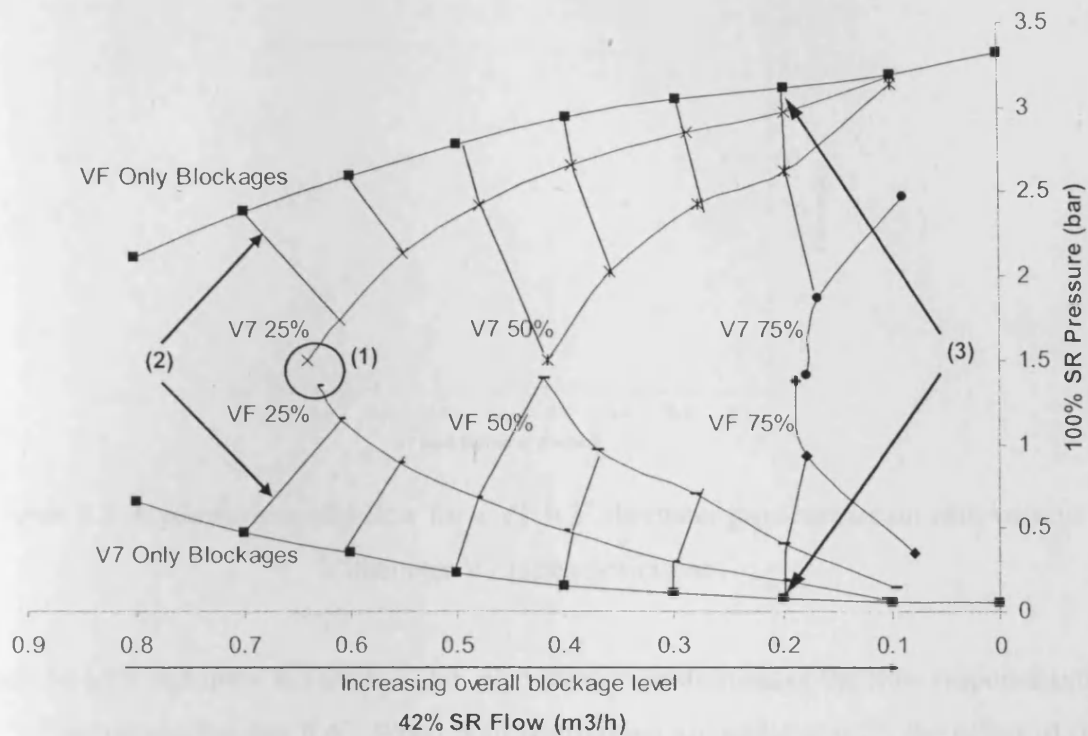


Figure 6.2: Combined VF and V7 blockage results showing synergistic behaviour.

The results for dominant blockages of the same level have been linked by illustrative lines in Figure 6.2. The gradients of the illustrative connecting lines shown in the figure are an indication of the level of synergistic behaviour. The points on the single blockage only lines represent the expected flow for the dominant blockage alone. A heavily sloping illustrative line indicates that the flow for the combined test was far less than expected. For the tests where the margin of dominance was small, such as the 25%/30% tests, indicated as (2), it can be seen that the slope of the line was severe suggesting a high level of synergy. However, for tests with a large dominance margin such as the 25%/80% tests, marked as (3), the line is almost vertical showing that the dominant fault was controlling the flow rate and the subordinate blockage was having little effect. This characteristic was also present in results gained from the theoretical Hydroflow model. In the model a VF restriction was added by reducing the diameter of the pipe to 0.2". A series of tests were then conducted with differing levels of V7 restriction, achieved by reducing the pipe diameter. The results obtained are shown in Figure 6.3.

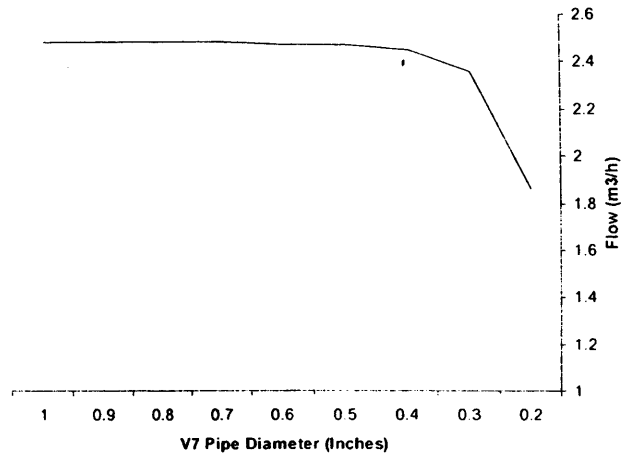


Figure 6.3: Hydroflow model flow for a VF 0.2” diameter pipe restriction with various diameter V7 pipe restrictions.

As can be seen in Figure 6.3 the 0.2” VF pipe restriction dominates the flow response until the V7 restriction reaches 0.4”. When both restrictions are equal at 0.2”, the effect of the synergistic behaviour becomes wholly apparent as the flow falls away sharply.

A partially closed valve causes the generation and dissipation of turbulent eddies in the high shear layer around the submerged jet [83]. It is hypothesised that the dominant blockage caused a reduction in flow proportional to its size. When a subordinate blockage was then applied, this resulted in a second submerged jet. If the subordinate blockage was small the velocity of the submerged jet was low and energy losses due to eddy formation were negligible. As the subordinate blockage reached the proportions of the dominant blockage, the velocity of the submerged jet caused by the subordinate blockage, increased in line with the law of conservation of momentum. This increased the velocity of the subordinate submerged jet, resulting in greater energy dissipation and lower overall flow rate, accounting for the synergistic behaviour.

6.2.4 V5 and VF Combined Testing

The test sets outlined in Tables 6.1 and 6.2 were now conducted using V5 in the place of V7. It was decided that, as usual, a ‘Flow Standardisation Period’ of 120 seconds at a speed request of 100% should be undertaken before each V5 test was performed. As such, the closure levels were first applied and the ‘Flow Standardisation Period’ was run, then

the speed request was set to 42% and the flow taken. The speed request was then ramped up to 100% again and the pressure taken.

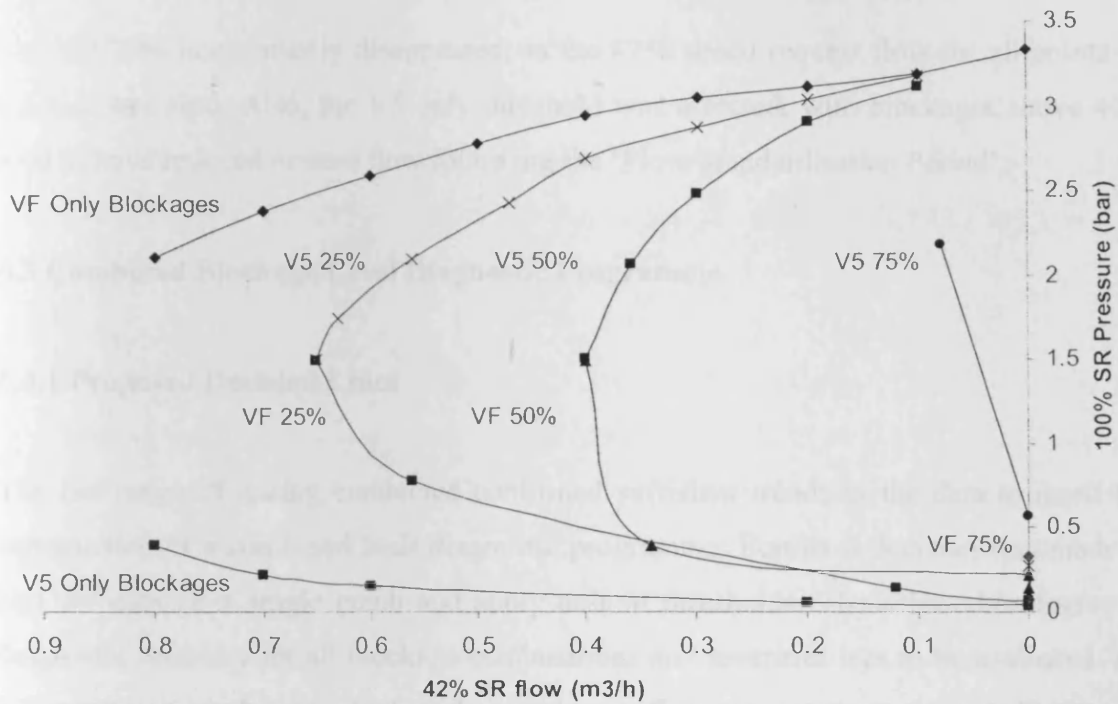


Figure 6.4: V5 combined blockage test results.

The pattern in Figure 6.4 was of the general configuration seen for the V7 combined tests but there were some differences. The pressures seen in the V5 dominant bottom half of the plot, appeared lower than V7. Also the V7 75% threshold line was virtually non-existent. These differences were caused by the V5 pump starvation characteristics. Following the ‘Flow Standardisation Period’, moderate to severe blockages always exhibited lower flow rates than seen before the ‘Flow Standardisation Period’. This led to lower PT3 pre-filter pressures.

For severe V5 blockages the flow was seen to fall to zero when returned to 42% speed request following the ‘Flow Standardisation Period’. The effect of this was very evident on the V5 75% line. The VF 90%/V5 75% point managed to maintain flow after the ‘Flow Standardisation Period’. However the next point on this line, the VF 80%/V5 75% point, had a flow of zero. It is believed that the severe VF restriction at the first point prevented the most severe pump cavitation behaviour during the ‘Flow Standardisation Period’. This allowed flow to still be generated at 42% speed request. The less severe VF

blockages allowed the pump to enter a state of severe cavitation during the 'Flow Standardisation Period', so the flow stalled when the speed request was returned to 42%.

The VF 75% line virtually disappeared, as the 42% speed request flow for all points on the line was zero. Also, the V5 only threshold was affected, with blockages above 40% seen to have reduced or zero flow following the 'Flow Standardisation Period'.

6.3 Combined Blockage Level Diagnostic Programme

6.3.1 Proposed Decision Lines

The full range of testing conducted confirmed sufficient trends in the data to merit the construction of a combined fault diagnostic programme. Further a decision was made to plot the data on a single graph and apply best fit thresholds. The achievable degree of diagnostic accuracy for all blockage combinations and severities was to be evaluated. All V5 combined blockages which had caused zero flow were not considered. Figure 6.5 shows the single graph, with thresholds chosen to best represent both V5 and V7 subordinate blockages labelled as VP (pipe work blockages).

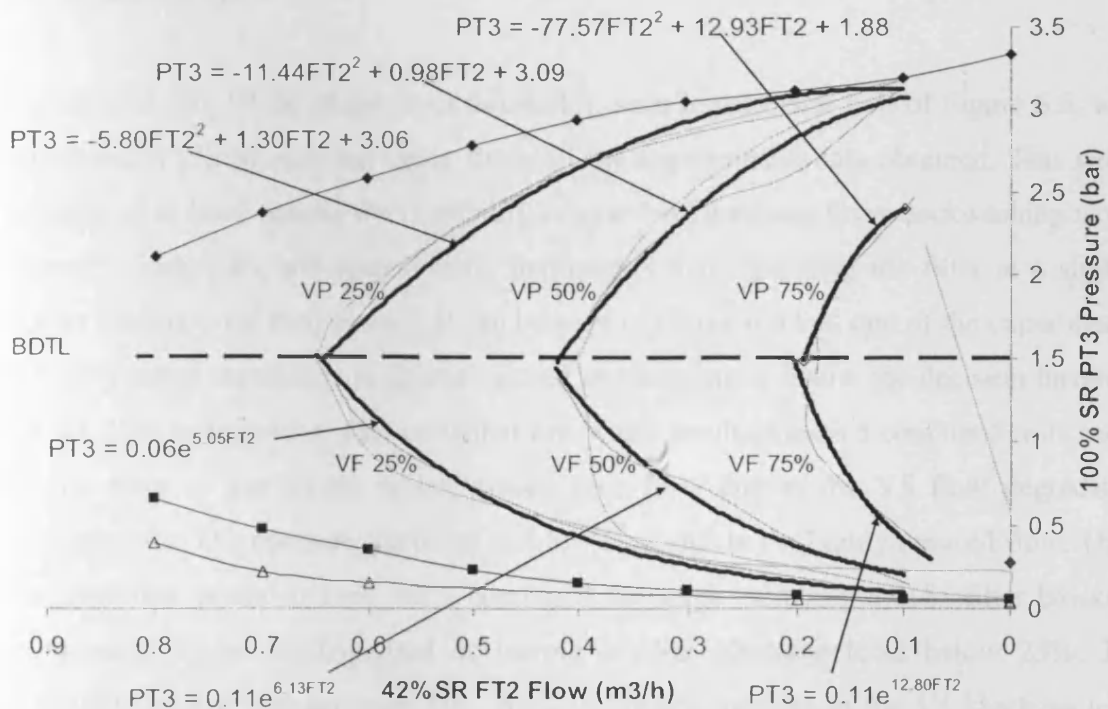


Figure 6.5: Combined VF and pipe valve blockage tests results with diagnostic thresholds.

It was clear that the tolerances between the measured relationships, and the best fit thresholds, would limit the accuracy of this diagnostic programme. However, a general indication of system condition could be obtained with sufficient accuracy to allow both approximate combined blockage diagnosis and reliable condition based backwash. It would have been possible to add further thresholds to improve accuracy. It was felt this would increase calibration and programming complexity to an unacceptable level, particularly for a programme which would only be activated under extreme fault circumstances.

For the cases where a V5 blockage was causing severe pump starvation, a system shut down would be triggered, and as such, diagnosis was not of great importance. It was also decided that any blockage greater than 90%, i.e. causing flow less than $0.1\text{m}^3/\text{h}$ at 42% speed request, would not be covered. This was due to the convergence of the thresholds and reduced accuracy in such cases. The positioning of the blockage dominance transition line (BDTL) was based on best fit methods. In a small proportion of cases this could lead to dominant filter bed blockages being diagnosed as subordinate and vice-versa. Although misdiagnosed as subordinate, the programme would still be able to categorise such faults in the correct broader category. The general state of the filter bed or pipe blockage would still be obtainable.

The subordinate VF blockage level thresholds, seen in the lower half of Figure 6.5, were intentionally placed near the upper limits of the experimental data obtained. This would prevent, or at least reduce, the possibility of over backwashing. Over backwashing would be more financially and operationally detrimental than operating the filter at a slightly higher fouling level than desired. It can be seen in Figure 6.5 that one of the experimental VF 50% actual thresholds is almost vertical and terminates below the decision threshold for VF 25% components. This particular line was a result of the V5 combined tests and is on the cusp of the results which caused zero flow due to the V5 flow degradation characteristic. The pressure has fallen to a low level due to the highly reduced flow. There was therefore potential here, for a combined blockage including a 50% filter blockage component, to be misdiagnosed as having a filter blockage level below 25%. The possibility of this was however low. Also any minor increase in the V5 blockage level would cause the flow to crash next time the diagnostic programme was run. As such this

result, which lay at the edge of the useable V5 data, was considered acceptable, meaning the proposed decision thresholds could still be used with a high degree of confidence.

6.3.2 Combined Blockage Diagnostic Programme Functionality

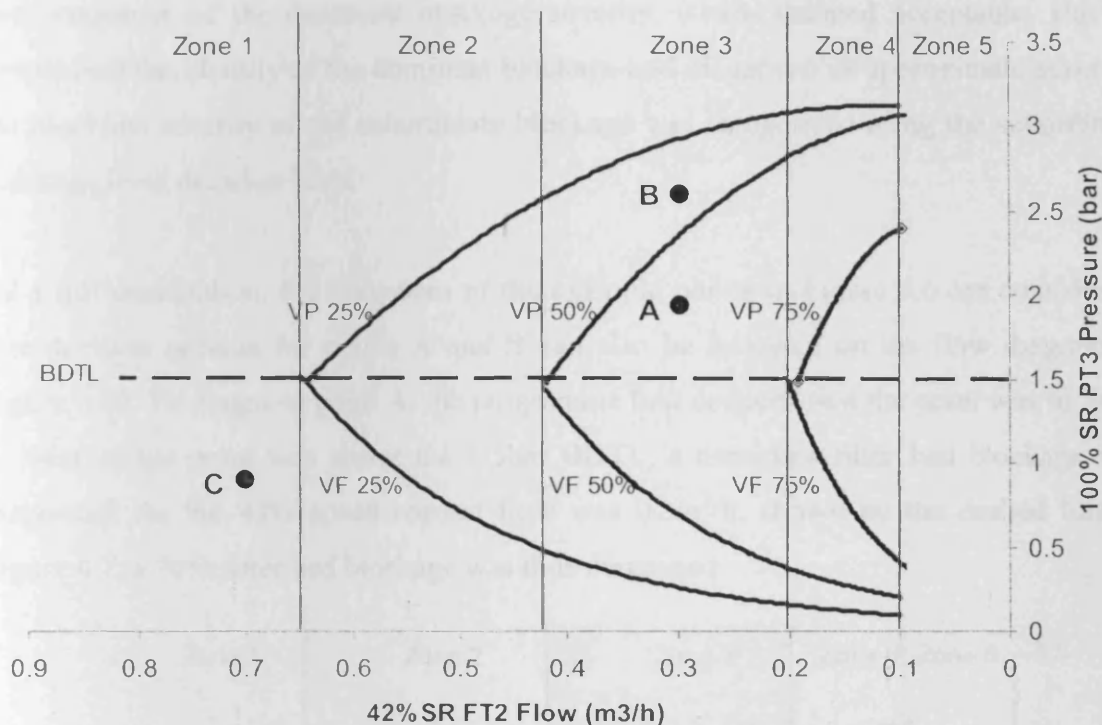


Figure 6.6: Threshold template.

The final decision threshold arrangement used in the combined blockage diagnostic programme is shown in Figure 6.6. The Figure represents the full range of combinations. The programme functionality is described in the following. Rather than always constructing the entire set of decision boundaries, the programme first narrowed down the zones of operation for any particular instance. By analysing the 42% flow recorded, the result was first categorised into one of Zones 1-5. Results with no flow triggered an on screen pop up box recommending system shutdown and the programme terminated. The position of the result relative to the BDTL was then ascertained. If the result fell below the BDTL a dominant pipe blockage was diagnosed and if above the BDTL, a dominant filter bed blockage was diagnosed. If the result fell into Zone 5 and a dominant filter bed blockage was diagnosed (i.e. above BDTL) backwash was recommended. A Zone 5 dominant pipe blockage (i.e. below BDTL) result recommended plant shutdown, as the blockage was too severe for sensible operation.

If the result fell in Zones 1-4, the approximate severity of the dominant blockage was deduced with reference to the 42% speed request flow. For example, if the 42% flow for a result was found to be $0.6\text{m}^3/\text{h}$, a 40% blockage level for the dominant fault was diagnosed. This method did overlook the previously mentioned synergistic behaviour in reduction of flow caused by combined blockage. As this would cause a maximum of 10% over diagnosis of the dominant blockage severity, it was deemed acceptable. Having ascertained the identity of the dominant blockage and diagnosed its approximate severity, the blockage severity of the subordinate blockage was categorised using the subordinate blockage level decision lines.

As a full explanation, the diagnoses of the example points in Figure 6.6 are considered. The decision process for points A and B can also be followed on the flow diagram in Figure 6.10. To diagnose point A, the programme first deduced that the point was in Zone 3. Next as the point was above the 1.5bar BDTL, a dominant filter bed blockage was diagnosed. As the 42% speed request flow was $0.3\text{m}^3/\text{h}$, shown by the dashed line in Figure 6.7, a 70% filter bed blockage was thus diagnosed.

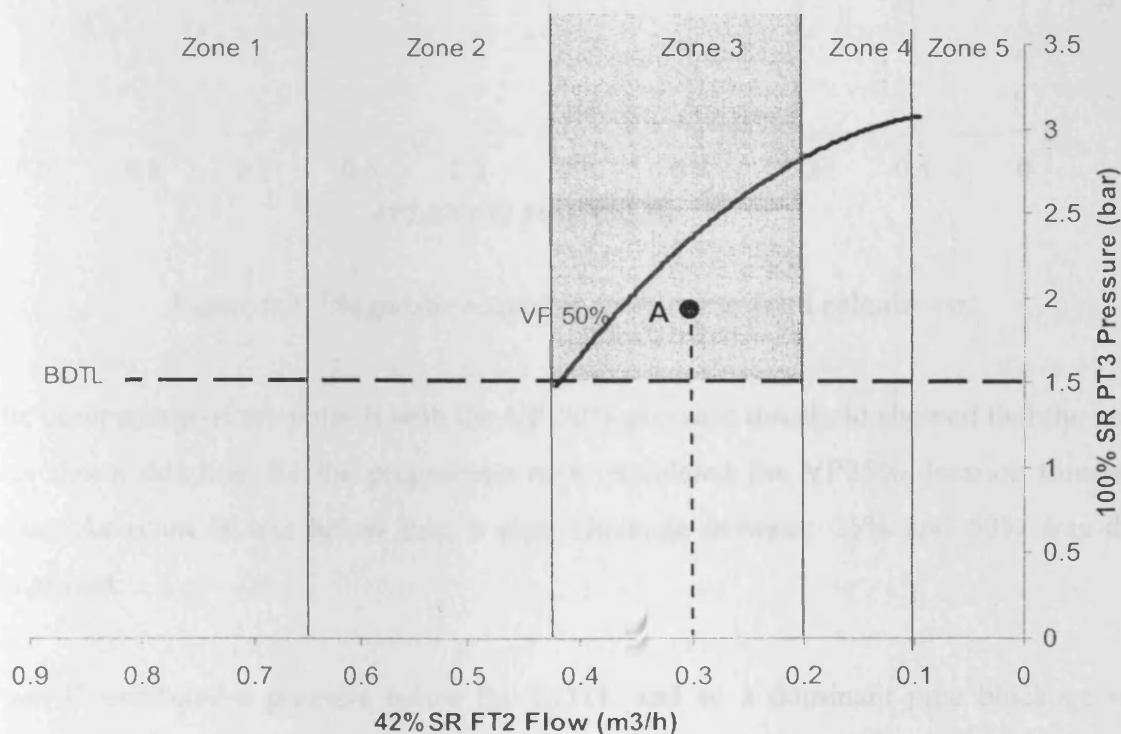


Figure 6.7: Diagnostic requiring single threshold calculation.

To diagnose the subordinate VP blockage category, the relevant subordinate blockage decision values were calculated. As the point was in Zone 3, there was no need to

calculate the VP 75% threshold pressure, as this blockage level was not possible in Zone 3. The VP 50% threshold pressure was calculated first and checked to see if the recorded pressure was below it. As this was the case, the subordinate pipe blockage level could be diagnosed as being between 50% and 75%.

If the point B is now considered, the same initial steps occurred with a dominant VF blockage of 70% diagnosed as shown by the dashed line in Figure 6.8.

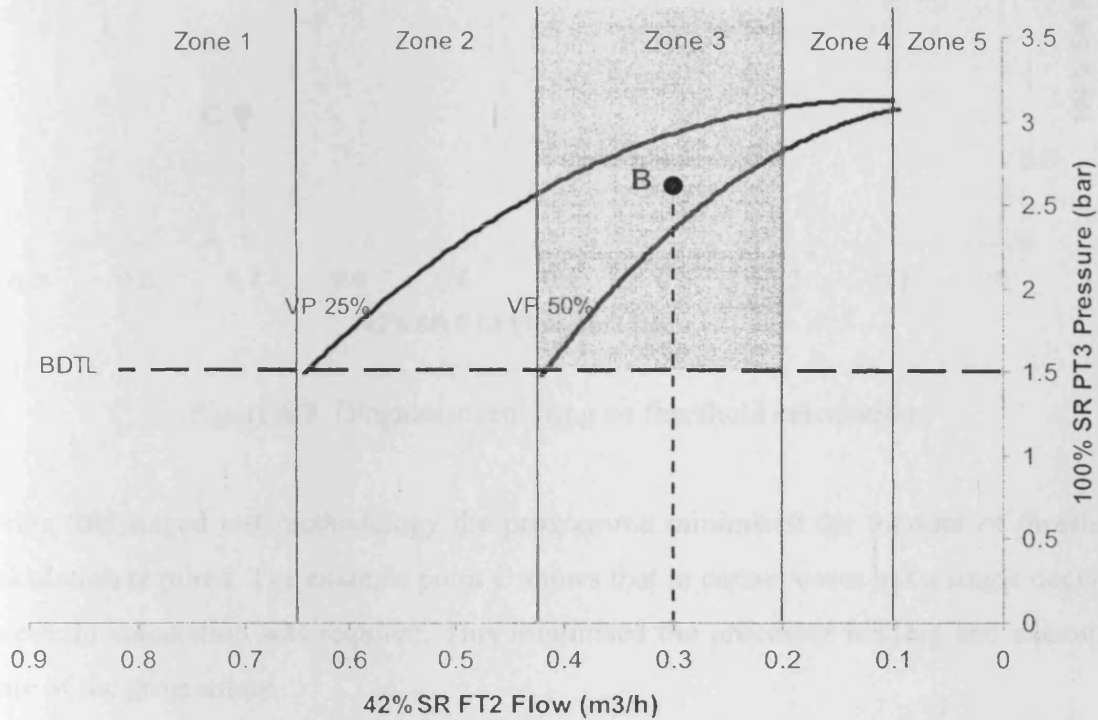


Figure 6.8: Diagnostic requiring double threshold calculation.

The comparison of the point B with the VP 50% pressure threshold showed that the point was above this line. So the programme now calculated the VP25% decision threshold value. As point B was below this, a pipe blockage between 25% and 50% was thus diagnosed.

Point C exhibited a pressure below the BDTL and so a dominant pipe blockage was diagnosed. A 30% pipe blockage was diagnosed based on the 0.7 m³/h flow at 42% speed request, as shown in Figure 6.9. A subordinate filter blockage between 0% and 25% was diagnosed as the point C was in Zone 1 and no subordinate blockage category decision threshold was present in Zone 1.

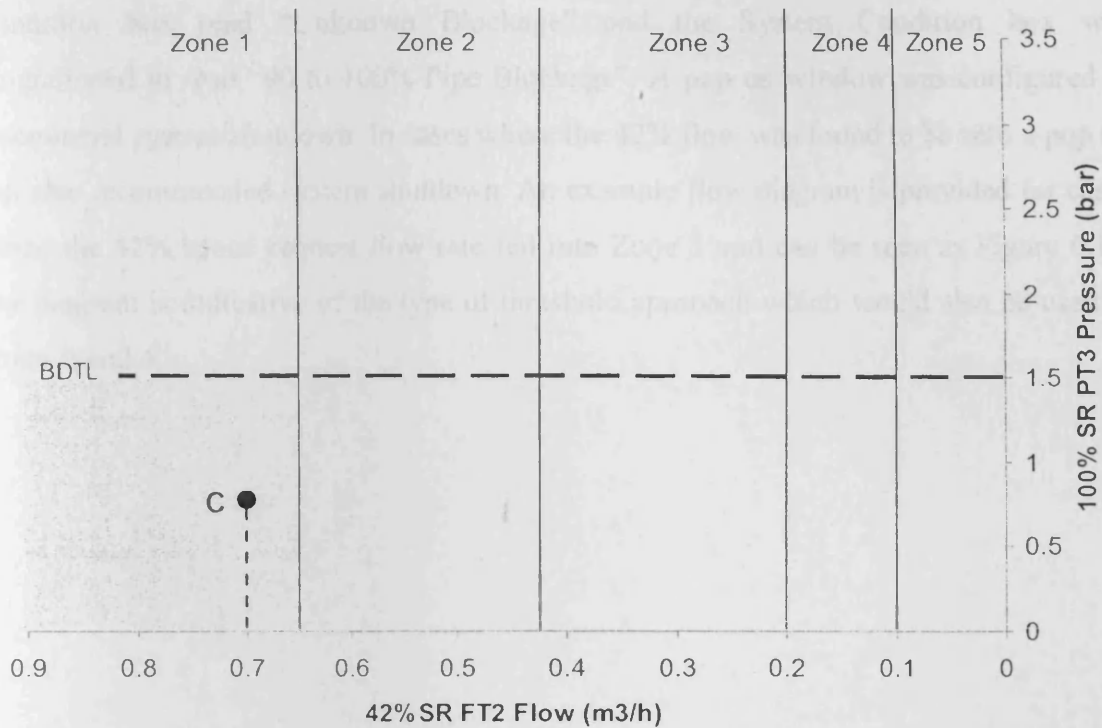


Figure 6.9: Diagnostic requiring no threshold calculation.

Using this staged test methodology the programme minimised the amount of threshold calculation required. The example point C shows that in certain cases not a single decision threshold calculation was required. This minimised the processor loading and execution time of the programme.

The operator interface, seen in Figure 5.17, was updated as a result of the programme outputs. The Filter Condition box stated the estimated blockage level to the nearest 10% for dominant blockages e.g. “Approximately 60% Blockage” and the category of blockage for subordinate blockages, for example “0 to 25% Blockage”. The System Condition box stated the estimated blockage level to the nearest 10% for dominant blockages “Approximately 70% Pipe Blockage”, and the category of blockage for subordinate blockages, for example “0 to 25% Pipe Blockage”.

For Zones 1 to 4, if the level of filter blockage reached the user defined preset, a pop up box was triggered recommending backwash, as was seen in the previous programme. In the Zone 5 cases described earlier the detection of dominant VF blockages updated the Filter Condition box to read “90 to 100% Blockage” and the System Condition box was programmed to read “Blockage of Unknown Severity”. A pop up box was triggered

recommending backwash. For Zone 5 pipe dominant combined blockages, the Filter Condition box read “Unknown Blockage” and the System Condition box was programmed to read “90 to 100% Pipe Blockage”. A pop up window was configured to recommend system shutdown. In cases where the 42% flow was found to be zero a pop up box also recommended system shutdown. An example flow diagram is provided for cases where the 42% speed request flow rate fell into Zone 3 and can be seen as Figure 6.10. The diagram is indicative of the type of threshold approach which would also be used in Zones 2 and 4.

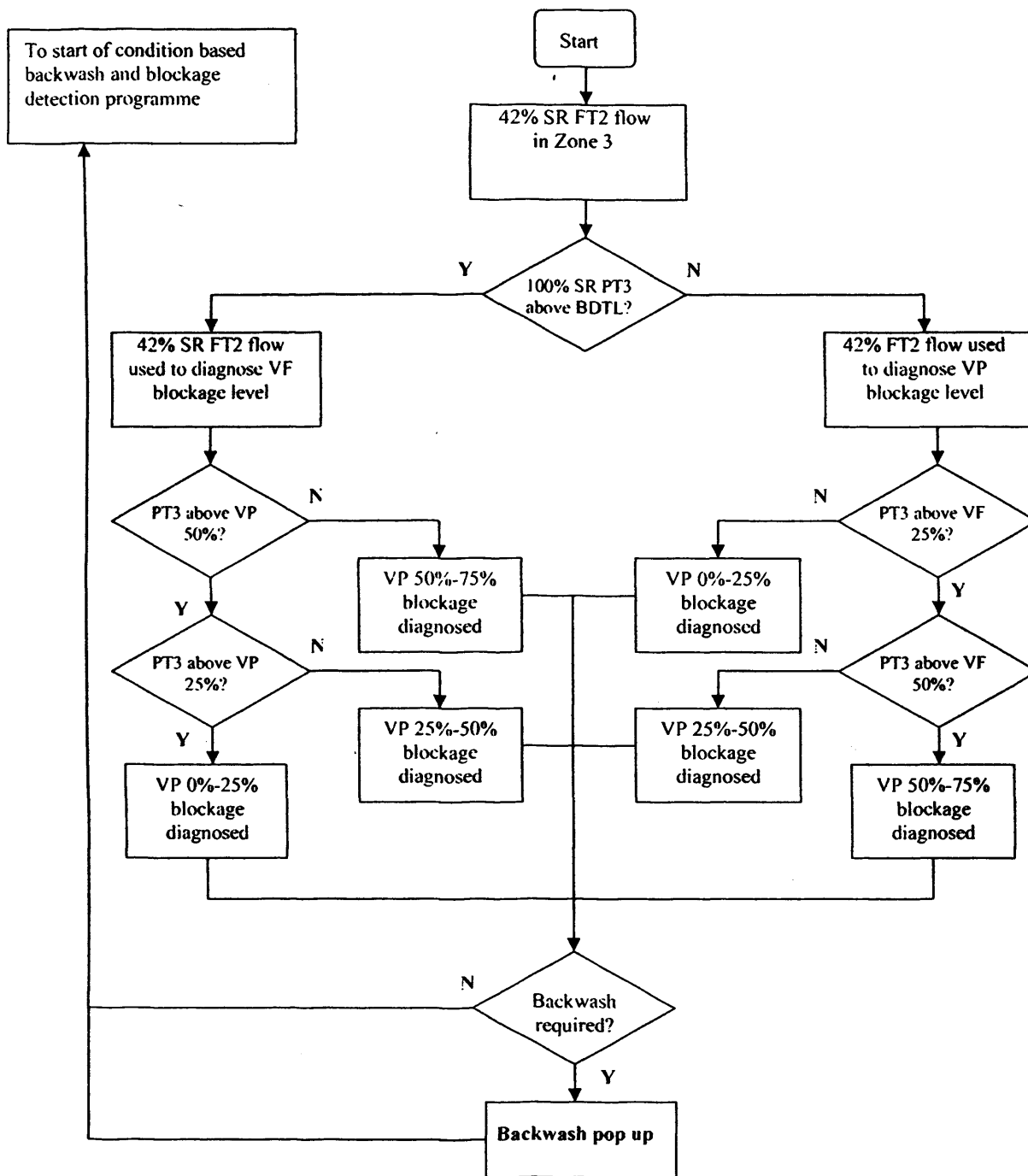


Figure 6.10: Flow diagram for case where the 42% speed request flow rate was in Zone 3.

6.3.3 Programme Testing

A matrix of tests was conducted to assess the performance of the developed approach across a representative range of possible eventualities and the results are shown in Table 6.3. The test blockage values are correct to within $\pm 3\%$. Diagnosed blockage level was assigned an 'OK' in the table if the dominant blockage was within 10% of the actual

blockage and the subordinate blockage was in the correct blockage category. Figure 6.11 explains the results with reference to the decision thresholds.

Table 6.3: Combined blockage diagnostic testing results.

V5	10%		20%		30%		40%		50%		60%		70%		80%		90%		100%	
VF	F	P	F	P	F	P	F	P	F	P	F	P	F	P	F	P	F	P	F	P
10%	OK	OK	OK	OK	OK	OK	OK	OK	OK	OK	OK	OK	OK	OK	OK	OK	OK	OK	SD	SD
20%	OK	OK	OK	OK	OK	OK	OK	OK	OK	OK	OK	OK	OK	OK	OK	OK	OK	OK	SD	SD
30%	OK	OK	OK	OK	OK	OK	OK	OK	OK	OK	OK	OK	OK	OK	OK	OK	OK	OK	SD	SD
40%	OK	OK	OK	OK	OK	OK	OK	OK	OK	OK	OK	OK	OK	OK	OK	OK	OK	OK	SD	SD
50%	OK	OK	OK	OK	OK	OK	OK	OK	OK	H	OK	OK	OK	OK	OK	OK	OK	OK	SD	SD
60%	OK	OK	OK	OK	OK	OK	OK	OK	OK	H	OK	OK	L	OK	SD	SD	SD	SD	SD	SD
70%	OK	OK	OK	H	OK	OK	OK	OK	OK	H	OK	OK	SD	SD	SD	SD	SD	SD	SD	SD
80%	OK	H	OK	H	OK	OK	OK	OK	OK	H	OK	OK	SD	SD	SD	SD	SD	SD	SD	SD
90%	OK	H	OK	H	OK	OK	OK	OK	OK	H	OK	OK	OK	H	SD	SD	SD	SD	SD	SD
100%	BW	BW	BW	BW	BW	BW	BW	BW	BW	BW	BW	BW	BW	BW	SD	SD	SD	SD	X	X
V7	10%		20%		30%		40%		50%		60%		70%		80%		90%		100%	
VF	F	P	F	P	F	P	F	P	F	P	F	P	F	P	F	P	F	P	F	P
10%	OK	OK	OK	OK	OK	OK	OK	OK	OK	OK	OK	OK	OK	OK	OK	OK	OK	OK	SD	SD
20%	OK	OK	OK	OK	OK	OK	OK	OK	OK	OK	OK	OK	OK	OK	H	OK	OK	OK	SD	SD
30%	OK	OK	OK	OK	OK	OK	OK	OK	OK	OK	OK	OK	OK	OK	OK	OK	OK	OK	SD	SD
40%	OK	OK	OK	OK	OK	OK	OK	OK	OK	OK	OK	OK	OK	OK	OK	OK	OK	OK	SD	SD
50%	OK	OK	OK	OK	OK	OK	OK	OK	OK	OK	H	OK	H	OK	H	OK	OK	OK	SD	SD
60%	OK	OK	OK	OK	OK	OK	OK	OK	OK	OK	H	OK	OK	OK	OK	OK	OK	OK	SD	SD
70%	OK	OK	OK	H	OK	OK	OK	OK	OK	OK	OK	OK	OK	OK	OK	OK	OK	OK	SD	SD
80%	OK	OK	OK	H	OK	OK	OK	OK	OK	H	OK	OK	OK	OK	OK	OK	SD	SD	SD	SD
90%	OK	H	OK	H	OK	L	OK	OK	OK	OK	OK	OK	OK	OK	BW	BW	BW	BW	SD	SD
100%	BW	BW	BW	BW	BW	BW	BW	BW	BW	BW	BW	BW	BW	BW	BW	BW	BW	BW	X	X

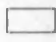
Key:

F = Filter blockage

P = Pipe blockage

 = Correct blockage diagnosis

 = Incorrect blockage diagnosis

 = Exceptional recommendation

OK = Correct blockage level diagnosed

H = Blockage over estimated

L = Blockage under estimated

SD = System Shutdown recommended

BW = Backwash recommended

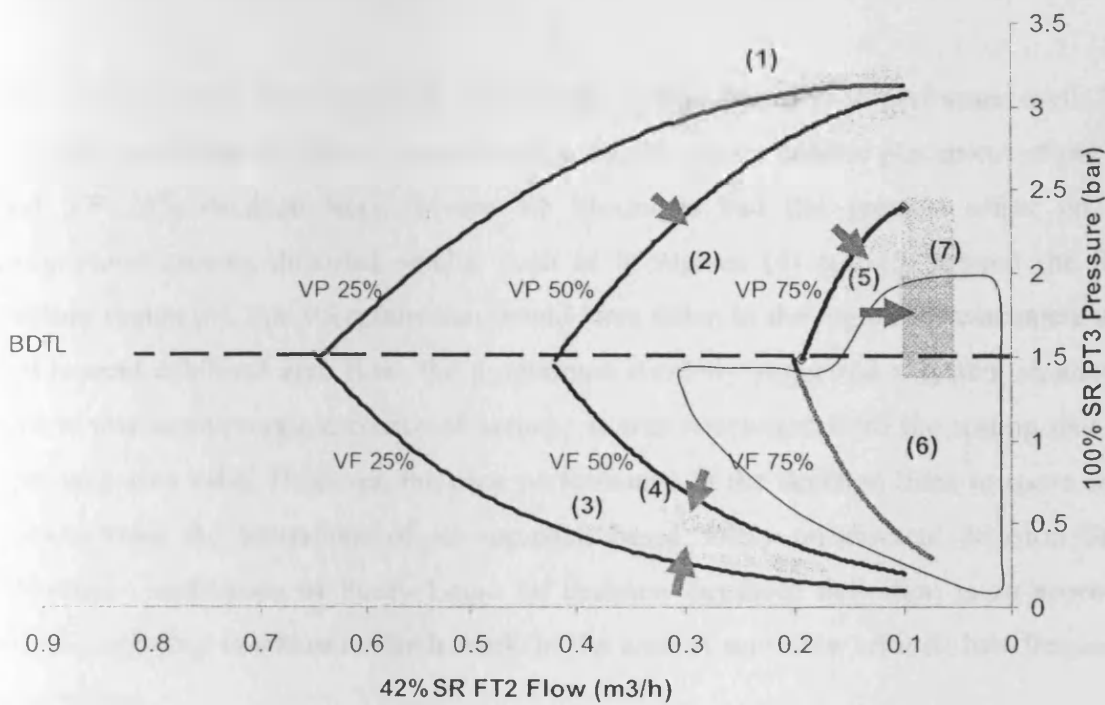
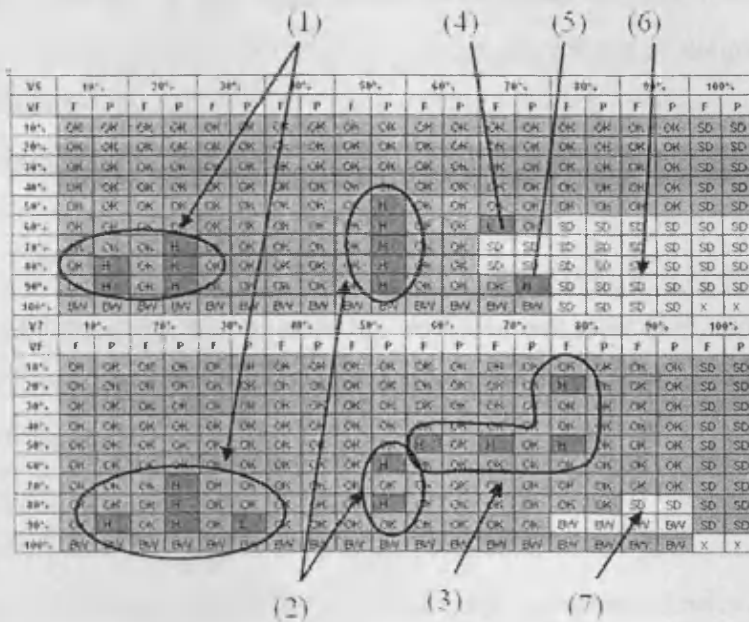


Figure 6.11: Explanation of combined blockage diagnostic test results.

Figure 6.11 highlights the decision line failure areas. The VP 25% decision line caused a number of over estimations and one under estimation, in the regions marked as (1). The narrowing of the margin for error at this higher blockage level end of the plot, combined with a poor placement of the decision line led to these errors. A better placement of the decision line section in region (1) would reduce these errors. The VP 50% decision line also caused a number of wrong diagnoses, with the pipe blockage level over diagnosed as

represented by region (2). In part these could be attributed to experimental error of the blockage levels. However, the V5 results were consistently over diagnosed suggesting that the decision threshold was possibly poorly placed for V5 combinations. In region (3) a number of subordinate VF blockages were over diagnosed. This was due to the reduced margin for error and a poor placement of the VF 25% decision line. The single results shown as (4) and (5) represent distortion which occurred due to the V5 starvation characteristic. In these cases the reduced flow and pressure effectively dragged the results across the decision thresholds into the wrong category. Region (6) represents all the severe V5 blockage cases where the starvation characteristics of V5 caused the flow to stall to zero, hence causing the programme to deliver a system shutdown recommendation. Finally region (7) represents the results where the synergistic behaviour of the combined blockages pushed the result into the mandatory backwash or shutdown region shown as Zone 5 in Figure 6.6.

The results showed that across the range of the system the method performed well. The accuracy in regions (1) and (3) could be improved by more precise placement of the VP and VF 25% decision lines. Severe V5 blockages had the greatest effect on the programme causing distorted results, such as in regions (4) and (5) around the flow stalling region (6). For V5 results that would have fallen in the region (6) catchment area but instead exhibited zero flow, the programme correctly suggested a system shutdown, which was an appropriate course of action. It was concluded from the testing that the approach was valid. However, the poor performance of the decision lines in some cases demonstrates the limitations of an approach based solely on discrete decision lines. Therefore, application of Fuzzy Logic for decision threshold definition is an approach worth exploring in future research work in the area of non-time critical, low frequency algorithms.

6.4 Chapter Summary

Through examination of the affects of combined blockages on FT2 flow and PT3 pre-filter pressure signals, a method for diagnosing the severity of combined blockages was developed and tested. The method was found to be capable of diagnosing dominant blockages to within 10% of the levels introduced in tests. Subordinate blockages could, in the majority of cases, be diagnosed to within 25%.

The Combined Blockage Level Diagnostic programme can be used to diagnose pipe blockage severity for any combined blockage scenario. For this purpose, the programme would be best applied by an operator who required this information.

If the programme were to be used to control backwash optimisation for combined blockages in the 'Maximum Speed Request Region', the programme could be configured to run automatically, allowing condition based backwash initiation to continue until the blockage could be remedied.

Further work would be required to assess the characteristics of internal pump blockages and integrate their behaviour into the Combined Blockage Level Diagnostic programme. It is concluded that the developed method was successful. Minimum processing power was utilised for calculation of the decision lines and the response of the programme was fast. It had been demonstrated that a non time critical, low data frequency approach can be implemented on a SCADA system for complete and complicated diagnostics, without undue overloading of system resources.

6.5 Overall WRAP Rig Programme Structure and Use

The overall structure and intended usage of the three developed programmes is summarised as follows: the timed repeating event triggers the speed request checking function, which in turn triggers the Condition based Backwash and Pipe Blockage Detection Programme. Following this, if normal filter fouling is diagnosed by the Condition Based Backwash and Blockage Detection programme, the level of blockage is compared with the backwash threshold and a backwash decision is made.

If an abnormal blockage is detected but the speed request is below 100% then the level of filter fouling is still correctly detected and an appropriate backwash decision is made. An on screen message is also issued alerting operators to the presence of an abnormal blockage.

Alternatively, if the speed request is above 100% the Combined Blockage Level Diagnosis programme outlined in this chapter is called. This gives a reasonable, but more

approximate, measure of the filter blockage level, allowing backwash initiation optimisation to continue despite the presence of a major blockage. The combined blockage severity diagnosis programme can also be triggered manually by an operator to evaluate the size of an abnormal pipe blockage. The operator may decide to do this even if the speed request is below 100%. Further, it is expected that the Blockage Location programme is always to be triggered manually by the operator when an abnormal blockage has been detected by the other programmes. This will allow the technician to correctly direct remedial attention.

6.6 WRAP Rig Research Conclusion

The research utilising the WRAP Rig had shown that a non-time critical low data frequency approach could be implemented using a standard SCADA package connected to a PLC for fault detection and diagnosis and condition based control. This could be achieved utilising already available process signal at standard resolution, either passively or through the use of active test cycles. The wider impact of the work is discussed further in Chapter 8. The final question considered in this thesis was whether a standard SCADA package could be deployed for efficiency monitoring to improve performance? Since the WRAP Rig was essentially used in a test rig configuration for this research, efforts were made to identify an operational process which could be use as the basis for such an investigation.

Chapter 7

Power Station and Gas Turbine Research Centre

7.1 Introduction

To further the aims of this research, a relationship was developed with the management team of a subcritical coal fired power station and an agreement was formulated allowing access to plant data and operating procedures. Due to the commercially sensitive nature of the data and information, the plant remains anonymous in this thesis and technical descriptions remain broad to prevent identification.

In this chapter the application of non-time critical low frequency algorithms to the problem of condenser efficiency monitoring in a coal fired power station is described. The condenser is essentially a heat exchanger, if considered in terms of the generalised cooling water infrastructure of Figure 7.1. The effectiveness of the condenser is impacted by factors relating to both the performance of the process and the cooling towers.

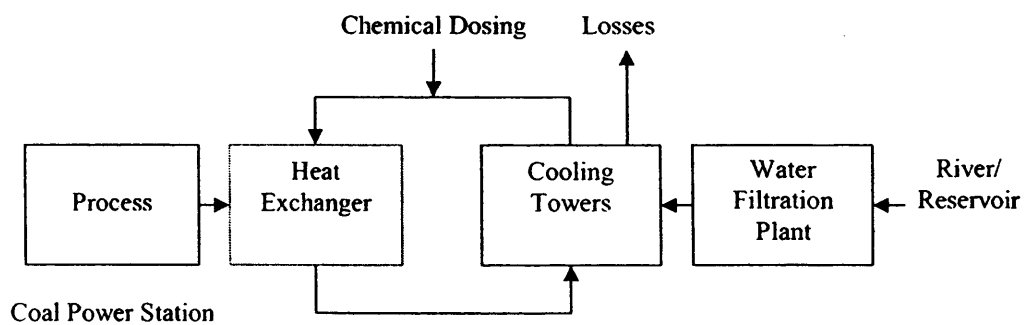


Figure 7.1: Simplified representation of the cooling water infrastructure in a generalised large scale industrial process with heat exchanger highlighted.

There are a large number of coal fired power stations world wide which could potentially benefit from improved condenser performance monitoring. It was considered that demonstrating this could be achieved, using the existing software in place at a power station, would make a significant academic contribution. Biomass, combined cycle gas

and nuclear power stations also utilise condensers and this broadened the relevance of the research.

The monitoring and management of condenser efficiency using non-time critical low frequency algorithms is considered in this chapter. A literature review covering cooling tower and condenser efficiency research is presented. Condenser back pressure deviation is identified as the key parameter for performance monitoring and an ideal back pressure surface equation is developed and implemented. A simulation is created using real coal fired power station data, within the SCADA software, which quantifies the deviation between the ideal back pressure and the actual back pressure in real time. The performance implications of this step are discussed and further possible applications of SCADA, for more in depth operational efficiency monitoring, are explored. Work undertaken at the University owned Gas Turbine Research Centre is also presented. This indicates the potential for application of SCADA across cooling water infrastructure, for efficiency monitoring an improvement.

7.2 Power Station Operation

In a typical subcritical coal fired power station pulverised coal and air is fed to a boiler where it is combusted producing flu gases and ash, as shown in Figure 7.2.

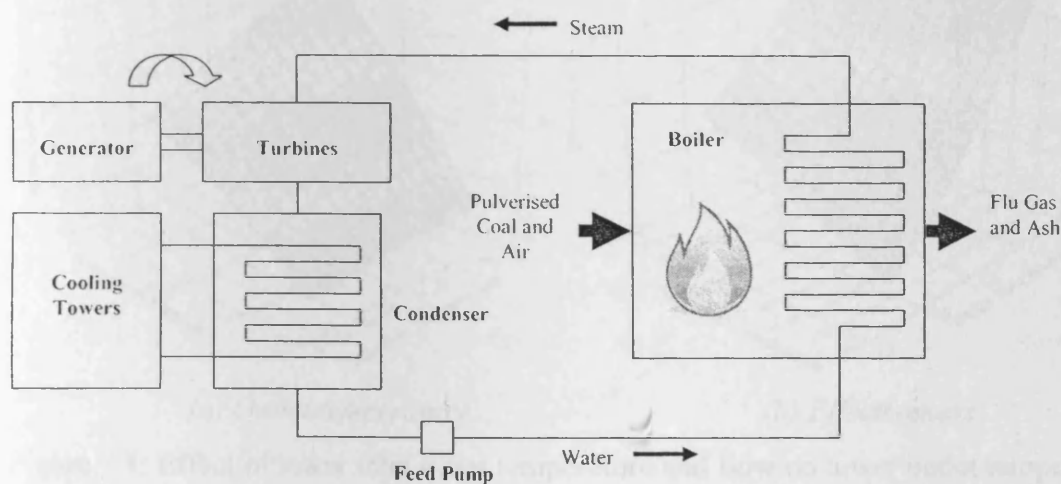


Figure 7.2: Simplified representation of a coal fired power station.

Highly purified water is fed to the boiler by a feed pump, where heat from the combustion of the coal turns it to steam. This high temperature high pressure steam is fed to the

turbines which are connected to the generator. After the steam has passed through the turbines it is fed to the condenser. Here the steam is turned back into water by exchanging heat to the cooling water, which is being pumped around the condenser from the cooling towers.

7.3 Literature Review

7.3.1 Cooling Tower Performance

Researchers have been analysing the thermal performance of wet cooling towers for many years. The first heat exchange model developed specifically for cooling towers was presented by Merkel [84] in 1925. Understanding the behaviour of cooling towers is important both to improve their design and also to optimise their operational efficiency.

Kim et al [85] modelled the relationship between cooling tower inlet flow rate and temperature, and the resulting outlet temperature as shown in Figure 7.3(a). Any increase in inlet temperature or flow rate, or a combination of the two, leads to an increase in outlet temperature.

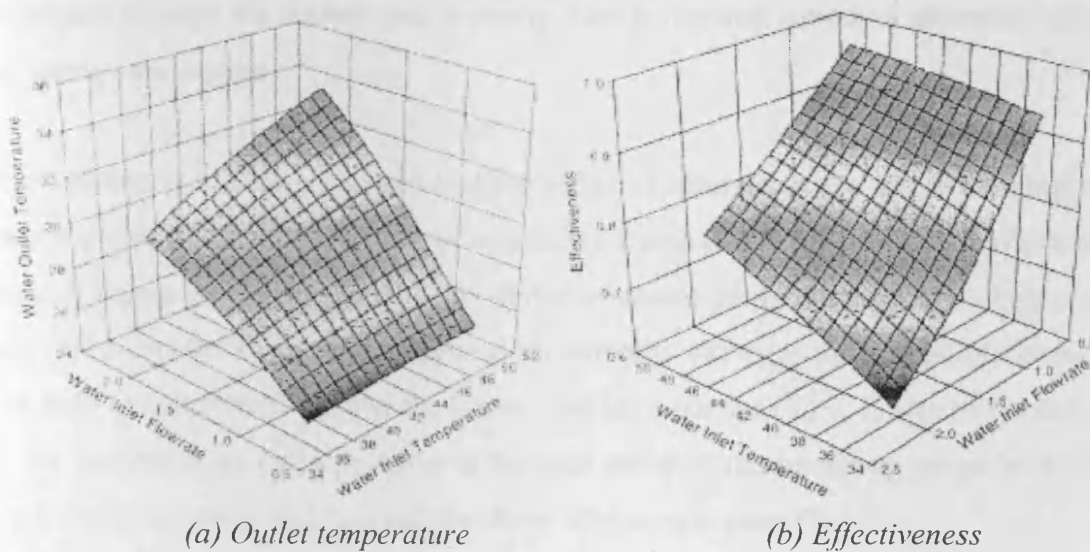


Figure 7.3: Effect of tower inlet water temperature and flow on tower outlet temperature and effectiveness (Kim et al [85]).

Kim et al [85] went further to define the effectiveness (e) of the cooling tower as the ratio of actual heat removal to the maximum attainable heat removal as shown in equation 7.1.

$$e = \frac{Q_{act}}{Q_{max}} \quad (7.1)$$

As can be seen in Figure 7.3(b), increases in inlet temperature have a positive impact on tower effectiveness, while increases in flow have a negative impact on tower effectiveness.

Picon-Nunez et al [86] described how temperature disturbances, which effect the outlet water temperature from the tower, propagate through the cooling systems in cycles until a steady state is reached. The two main reasons for a temperature disturbance are stated to be changes in ambient conditions at the tower end and changes in the heat load at the process end. The key ambient factors, which dictate the minimum water temperature attainable by the cooling tower, are stated to be the wet bulb temperature and the relative humidity. The two possible fluctuations in the heat load at the exchanger are variations in the process side flow rate and variations in the process flow temperature. If the process heat load is increased then the tower input temperature will rise, leading to a higher output temperature, as shown by Figure 7.3. Also if the ambient factors reduce the efficiency of the tower there will be a rise in output temperature. If these rises are not controlled, they propagate through the system until a steady state is reached, which is above the intended operating temperature.

Picon-Nunez et al [86] postulated that the effect of changes in the wet bulb temperature can be predicted by consideration of a quantity know as the tower thermal effectiveness (ϵ_{Tower}). Figure 7.4 shows the enthalpy verses temperature diagram for a cooling process. f_{R+A} represents the slope of the saturated air enthalpy curve, at the mid point between the wet bulb temperature (T_{wb}) and the tower inlet temperature (T_{w1}). f_R represents the slope of the saturated air enthalpy curve at the mid point of the operating range between the tower outlet temperature (T_{w2}) and the tower inlet temperature (T_{w1}).

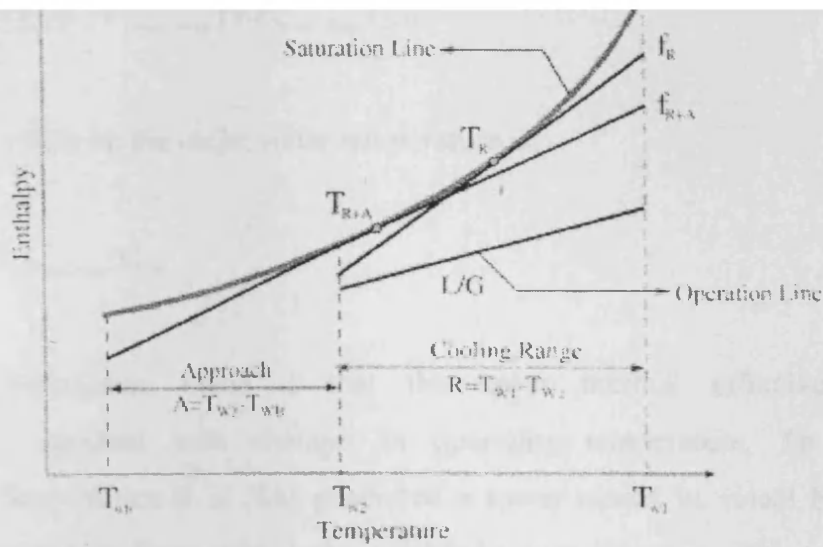


Figure 7.4: Enthalpy versus temperature diagram for a cooling process. (Picon-Nunez et al [86])

Based on this diagram El-Dessouky et al [87] derived the following equation for the rigorous thermal effectiveness of a cooling tower.

$$\epsilon_{Tower} = \frac{f_R(T_{w1} - T_{w2})}{f_{R+A}(T_{w1} - T_{wb})} \quad (7.2)$$

It is asserted that tower thermal effectiveness is a design parameter which remains as a constant when temperature changes enter the system. For example, a change in T_{wb} alters the slope of f_R and f_{R+A} which counteracts changes in the temperature difference ratio. Due to the difficulty of calculating f_R and f_{R+A} in a practical application Picon-Nunez et al [86] propose a simplified tower thermal effectiveness expression;

$$\epsilon_{Tower, simp} = \epsilon_{Tower} \frac{f_{R+A}}{f_R} = \frac{(T_{w1} - T_{w2})}{(T_{w1} - T_{wb})} \quad (7.3)$$

It is thus clear that the simplified tower thermal effectiveness can be used to calculate the changes in outlet temperature that will occur as a result of changes in the inlet or wet bulb temperature. For example, if a change results in a new wet bulb temperature of T_{wbN} then, the new outlet temperature T_{w2N} can be calculated by a rearrangement of equation 7.3, as follows.

Therefore the effect on the outlet water temperature is;

$$\Delta T_{w2} = \varepsilon_{Tower, simp} \Delta T_{wb} \quad (7.5)$$

The major assumption made is that the tower thermal effectiveness remains approximately constant with changes in operating temperature. To validate this assumption Picon-Nunez et al [86] generated a tower model in visual basic code and validated it against cooling tower data available in open literature. This model was then used to assess the tower thermal effectiveness equation, with the conclusion being that it was valid. The findings published clearly provide potential for online calculation of the loss of tower performance caused by changes in ambient conditions, if the problem of automated wet bulb temperature monitoring can be overcome.

Muangnoi et al [88] explored the effect of ambient air temperature and humidity on the performance of a counter flow wet cooling tower using an exergy based analysis. In simple terms exergy can be described as the maximum work which can be used from a system. The exergy analysis model used was validated against experimental data from a purpose built cooling tower. The model was then used to analyse the effects of varying inlet air temperature and humidity on the performance of the tower. The results can be seen in table 7.1 where T_{db} is the dry bulb temperature, Φ is the humidity and T_{wb} is the wet bulb temperature.

Inlet air condition			Exit air condition			Required dry air flow rate
$T_{db,i}$ (°C)	ϕ_i (%)	$T_{wb,i}$ (°C)	$T_{db,e}$ (°C)	ϕ_e (%)	$T_{wb,e}$ (°C)	G_{req} (kg/s)
32.40	40.0	21.91	34.30	96.5	34.08	0.0726
32.40	45.0	22.97	34.08	96.0	33.78	0.0806
32.40	50.0	23.98	33.82	97.2	33.41	0.0914
32.40	55.0	24.96	33.51	96.0	32.92	0.1073
32.40	60.0	25.90	33.14	94.1	32.27	0.1271
32.40	65.0	26.81	32.73	90.8	31.36	0.1725
32.40	70.0	27.69	32.36	84.2	29.99	0.3750
32.40	72.0	28.00	32.30	79.7	29.20	0.7400
27.00	70.0	22.77	33.83	100	33.83	0.0788
28.00	70.0	23.68	33.58	99.6	33.52	0.0877
29.00	70.0	24.59	33.28	98.2	33.02	0.1004
30.00	70.0	25.50	32.49	97.4	32.11	0.1205
31.00	70.0	26.41	32.58	94.6	31.79	0.1580
32.00	70.0	27.32	32.33	88.6	30.64	0.2685
33.00	70.0	28.12	32.88	73.0	28.65	2.1100

Constant input data: $L_i = 0.167$ kg/s, $T_{w,i} = 35.5$ °C, $T_{w,e} = 29.7$ °C, $Ka = 2.383$ kg/m³s, $A = 0.196$ m², $H = 0.5$ m, and $Le_i = 1.0$.

As can be seen, increases in the inlet air relative humidity and wet bulb temperature, at a constant dry bulb temperature, require an increase in tower air mass flow to achieve a given cooling water temperature drop. Similarly, increasing inlet air dry bulb and wet bulb temperatures, at a constant humidity, require an increase in tower air mass flow to achieve a given cooling water temperature drop. Both cases seem to exhibit a steep increase in required air mass flow with increasing ambient conditions.

Papaefthimiou et al [89] explored the effects of ambient conditions and tower control parameters using an involved computational model. The model was once again validated against real tower data, this time obtained from open literature. Three cases of surrounding air conditions were evaluated representing the mid-winter, mid-summer and average conditions in the city of Athens, Greece. In their findings they state that the ability of inlet air to absorb moisture is increased as the wet bulb temperature of the inlet air decreases. As evaporation is a major factor governing the thermal performance of the tower, the cooling efficiency and temperature drop across the tower increase with decreasing wet bulb temperature. A profound interrelation between the inlet air wet bulb

In the same study the results of varying the mass flow rate of water through the tower, otherwise known as the recirculation rate, were examined. It was found that the dry bulb temperature and humidity of the constant airflow leaving the tower increased, with the increasing mass flow rate of the cooling water stream. However, the actual temperature drop in the cooling stream decreases with increasing mass flow rate. This therefore, has a detrimental effect on the cooling capacity and thermal efficiency of the tower. Increases in the temperature of the tower input cooling water stream were examined and it was found that the temperature drop across the tower increased along with the evaporation rate.

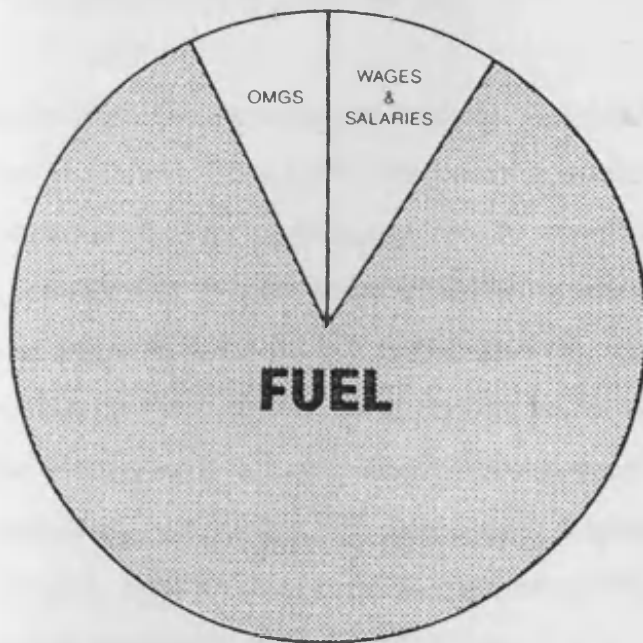
The cooling tower literature review conducted revealed that a number of operational factors can affect the efficiency of the cooling towers. Ambient conditions, in the form of the wet bulb temperature and relative humidity of the air, greatly alter the amount of heat which can be dissipated by the towers. The ambient conditions can obviously change in a matter of minutes and are beyond the control of the operator. Cooling water flow rate, or recirculation rate, is also a major factor but this variable can usually be controlled by the operators. Finally, the tower water inlet temperature was identified as factor in the performance of the towers. This variable is dependant on the process. It is therefore usually under the control of the operator. However, with the process being the dominant consideration in a plant, it is not practical to alter the process temperature in order to improve tower efficiency. The cooling towers must therefore be optimised to perform as well as possible considering the current process temperature.

7.3.2 Condenser Performance

The condenser turns steam from the turbines into condensate. Power station condensers are usually of a shell and tube construction. Cooling water flows through the condenser tubes. Steam enters one side of the shell and condensate emerges from the other, following heat exchange, as shown in Figure 7.2.

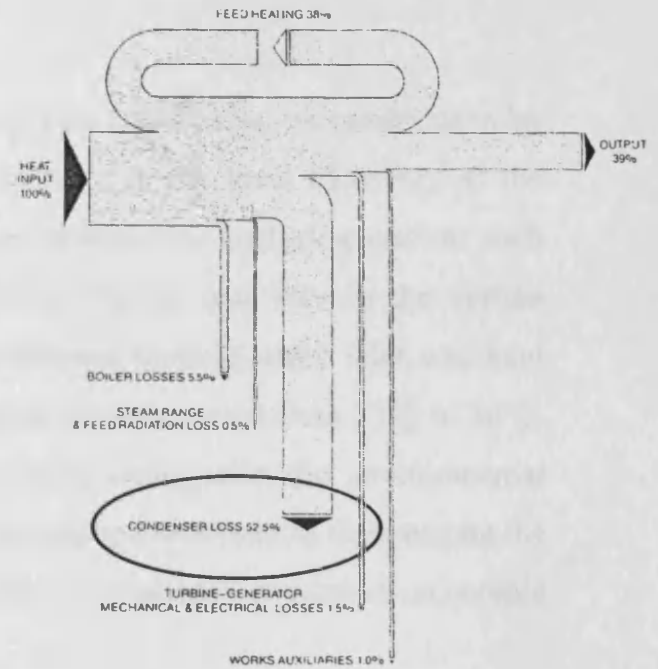
Gill [90] stated that "Condenser performance is undoubtedly the most important operating parameter on a unit." The back pressure in the condenser is important because the work

due to the extra heat required to produce a given output. Figure 7.5 taken from Gill [90] illustrates why the condenser is so important in terms of overall plant efficiency.



(OMGS: Other Materials, Goods and Services)

(a) Relative costs



(b) Sankey Diagram

Figure 7.5: Relative costs of running a medium size station and Sankey diagram of heat flow for a 500MW generating unit. (Gill [90])

As can be seen in Figure 7.5(a), by far the biggest expense of running a power station is fuel. Figure 7.5(b) demonstrates that the condenser actually dissipates more of the energy produced by this fuel, than is output from the station as electricity. This is shown by the condenser loss component circled in the figure. Therefore, any slight increase in condenser efficiency actually has a large impact on the operational efficiency of the station.

Rosen [91] performed an energy-based analysis of coal fired and nuclear power plants. A process simulation was used to deduce how the energy input into the station was consumed. For the two plants studied, it was found that 56% of the coal energy produced and 69% of the fusion heat produced was transferred to the cooling water via the

has also been undertaken to model the thermoeconomics of coal fired power stations, including condensers, as summarised and contributed to by Rosen et al [93]. In this work the ratio of thermodynamic loss rate to capital cost was examined with a view to the improvement of future plant design.

An in depth thermoeconomic analysis, focussed solely on condensers, was undertaken by Can et al [94]. This work utilised an economic analysis of the level of exergy of the condenser. Exergy analysis was chosen to be the best method for analysing systems such as condensers, where flows of differing energy are entering and leaving the system boundaries simultaneously. In the analysis, the condenser cooling water inlet was kept constant at 18°C and the outlet cooling water temperature was varied from 25°C to 36°C. The temperature and pressure of the saturated steam, along with the environmental conditions, were assumed to be constant. A graphical method was used to demonstrate the optimum operation point of the condenser, based on variations in external economic factors, as demonstrated in Figure 7.6.

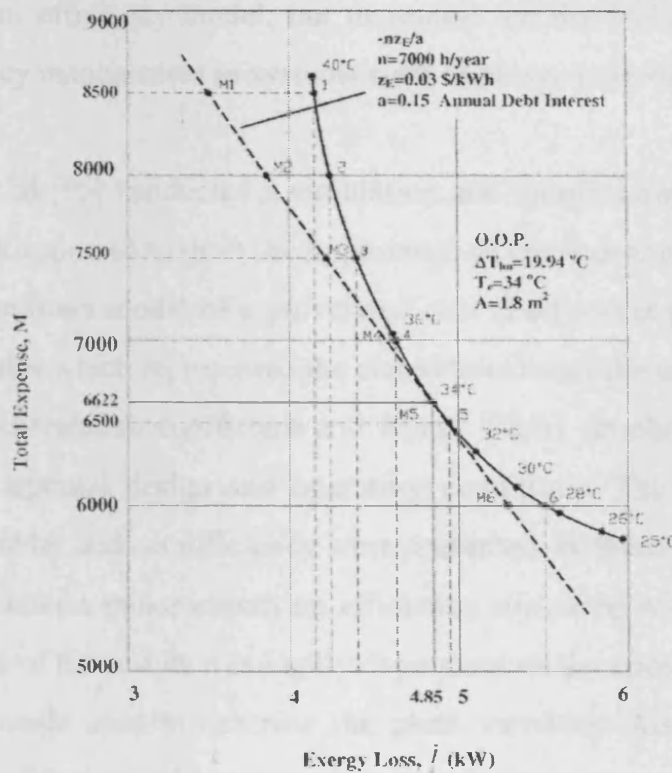


Figure 7.6: Optimum operating point (Can et al [94])

Each plot showed two lines, with the first being a curve relating operational expense to total exergy loss by variation of the cooling water exit temperature. The second line was straight and termed the expense line. This was a function of the hours run per year, the unit price of electrical energy and the annual debt interest of the plant. The point at which the expense line was tangential to the exergy variation line was found to be the optimum operation point (O.O.P in Figure 7.6). By varying the unit price of electrical energy and the annual debt interest, it was demonstrated that the economic optimum operating point, in terms of cooling water temperature rise across the condensers, was drastically affected by these external economic factors.

The work was highly focussed on the condenser and therefore did not account for the economics of other parts of the station. For example, the ambient conditions were considered to be constant. In a real power station this is not the case. If the ambient conditions change then cooling water flow rates may be altered to produce the optimum cooling water temperature rise across the condenser. This will then have an impact on pump power consumption, which could alter the optimum operation point. This analysis of the work is made not to undermine the approach taken by Can et al, which could form a building block of an efficiency model, but to remark on the highly complex nature of operational efficiency management in systems such as power stations.

Sanpasertparnich et al [95] conducted a simulation and optimisation of coal fired power plants, which at first appeared to limit the importance of condenser pressure on efficiency. A process based computer model of a pulverised coal fired power plant was constructed by combining modules which represented the characteristics of the component parts of the system. The Rank correlation coefficient and Monte Carlo simulation approaches were used to derive the optimal design and operating conditions. The correlations between certain process variables and net efficiency were presented. In these results, the condenser pressure appears to have a minor impact on efficiency compared with the other variables. However, the nature of the results was highly dependant on the construction of the station model and the rationale used to describe the plant variables. Also, a clear distinction between the effects of design and operation is not explained in the paper. For example one of the variables having the biggest impact on efficiency was described as the 'Boiler efficiency'. Indeed, boiler efficiency is of great importance but as no distinction is drawn between the design efficiency and operational efficiency it is not possible to contextualise

the data by understanding which of these was affecting the sensitivity analysis. If the condenser in a real station is considered, a loss of coolant flow through the condenser would result in a reduced pressure difference across the turbine, which would stop the generating process. Therefore, it could be argued that condenser efficiency has as high an impact on net efficiency as the boiler. The style of work undertaken by Sanpasertparnich et al is undoubtedly of value in the analysis of power station performance but the above description illustrates the difficulties which efficiency practitioners can face when trying to interpret and apply academic findings.

Further evidence of the perceived importance of condenser efficiency is provided by the large amount of research which has been conducted, in matters which affect the heat transfer possible in the condenser. For example Shaosheng et al [96] developed a combined fuzzy logic and genetic algorithm approach for online measurement of condenser tube fouling. This was intended to allow an economic cleaning schedule to be devised, which balanced the cost implications of reduced heat transfer efficiency with costs of condenser tube cleaning.

Wakui et al [97] also examined heat transfer issues in the condenser and developed a system for the online performance monitoring of shell and tube type heat exchangers. They used a test rig which mimicked the systems seen in fossil fuelled power stations, including a mechanical draft cooling tower. The flow rate and upstream pressure of the steam and the cooling water flow rate and condensate level were controlled via PID loop action, to simulate operational conditions. The intended use of the developed online performance measurement was to detect the gradual loss of performance associated with a build up of air on the steam side of the condenser. To do this, a mathematical steady state model of the heat exchanger was developed and executed using PROPATH software. Based on the input variables to the condenser, the steady state model was used online to predict the expected output variable values of cooling water outlet and condenser steam pressure with no air ingress. The actual measured output variables were then compared with this ideal response, to give an indication of the performance of the heat exchange process. The experimental results showed that as the amount of air present in the exchanger slowly grew, the deviation of the actual output variables from the expected steady state model variables, also increased. The model was tested and validated across a range of input conditions and shown to be effective. Within the steady state model a

performance correction factor was included, which was derived empirically through tests on the condenser. This was used to account for the slight discrepancies between the theoretical performance of the condenser and the actual operational reality. A major step outlined by the researchers, for further work, was to configure online update of the correction factor, to account for the effects of ambient conditions.

The research reviewed demonstrated that condenser performance was both highly important to plant efficiency but also difficult to manage. Ambient conditions, operator performance and mechanical malfunction are all factors impacting on the performance of this important system.

7.4 Coal Fired Power Station

7.4.1 Power Station Description

The plant was built in the 1960's and comprises of three generating units. The units can be considered typical and operate based on the principals which govern traditional subcritical coal fired power stations. Each unit is self contained, with a pulverised coal fed boiler heating purified water into steam which is fed to high, medium and low pressure turbines. These turbines are connected to a shared shaft, which translates the rotation of the turbines to an alternator generating a three phase power output. The steam is then fed from the turbines to a condenser, which lowers the temperature of the steam until it is condensed back into water. The condensate is then re-circulated back to the furnace after a de-aeration process. The steam is condensed, in the condensers, by exchange of heat to the water of the cooling system. The condenser in each unit is supplied with cooling water from a cooling system which is common to all three units. The cooling system comprises a large number of mechanical draft counter flow cooling towers, which share a common pond. The cooling water is re-circulated by three pumps each capable of producing a volumetric flow rate of 20000m³/h. Each unit has a separate control room usually manned by two operators. The units can communicate by telephone but there are no shared operator screens.

.....

In discussions with plant management it became clear that operational efficiency was important and that efforts had been made to monitor and optimise condenser performance. The key cooling performance indicator utilised centred on monitoring the disparity between the design back pressure and the actual measured back pressure, for each of the three condenser units. The back pressure indicated how effectively the steam was being condensed, which is a key parameter for optimising the efficiency of the generating process. A table, which was originally supplied with the condenser equipment on installation, related the generated load and condenser cooling water inlet temperature to give a value for the design back pressure. If the system was not running at optimum efficiency the measured back pressure in the condenser would be above that of the design. In real terms, this infers that the maximum possible power generation is not being realised from the chemical energy of the coal fed to the furnace. Based on this fact, an equation which included the price of coal was used by engineers at the plant to convert the back pressure difference in to an actual financial cost penalty.

Operationally the personnel controlling the units would attempt to optimise the system by minimising the difference between design and actual backpressure. However, the only method available for deriving the design backpressure was by manually using a copy of the design back pressure table, shown as Table 7.2, which was attached to the operator console in each control room. This involved reading the current generated load and condenser cooling water inlet values and cross referencing them in the table, to find out the design back pressure. When the generated load and cooling water temperature values fell between those provided in the table, an estimated design back pressure would be used. This method was labour intensive and inaccurate. In an attempt to provide some level of historical trending of the cost penalty, efforts were made to measure and record the back pressure difference on each unit once a day. This was then used to calculate the cost penalty per hour, at that moment, and then multiplied by the number of hours operated to give an indication of the cost penalty for the full period of operation. Once again this method led to inaccuracies due to the error associated with using the back pressure table. More significantly the calculation of cost penalty for the period of operation was inferred from a single instantaneous measurement. The generated load profiles, along with other variables, fluctuate throughout a period of operation leading to an ever changing

difference between design and actual back pressure. As a result multiplying the cost penalty for a given hour, by the number of hours operated, could not provide an accurate reflection of the true cost penalty.

7.5 Design Back Pressure Table Assimilation

7.5.1 Design Back Pressure Equation Development

It was decided that the first step towards improving condenser efficiency monitoring was to assimilate the design back pressure table into the SCADA software. This would then facilitate the automated real time indication, of the deviation of the actual measured back pressure, from the design back pressure. This would allow the operators to rapidly assess condenser efficiency and act to improve the situation, which was not possible previously. The accurate logging of associated cost penalty data could also be achieved. This would facilitate accurate cost management. The design back pressure table used by the operators is shown in Table 7.2. The design back pressure is expressed in inches of mercury.

CW Inlet Temp. °C	Generated Load MW (%MCR)								
	36 (30%)	48 (40%)	60 (50%)	72 (60%)	84 (70%)	96 (80%)	108 (90%)	120 (100%)	132 (110%)
2	0.452	0.494	0.543	0.601	0.668	0.744	0.834	0.938	1.060
3	0.475	0.519	0.568	0.627	0.695	0.772	0.862	0.967	1.090
4	0.498	0.543	0.594	0.653	0.722	0.800	0.891	0.996	1.119
5	0.525	0.571	0.623	0.683	0.753	0.833	0.925	1.032	1.156
6	0.552	0.599	0.652	0.714	0.785	0.866	0.959	1.067	1.193
7	0.583	0.630	0.685	0.748	0.821	0.904	0.999	1.109	1.236
8	0.613	0.662	0.718	0.783	0.858	0.942	1.039	1.151	1.280
9	0.647	0.698	0.756	0.823	0.899	0.985	1.085	1.199	1.330
10	0.682	0.734	0.793	0.862	0.941	1.029	1.131	1.247	1.381
11	0.720	0.774	0.836	0.907	0.987	1.078	1.183	1.302	1.439
12	0.759	0.815	0.878	0.951	1.034	1.127	1.235	1.357	1.497
13	0.802	0.860	0.925	1.001	1.087	1.183	1.293	1.419	1.563
14	0.845	0.905	0.973	1.051	1.140	1.238	1.352	1.481	1.628
15	0.894	0.956	1.026	1.107	1.198	1.300	1.417	1.550	1.702
16	0.942	1.006	1.079	1.163	1.257	1.363	1.483	1.620	1.776
17	0.996	1.063	1.139	1.225	1.323	1.432	1.556	1.697	1.858
18	1.050	1.119	1.198	1.287	1.389	1.501	1.630	1.775	1.941
19	1.110	1.182	1.264	1.357	1.462	1.578	1.711	1.862	2.033
20	1.170	1.245	1.329	1.426	1.535	1.655	1.793	1.948	2.125
21	1.237	1.315	1.403	1.503	1.616	1.741	1.884	2.044	2.227
22	1.303	1.385	1.476	1.580	1.697	1.827	1.974	2.140	2.329
23	1.377	1.462	1.557	1.665	1.787	1.922	2.075	2.247	2.443
24	1.451	1.539	1.638	1.751	1.877	2.017	2.175	2.354	2.556

As can be seen the magnitude of the divisions between data could lead to significant error, when using the table manually. Due to the age of the equipment, no information was available on the exact method originally used to derive the table and no underlying equation was available. It was decided that the best way to assimilate the table into the monitoring system would be to derive an equation for the surface generated by the table. This would allow the software to operate with values which fell between the categories in the table, minimising error and programme work load. The actual surface produced by the design back pressure data in Table 7.2 can be seen in Figure 7.7.

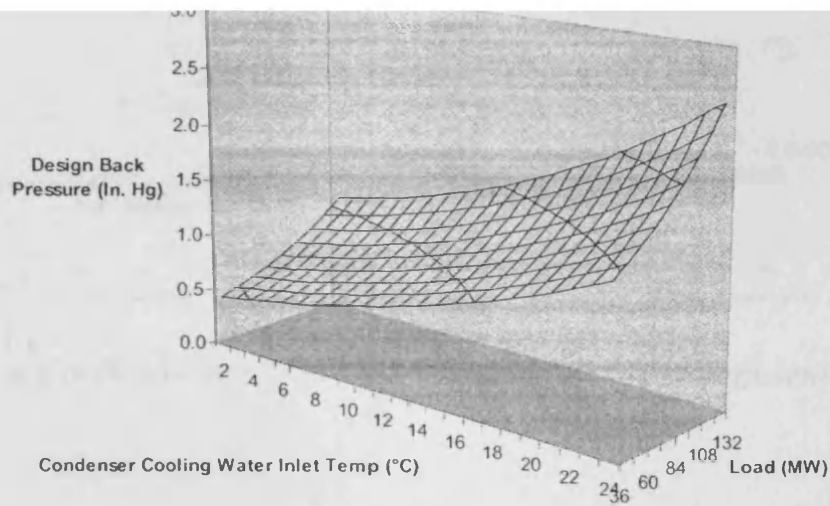
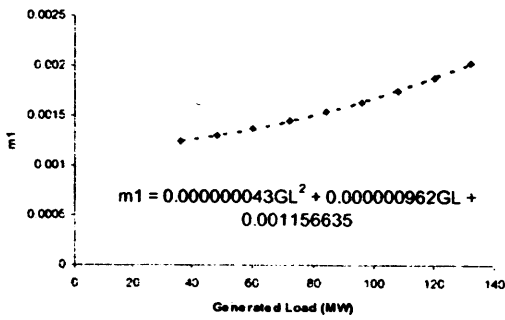


Figure 7.7: Design condenser back pressure related to condenser cooling water inlet temperature and generated load.

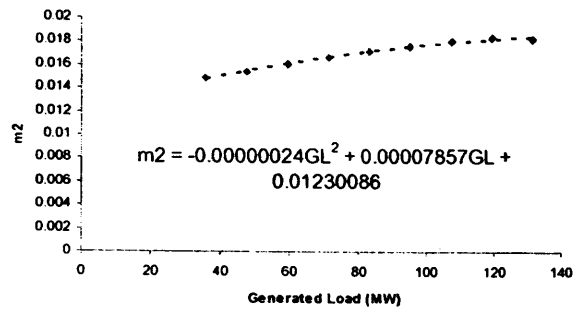
The surface seen in Figure 7.7 was composed of a series of curves for each finite value of generated load. Each of the generated load curves could be described mathematically, by a simple second order polynomial equation of the form shown as equation 7.6, where CW is the condenser cooling water inlet temperature.

$$\text{Design Back Pressure} = m_1 \times CW^2 + m_2 \times CW + c \quad (7.6)$$

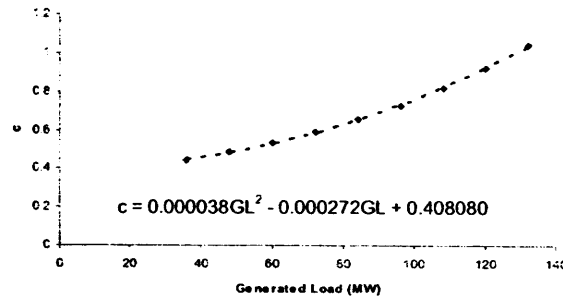
To obtain the equations, the individual curves for the nine available generated loads were plotted two dimensionally in a spreadsheet. The equations of each of the lines were then derived. Having obtained the nine second order equations, the nine values of m_1 , m_2 and c were plotted. The Excel Trendline function was used to obtain a second order polynomial equation for these curves, as can be seen in Figure 7.8.



(a) Coefficient m_1



(b) Coefficient m_2



(c) Constant c

Figure 7.8: Variation of coefficients and constant of equation 7.6 with varying generated load.

The derived equations shown in Figure 7.8 described how the coefficients and constant of equation 7.6 varied with generated load. The equations were substituted into equation 7.6 to give an overall equation for the surface, which would allow the design back pressure to be calculated based on the condenser cooling water inlet temperature and the generated load.

7.5.2 Back Pressure Equation Error Analysis

The new surface equation was used to generate design back pressure values for all the combinations of generated load and cooling water inlet temperature provided in the original design back pressure table, shown as Table 7.2. It was possible to compare the surface equation generated values, with the actual table values, and provide a sum of squared errors between the two. The spreadsheet solver function was used, along with manual manipulation of the equation, in an attempt to minimise the discrepancy between the table and surface equation values, as quantified by the sum of squared errors.

The best fitting equation had a sum of squared errors of 0.028. However, the error profile was not uniform across the surface, as can be seen in Figure 7.9. The usual operating region of the condensers was between 16°C and 24°C for cooling water inlet temperature and 80MW to 120MW for Generated Load. This fell in an area where the errors were larger and all of identical sign. If left uncorrected this would generate a cumulative systematic error, over the course of an operational period, if used to sum cost penalty.

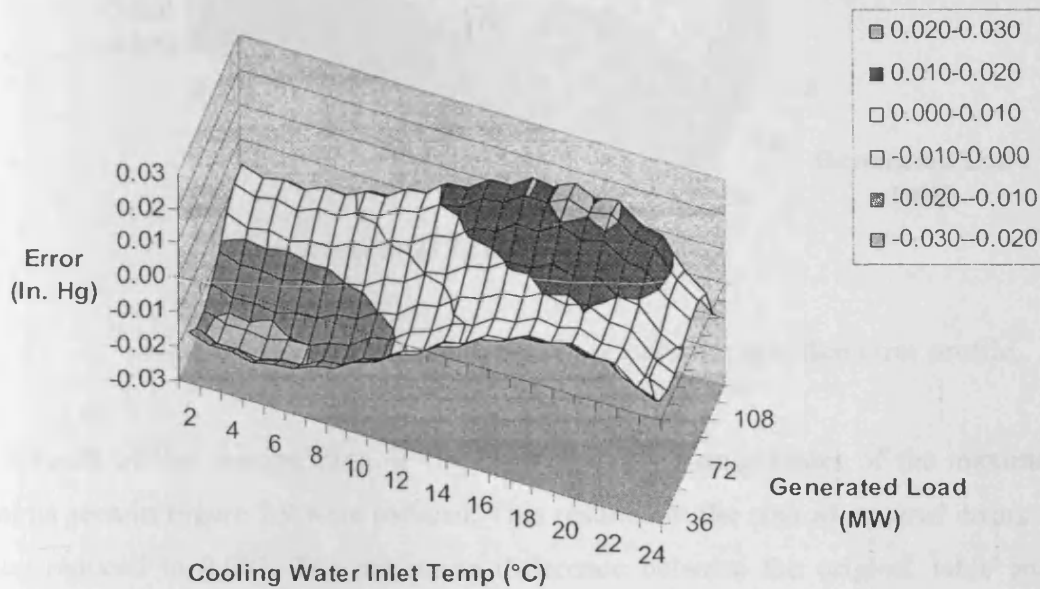


Figure 7.9: Design back pressure equation error profile.

The error was significant but the equation was to be implemented using the SCADA software. Therefore, it was considered possible to manipulate the values generated by the design back pressure equation using conditional executers. This would allow the selective reduction of the worst errors, as embodied by the trough and peak regions seen in Figure 7.9. To see how this would affect the error profile the values in the error table used to generate Figure 7.9 were manipulated by either adding or subtracting quantities. After a period of trial and error, it was decided to add 0.12 to all cells with a cooling water inlet temperature of 2°C to 11°C and a generated load of 36MW to 84MW, to reduce the depth of the trough. To reduce the height of the peak, 0.14 was added to all cells with a cooling water inlet temperature of between 14°C and 22°C and a generated load of between 84MW and 132MW. The new error profile shown in Figure 7.10 resulted.

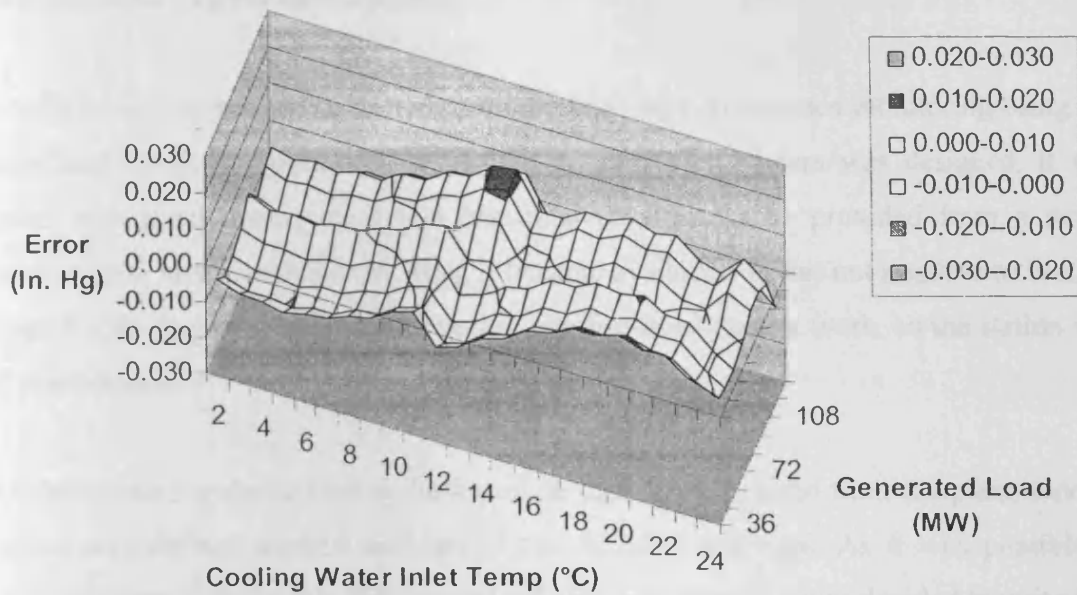


Figure 7.10: Manipulated design back pressure equation error profile.

As a result of this manipulation, it can be seen that the magnitudes of the maxima and minima seen in Figure 7.9 were reduced. This resulted in the sum of squared errors value being reduced to 0.007. The maximum difference between the original table and the devised method, in the usual operating region, was now 0.008 In. Hg. This represented an error of 0.38% of the full scale of the table. As a result, any discrepancy between the equation and the table would be small and not influence the decision making of the operator. The average difference in the operating region was 0.0025 In. Hg, which represented an error of 0.12% of the full scale of the table. Therefore, any cumulative error in the calculation of cost penalty would also be insignificant. It should also be noted that no information on the origins of the back pressure table were available. Therefore, the error between the table values and the equation values may be influenced by the construction of the original table. For example, it is possible that the table was constructed by mathematical extrapolation of test data from the condenser. This could have led to an irregular surface. As the data in the table is used for performance monitoring at the station, it would be advisable to recheck and confirm the validity of the data. This was however, outside the remit of the research. Any future updates could be quickly assimilated into the new system using the defined methods.

7.6 Simulation System Development

In order to implement and test an algorithm providing performance monitoring using the assimilated condenser performance surface, a simulation system was designed. It was agreed with plant management that historical data would be provided from a newly installed plant historian database, when it became available. It was not possible to link the research software directly into the existing site for development work, as the station was fully operational.

In order to run simulations using the historical data files obtained from the plant, a novel method was devised to feed the data to the SCADA software. As it was possible to manipulate data tags directly from embedded Citect functions, it was decided to write data feed functions into which data sets from the historical files could be pasted. This data would then be uploaded to the relevant on screen tags to produce a simulation. An 'Event' was configured in Citect to repeatedly trigger the simulation update at set intervals.

For each variable to be fed into the system a separate data feed function was written containing a one dimensional array. On initialisation, this array was populated with the relevant data set, which had been pasted into the actual code of the function before it was compiled and run. For example, a column of generated load data representing a day of operation would be pasted into the generated load data feed function. The array defined in this function was populated sequentially with this data when the function was called.

A global counter variable, which was independent of all of the Cicode functions, was configured. This incremented each time the main simulation function was run by the 'Event'. This global counter was used by the data feed functions to select the array element to be uploaded to the on screen variable tag. So on the first cycle of the simulation, element 0 of each of the arrays in the data feed functions was fed to the relevant on screen tag. On the next cycle element 1 of the arrays was uploaded. As a result the on screen variable tags were updated with the next set of historical process data. This had the effect of producing a simulated replay of the plant process variables.

A function was written which read the current generated load and condenser cooling water inlet temperature. This was then substituted into the developed design back pressure

equation (7.6). The conditional executors were then applied, by the function, to minimise the error, as described previously in Section 7.5.2. Following this, the calculated design back pressure was compared to the actual back pressure, which had also been read into the function at the start of the cycle. This produced a value for the difference between the two.

As mentioned previously, an equation which calculated the cost penalty, based on the difference between design and actual back pressure, taking into account the price of coal, was available. The equation was a multiplication of the back pressure, coal price and a weighting value. This simple equation was assimilated into the function allowing the cost penalty per hour to be generated and displayed. Finally a measure of the cost penalty accumulated over the current period of operation was calculated. The functionality of the simulation programme is represented in the flow diagram of Figure 7.11.

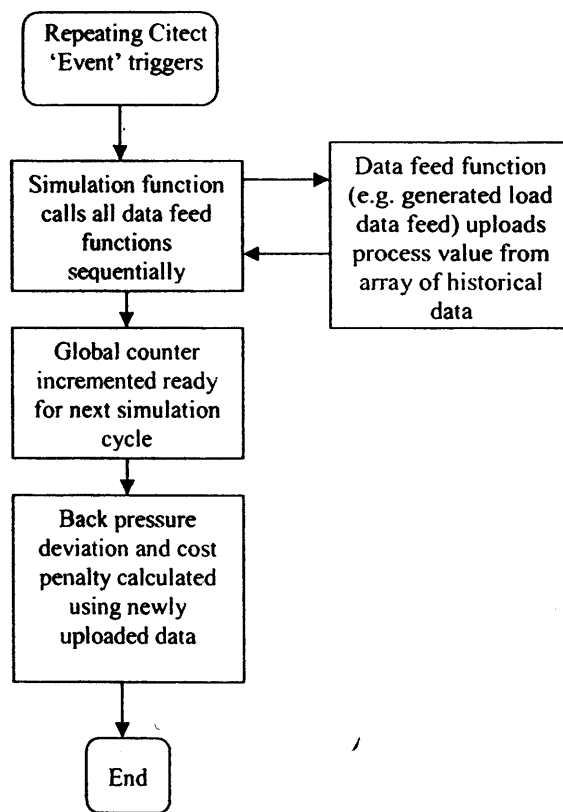


Figure 7.11: Simulation system functionality.

To accompany the simulation a process mimic for each of the three generating units was produced, as shown in Figure 7.12. A back pressure information pane was constructed displaying the key efficiency information now being calculated using the ideal condenser performance curve. Various key process variables were also displayed next to the

appropriate sections in the plant mimic diagram. These were all updated during the simulation by the relevant data feed function.

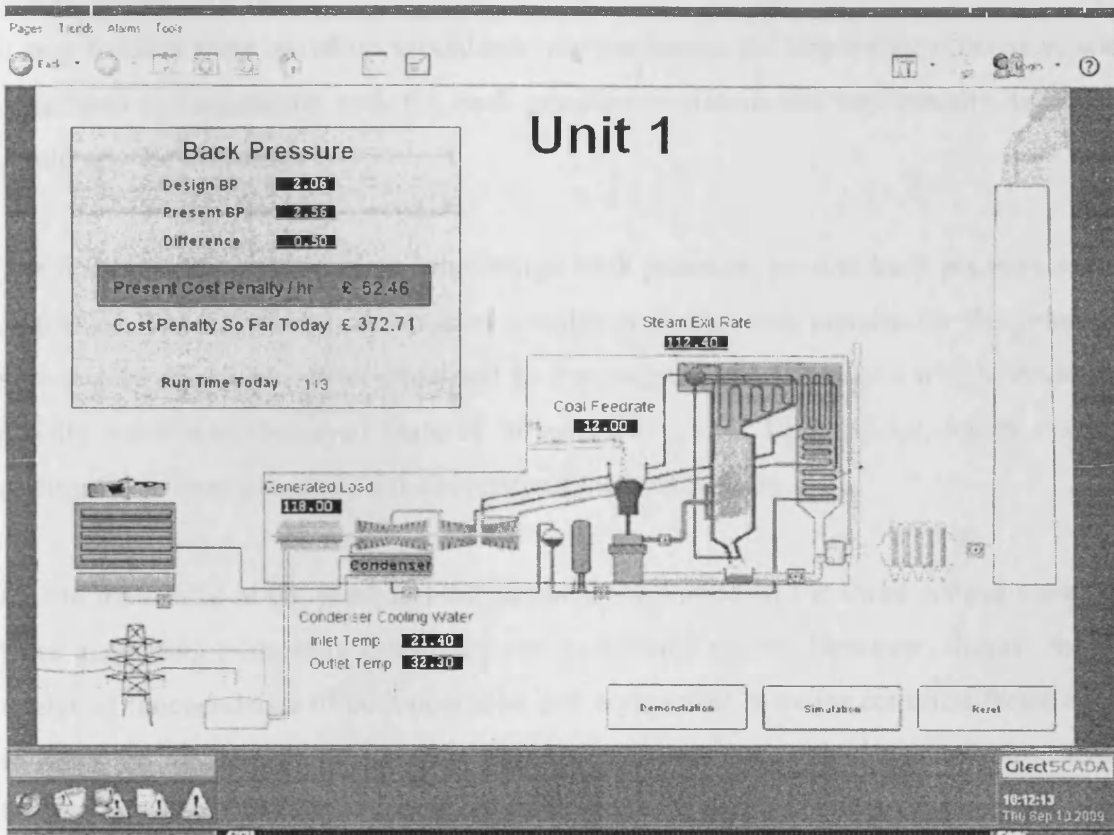


Figure 7.12: Process mimic for one of the three generating units.

The mimic screen in Figure 7.12 shows an overall process view, one step removed from the highly detailed and fragmented control screens which are in place in the control rooms. The current control screens which allow manipulation of numerous small plant elements (such as valves for example), required a comprehensive representation of the plant for obvious reasons. Due to the level of complexity this was achieved by a number of focused mimic screens, showing only certain elements of the whole plant. While this was a necessity for the safe and correct operation of the plant, it was felt a significant advantage could be achieved in this research by configuring a far less detailed overview screen. This would provide a greater opportunity for a systems approach to the efficient running of the plant. A number of key governing variables, as discussed and outlined with the plant management, were included on the screen and updated by the data feed functions:

- Generated load
- Condenser cooling water inlet temperature

- Condenser cooling water outlet temperature
- Coal feed rate to the furnace
- Steam flow rate

It was felt that these variables would provide the basics for improving efficiency, when considered in conjunction with the back pressure deviation and cost penalty data which would now be available.

The Back pressure pain displayed the design back pressure, present back pressure and the difference. The associated current cost penalty and total cost penalty for the generating period were also displayed as calculated by the programme. The bar on which present cost penalty value was displayed featured an adaptive traffic light colour, which could be configured to change based on the severity of the cost penalty.

Due to the nature of the plant and the physical separation of the three control rooms, the three generating units were essentially run as isolated plants. However, despite the high degree of independence of both operation and equipment, a major common factor existed in the form of the shared cooling system. In discussions with plant management, it became apparent that little was known about the interrelation between the generating units. Indeed it was suggested that potentially operators in the three units could be working at cross purposes in their use of the cooling system. Due to the lack of data, there was however no evidence to support this. Once again, the prospect of a system overview approach to efficiency monitoring was considered to be of value to the management, in this case on a station wide basis. As a first step to exploring the potential of this functionality, a station overview screen was created combining information from all three units as shown in Figure 7.13.

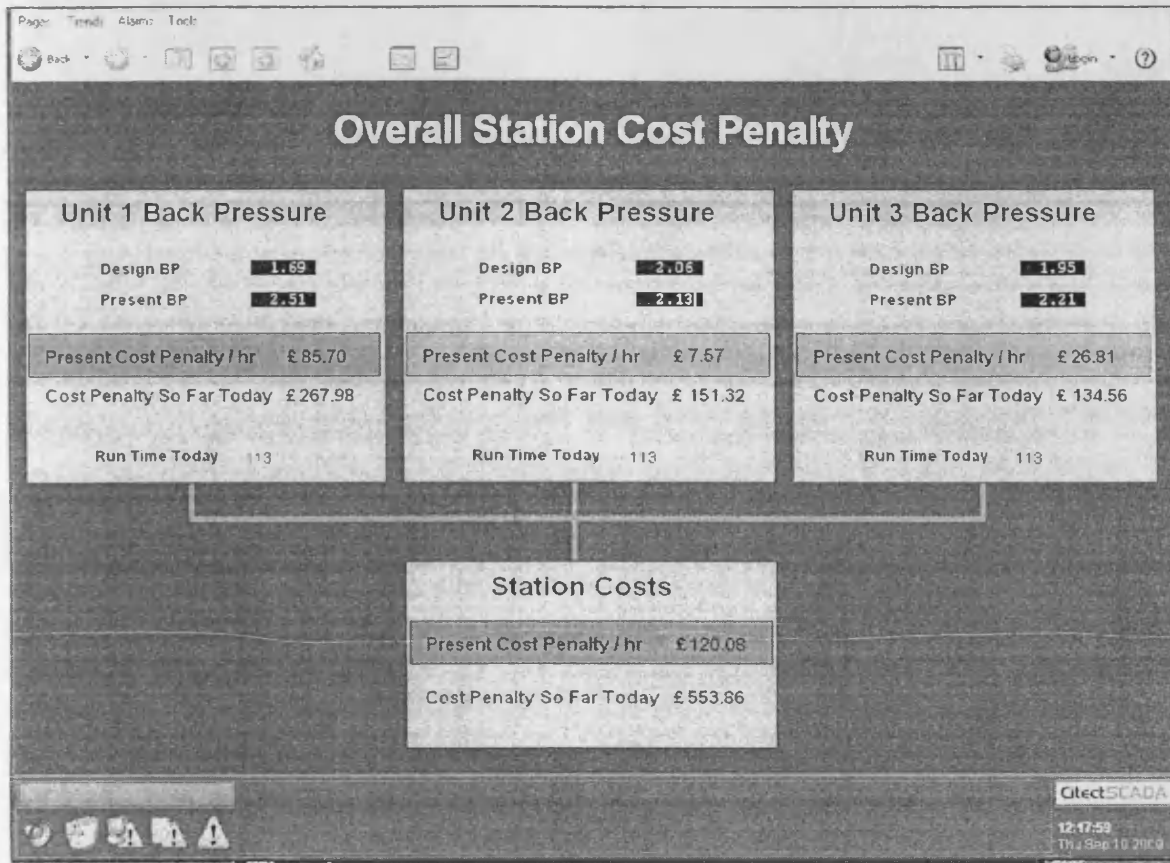


Figure 7.13: Station-wide condenser efficiency overview screen.

In Figure 7.13 it can be seen that the station overview screen provides cost penalty information from all three units and then combines this to show an overall cost penalty for the station. The cost penalty per hour for the station is once again presented on a dynamically coloured bar, similar to the individual units, to draw attention to high values. From the station manager's perspective, this could allow an instant appraisal of the current state of the station efficiency and also identification of which units were responsible for problems. It was also deemed to be of value by the management team as, according to them, it would generate competition between the operators in the three units, driving them to focus on improving condenser efficiency.

Recent data, representing one month of operation, was provided by the station for simulation. The data was recorded at a frequency of one hour. Data was actually captured and stored by the station at 10 second intervals, providing operators with detailed trends. However, the data was only stored at this resolution for 24 hours. After this period, all data recorded during the hour was discarded and only the data point recorded on the hour was retained. This was done to reduce the storage requirements of the historian database.

The data provided was of a low frequency of one sample per hour and only one month of data could be obtained. The plant was also not being run near maximum capacity, due partly to the fact that the data was taken during the summer months, when demand is lower but largely due to the fact that all the units were shut down for maintenance at some point during the month.

The data provided was pasted into the data feed functions and the project compiled and run. In the runtime environment the simulation using real historical data now began. It was possible to see and trend the difference between design back pressure and actual back pressure, the current cost penalty and the accumulated cost penalty for the real plant data.

7.7 Simulation Results and Potential System Applications

7.7.1 Cost Penalty Monitoring

The original method for calculating the cost penalty employed by the station involved manually entering the process values, taken at some point during an operating period for a unit, into a spreadsheet. The design back pressure was manually derived from the design back pressure table and entered into the spread sheet. Finally the period in hours which the unit was run for was manually entered. The cost penalty equation calculated the cost penalty per hour based on the instantaneous data point provided and then multiplied this by the run time in hours for the operating period, to give a total cost penalty. It was believed that this approach was highly inaccurate due to the fluctuating nature of the generation profile and the error associated with manual use of the back pressure table. This was proven to be the case by analysis of the cost penalty values produced by the simulation. An example of this is shown using two successive periods of operation taken from Unit 1, as shown in Figure 7.14. In the figure, only the generated load and cost penalty trends are shown for clarity, although the trends for all the on screen variables, listed previously in Section 7.6.1, were available.

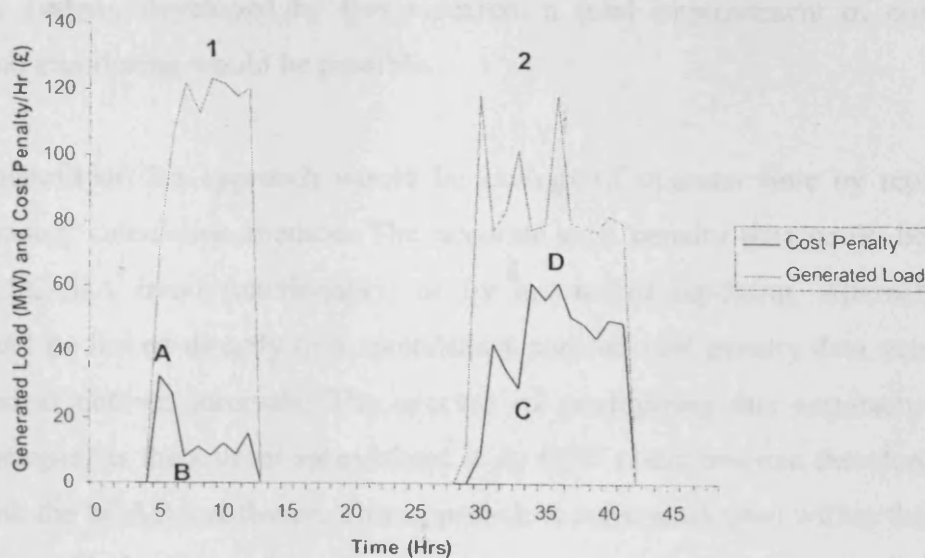


Figure 7.14: Two successive generating periods of Unit 1.

As can be seen in the example of Figure 7.14, there was a high level of variation in the cost penalty over a given generating period. The possible errors which would result using the old method are shown in Table 7.3. The errors are calculated based on the data that would have been logged if the system was sampled at its most and least efficient points, in terms of cost penalty, compared with the accurate cost penalty data produced by the research system. The error is expressed in terms of cost penalty per hour, to provide a relative measure of inaccuracy.

Table 7.3: Example of cost penalty error.

Period	Correct cost penalty values		Highest possible erroneous cost penalty using manual method			Lowest possible erroneous cost penalty using manual method		
	Total	Average /hr	Cost penalty/hr used	Total based on penalty used	Average error /hr	Cost penalty/hr used	Total based on penalty used	Average error /hr
1 (9hrs)	£124.31	£13.81	£32.69 (A)	£294.21	165.7%	£8.03 (B)	£72.27	41.9%
2 (12hrs)	£542.25	£45.19	£61,80 (D)	£741.6	36.18%	£9 (C)	£108	80.1%

Table 7.3 illustrates the level of error possible using the existing method. Based on this data it can be argued that the existing method of cost penalty monitoring was inaccurate to the point of being ineffective and misleading. By fully implementing the cost penalty

monitoring system, developed by this research, a total improvement of cost penalty performance monitoring would be possible.

The first benefit of this approach would be savings of operator time by replacing the existing manual calculation method. The accurate cost penalty data could be recorded using the SCADA trend functionality, or by automated reporting. Alternatively, the system could be linked directly to a spreadsheet and the cost penalty data automatically downloaded at defined intervals. The process of configuring this approach would be relatively simple, as the current spreadsheet is an OPC client and can therefore interface directly with the SCADA software. This approach is commonly used within this industry. The system could also be configured to provide a manual input box in which the current price of coal would be set. This would then be automatically substituted into the cost penalty equation, ensuring the cost penalty values were up to date.

Cost penalty is a useful measure for plant management, as it helps to assess the financial viability of the station. Accurate records of cost penalty data allow important operational and financial decisions to be based on facts rather than estimated values. Once accurate data was available, it could be formatted in a number of ways to provide Key Performance Indicators. For example, cost penalty totals could be divided by generation totals for a period to give a cost penalty per KW value for the condensers.

The accurate cost penalty data would also facilitate cost benefit analysis procedures. The percentage condenser efficiency improvement, associated with a proposed plant upgrade or maintenance action, could be estimated. The cost of the work could then be compared with the potential savings calculated from the historical cost penalty data and a payback period calculated. For example, it had been stated by the plant managers that the cooling tower fans suffered from relatively low reliability. Due to the nature of the system, if a single fan went down the other four fans in this cell were also disabled. This then had a detrimental affect on the cooling capacity, which in turn increased back pressure deviation. Through proper record keeping of fan down time and a correlation of these records with cost penalty and back pressure deviation data, the real cost of this down time could be calculated. Then a cost benefit analysis could be performed on a predictive maintenance system. This system would allow early stage fan problems to be identified and then remedied at the earliest off-load opportunity, rather than the unit failing during

an operational period and causing increased back pressure deviation and associated cost penalty.

7.7.2 Back Pressure Deviation Display Benefits

The real time display of back pressure performance, as seen in Figure 7.13, was now possible. This would have a number of immediate impacts on the way condenser efficiency was handled even without further refinement of the system. The screens would provide a focal point for condenser management in the control rooms of the three units. Operators would be aware of large back pressure deviation events eliciting a corrective response. A trend display of the back pressure deviation could also potentially provide early warning information. This would alert operators to a gradually worsening back pressure, allowing corrective action to be taken, before a serious back pressure deviation occurred. A simple real time indication of performance could have the effect of empowering operators and allowing them to perform more effectively, as was the case in the performance monitoring system described by Kim et al [43]. Over time, these continual indications of the condenser efficiency behaviour would allow operators to learn more efficient operating strategies and to develop an understanding of efficiency disturbances. It is therefore likely that efficiency would be improved, just by the real time indication of back pressure deviation.

The plant overview screen shown as Figure 7.13 would also help to focus operators and plant managers on condenser efficiency. The plant managers indicated in discussions that they saw potential to implement the overview screen in all three control rooms. This would generate natural cross-unit competition. Operators could be further incentivised to improve condenser efficiency by the addition of a bonus scheme which rewarded the best performing operators. Managers also commented, that the overview screen would allow them to exercise far greater managerial control over the operators. Currently, a shift manager would be required to visit each control room in turn to assess the performance of each unit. The shift manager has a number of other duties and as such this form of supervision is highly impractical. The sporadic snapshot of performance obtained from these short visits does not allow a high degree of managerial control. However, the overview screen would allow the shift manager to assess the performance of all three units at once. The traffic light indication would make this process more intuitive. As a result,

the shift manager could conduct their normal duties focussing direct management time on poorly performing units.

7.7.3 Scope for Further Operator Guidance

In the event of high back pressure deviation the system also provides the potential to indicate what action, if any, should be taken by the operators. This could be based on a more in depth analysis of the condenser and cooling system state. Gill [90] states that the three main factors affecting condenser efficiency are; condenser cooling water inlet temperature, cooling water flow rate and interference with heat transfer in the condenser pipes, caused by fouling or steam side air blanketing. An operational method is presented by Gill [90], which allows the variation in back pressure caused by each of these factors to be manually calculated. The method relies on the design back pressure table which was already assimilated into the system and an additional two ideal performance curves for the condenser. The first of these two characterises is the variation of cooling water temperature rise across the condenser with respect to load. The second maps the Terminal Temperature Difference (TTD), with respect to load. The TTD is the temperature difference between the condenser cooling water outlet temperature and the steam temperature in the condenser. A representative plot of the ideal temperature rise and TTD for a typical condenser is shown as Figure 7.15.

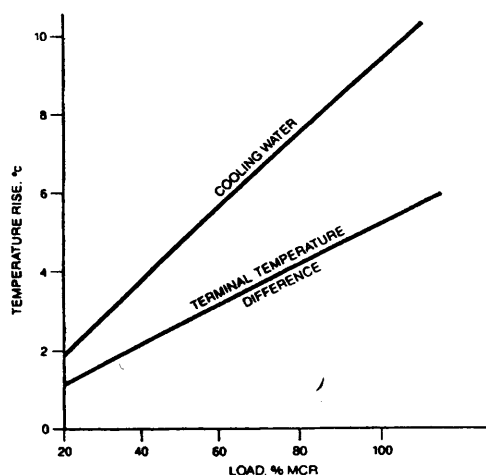


Figure 7.15: Condenser cooling water temperature rise and TTD for a typical condenser.

(Gill [90])

It was recognised that the two lines shown in Figure 7.15 could be easily assimilated into the system by deducing their line equations. As a result the ideal cooling water rise and TTD could be calculated in real time based on the generated load of a unit. This would allow the method outlined by Gill [90] to be applied in real time. The method is summarised in Table 7.4.

Table 7.4: Method for deducing back pressure deviation causes (Gill [90])

Back Pressure Variation Cause	Level of Back Pressure Variation
Condenser cooling water inlet temperature	$CW_I - CW_{Rise} + TTD - BP_{Des}$
Cooling water flow rate	$CW_O + TTD - CW_I + CW_{Rise} + TTD$
Air/dirty tubes	$BP_{Act} - CW_O + TTD$

In Table 7.4, CW_I is the condenser cooling water inlet temperature, CW_O is the condenser cooling water outlet temperature, BP_{Des} is the design back pressure, BP_{Act} is the actual back pressure, TTD is the ideal terminal temperature difference and CW_{Rise} is the ideal condenser cooling water temperature rise across the condenser. The summarised method equations in Table 7.4 could be coded into the SCADA system allowing the back pressure variation causes to be displayed and prioritised on screen.

Having an accurate on screen breakdown of the factors responsible for a high back pressure deviation event would help to improve operator response in a number of ways. If cooling water inlet temperature was causing major deviation, more towers could potentially be brought online. If cooling water flow was identified as a major cause, the position of cooling water outlet valves and the number of pumps in service could be optimised, lowering back pressure. The level of deviation caused by air blanketing or tube fouling could be used as an indicator for deciding when to take remedial maintenance action on the condensers. As this functionality may only be required during high back pressure deviation events, its execution could be linked to an on screen button. This would reduce the processor loading, as the calculations would only be performed when required by the operator.

Gill [90] comments on the fact that increasing the cooling water flow can often have a positive effect on back pressure. It is suggested in the text, that this fact should be used by operators in times of poor back pressure performance, by increasing the number of pumps

on line for example. However, it is also stated that the operator should make the decision to follow this course of action based on whether the benefit of the improvement in back pressure is greater than the cost of the extra power used. If this decision is based on financial implications, determination of the correct course of action can only be made if the price of coal and the sale price of electricity are correlated with the improvement produced in the back pressure. In a real time situation, it is unlikely that the operator will have the resources and time to make the correct decision. The research system could however, be programmed to calculate the best course of action immediately using encoded equations and thus recommending the correct course of action to the operator.

7.7.4 Back Pressure Performance Benchmarking

The accurate back pressure deviation data, which would now be available, offered long term performance monitoring benefits, as well as real time operational optimisation improvements. Figure 7.16 shows the back pressure deviation data for the simulation run using the month of data provided by the station.

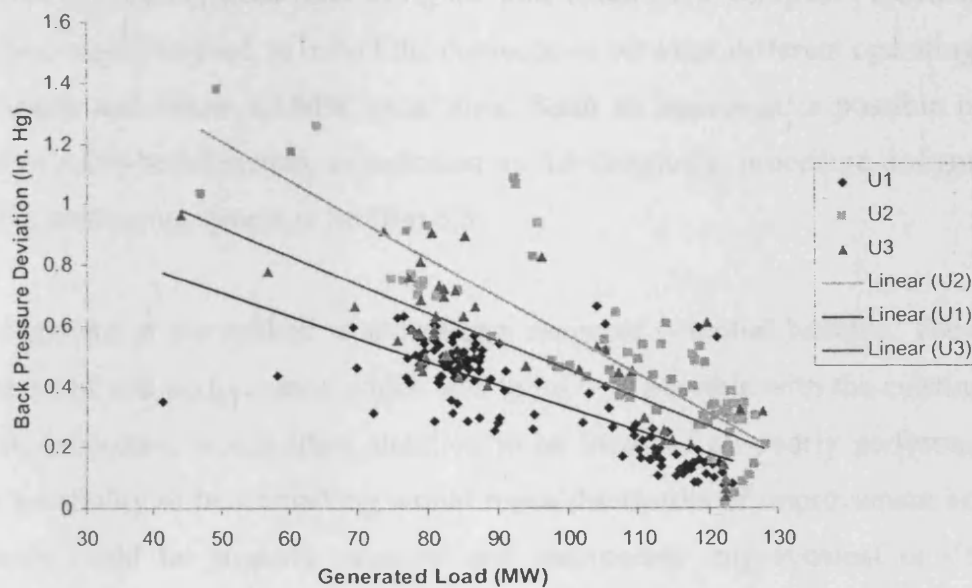


Figure 7.16: Back pressure deviation data with lines of best fit for each unit.

The lines of best fit for each unit have been included in Figure 7.16 to help in the explanation of how this new condenser performance monitoring data could be used. The spread of data around the lines of best fit, is the result of operational and climate conditions impacting on the back pressure. It also appears that there is an inversely proportional relationship, between back pressure deviation and generated load, and this is

discussed in the next section. It is clear from the lines of best fit that there is a marked difference between the back pressure performances of the units, across the generating range. In this month it was clear that, on average, Unit 1 operated most efficiently, with Unit 3 in second place and Unit 2 performing worst. In concept, a line of best fit approach could be applied to the data every month, allowing a direct performance comparison, thus facilitating benchmarked continuous improvement activity.

To enact this system, a considered and standardised approach would have to be developed for production of the lines of best fit. This is important, as it can be seen that Unit 2 was operated far above 120MW on a number of occasions, unlike the other units. In this very high output region, the Unit 2 back pressure deviation is minimal and as a result the line of best fit is skewed, with a steep gradient. This is because the high generation end of the trend line is pulled down by this grouping of points. If the plot only contained points below 120MW, the Unit 2 line would be far shallower providing a more accurate reflection of the Unit 2 performance, across the standard operating range. If analysis of a number of month's data were conducted a methodology for the application of performance monitoring trend lines using the plot could be developed. Potentially, more than one line would be used, to reflect the distinctions between different operating regions such as above and below 120MW generation. Such an approach is possible using the deployed SCADA-based system, as indicated by the diagnostic procedure designed in the WRAP Rig monitoring system in Section 6.3.

The development of the method would offer a range of potential benefits. The accurate measurement of unit performance, which was in no way possible with the existing station monitoring procedure, would allow attention to be focussed on poorly performing units. The new possibility of benchmarking would mean the results of improvement action and maintenance could be properly assessed and unexpected improvement or decline in performance could be spotted and investigated. This should also lead to early fault detection, as a fault affected unit would show a marked increase in back pressure deviation, resulting in the benchmark line of best fit being far above the line for the previous month. This would reveal the presence of a problem. As a result, the problem could be isolated and remedied immediately, rather than potentially going unnoticed for an extended period.

7.7.5 Real Time Contextualisation of Back Pressure Deviation Data

The data seems to indicate that there is an inversely proportional relationship between back pressure deviation and generated load. This was also the opinion of plant operators when questioned. It is probably due to the system being originally optimised to operate most efficiently near the maximum generated load. Using the new system, operators would be informed of the back pressure deviation in real time. This could allow them to apply their accumulated knowledge to attempt to lower the back pressure discrepancy and increase efficiency. However, at lower generated loads a higher deviation should be expected. As there is no indication of what the expected difference should be; operators would have no way of knowing whether the difference was significant or not. Therefore, it is quite possible that a high back pressure deviation would be ignored by an operator at low generation loads. It would be attributed to the normal poor, low generation performance, which has been noted over the years. On the other hand, a normal higher back pressure difference, at low generated load, may prompt a different operator to try and rectify a non-existent problem. Without the ability to contextualise data, thus producing actual performance information, the knowledge and expertise of the operators is wasted.

The work done on the WRAP Rig in Section 5.8 had indicated that an approach could be implemented to remedy this situation. A line of best fit could be generated for a particular unit, for a number of months, until a representative bench mark trend line was developed. The equation of this line could then be assimilated into the SCADA software and used to create a normal operation envelope, as was applied to filter pressure for abnormal blockage detection. A representation of how this would be applied is shown in Figure 7.17.

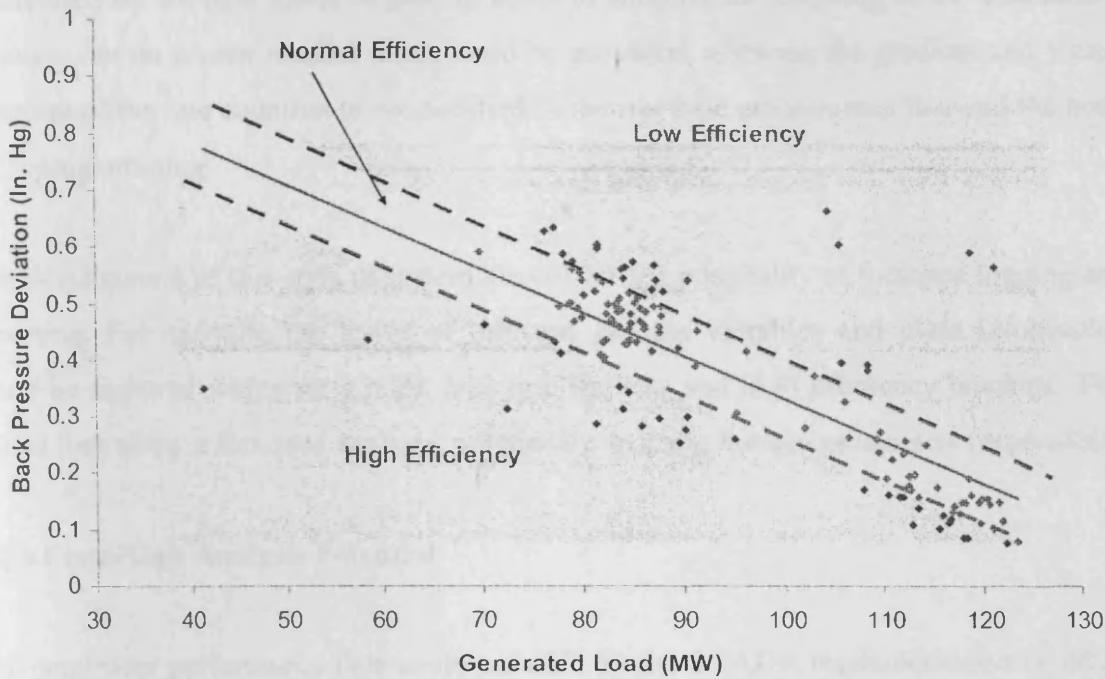


Figure 7.17: Efficiency level contextualisation using performance bench mark envelope.

The equation of the example line of best fit, shown in Figure 7.17, would be assimilated into the system. Taking in values for back pressure difference and generated load, the expected value for back pressure deviation would be calculated. Using conditional executors the programme would then determine if the actual back pressure difference was within the upper and lower threshold of normal performance, calculated with reference to the line of best fit. This data could then be used update the on screen traffic light indicator, based on the colours shown in Figure 7.17. It would also be possible to quantify on screen, in a separate box, the extent to which the back pressure difference was out of tolerance, giving even deeper insight. The outlined approach would unlock the skills of the operators allowing them to use their extensive knowledge of the plant, to act when low efficiency was highlighted.

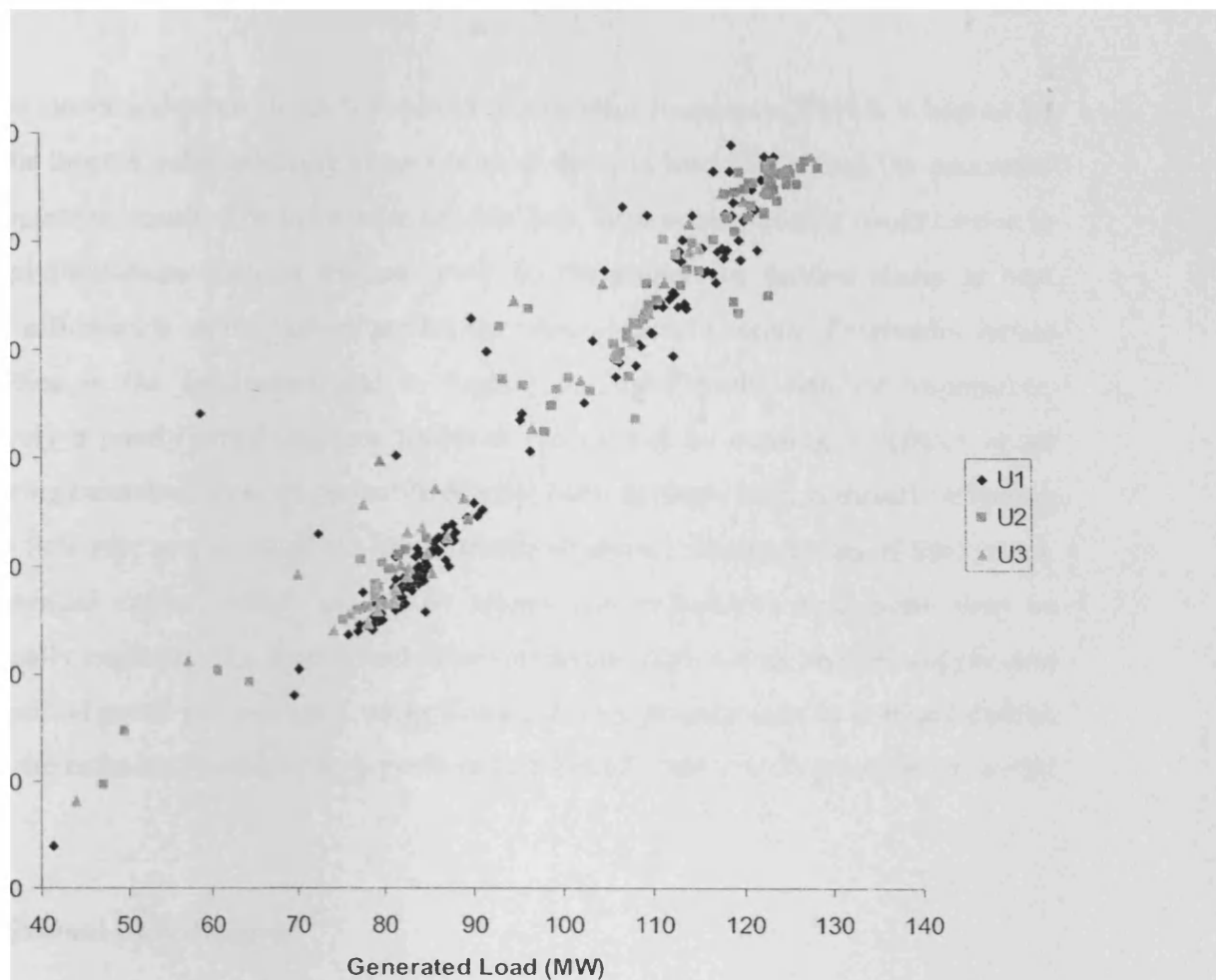
As is key in all continuous improvement strategies, the contextualisation system would require maintenance to reflect improvements. The equation would have to be updated if the efficiency benchmark improved, so that operators were compelled to strive for higher and higher efficiency. Any seasonal variations caused by the affects of ambient conditions on cooling tower performance, as outlined in the literature review, would also have to be taken into consideration. Operators should be consulted when changes are made to the equation, to ensure that knowledge and confidence gained is not lost or apparently

discredited by the new lower targets. In order to simplify the updating of the benchmark equation, an on screen manual input could be provided, allowing the gradient and y axis intercept of the line equation to be modified in the run time environment to avoid the need for reprogramming.

The development of this style of system also offers the possibility of focussed logging and reporting. For example the status of relevant process variables and plant information could be captured whenever a point falls into the low and high efficiency brackets. This would then allow a focussed analysis, potentially spotting the key parameters responsible.

7.7.6 Cross Unit Analysis Potential

The condenser performance data made possible by the SCADA implementation could be used to support the root cause analysis of back pressure inefficiencies. The disparity between unit performance data offers one possible approach. By plotting similar variables from all units against each other, it is potentially possible to pinpoint root causes of inefficiencies in the failing units. Figure 7.18 shows the data for the steam circuit flow rate for each unit, plotted against the generated load.



7.18: Steam rate characteristics for the three units across the generating range.

which is not presented as statistically significant data but it does indicate how differences in process variables, between units of differing efficiency levels, could be identified by the analysis of the produced information. It can be seen that Unit 2, which has the worst back pressure performance data in Figure 7.16, tends to exhibit a higher steam rate than Unit 1, which had the best back pressure performance. Unit 3 is placed in between the other units, as occurred in the back pressure plot. If, over a number of observations, this relationship was shown to be significant, a root cause analysis could then be performed to identify the origin of the inefficiencies.

A root cause consideration was performed to indicate how this would be controlled. The first possibility was a systematic error from the flow meter, which would require recalibration. In general terms the steam rate is controlled by the amount of steam generated per second. More refined control is then required to respond to grid frequency fluctuations. To perform this control, throttle valves in the steam circuit are slaved by a feedback loop to the grid frequency. If the grid load exceeds the generated load

the turbine slows and more steam is required to maintain frequency. This is achieved by opening the throttle valve allowing greater flow. If the grid load is less than the generated load the opposite occurs. The difference seen in flow rates between units could be due to mechanical limitations such as friction levels in the respective turbine shafts or heat exchange efficiencies in the boilers producing lower pressure steam. Potentially innate inefficiencies in the condensers due to fouling or leaks could also be responsible. Alternatively a poorly tuned negative feedback loop could be causing overshoot or set point hunting behaviour. It is also possible that the back pressure level is directly affecting the steam flow rate as a result of the innate thermodynamic characteristics of the system. These potential causes, which are by no means an exhaustive list, could then be systematically explored. If a mechanical fault was pinpointed, a cost benefit analysis and payback period could be generated, using historical cost penalty data as outlined earlier, based on the estimated back pressure performance benefit that improvement work would yield.

7.7.7 Individual Unit Analysis

The newly available back pressure data could also be recorded and analysed for single units. It would be possible to compartmentalise data in order to effectively extract meaning. The system can easily be programmed to perform this specific data capture function. This could be applied, for example, by examining how cooling water was affecting the back pressure. The station management and operators had expressed a belief that the cooling system was under capacity and thus limited efficiency. This may well have been the case when all three units were in operation but it was decided to use the system to pinpoint times during the month of operation when the cooling system could not have been over capacity and assess the effects of cooling in these times. Unit 1 had a 5 day operating period where the generated load averaged around the 80MW mark. No other units were running during this period. In this situation, the cooling system could not have been under capacity. It was decided to select and log the condenser inlet temperature for all points which had a generated load between 80MW to 85MW. A code segment was written which tested all data during the simulation using conditional executors. A report was then generated containing only the data points with generated loads in this range. Analysis was then performed on the data resulting in the data plotted in Figure 7.19.

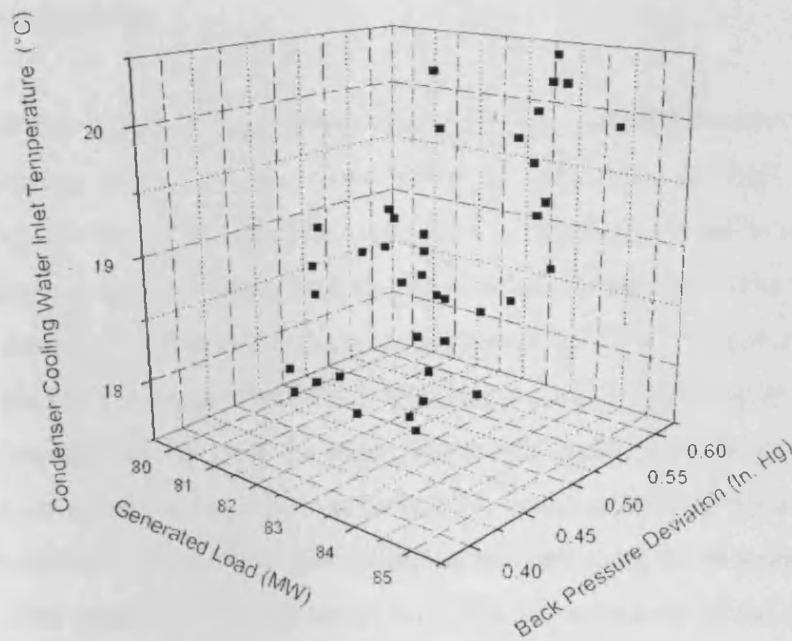


Figure 7.19: Effects of condenser cooling water inlet temperature on back pressure deviation for a limited range of generated load.

The general trend indicated by this data was that back pressure increased with increasing condenser cooling water inlet temperature, across this small range of generated load. The effect of the inverse relationship between generated load and cost penalty was limited due to the small range of generated load plotted. As a result the temperature was the key factor which shaped the plot in Figure 7.19. It is possible that the atmospheric conditions (specifically the wet bulb temperature) limited the performance of the cooling system, so putting the control of the condenser cooling water inlet temperature beyond the operator's influence. Unfortunately, the wet bulb temperature data was not available to examine this possibility. However, it is also possible that having a number of towers shut down for maintenance, or having a number of towers purposely shut down by operators, was responsible for the higher temperature and lower efficiency portion of the data. During visits to the station it was noticed that when only a single unit was running half the towers would be disabled to save electricity. This was not based on a scientific approach and may have led to a larger cost penalty, in terms of coal use, than was saved in electricity. It would provide context to the data if the number of units available for service were known. At present this data is not recorded. Within the SCADA-based system it would be possible to implement a pop up which requested information on the number of fans available for service. This could then be logged and reported along with the other data.

7.7.8 Potential Savings

Based on the data in Figure 7.16 and the relative cost penalty information provided by the station, bringing Unit 3 to the same level of efficiency as Unit 1 would save approximately £40/hr. Improving Unit 2 to Unit 1 standards would save approximately £20/hr. If these savings are multiplied by the number of hours the units were run during the month examined and then this data is multiplied by 12 to extrapolate over the year, this would lead to a saving of £60,000. If all units were then improved by £10/hr, through the more controlled operation of the plant, this would result in a £38,760 saving over the year. Based on current coal prices from the API index and CO₂ emissions per tonne of coal data from the Carbon Trust, this would convert into over 4500 tonnes of saved CO₂ emissions. This potential saving is based on a highly limited set of data and the level of improvement suggested may not be entirely possible due to technical or financial constraints. However, given that the levy on CO₂ is only set to rise, the positive implications of reducing CO₂ are likely to become of greater benefit as time progresses. There are clearly other elements in the operation of cooling towers that could also benefit from this approach. Some of these were demonstrated in relation to a university owned facility that utilised cooling towers.

7.8 Cooling Water Monitoring and Control

The Gas Turbine Research Centre (GTRC) based at The Engineering Centre for Manufacturing and Materials (ECM²) Centre in Port Talbot is a facility used to study combustion characteristics of modern fuels. In order to dissipate the heat loads generated, a mechanical draft cooling tower system is incorporated into the plant, as shown in Figure 7.20. Development work conducted based on the plant information is briefly described here, to discuss further the scope for improved monitoring and management, through extended supervisory system functionality.

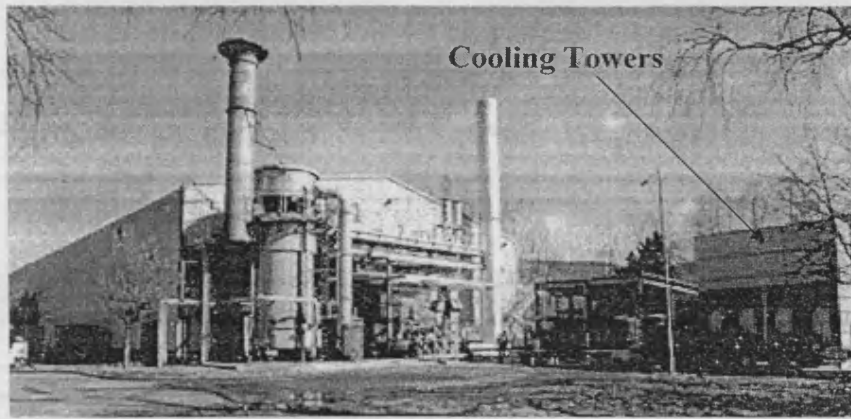


Figure 7.20: Gas Turbine Research Centre.

The cooling water at the Centre is chemically dosed with a combination of biocide, bio-dispersant, scale and corrosion inhibiting and pH regulating chemicals. The dosing of these chemicals is performed by a proprietary controller, supplied by a subcontracting water management company. Chemicals are automatically dosed to maintain a set level. The water management company consultant visits the site monthly, conducting tests and writing a report. Personnel at the GTRC monitor the cooling water daily and conduct testing and record keeping activities to conform to the L8 legislation. This legislation deals with the control of legionella, which is the bacterium responsible for Legionnaires' disease. The most important check made is on the level of biocide, which needs to be maintained in order to kill the legionella bacteria. A number of other chemical readings are taken daily as a matter of course. All the record keeping undertaken during the daily checks is handwritten in a folder. The proprietary controller supplied by the water treatment company is not linked to the site DCS in any way. The general set up and procedure described can be considered standard practice within industry and would need to be enacted in the cooling towers referred to earlier in this chapter.

In practice the tower water management is usually completely separate from the operation of the cooling tower and is effectively ignored by the operators, as it is absent from the control screens. All the data collected daily on chemical levels and chemical use is handwritten and then filed remaining unutilised.

A screen was developed by the author, as shown in Figure 7.21, which allowed the information gathered during the daily checks to be input directly into the SCADA system. A hard copy report could be printed in line with the L8 requirements. Implementing this

approach would allow information on chemical use trends to be readily available for efficiency monitoring purposes, rather than being lost in the paper filing system. Also the system could trigger an alarm if the mandatory daily checks were not performed ensuring that legal requirements would be fulfilled.

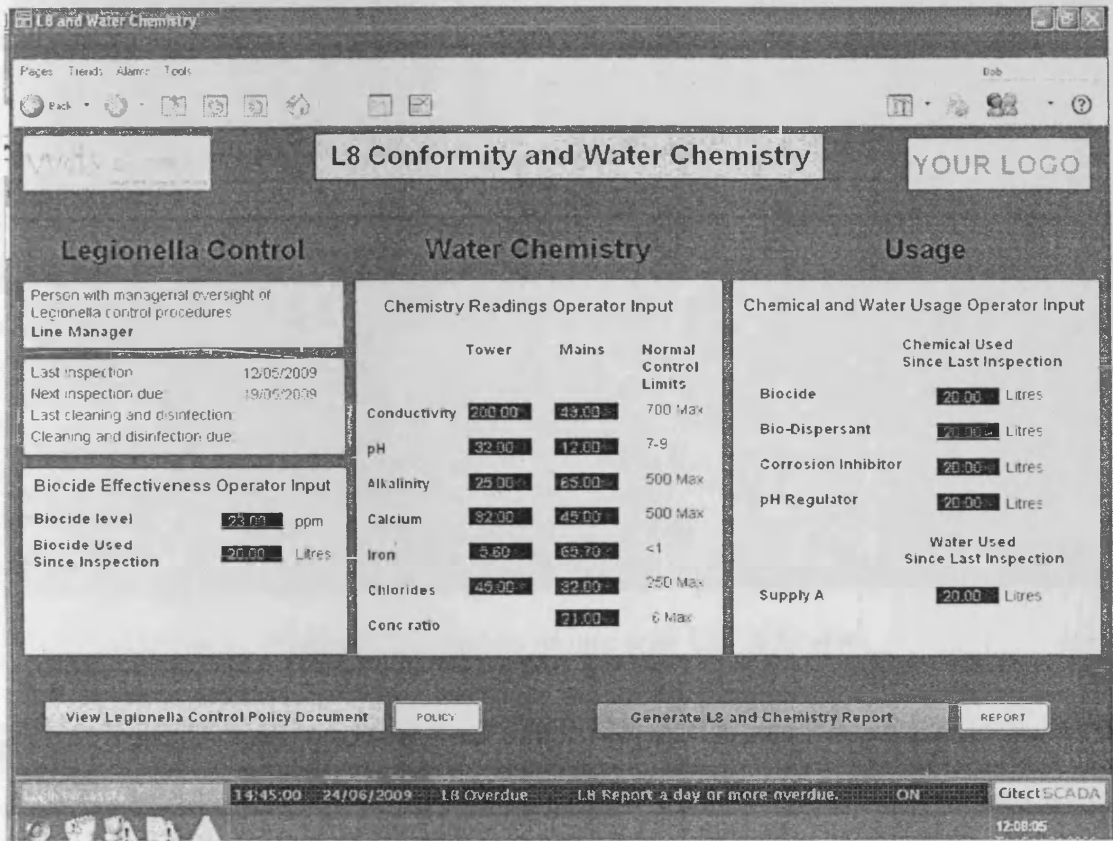


Figure 7.21: L8 and chemical use manual input page.

As the proprietary controller which managed the automated chemical dosing at the GTRC was not linked to the site DCS, this meant that potentially useful information about the water quality was also lost. For example, the conductivity and pH could be utilised to calculate the scale potential of the water using the Langelier Saturation Index (LSI). This task can be performed by the Walchem Web Master One [53]. This is a specialised water controller covered in the commercial system review in Section 3.7.3. The build up of calcium carbonate as scale is highly detrimental, as it reduces the heat transfer possible in the heat exchanger and could force replacement of the heat exchanger. To demonstrate that the SCADA software could be used to monitor LSI, a function was written which calculated the index using appropriate variables and displayed the value on screen using a traffic light severity scale, as shown in Figure 7.22.



Figure 7.22: Process mimic with LSI indicator.

It is suggested that having this value displayed in real time could aid energy efficiency in a mechanical draft cooling system. Water temperature is a key parameter of the LSI, with increasing temperature increasing the scale potential of the water. If for example, the scale potential of the water was low and the process heat load was low, it may be possible to reduce the number of tower fans in operation saving energy. This would increase the temperature of the cooling water but as long as the scale potential remained reasonably low, as monitored by the LSI, there would be no detrimental effect. The pH of the water is also a critical factor. It could be possible using the new system to find an optimum efficiency balance between pH regulation and fan control.

Finally, if the new data available from the SCADA-based L8 and chemical use input page and the process mimic page with LSI monitoring were combined, it could be possible to facilitate an integrated approach to tower water management. This would allow consideration of all the factors affecting the tower. A functional screen was developed using the SCADA software, as shown in Figure 7.23, which could calculate cost savings compared to a benchmarked value, for both chemical and fan use. This offered a holistic

overview of tower efficiency. A system such as this is in contrast to the current situation, where separate electronic systems and personnel manage strongly interdependent aspects of the same cooling system.

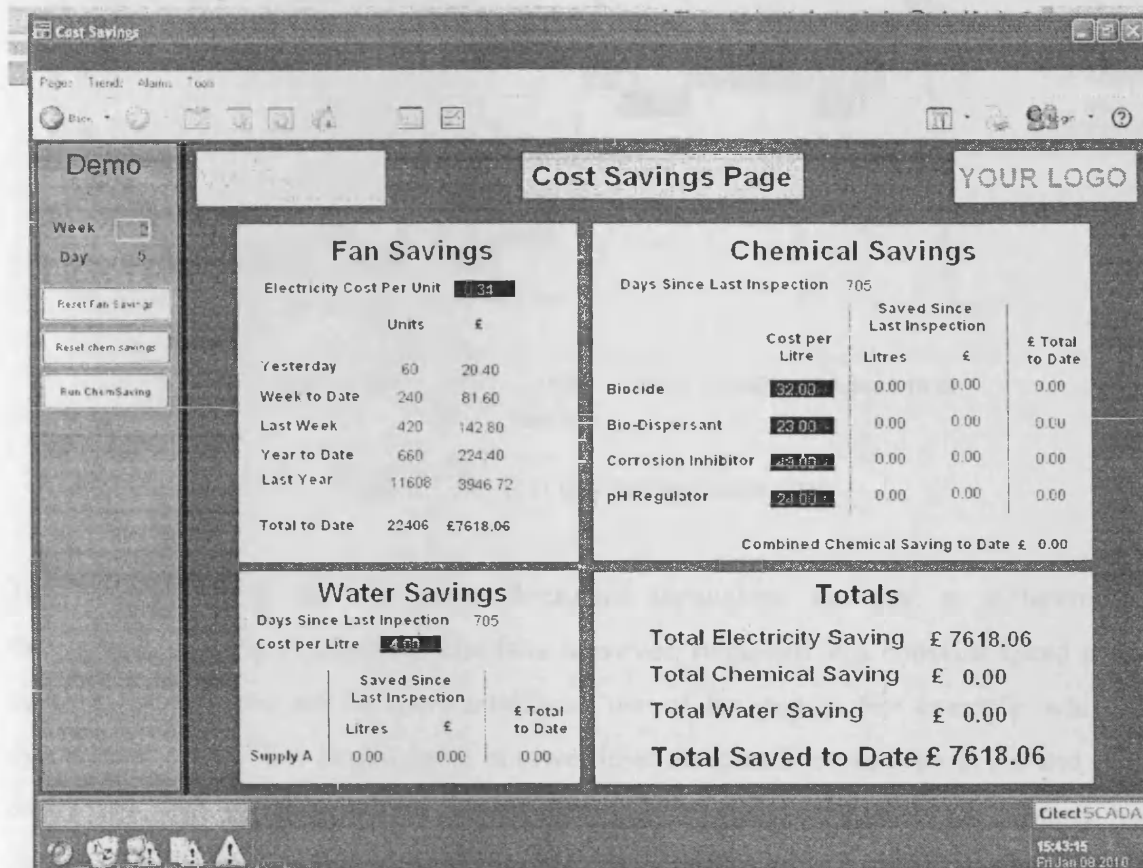


Figure 7.23: Cooling tower cost savings page.

Tower inlet and outlet water temperature data for a single days testing was captured during the time at the GTRC. The temperature profile produced, shown in Figure 7.24, indicated the potential for applying the style of monitoring outlined in this section.

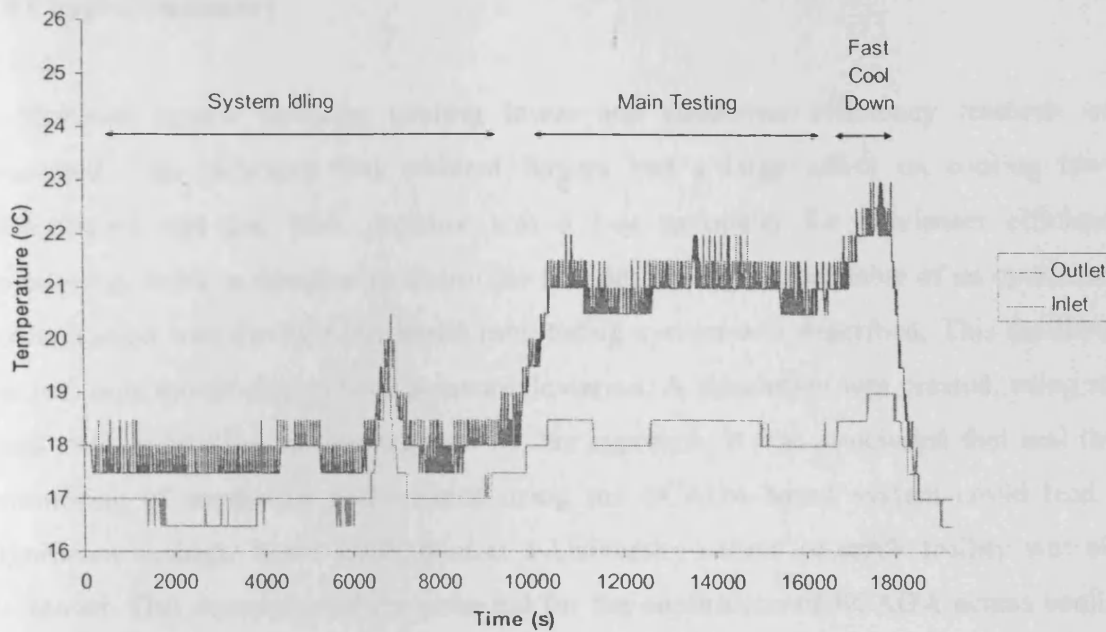


Figure 7.24: Test day temperature data.

The temperature of the inlet water fluctuated throughout the day, as different heat dissipation levels were required. The fans however, remained at a constant speed and as such there was potential for more intelligent use of fan power. For example, while the system was idling. The largest spike in tower inlet temperature was seen at the end of the day. This was the result of the cooling water flow rate, around the process heat exchangers, being increased to maximum. This action was taken to quickly cool the system, so that the personnel could leave on time. It is likely that the water was at its highest scale potential during this period. Monitoring of LSI would allow more informed decisions to be made in such situations, preventing potentially costly actions such as this.

The work conducted at the GTRC is not fully presented as the systems developed utilised basic SCADA programming methods and in depth experimental work was not possible due to a lack of test days at the Centre. It was included to further demonstrate the potential for applying SCADA software across cooling water infrastructure; using the SCADA system to tie in disparate elements, forming a systems approach to efficiency monitoring and improvement.

7.9 Chapter Summary

A literature review covering cooling tower and condenser efficiency research was presented. This indicated that ambient factors had a large effect on cooling tower performance and that back pressure was a key parameter for condenser efficiency monitoring. Work undertaken to assimilate the ideal back pressure table of an operational power station into the SCADA-based monitoring system was described. This facilitated the real time monitoring of back pressure deviation. A simulation was created, using real plant data, to explore the implications of this approach. It was concluded that real time monitoring of condenser performance using the SCADA-based system could lead to significant savings. Work undertaken at a University owned research facility was also presented. This demonstrated the potential for the application of SCADA across cooling water infrastructure, for efficiency monitoring and improvement.

7.10 Conclusion

This chapter has demonstrated that in depth efficiency monitoring can be enacted using non-time critical low frequency algorithms implement in a modern SCADA package; the laborious and inaccurate manual monitoring approach can be replaced. The real time nature of the monitoring also offers many potential benefits. As well as the specific impacts on operators and managers outlined, the continual presence of performance monitoring on the control system can only serve to raise the profile of this important factor, leading to increased improvement activity.

Chapter 8

Discussion

8.1 Relevance and Scope of Developed Methods

8.1.1 WRAP Rig

The work conducted on the WRAP Rig was considered in the context of water treatment in an industrial cooling water infrastructure, as represented in Figure 1.1. Similar pumped deep bed filtration plants are however, utilised in a variety of other applications. Industrially, such plants are used to supply low turbidity water to manufacturing and process facilities and for the extraction of post process water contaminants before discharge. They are also widely used to filter drinking water from boreholes. The developed system could be deployed on filtration plants in all such applications. Therefore, the research conducted on the WRAP Rig forms the building blocks of a generic, pumped deep bed filtration plant, performance monitoring and optimisation approach.

The blockage identification research, presented in Chapter 4, is considered generic as it relies on the cavitation behaviour of the centrifugal pump. The main body of the programme created could be applied to other pumped systems. To calibrate the system, tests would be conducted with downstream blockages. These results would provide the expected downstream blockage response for use in the CUSUM process, as demonstrated in Section 4.9.1. Tests on upstream blockages would also be conducted. These would be used to examine any areas of ambiguity between upstream and downstream results as was undertaken in Section 4.9.2. Two other tests would be required to extend the range of the programme, as was explained in Section 4.10.2. Thus, it is considered relatively simple to update the programme for use with other plant. It should be noted that the developed method was an either or test, between upstream and downstream blockages. However, as discussed in Section 4.11, other restrictions could potentially be added to the diagnostic, as they too would affect the cavitation behaviour of the pump.

In a wider context, the research done on blockage diagnostics also has potential applications in other parts of an industrial installation. Blockage location could improve both energy and maintenance efficiency in a variety of pumped systems other than filtration plant. For example, cooling towers are pumped systems and problems such as biofouling can lead to blockages. These could be more effectively remedied if the location of the blockage were known.

The filter bed monitoring work, presented in Chapter 5, embraced the concept of combining control and fault detection, as set out by Venkatasubramanian et al [27]. The concept was shown to be generic by investigation using a theoretical software model of the WRAP Rig. As all pumped deep bed filtration plant work in a similar fashion, the developed programme could be quickly applied to other plant. This procedure would be simple, with approximately eleven tests required to develop the filter only blockage response of the system, as demonstrated in Section 5.8. Two extra tests would then be sufficient to set the exceptional thresholds required near the 'Speed Request Transition Line' as discussed in Section 5.8.3. The equations of the two lines of best fit would be pasted into the existing programme. This process would take no longer than a few hours.

As well as condition based back wash initiation and blockage detection, the approach outlined in Chapter 5 would also provide other benefits. Filter performance decay data, previously disguised by the corrective action of the PID loop before SCADA was utilised, would now be available. This new data could provide an insight into efficiency performance, analogous to that realised by the real time calculation of back pressure and cost penalty data for the power station. This may then provide opportunities to refine operating parameters and discover the root cause of problems.

The closer monitoring of the state of the filtration system also leads to the potential for circumstance based adaptive control. For example, if the current price of electricity per unit and the current cost of discharge to drain were known to the system, the level of blockage which triggered back wash could be automatically updated to minimise cost. If the price of electricity was low and the price of discharge high, the allowable blockage level might be raised, providing it was decided that the extra motor and pump wear was

not an issue. The relationship used to make this decision could be described using an equation based on the two parameters and encoded into the software.

The method outlined for combined blockage diagnostics, set out in Chapter 6, could also be applied to other pumped deep bed filtration systems. The recalibration activity required would be relatively involved, requiring a matrix of tests as set out in Section 6.2. However, in general terms, the use of multiple complicated thresholds by the SCADA system could have varied uses. For example, much of the equipment used in the coal fired power plant is governed by complicated relationships. The style of approach used, where multiple boundaries were encoded into the system and used to analyse automated test data, could potentially be applied to the station equipment. Much of the regular maintenance in a power plant involves the testing of equipment performance. The SCADA system could be used to generate repeatable tests cycles and log and analyse data, improving the efficiency of performing these tasks.

The research presented from the WRAP Rig would require further work to provide a fully robust solution. The impact of other faults would have to be considered either to make them part the diagnostic or prevent them from undermining the system. One such fault not mentioned would be pump motor malfunction. This style of fault was not outlined by Higham et al [61] as one of the four main pump faults and did not come as high as other faults in the FMEA of Appendix A. However, this style of fault is certainly possible over the extended life of a plant and would have implications to the functionality of the algorithms developed in this research. For example, bearing wear will increase the power consumption of the motor and require a higher speed request from the PID loop to maintain flow. This could give a similar speed request response to a small blockage. However, it is likely that this fault would give a differing pressure response to a pipe blockage. Therefore, by research into the range of possible faults and extended multivariate analysis of available system signals, it is postulated that a highly robust FDD and condition based backwash initiation system could be fully realised.

The research conducted in The WRAP Rig showed that FDD and condition based control strategies could be implemented using SCADA software. This was achieved on an industrial plant, containing industry standard sensors and instrumentation, at normal operational data frequencies. Algorithms were developed for these applications which

required no extra hardware. In a wider sense, this demonstrates the potential for developing such algorithms for seamless inclusion into the SCADA system of any industrial installation.

8.1.2 Coal Fired Power Station and Gas Turbine Research Centre

The research conducted on condenser monitoring using SCADA software in the power station, in Chapter 7, has significant relevance. The work demonstrated that ideal performance curves can be assimilated into a standard SCADA package. Once the equation of a performance curve or surface has been defined, it is relatively simple to assimilate this into the SCADA programme. As such, manual performance monitoring tasks, in a wide variety of industrial applications, could potentially be automated and improved, using the existing software infrastructure. The approaches outlined for use at the coal fired power station are readily configurable to match the requirements of any steam cycle power plant. The general approach of applying efficiency monitoring using an installed SCADA system could have applications across industry and the commercial sector. For example, Building Management Systems are prevalent in most large commercial and domestic buildings. One such example is the Trend system [59], covered in Section 3.8. These systems share many of the attributes of SCADA software. As such, it is also conceivable that the approaches set out in this research could be applied to existing buildings for improved management of HVAC systems, using ideal performance curves and condition based control.

The method developed for enacting simulations using real power plant data, covered in Section 7.6.2, is very relevant in the context of this research. If the extended functionality of SCADA software is to be fully utilised at an industrial site, the ability to develop and refine new algorithms, off line, is of great value. The method gives an opportunity to test and showcase a newly programmed SCADA module improving the prospect of a successful implementation.

The work undertaken at the Gas Turbine Research Centre, presented in Section 7.7, further widened the scope for applying SCADA technology to efficiency control. The developed programmes sought to digitise current paper based procedures, therefore utilising previously discarded efficiency information. It was put forward that installed

SCADA systems have the potential to break down established operational boundaries, allowing a systematic approach to efficiency management of the cooling system. Once again the programmes developed are highly generic and could be applied to any cooling tower system with a minimum of effort.

The power station and Gas Turbine Research Centre work demonstrated that SCADA software can be effectively used to perform efficiency monitoring tasks. The rich graphics can be used to enhance operator understanding and involvement. Utilising the SCADA system for the task of efficiency management therefore offers a flexible and readily configurable tool, for the efficiency practitioner to implement continuous operational improvement, at a given industrial installation.

8.2 Systems Approach to Efficiency Using Supervisory Infrastructure

8.2.1 Systems Approach

The overriding concept, to which the work presented contributes, is that a systems approach to the management of efficiency in industry can be achieved through the innovative reapplication of the software infrastructure, which is already in place. A systems approach is defined, in the context of this thesis, as the collective consideration of all sub-systems and their interrelations to produce an overall efficiency management system. It is put forward that the supervisory system offers the ideal platform for a systems approach, as it is integrated into all subsystems in the installation giving access to all the data required.

8.2.2 Benefits of a Systems Approach

In industrial installations a systems approach to efficiency is important for a number of reasons. In practice, the personnel working within a large industrial system may be highly compartmentalised. This can be a result of organisational planning, geographical separation or safety protocols. The majority of personnel have specialised knowledge about their specific area of the plant and often work as part of an isolated sub-system, which is essentially a step removed from the overall system. However, the operation of their plant will undoubtedly impact on the operation of other parts of the system. Without

a systems approach, which considers such interrelations between sub-system, optimum plant efficiency cannot be achieved.

Due to the large numbers of staff and complicated nature of the tasks involved, the communication and implementation of an overall efficiency approach can be difficult. In many cases a deployed efficiency approach will soon be abandoned, in favour of a custom and practice approach, where personnel take action referencing what previous operators have done, rather than examining and following official guidelines. The application of an integrated efficiency procedure, enacted using the all pervasive supervisory system, could potentially provide a tangible plant wide focal point for efficiency activity. Separate departments could then be brought under the remit of the overall plant efficiency strategy, rather than relying on their own segmented interpretation of what makes their specific department efficient. The development of this approach would produce the outcome of defining efficiency for the installation as a whole. For example, in power stations different departments and management levels may define efficiency on a financial, energy use or emissions basis, which could lead to conflicting approaches. An integrated efficiency system ensures all departments are working towards complimentary goals.

The efficiencies of the individual components of large industrial systems, such as the alternators or cooling towers of a power station, are often very high. The designs have been refined by manufactures, producing small improvements with each new model. However, if these individual components are not operated well in unison, the efficiency implications can be vast, as demonstrated by the ramifications of high back pressure deviation in the power station. This further explains why the development of a systems approach to efficiency, in all large industrial systems, could have a significant affect on world energy use and emissions.

8.2.3 Structure of a Systems Approach

The final goal would involve the development of algorithms relating to all the individual subsystems of an installation. The outputs of these performance monitoring algorithms would then be drawn together by an overriding master function, which would calculate key performance indicators for the plant as a whole. It is the long term monitoring of

these performance indicators which offers the potential to expose how sub-system interrelationships were affecting overall efficiency.

For example if the efficiency of the power plant system of Chapter 7 is considered, in terms of energy conversion of chemical energy into electrical energy delivered to the grid, the supervisory system could potentially be utilised to monitor and improve efficiency as shown Figure 8.1.

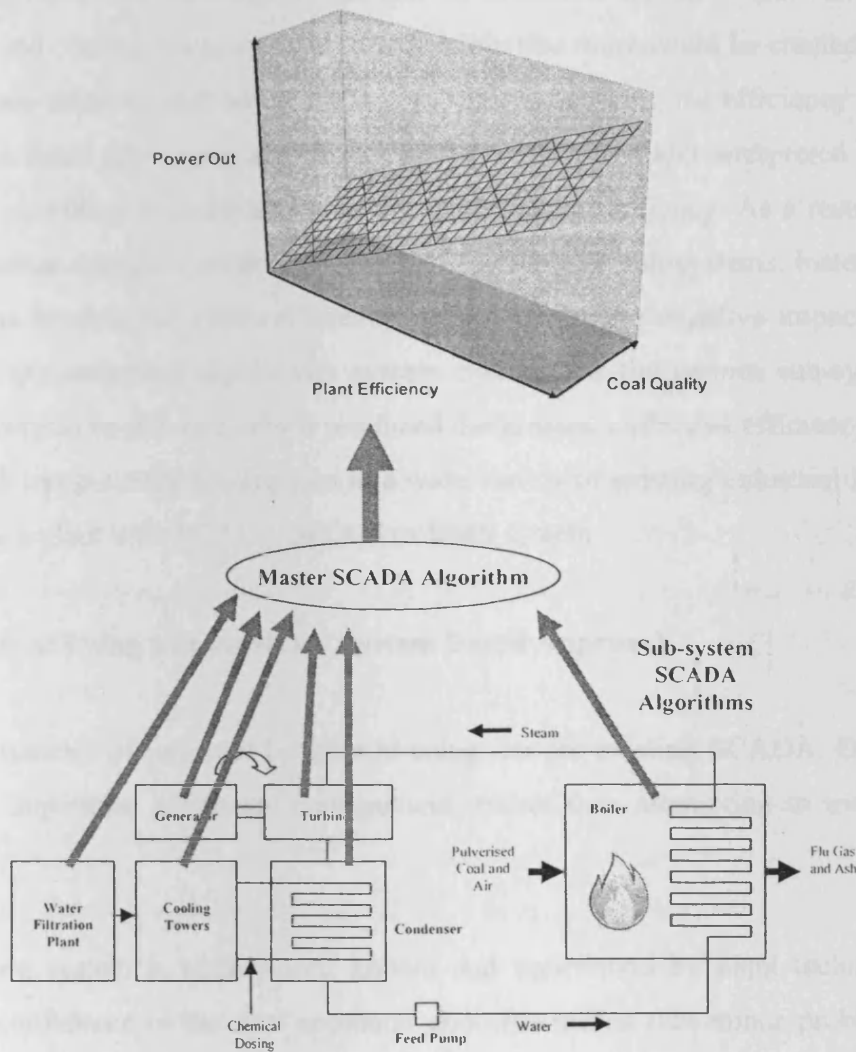


Figure 8.1: Simplified representation of a SCADA based efficiency management system for a coal fired power plant.

In the Figure, the efficiency surface, situated at the top of the diagram, illustrates that the power actually provided to the grid from a given quantity of chemical energy put into the station, is a function of the quality of the coal and the mechanical and operational

efficiency of the plant. Coal quality can be highly variable, based both on chemical properties and moisture content. This factor is beyond the control of the operators but must be properly considered when analysing overall station performance.

It is envisaged that the supervisory system could be used to monitor and improve the efficiency of the mechanical plant and its operational orchestration. Appropriate algorithms could be developed for all the sub-systems. The work presented in this thesis has demonstrated that such algorithms can be produced for the water filtration plant, condenser and cooling tower systems. It is feasible that more could be created for the rest of the system elements such as the boilers. In the final system, the efficiency information output from these sub-system algorithms would be collected and interpreted by a master algorithm, providing an integrated measure of the plant efficiency. As a result, the plant could be run as a single system rather than an assembly of sub-systems. Instead of all the sub-systems striving for 100% efficiency, regardless of the negative impact on overall efficiency, the integrated supervisory system could allow the various sub-systems to be controlled within boundaries, which produced the greatest collective efficiency. This style of approach has potential applications in a wide variety of existing industrial installations, which have a plant wide SCADA or DCS or BMS system.

8.3 Benefits of Using a Supervisory System Based Approach

There are number of potential benefits to using the pre-existing SCADA, DCS or BMS system to implement efficiency management, rather than attempting to use an add-on system.

The existing system is usually well known and understood by plant technicians. This increases confidence in the new approach and also means that minor problems can be overcome economically and in a timely manner, in-house.

Large industrial systems can be highly intense environments. As they age the number of breakdowns may increase and the complexity of fixing them may often be increased by the addition of upgraded equipment over the years. As a result, much of the day to day running of a plant involves tackling immediate problems which threaten the core functionality of the facility. This is often referred to as 'Fire Fighting'. Therefore, the

success of newly implemented systems often depends on their simplicity and ease of use. The new system must compete for time with the demands of general 'Fire Fighting' activity. Using the pre-existing control system utilises the existing skill set of technicians. As a result, maintenance of the efficiency system can be added to the general maintenance of the supervisory system and is more likely to be completed.

External or add-on systems require a communication infrastructure and may be programmed in a different language and configured in a different virtual environment to the supervisory system. As a result, it is far less likely that technicians will have the time to fully understand the new system, or the experience to maintain it and trouble shoot problems.

As discussed in the SCADA Background section, the communications infrastructure in an industrial plant can be highly complicated. Attempting to interface a new system, either directly to the existing SCADA or to field devices, can bring a range of potential problems. The communications infrastructure could be compromised. If this was the case then the new system would be immediately disabled and could then potentially fall out of use permanently. However, if the existing supervisory system is used, the most difficult part of the integration process has already been achieved. The use of only existing sensors is also a major advantage. Implementation costs are lowered and no extra maintenance and calibration burden is added. There is no increase in data transfer and no extra data points are required, so there is no added software licence extension expense.

Although the specific techniques outlined in this thesis may not be suitable for all plants, the general approach used is indicative of the potential for using the supervisory system. The approach could be applied to other industrial systems such as steel works, petrochemical plants and even large buildings. Paper based ideal performance characteristics could be assimilated into the supervisory system in a similar fashion to the work done with the back pressure deviation. For any plant where performance indicators can be devised, a bespoke efficiency monitoring approach can be implemented within the supervisory system provided the rules for practical application outlined in Section 8.4 are followed.

8.4 Practical Application

To safely and successfully implement the extended supervisory system functionality suggested, a good level of practical software and instrumentation knowledge and experience would be required. A level of expertise in efficiency monitoring would also be required, to effectively define the scope of the system. Much of this may exist within the company. Most large industrial sites will have in-house engineers, capable of making modifications to supervisory system and PLC programming and may have personnel already tasked with examining efficiency. The successful implementation will in some cases, also need to involve external contractors. For example, it is advisable to consult dedicated system integrators with direct knowledge of the supervisory system involved, before undertaking major change. These people can provide informed opinions on how the addition of extra programming could impact on the performance of the system, both in terms of reaction time and reliability. The help of an external efficiency consultant may also be of benefit, as internal experts will often have become susceptible to the culture of custom and practice which develops over time in a large industrial system. An outside perspective can often spot glaring inefficiencies, which have become masked by procedure and familiarity in the eyes of people who are permanently involved with the plant.

The most important factor to consider is the robustness of the system. If the efficiency monitoring functionality implemented compromises safety, or leads to plant down time, the possible savings will be far outweighed by the financial implications of these secondary problems. The strategies embodied in the software must also be robust enough to function despite being subordinate to all critical supervisory system tasks, in terms of processor usage. This means that the algorithms used should not be highly time critical but must be able to deliver the correct outcome despite pauses of a few seconds in the execution of the code. As with all software, new functions need to be thoroughly tested and a staged implementation is advisable.

The processing limitations of the existing supervisory system must be examined. It is impossible to make a generalised statement about the potential processing limitations of the range of SCADA, DCS and BMS systems deployed around the world. This depends on the processing power of the PC or networked PC's that the software is implemented

on. It also depends on the age and innate efficiency of the software package and the efficiency of the implementation and configuration of that software. There may well be deployed systems which are very close to overloading the available processing power. In such cases it would not be advisable to apply new algorithms to the system, as this could reduce reaction times or, if poor programming was used, cause a system crash. However, on systems which have a large excess of processing power it may be possible to implement highly complex algorithms as long as consideration is given to ensuring the priority of core tasks.

If the Citect SCADA software used in this research is considered, the scope for extended application of the system is clear. The first large implementation of Citect took place in 1992 at the Argyle Diamond mine. This implementation included 33,000 digital and 16,000 analogue I/O points and 50 networked PC's. Using distributed processing techniques and network optimisation, reliable implementations in excess 450,000 I/O points are possible. In systems such as this, it is viable to simply add another PC to the network, running a sub-project containing the new efficiency algorithms. This will ensure there is enough processing capability available. The algorithms developed in this research used minimal processing power but more importantly were configured to maintain the priority of core tasks. As a result the algorithms essentially only use 'free' processing time within the CPU. Therefore, even if the processing limits are reached, the core SCADA functionality should remain intact and responsive, even if the new algorithms fail to function properly due to highly extended execution times. The Citect software is designed to be capable of running multiple Cicode algorithms while maintaining core functionality. There are over 650 pre-programmed Cicode programmes already available for use within Citect. These cover the full range of activities from data management to advanced graphics configuration. Therefore, safely adding efficiency related algorithms to Citect SCADA or any other supervisory system is matter of good programming, good systems integration practice in terms of ensuring acceptable processor demand and adequate testing.

Items which offer the greatest potential reward, for the least risk and cost, should be attempted first. In the power station for example, the addition of automatic back pressure deviation calculation can actually be achieved with a relatively simple code segment. The same is true for the backwash optimisation in the WRAP Rig. The timing of the execution

of these functions was not critical, so they can be configured to run at well spaced intervals, preventing processor overloading. They can also be assigned a low priority, ensuring that critical SCADA tasks are not affected. The execution of repeating functions could also be staggered to provide an even distribution of processor demand. Items such as the Blockage Location test cycle in the WRAP Rig, or the back pressure deviation cause analysis, suggested for the power station, should be configured to run only on the command of the operator and an abort function should be available.

The role of operators, as a key part of the supervisory system, must not be overlooked. Implementation of higher level functionality in the supervisory system, with no explanation of function and objective, will inevitably lead to distrust from the operators. It is advisable to provide explanatory notes linked to buttons and on screen indicators associated with the new functions. Any alarms should be as self explanatory as possible. The use of alarms as part of the efficiency system should be considered in detail. The problem of alarm showering has been widely documented and it is questionable whether any alarms which do not pertain to safety issues or serious plant malfunctions should be included. The use of on screen indicators, such as the text strings and traffic light colours, described in earlier chapters, are preferable to the use of alarms.

Overall, the relative simplicity of the implementation should be considered at all stages. Due to the high stress environment and 'Fire Fighting' activity, described earlier, it is suggested by the author that in most cases, highly complicated systems will not receive the attention and maintenance required. In some cases systems which are ill understood and maintained will be counter productive. Operational efficiency is a flexible concept, as the inevitable changes to equipment and procedures can drastically alter characteristics. A simple system may not realise the maximum benefits possible at implementation but it is far more likely to continue reaping efficiency benefits into the future, as it will be easier to maintain and upgrade, reflecting plant changes.

Chapter 9

Conclusions and Further Work

9.1 Main Contributions of the Research

The pivotal aim of the thesis was to research non-time critical standard low data frequency applications, suitable for deployment using existing on site software, such as the SCADA system. It was shown that Fault Detection and Diagnosis (FDD), condition based control and performance monitoring were possible using this approach demonstrating its validity and flexibility. The research was undertaken in the context of improving the efficiency of industrial water systems, while also indicating the possible potential for applying this approach across other areas. The research produced the following important contributions to engineering knowledge:

- The programme demonstrated in Chapter 4 proved that SCADA software can be used to run repeatable active test cycles by controlling the variable pump speed request. This is an innovative, yet practical, step in pump diagnostics.
- Chapter 4 also demonstrated that a non-time critical, low data frequency algorithm can be used to diagnose the relative location of pipe blockages. A novel approach using an active pump test cycle and resulting flow rate data successfully achieved this outcome. In more general terms, it was shown that blockages up stream of a pump create starvation characteristics. These alter with variation and duration of pump effort and differ significantly and identifiably from flow characteristics of downstream restrictions.
- The methods described in Chapter 5 demonstrated that non-time critical, low data frequency algorithms can be used to passively monitor standard process variables of a filtration plant. This provided an indication of filter bed fouling and supported the detection of abnormal system conditions, such as pipe blockages. The innovative approach, made possible by this research, performed this task despite the disguising action of the PID control loop. It was shown that this functionality

can be used to provide a robust, fault tolerant, condition based control strategy for back wash initiation. This is an important contribution to furthering the operational efficiency of such systems.

- Chapter 6 demonstrated that non-time critical, low data frequency algorithms can be used to diagnose the relative severity of combined blockages in a filtration plant. This was performed using an active test cycle and a threshold based analysis of standard process variable responses. The novel approach showed that a complicated threshold based analysis, which was programmed in such a way as to minimise workload, could perform this task. In more general terms, this demonstrates that pressure and flow signatures from combined blockages can be used to diagnose the relative severity of the component restrictions.
- The research conducted proved that effective and non-time critical SCADA software algorithms can be programmed. These can function correctly despite varying execution time, caused by the processor demands of higher priority core SCADA functions. This demonstrates that SCADA does possess the capability to be applied for monitoring and non-critical control duties.
- The software described in Chapter 7 demonstrated that an ideal condenser performance surface can be successfully assimilated into SCADA infrastructure. Thus, vastly improving on existing manual monitoring approaches and providing operators with real time efficiency information.
- Chapter 7 proved that SCADA programming functionality can be used to selectively modify assimilated surface equations to minimise error. It can also be used to provide focussed logging of process variables. This research has thus advanced the potential applications of utilising SCADA functionality, in the context of process management.
- Chapter 7 also demonstrated that SCADA software can be modified to replay process data, allowing the safe offline development of advanced SCADA applications, based on actual plant data. This is a significant contribution in the context of applying extended SCADA functionality to industry.

- Finally Chapter 7 demonstrated that algorithms suited to the SCADA infrastructure can potentially be used for the innovative real time contextualisation of power station performance data, based on benchmarking of previous SCADA produced information. It can also potentially be used for real time indication of the causes of inefficiency.
- Chapter 8 defined the concept of utilising a plant supervisory software and infrastructure to provide a plant-wide systems approach to efficiency. This contribution infers the large potential scope for other researchers from all disciplines of engineering to consider utilising existing supervisory infrastructures for applying their research outcomes to the problem of operational efficiency.
- The research conducted proved that non-time critical, low data frequency algorithms can be generated to conduct FDD, adaptive control and efficiency monitoring. The approach used is suitable for application using SCADA software and potentially DCS and BMS software. This can be achieved robustly and using only existing process signals at industry standard frequencies.
- The application of the approach to a selection of functioning industrial plants indicates there is strong potential for applying non-time critical, low data frequency algorithms to a range of systems. This opens possibilities for interim and long term research to address the problem of operational efficiency through the more extensive merging of academic and industrial strategies and technology.

9.2 Conclusion

It is standard practice to have a SCADA, DCS or BMS system connected to all the subsystems in an industrial or commercial installation. This thesis has shown that the non-time critical, low frequency, algorithms required to produce a systems approach to efficiency, in industrial water infrastructure, can be implemented using representative SCADA software. This is a strong indication that the potential exists to improve process monitoring and efficiency by applying this approach to all the sub-systems of industrial installations using the supervisory system.

This thesis has demonstrated a number of the potential benefits. Work on blockage location, presented in Chapter 4, could result in faster maintenance and less down time. The reduction of the work required to remedy a blockage could also decrease time personnel spend operating in dangerous environments.

Application of the research on filter bed monitoring, described in Chapter 5, would lead to early detection of energy wasting abnormal blockages. The condition based initiation of backwashing would also save energy, by preventing the pump straining against a heavily fouled filter bed. Energy wastage caused by backwashing a relatively clean filter would also be avoided. In the longer term filter fouling decay profiles, exposed by the system, could lead to improved operation. Advanced overall filter plant management strategies could also be developed using the supervisory system. Operational strategy decisions could be made in real time based on financial factors as mentioned in Section 8.1.1.

The work on combined blockages, presented in Chapter 6, demonstrated that SCADA software could be employed to provide efficiency management even under severe fault conditions. This could have major benefits in remote water filtration plant applications where maintenance action may not be possible for some time.

There are a vast number of pumped deep bed filtration plants operating globally. If the work conducted on filtration in this thesis is considered in that context, the contributions made could have wide spread applications.

The work presented on the coal fired power station in Chapter 7 demonstrated that ideal performance surfaces can be assimilated into SCADA architecture. This contribution has wide reaching implications. It demonstrates that an installed SCADA or similar system, in any plant or building, could be rapidly upgraded to give in depth efficiency monitoring. Further more, contextualisation of the data produced can be used to inform the actions of operators and drive efficiency improvement.

The work on the Gas Turbine Research Centre, presented in Chapter 7, further demonstrated how SCADA software can be used to draw together disparate sub-systems and utilise currently discarded information.

All the contributions made in this thesis support the hypothesis that an installed supervisory system can be used as a focal point for efficiency management. Many of the plants which would benefit from a systems approach to efficiency management in the UK and world wide today will be operating for many years to come. The percentage of global emissions produced by plants that are already in service today is likely to remain high throughout the action periods of emission reduction treaties such as the Kyoto agreement. Therefore, the reduction of operational wastage in existing plant has a key role to play in achieving targets and also helping to conserve dwindling resources.

It is concluded as a core outcome of this research, that the potential for researching and developing non-time critical, low frequency, algorithms for efficiency improvement activity has been demonstrated. These algorithms are suitable for application using the supervisory systems of existing and future plant. This is of merit to the research community as it broadens the scope for the application of research findings to real world plant.

9.3 Further Work

- Research and include the effects of internal pump blockage and motor faults in the algorithms designed for the WRAP filtration rig.
- Refine and deploy the Condition Based Backwash and Blockage Detection algorithm on an operational deep bed filtration plant.
- Research the potential for applying Fuzzy Logic and off line Neural Network approaches using non-time critical, low frequency algorithms.
- Deploy the developed power station back pressure deviation monitoring approach on a power station SCADA or DCS and assess performance.
- Conduct a wider study of the functionality and execution time impact of running multiple sub-algorithms on industrial SCADA and DCS systems.

- Develop and implement a SCADA based efficiency management system at an appropriate industrial installation.

References

1. Bailey, D., *Practical SCADA for Industry*. 2003, Elsevier: London. p. 1-17.
2. Bailey, D., *Practical SCADA for Industry*. 2003, Elsevier: London. p. 148-168.
3. *Good Practice Guide: Process Control and SCADA Security*. 2005, Centre for the Protection of National Infrastructure. p. 3.
4. Cai, N., J. Wang, and X. Yu, *SCADA system security: Complexity, history and new developments*, in *6th IEEE International Conference on Industrial Informatics*. 2008. p. 569-574.
5. Blaha, M., *A retrospective on industrial database reverse engineering projects - part 2*, in *Proceedings. Eighth Working Conference on Reverse Engineering*. 2001. p. 147-153.
6. Garrett, M.T., *Instrumentation, control and automation progress in the United States in the last 24 years*. Water Science and Technology, 1998. 37: p. 21-25.
7. Dieu, B., *Application of the SCADA system in wastewater treatment plants*. International Society of Automation Transactions, 2001. 40(3): p. 267-281.
8. Patel, M., G.R. Cole, and T.L. Pryor, *Development of a novel SCADA system for laboratory testing*. International Society of Automation Transactions, 2004. 43(3): p. 477-490.
9. Ozdemir, E. and M. Karacor, *Mobile phone based SCADA for industrial automation*. International Society of Automation Transactions, 2006. 45(1): p. 67-75.
10. Trung, D. *Modern SCADA systems for oil pipelines*. in *Petroleum and Chemical Industry Conference. Record of Conference Papers., Industry Applications Society 42nd Annual*. 1995. Denver Colorado, USA.
11. Theakston, J., *Selecting and Installing a Software-Based Leak Detection System*. Pipeline & Gas Journal, 2002(october): p. 52-53.
12. Chan, E.K. and H. Ebenhoh, *The implementation and evolution of a SCADA system for a large distribution network*. IEEE Transactions on Power Systems, 1992. 7(1): p. 320-326.
13. Valsalam, S.R., A. Sathyan, and S.S. Shankar, *Distributed SCADA system for optimization of power generation*, in *INDICON 2008*. 2008. p. 212-217.

14. Bernard, J.P. and D. Durocher, *Expert system for fault diagnosis integrated in existing SCADA systems*. IEEE Transactions on Power Systems, 1994. 9(1): p. 548-554.
15. Reynard, S., O. Gomis-Bellmunt, and A. Sudria-Andreu, *Flexible manufacturing cell SCADA system for educational purposes*. Computer Applications in Engineering Education, 2008. 16(1): p. 21-30.
16. Yang, S.H., X. Chen, and J.L. Alty, *Design issues and implementation of internet-based process control systems*. Control Engineering Practice, 2003. 11: p. 709-720.
17. Chun, S.K.a.J., *Remote Monitoring and Control of Agricultural Storage Facility using Internet*, in AFITA. 2000. p. 179.
18. Prickett, P.W. and R.I. Grosvenor, *Non-sensor based machine tool and cutting process condition monitoring*. Journal of COMADEM, 1999. 2: p. 31-37.
19. Frankowiak, M.R., R.I. Grosvenor, and P.W. Prickett, *A Petri-net based distributed monitoring system using PIC microcontrollers*. Microprocessors and Microsystems, 2005. 29(5): p. 189-196.
20. Ahsan, Q., R.I. Grosvenor, and P.W. Prickett, *Distributed On-Line System for Process Plant Monitoring*. Proceedings of the Institution of Mechanical Engineers, Part E: Journal of Process Mechanical Engineering, 2006. 220(2): p. 61-77.
21. Alyami, M., R.I. Grosvenor, and P.W. Prickett, *A pressure based approach to the monitoring of a pneumatic parallel gripper using a dsPIC*, in COMADEM. 2008. p. 33-42.
22. Alyami, M., R.I. Grosvenor, and P.W. Prickett, *A microcontroller-based approach to monitoring pneumatic actuators*. International Journal of Production Research, 2009: p. 1-13.
23. Isermann, R., *Model-based fault-detection and diagnosis - status and applications*. Annual Reviews in Control, 2005. 29(1): p. 71-85.
24. Isermann, R. and P. Ballé, *Trends in the application of model-based fault detection and diagnosis of technical processes*. Control Engineering Practice, 1997. 5(5): p. 709-719.
25. Venkatasubramanian, V., R. Rengaswamy, and K. Yin, *A review of process fault detection and diagnosis - Part I: Quantitative model-based methods*. Computers and Chemical Engineering, 2003. 27: p. 293-311.
26. Venkatasubramanian, V., R. Rengaswamy, and S.N. Kavuri, *A review of process fault detection and diagnosis: Part II: Qualitative models and search strategies*. Computers and Chemical Engineering, 2003. 27(3): p. 313-326.

27. Venkatasubramanian, V., R. Rengaswamy, and S.N. Kavuri, *A review of process fault detection and diagnosis: Part III: Process history based methods*. Computers & Chemical Engineering, 2003. 27(3): p. 327-346.
28. Zumoffen, D. and M. Basualdo, *Improvements in fault tolerance characteristics for large chemical plants: 1. Waste water treatment plant with decentralized control*. Industrial and Engineering Chemistry Research, 2008. 47(15): p. 5464-5481.
29. Xin, X.Z. and A.R. Simpson, *Expert system for water treatment plant operation*. Journal of Environmental Engineering, 1996. 122(9): p. 822-829.
30. Grieu, S., A. Traore, and M. Polit, *Fault detection in a wastewater treatment plant*, in *IEEE Symposium on Emerging Technologies and Factory Automation, ETFA*. 2001: Antibes-Juan les Pins, France. p. 399-402.
31. Chen, Y. and L. Lan, *A fault detection technique for air-source heat pump water chiller/heaters*. Energy and Buildings, 2009. 41(8): p. 881-887.
32. Cho, S.-H., H.-C. Yang, and M. Zaheer-uddin, *Transient pattern analysis for fault detection and diagnosis of HVAC systems*. Energy Conversion and Management, 2005. 46(18-19): p. 3103-3116.
33. Thornhill, N.F., J.W. Cox, and M.A. Paulonis, *Diagnosis of plant-wide oscillation through data-driven analysis and process understanding*. Control Engineering Practice, 2003. 11(12): p. 1481-1490.
34. Bloch, G. and T. Denoeux, *Neural networks for process control and optimization: Two industrial applications*. International Society of Automation Transactions, 2003. 42(1): p. 39-51.
35. Soyguder, S. and H. Alli, *Fuzzy adaptive control for the actuators position control and modeling of an expert system*. Expert Systems with Applications, 2009. 37(3): p. 2072-2080.
36. Tzoneva, R., *Optimal PID control of the dissolved oxygen concentration in the wastewater treatment plant*, in *AFRICON*. 2007. p. 1-7.
37. Radhakrishnan, V.R., *Model based supervisory control of a ball mill grinding circuit*. Journal of Process Control, 1999. 9(3): p. 195-211.
38. Cembrano, G., J. Quevedo, and M. Salamero, *Optimal control of urban drainage systems. A case study*. Control Engineering Practice, 2004. 12(1): p. 1-9.
39. Gao, Z., M. Peek, and P.J. Antsaklis, *Learning for the adaptive control of large flexible structures*, in *Proceedings of the 3rd International Symposium on Intelligent Control*. 1988, Publ by IEEE: Arlington, VA, USA. p. 508-512.

40. Prasad, G., E. Swidenbank, and B.W. Hogg, *Novel performance monitoring strategy for economical thermal power plant operation*. IEEE Transactions on Energy Conversion, 1999. 14(3): p. 802-809.
41. Studinski, J., *Application of monitoring technologies in environmental engineering*, in *Quality, Reliability and maintenance*. 2004. p. 43-46.
42. Sardeshpande, V., U.N. Gaitonde, and R. Banerjee, *Model based energy benchmarking for glass furnace*. Energy Conversion and Management, 2007. 48(10): p. 2718-2738.
43. Kim, S.-M. and Y.-J. Joo, *Implementation of on-line performance monitoring system at Seoincheon and Sinincheon combined cycle power plant*. Energy, 2005. 30(13): p. 2383-2401.
44. *Red Lion Website*. [Web page] [cited 2007 August 22nd]; Available from: <http://www.redlion.net/Products/HumanMachineInterface/DataStationPlus/DataStationPlus.html>.
45. *ACT'L Website*. [cited 2007 August 22nd]; Available from: <http://ewon.be/PresEWON.htm>.
46. *MSL Website*. [cited 2007 August 22nd]; Available from: <http://www.measurementsystems.co.uk/displaysubcat.asp?id=113&cid=1>.
47. *Nortech NX-30 Web Page*. [cited 2007 September 4th]; Available from: http://www.nortechonline.co.uk/products.php?page_id=86.
48. *Powelectrics Website*. [cited 2007 September 24th]; Available from: http://www.in4ma.co.uk/products/in4ma_pc.html.
49. *Sentry GSM3D Multi Web Page*. [cited 2007 September 25th]; Available from: <http://www.sentrytelemetry.co.uk/products/sentrygsm3dmulti.html#Downloads>.
50. *SentryGSM3DLogger Web Page*. [cited 2007 September 25th]; Available from: <http://www.sentrytelemetry.co.uk/products/sentrygsm3dlogger.html>.
51. *IPC systems i-LOG EDM Web Page*. [cited 2007 October 3rd]; Available from: <http://www.assetmonitoring.eu/edm.html>.
52. *Pulsar Zenith 140 Web Page*. [cited 2007 8th October]; Available from: http://www.pulsar-pm.com/pages/zenith_140.htm.
53. *Walchem Web Master Web Page*. [cited 2007 9th October]; Available from: <http://www.walchem.com/nav/cm.aspx?cmid=98>.

54. *Wonderware Web page.* [cited 2009 24th July]; Available from: <http://www.wonderware.co.uk/>.
55. *GE Fanuc Web Page.* [cited 2009 24th July]; Available from: <http://www.gefanuc.com/>.
56. *ABB Website.* [cited 2009 24th July]; Available from: <http://www.abb.com/>.
57. *Siemens Automation Website.* [cited 2009 25th July]; Available from: <http://www.siemens.co.uk>.
58. *Rockwell Automation Website.* [cited 2009 25th July]; Available from: <http://www.rockwellautomation.com>.
59. *Trend Website.* [cited 2007 19th November]; Available from: <http://www.trend-controls.com>.
60. Ford, *Potential failure mode and effects analysis for manufacturing and assembly processes (Process FMEA) instruction manual.* 1984.
61. Higham, E.H., Perovic, S., *Predictive maintenance of pumps based on signal analysis of pressure and differential pressure (flow) measurements.* Transactions of the Institute of Measurement and Control, 2001. vol. 23: p. 226-248.
62. *Cylon Website.* [cited 2007 October 16th]; Available from: <http://www.cylon.com/>.
63. *OPC Foundation Website.* [cited 2009 March 4th]; Available from: <http://www.opcfoundation.org>.
64. *Citect website.* [cited 2008 14th May]; Available from: www.citect.com.
65. Parrondo, J.L., S. Velarde, and J. Pistono, *Diagnosis based on condition monitoring of fluid-dynamic abnormal performance of centrifugal pumps,* in *Proceedings of the 23rd International Conference on Noise and Vibration Engineering, ISMA.* 1998, Katholieke Universiteit: Leuven, Belgium. p. 309-316.
66. Wang, X.-J., M.F. Lambert, and A.R. Simpson, *Detection and Location of a Partial Blockage in a Pipeline Using Damping of Fluid Transients.* Journal of Water Resources Planning and Management, 2005. 131(3): p. 244-249.
67. Lee, P.J., J.P. Vitkovsky, and M.F. Lambert, *Discrete Blockage Detection in Pipelines Using the Frequency Response Diagram: Numerical Study.* Journal of Hydraulic Engineering, 2008. 134(5): p. 658-663.

68. Scott, S.L. and L.A. Satterwhite, *Evaluation of the Backpressure Technique for Blockage Detection in Gas Flowlines*. Journal of Energy Resources Technology, 1998. 120(1): p. 27-31.
69. Stephens, M., M. Lambert, and A. Simpson, *Field Tests for Leakage, Air Pocket, and Discrete Blockage Detection Using Inverse Transient Analysis in Water Distribution Pipes*. 2004, ASCE: Salt Lake City, Utah, USA. p. 474-474.
70. Page, E.S., *Cumulative Sum Charts*. Technometrics, 1961. 3(1): p. 1-9.
71. Angelo, S.P., *Monitoring quality of liquid in backwashing filter beds*. Filtration & Separation, 1997. 34(3): p. 212.
72. Amburgey, J.E., *Optimization of the extended terminal subfluidization wash (ETSW) filter backwashing procedure*. Water Research, 2005. 39(2-3): p. 314-330.
73. Chipps, M.J., Logsdon, G.S., Hess, A.F., Bayley, R.G.W., Pressdee, J.R., Rachwal, A.J., *Advances in Rapid Granular Filtration in Water Treatment*. Proceedings Chartered Institution of Water and Environmental Management (CIWEM), 2001: p. 183-197.
74. Colton, J.F., P. Hillis, and C.S.B. Fitzpatrick, *Filter backwash and start-up strategies for enhanced particulate removal*. Water Research, 1996. 30(10): p. 2502-2507.
75. Suthaker, S., Smith, D.W., Stanley, S.J., *Optimisation of filter ripening sequence*. J. Water Supply: Res. Technol, 1998. 3 p. 107-118.
76. Bhargava, D.S. and C.S.P. Ojha, *Theoretical analysis of backwash time in rapid sand filters*. Water Research, 1989. 23(5): p. 581-587.
77. Delgrange-Vincent, N., C. Cabassud, and M. Cabassud, *Neural networks for long term prediction of fouling and backwash efficiency in ultrafiltration for drinking water production*. Desalination, 2000. 131(1-3): p. 353-362.
78. Yigit, N.O., G. Civelekoglu, and I. Harman, *Effects of various backwash scenarios on membrane fouling in a membrane bioreactor*. Desalination, 2009. 237(1-3): p. 346-356.
79. Smith, P.J., S. Vigneswaran, and H.H. Ngo, *A new approach to backwash initiation in membrane systems*. Journal of Membrane Science, 2006. 278(1-2): p. 381-389.
80. Svarovsky, L., *Solid-Liquid Separation*, in *Monographs in Chemistry and Chemical Engineering*. 1981, Butterworth and Co Ltd: London. p. 290-292.

81. Tullis, J.P., *Hydraulics of Pipelines: Pumps, Valves, Cavitation, Transients*. 1989, J. Wiley and Sons, Inc. p. 12-13.
82. *Hydroflo Website*. [cited 2009 6th May]; Available from: <http://www.tahoessoft.com/html/hydroflo.htm>.
83. Tullis, J.P., *Hydraulics of Pipelines: Pumps, Valves, Cavitation, Transients*. 1989, J. Wiley and Sons, Inc. p. 89.
84. Merkel, F., *Verdunstungskühlung*. VDI Forschungsarbeiten, 1925(275).
85. Kim, J.-K. and R. Smith, *Cooling water system design*. Chemical Engineering Science, 2001. 56(12): p. 3641-3658.
86. Picon-Nunez, M., C. Nila-Gasca, and A. Morales-Fuentes, *Simplified model for the determination of the steady state response of cooling systems*. Applied Thermal Engineering, 2007. 27(7): p. 1173-1181.
87. El-Dessouky, H.T.A., A. Al-Haddad, and F. Al-Juwayhel, *A modified analysis of counter flow wet cooling towers*. Journal of Heat Transfer, 1997. 119(3): p. 617-626.
88. Muangnoi, T., W. Asvapoositkul, and S. Wongwises, *Effects of inlet relative humidity and inlet temperature on the performance of counterflow wet cooling tower based on exergy analysis*. Energy Conversion and Management, 2008. 49(10): p. 2795-2800.
89. Papaefthimiou, V.D., T.C. Zannis, and E.D. Rogdakis, *Thermodynamic study of wet cooling tower performance*. International Journal of Energy Research, 2006. 30(6): p. 411-426.
90. Gill, A.B., *Plant Performance and Performance Monitoring*, in *Modern Power Station Practice*, E.J. Davies, Editor. 1991, Pergamon Press PLC: Oxford. p. 514-519.
91. Rosen, M.A., *Energy- and exergy-based comparison of coal-fired and nuclear steam power plants*. Exergy, An International Journal, 2001. 1(3): p. 180-192.
92. Roy, R.P., M. Ratisher, and V.K. Gokhale, *A computational model of a power plant steam condenser*. Journal of Energy Resources Technology, Transactions of the ASME, 2001. 123(1): p. 81-91.
93. Rosen, M.A. and I. Dincer, *Thermoeconomic analysis of power plants: an application to a coal fired electrical generating station*. Energy Conversion and Management, 2003. 44(17): p. 2743-2761.

94. Can, A., E. Buyruk, and D. Eryener, *Exergoeconomic analysis of condenser type heat exchangers*. *Exergy, An International Journal*, 2002. 2(2): p. 113-118.
95. Sanpasertparnich, T. and A. Aroonwilas, *Simulation and optimization of coal-fired power plants*. *Energy Procedia*, 2009. 1(1): p. 3851-3858.
96. Shaosheng, F. and Z. Renjun, *A novel approach based on fuzzy-GA modeling for online measurement of fouling in steam condenser*. 2005, Institute of Electrical and Electronics Engineers Inc.: Kowloon, Hong Kong, China. p. 1307-1310.
97. Wakui, T. and R. Yokoyama, *On-line model-based performance monitoring of a shell-and-tube type heat exchanger using steam and water*. *Energy Conversion and Management*, 2008. 49(10): p. 2669-2677.

Appendix A: Failure Modes and Effects Analysis for the WRAP Filtration Rig

Part Name	Function	Potential Failure Mode	Potential Effect(s) of Failure	Potential Causes of failure	Secondary Cause	Current Controls	Occurrence	Severity	Detection	RPN
Pipe work	Water transport	Leak	Flood	Frost damage		Heater	3	7	7	147
				Impact		None	2	7	7	98
				loose/defective union		None	4	7	7	196
				Sample point left open		None	2	7	7	98
				Hose disconnection		None	2	7	7	98
		Blockage	Reduced/no flow	Valve closure		None	3	7	4	84
				Sludge/foreign body		None	5	6	7	210
Pumps	Pump water	Pump stops during operation	No flow/production halted	Excessive current VSD cut out		Health signal to PLC	4	7	1	28
				High flow alarm	High flow	Alarm	2	7	1	14
					Faulty sensor	None	2	7	2	28
				Low tank level alarm	low tank level	Alarm	3	7	2	42
					Faulty sensor	Alarm	2	7	1	14
				Motor burn out		Low flow alarm	1	7	5	35
				Bearing failure		Low flow alarm	2	7	4	56
				Sludge/foreign body		Low flow alarm	4	7	4	112
		Pump will not start		Low tank level alarm	low tank level	Alarm	3	7	4	84
					Faulty sensor	None	3	7	2	42
				Seized bearings		Low flow alarm in extreme cases	2	7	2	28
				Sludge/foreign body		Low flow alarm in extreme cases	2	7	2	28
		Poor performance		Bearing wear		Low flow alarm in extreme cases	5	5	6	150

Back wash controller	Control three way valve	Not actuating	Backwash or filtering prevented	Internal malfunction		none	1	7	5	35
		Not in sequence	Backwash/Filtering prevented	Timing pins changed		none	3	7	5	105
				Filter/backwash duration altered in Chemwatch		none	2	6	5	60
				Internal malfunction		none	1	7	5	35

FT - FLOW TRANSMITTER
 TYPE: MAGFLOW (INSERTION)
 RANGE: 0-3m³/hr
 OUTPUT: 4-20mA
 LOCAL DISPLAY

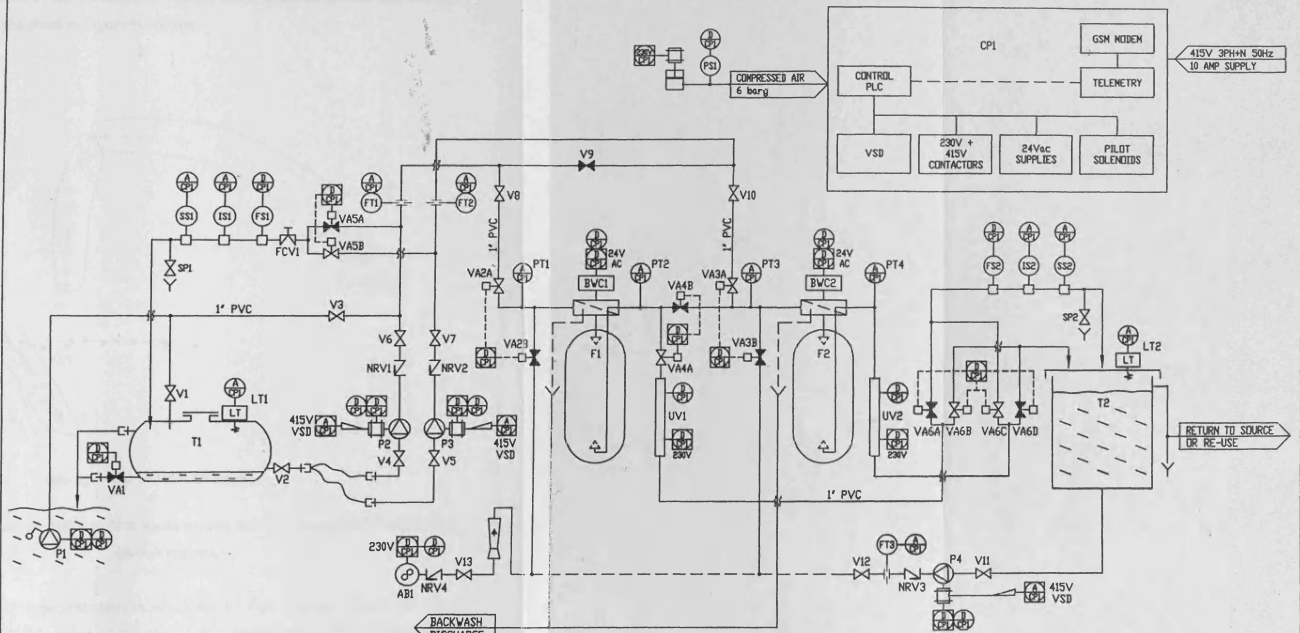
SS - SUSPENDED SOLIDS ANALYSER
 TYPE: OPTICAL/TURBIDITY
 RANGE: 0-3000mg/l
 OUTPUT: 4-20mA
 LOCAL DISPLAY

IS - ION SPECIFIC ANALYSER
 TYPE: COLOURMETRIC
 SPECIFIC ION: PROCESS SPECIFIC
 RANGE: TBA
 OUTPUT: 4-20mA

PT - PRESSURE TRANSMITTER
 TYPE: TRANSDUCER
 RANGE: 0-3bar
 OUTPUT: 4-20mA
 LOCAL DISPLAY

UV - ULTRAVIOLET STERILISER
 DESIGN FLOW: 2m³/hr
 FLOW CAPACITY: 3m³/hr
 TRANSMITTAL ALLOWANCE: 50%

LT - LEVEL TRANSMITTER
 TYPE: ULTRASONIC
 RANGE: 0-5 METRES
 OUTPUT: 4-20mA
 LOCAL DISPLAY



P1 - SUBMERSIBLE PUMP
 DUTY: RAW LIQUOR PUMP
 TYPE: CONTINUOUS OPERATION
 FLOW (DESIGN): 3m³/hr
 PRESSURE: 10 bar
 POWER: 240V

T1 - BALANCE TANK
 CAPACITY: 2000 LITRES
 CONSTRUCTION: NYPE MOULDED
 CONFIGURATION: HORIZONTAL CYLINDER
 COLOUR: GREEN

P2, P3 - FILTER PUMP
 TYPE: PROGRESSIVE CAVITY PUMP
 FLOW (DESIGN): 2m³/hr CAPACITY
 CONTROL: INVERTER SPEED CONTROL
 PRESSURE: 3 bar
 POWER: 415V

AB1 - AIR BLOWER
 TYPE: BLOWEN
 FLOW: 1000 L/min
 PRESSURE: 240V

F1, F2 - FILTER VESSELS
 TYPE: VERTICAL DEEP BED
 SIZE: 14 x 65
 CROSS SECTION: 01
 DN LINE FLOW: 1 TO 5m³/hr
 01 TO 10m³/hr
 BACKWASH FLOW: 30 TO 45m³/hr
 3 TO 4.5m³/hr
 FLEX: BWC

P4 - BACKWASH PUMP
 TYPE: PROGRESSIVE CAVITY PUMP
 FLOW (DESIGN): 3 TO 4.5m³/hr CAPACITY
 CONTROL: INVERTER SPEED CONTROL
 PRESSURE: 3 bar
 POWER: 415V

T2 - TREATED STORAGE TANK
 CAPACITY: 1500 LITRES
 CONSTRUCTION: NYPE MOULDED
 CONFIGURATION: VERTICAL CYLINDER
 COLOUR: NATURAL TRANSLUCENT

Appendix B: WRAP Rig Piping and Instrumentation Diagram

Appendix C: V5 Restriction Behaviour

The V5 results obtained (Tests described in Section 4.9.1) could be divided into distinct regions which are highlighted in Figure 1C below.

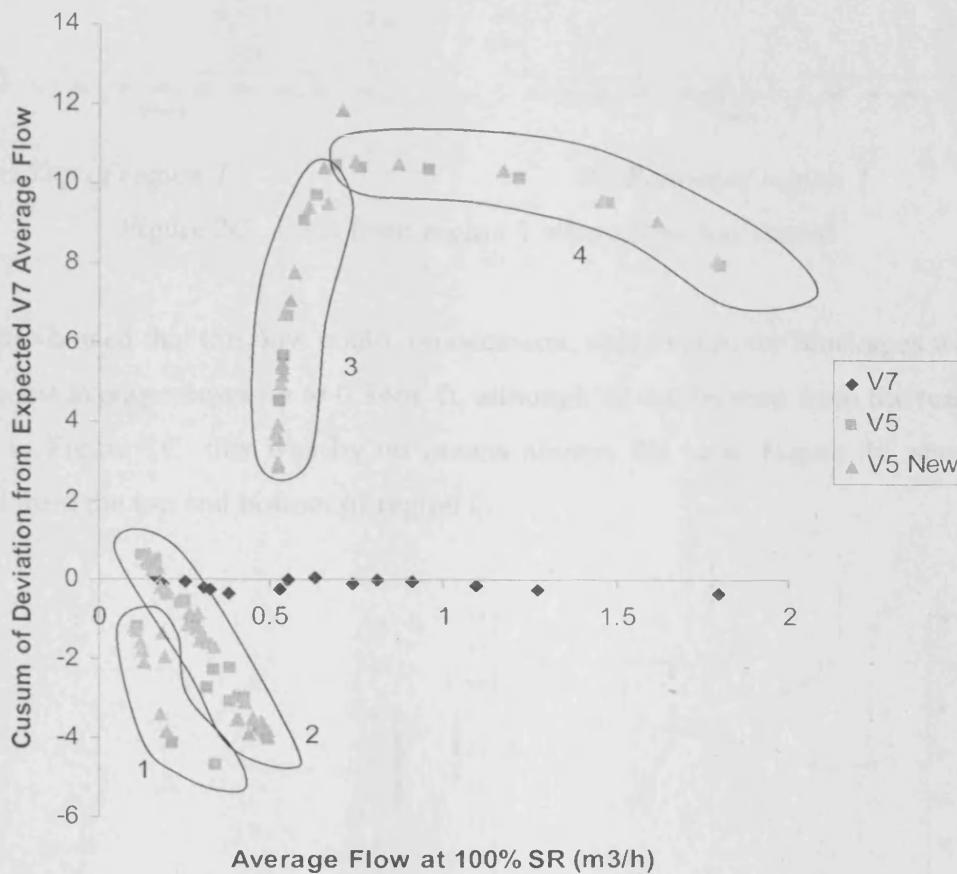
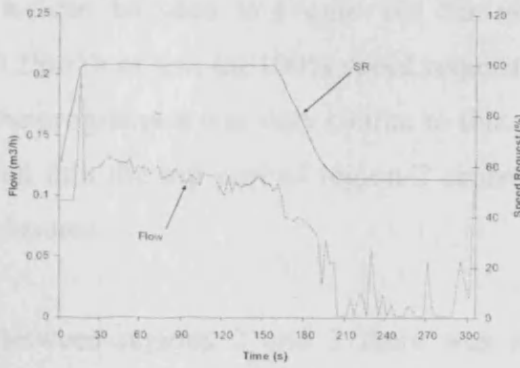
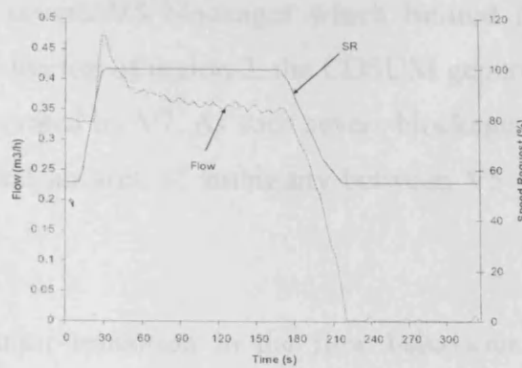


Figure 1C: Test results for 100% to 55% speed request test cycle programme highlighting distinct regions.

Region 1 in Figure 1C represents tests in which the V5 flow response stalled and fell to zero during the CUSUM period of the test cycle. During the 'Flow Standardisation Period' the flow reached a higher level than when the valve was first closed at 55% speed request but crashed to zero when the flow was returned to 55% speed request. Examples from the top and bottom of this region can be seen in figure 2C.



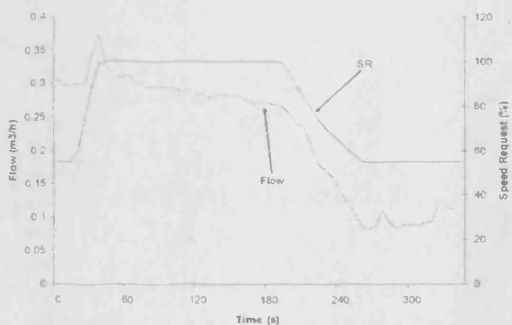
(a) Top of region 1



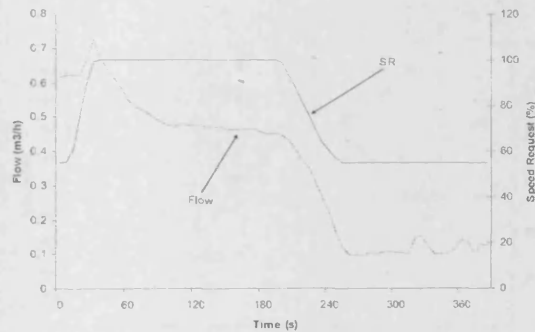
(b) Bottom of region 1

Figure 2C: Tests from region 1 where flow has stalled

These tests showed that the flow could, on occasion, stall to zero for blockages with 100% speed request average flows up to $0.34\text{m}^3/\text{h}$, although as can be seen from the results from region 2 in Figure 1C, this was by no means always the case. Figure 3C shows some examples from the top and bottom of region 2.



(a) Top of region 2



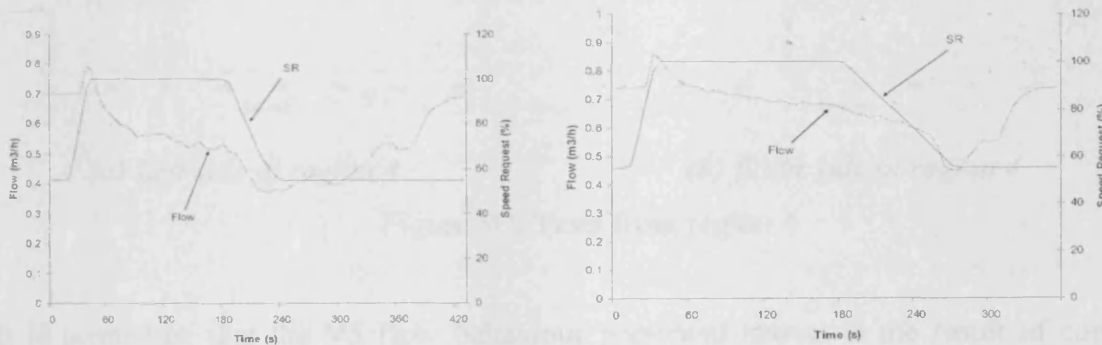
(b) Bottom of region 2

Figure 3C: Tests from region 2 where flow fluctuates about a constant level in the CUSUM period.

As can be seen in Figure 3C, for V5 test cycles which fell in region 2, the flow fell to a relatively steady value when the speed request was returned to 55%, following the 'Flow Standardisation Period'. Also different from region 1 tests was the fact the flow during the 'Flow Standardisation Period' actually fell to levels below that seen when the valve was first closed at 55% speed request. This fall actually became greater as the blockage severity decreased in region 2.

As can be seen in Figure 1C, for very severe V5 blockages which limited flow to $0.25\text{m}^3/\text{h}$ or less (at 100% speed request) at the top of region 2, the CUSUM generated by the programme was very similar to that generated by V7. As such severe blockages which fell into the top part of region 2 represented an area of ambiguity between V5 and V7 closures.

Between regions 2 and 3 there was a major transition in the flow behaviour of V5 blockages. In region 3 the flow suddenly stopped falling to such a large extent during the ramp down. Also the flow almost immediately showed a tendency towards flow recovery when the speed request stabilised at 55%. Also, as blockage severity decreased, the fall in the flow (during the 'Flow Standardisation Period') to levels lower than the initial flow, began to decrease. Further more, the flow was eventually able to recover to the level it was at before the 'Flow Standardisation Period'. This was actually higher than that obtained when the 100% speed request average was taken, immediately following the 'Flow Standardisation Period'.



(a) Bottom of region 3

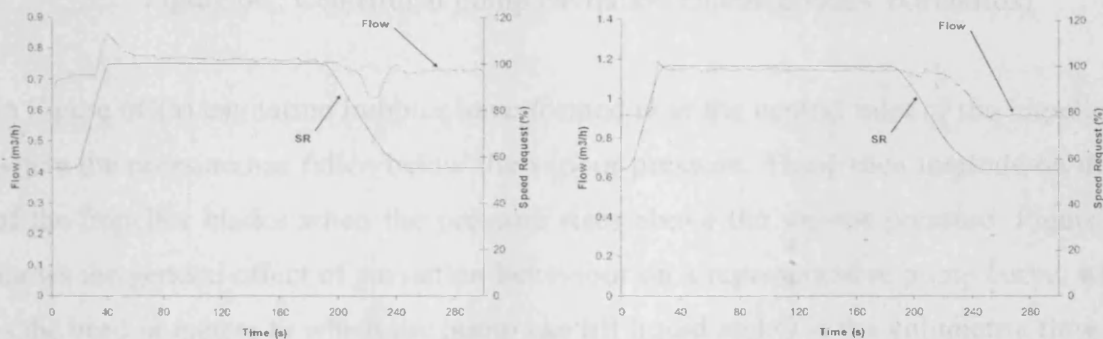
(b) Top of region 3

Figure 4C: Tests from region 3

Figure 4C(a) shows that as blockage level decreases, the flow recovery becomes even faster. This explains why the region 3 CUSUM climbs so sharply in Figure 1C. The change in characteristics between region 2 and 3 appeared to be due to the flow recovery phenomena which happened following the 'Flow Standardisation Period' in region 3 results but was not present in region 2. This had the effect of greatly increasing the CUSUM as the flow recovery resulted in the measured flow being far greater than the modelled V7 flow. The emergence of flow recovery behaviour appeared to occur suddenly at the bottom of region 2 and had the drastic effect of changing the sign of the

CUSUM results. The transition into flow recovery behaviour occurred instantaneously and this is believed to explain why ambiguous results between region 2 and 3 did not occur.

Finally in region 4 the flow once again reached a level equal to, or higher than, the initial flow obtained at 55% speed request when put into the 'Flow Standardisation Period' at 100% speed request. When returned to 55% speed request for the CUSUM period the flow obtained the level seen initially. In the more severe blockages in this group, as represented by Figure 5C(a) the flow dipped below the initial rate for a short period. For the less severe blockages such as Figure 5C(b) the flow falls straight to the initial level with no dip.



(a) Left side of region 4

(b) Right side of region 4

Figure 5C: Tests from region 4

It is postulated that the V5 flow behaviour presented above, is the result of cavitation behaviour in the pump, which is caused by the upstream restriction starving the pump of fluid. As explained by Tullis [81], cavitation occurs in a water pump when the local pressure falls below the vapour pressure of the water. In these conditions, vapour cavities form and if the conditions persist, the cavities rapidly expand. If the surrounding pressure is above the vapour pressure the bubbles becomes unstable and implode. The energy released from this collapse, causes noise and vibration. A diagrammatic representation of the cavitation behaviour in an impellor, of the type used in the WRAP rig pumps, is shown as Figure 6C(a).

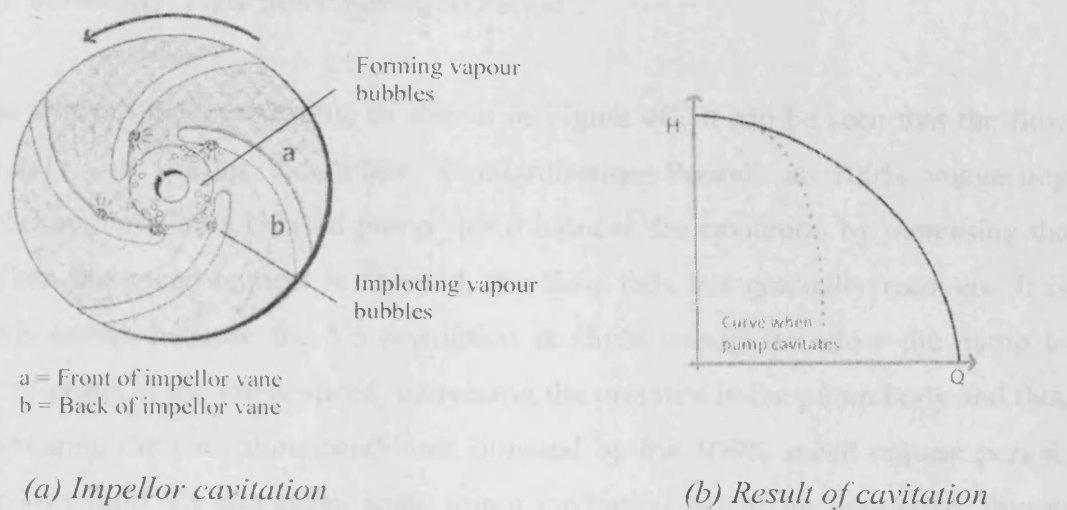


Figure 6C: Centrifugal pump cavitation characteristics. (Grundfos)

In Figure 6C(a) cavitation bubbles have formed near the central inlet of the impellor disc, where the pressure has fallen below the vapour pressure. These then implode on the back of the impellor blades when the pressure rises above the vapour pressure. Figure 6C(b) shows the general effect of cavitation behaviour on a representative pump curve, where H is the head in meters to which the pump can lift liquid and Q is the volumetric flow rate in m^3/h . As can be seen, cavitation has a pronounced effect on the flow rate. It is believed that a restriction in the upstream V5 causes the Net Positive Suction Head (NPSH) of the pump to enter a negative region. NPSH is the difference between the local pressure in the pump body and the vapour pressure of the pumped fluid, in this case water. An upstream blockage increases the level of suction required, which in turn lowers the pressure inside the pump, potentially making the NPSH negative and leading to cavitation.

It is likely that for severe blockages of V5, as represented by regions 1 and 2 in Figure 2H, the 'Flow Standardisation Period' at 100% speed request causes severe cavitation behaviour in the pump. This theory is supported by the presence of excess noise and vibration emanating from the pump during these periods. As can be seen in the results from Figures 2C and 3C, the flow rate falls during the 'Flow Standardisation Period'. This is potentially the result of worsening cavitation behaviour as pressure in the pump body falls and increasingly large cavitation bubbles are formed. When the speed request is returned to 55%, it can be seen that the flow does not recover fully. This is potentially a

result of the now lowered pressure in the pump body still causing worse cavitation than was present before the 'Flow Standardisation Period'.

For the less severe blockage results, as shown in Figure 4C, it can be seen that the flow does gradually fall during the 'Flow Standardisation Period' at 100% suggesting cavitation behaviour. The increased pump speed induces the cavitation by increasing the suction. When the speed request is reduced, the flow falls but gradually recovers. It is believed this occurs because the V5 restriction is slight enough to allow the pump to effectively re-prime at the lower speed, increasing the pressure in the pump body and thus slowly eradicating the cavitation conditions initiated by the 100% speed request period. Finally for very mild V5 blockages some minor cavitation behaviour may occur during the 'Flow Standardisation Period' but this is quickly overcome when the speed request is returned to 55%. It is also worth mentioning that cavitation can also occur immediately following partially closed valves. It is believed that this behaviour was also occurring, as noise and vibration could be detected coming from V5 during severe closures.

Appendix D: Published Papers

An Approach to the Characterisation of Faults in a Water Treatment Plant. Published in COMADEM 2009 Proceedings. ISBN 978-84-932064-6-8

Practical Implementation of a SCADA Based Water Treatment Optimisation System. Submitted to ISA Transactions and currently under review.

